Spatial and Temporal Regulation of IL4Rα Expression.

Elizabeth M. Smith

Thesis submitted to the University of Cape Town in fulfilment of the degree
Doctor of Philosophy
Department of Immunology
Faculty of Health Sciences
University of Cape Town
February 2008

Declaration

I, Elizabeth M. Smith, hereby declare that the work on which this thesis is based, is my original work (except where acknowledgments indicate otherwise) and that neither the whole work or any part thereof has been, is being or is to be submitted for another degree in this or any other University.

I empower the University of Cape Town to reproduce for the purpose of research either the whole or any portion of the contents in any manner whatsoever.

Signed by candidate

Elizabeth Maria Smith

February 2008

Acknowledgements

I would like to express my sincere gratitude and thanks to all the people who have supported me and contributed to the completion of this thesis.

To my supervisors, Prof. F. Brombacher and Dr W. Horsnell for the support, advice and scientific enthusiasm.To my colleagues and friends at the department of Immunology for motivation, advice and friendship, especially Reece and Frank. I am extremely grateful towards all the technicians and administrative staff, especially Hiram, Berenice, Reagon and Wendy. Furthermore, I wish to acknowledge the National Research Foundation and University Research Council for funding.

A special thanks to my family and friends for all the love and support, it would not have been possible without you!
Lastly, I would like to thank David, for all the love, patience, support and keeping me sane. Congratulations on your PhD!! – Baie, Baie Liefde!

Chapter 1: General Introduction

Chapter 2: Inducible deletion of IL-4Rα expression

Chapter 3: Dendritic Cell Specific Expression of Cre Recombinase.

Chapter 4: Generation of molecular tools for the neutralization of signalling via IL-4Rα and IL-13Rα$_2$.

Chapter 5: Discussion.

Appendix A

References

Abstract

In order to design new therapies in the fight against infectious diseases it is necessary to understand how the human immune response controls infection. Mouse models, particularly gene-targeted mice, are invaluable in studies into immune responses (Goosen and Bujard, 2002). A central regulator of immune responses is IL-4Rα, the receptor for the IL-4 and IL-13, Th2 cytokines (Paul, 1997). The generation of IL-4Rα deficient mouse models has been invaluable in identifying the roles of IL-4/IL-13 and IL-4Ra in numerous studies (Mohrs *et al.,* 1999). In order to enhance these findings the development of new models and molecular tools targeting specific cell populations and/or taking advantage of new genetic technologies allow for the spatial and temporal deletion or reconstitution of the gene of interest. In this study, we generated a new mouse model, which allows both inducible and cell-specific deletion and reconstitution of IL-4Rα expression. This model has the potential to add a new dimension to our understanding of IL-4Rα biology. This has been achieved by using the established Tet System (Goosen and Bujard, 1992) where the crossing of two complementary transgenic mouse lines enable the generation of the final double transgenic model. The first line expresses the transactivator, tTA, from the Tet-Off expression cassette driven by the Vav hemapoeitic specific promoter (Wiesner *et al.,* 2005). The second mouse line expresses IL-4Rα cDNA under the dictates of a cytomegalovirus (P^{CMV}) minimal promoter supplemented with seven tet operon (Tet_O) sequences which serves as a binding site for the transactivator. Backcrossing these lines to an IL-4Rα$^{-/-}$ BALB/c genetic background, the two transgenic lines were crossed, generating a double transgenic mouse on an IL-4Rα$^{-/-}$ backbone. In these double transgenic mice, the transactivator was synthesized in a cell specific manner leading to haematopoietic cell IL-4Rα reconstitution on an IL-4Rα$^{-/-}$ background. As this binding of the transactivator to the Tet_O is inhibited by tetracycline, oral administration of tetracycline can turn off IL-4Rα expression.

To investigate the importance of IL-4Rα on dendritic cells (DCs), we constructed and characterised vectors to generate a dendritic cell (DC) specific IL-4Rα deficient mouse model (CD11c-Cre-IL-4Rα$^{lox/-}$). In this model, Cre recombinase transgene expression will be directed exclusively to DCs due to the incorporation of the appropriate cell specific promoter (CD11c). Cre expression will lead to the inactivation of the lox P flanked IL-4Rα gene. Here we describe the molecular cloning and characterisation of the eukaryotic expression vectors containing the mouse dendritic cell specific promoter (CD11c, Broker *et al.,* 1997). Vectors were designed for optimal expression, directed via CD11c, of the

Cre Recombinase and Green Fluorescent Protein (GFP) transgenes. *In vitro* functional analysis of these constructs confirmed cell specific transcription and translation of the transgenes.

In the final part of the project soluble receptors were generated for the blocking of IL-4 and IL-13 signalling. Such blockers have proven to be powerful tools in studying cytokine function (Goldenberg et al., 1999; Grunig *et al.*, 1998). Here we aimed to build on this body of knowledge by generating F_c-tagged soluble receptor blockers for IL-4Rα, IL-13Rα_2 and the IL-2Rγ-IL-4Rα receptor complex. These Fc-tagged blockers allow the inhibition of cytokine function *in vitro* and *in vivo*. The design and generation of these fusion proteins were analogous to those previous described IL-4 and IL-13 cytokine blockers but with specific refinements. These refinements are in the construct design where we specifically used cDNA of a BALB/c genetic background (to skew the immunological Th1 / Th2 response), and a mutated human F_c-tag which decreases non-specific binding by the recombinant proteins. All three cytokine blockers demonstrated cytokine blocking activity and biological functionality was confirmed for two of the generated blockers.

Together these strategies allow for the precise determination of the role of IL-4Rα and its associated cytokines in immune responses and will provide useful information which is likely to be of use in the development of new medical treatments.

Contents

	Page
Abstract.	*viii*
List of figures and tables.	
Abbreviations.	
Chapter 1: General Introduction.	**2**
1.1 The immune system.	2
1.1.1 Innate Immunity.	4
1.1.2 Adaptive Immunity.	6
1.1.2.1 B lymphocytes.	6
1.1.2.2 T lymphocytes.	8
1.1.2.3 T lymphocytes and Th1/Th2 differentiation.	10
1.2 Cytokines and immune system communication.	13
1.3 Interleukin-4 and Interleukin-13.	14
1.3.1 Interleukin-4.	15
1.3.2 Interleukin-13.	15
1.4 IL-4Rα.	17
1.4.1 Soluble receptors.	19
1.4.2 IL-4Rα and cytokine signalling pathways.	20
1.5 Molecular manipulation of gene function.	22
1.5.1 Conventional transgenics.	23
1.5.2 Gene targeting using embryonic stem cells.	24
1.5.3 Conditional transgenics.	26
1.5.3.1 Site-specific recombinase systems.	27
1.5.3.2 Tissue specific knockouts.	28
1.5.4 Conditional control of transcription.	31
1.6 Molecular manipulation of IL-4Rα.	35
1.6.1 *Leishmania donovani*.	35
1.6.2 *Nippostrongylus Brasiliensis*.	36
1.6.3 *Schistosoma mansoni*.	37

Chapter 2: Inducible deletion of IL-4Rα expression. **38**

2.1 Introduction. 39

2.2. Methods and Materials. 42

2.2.1 Cloning of the construct.

2.2.1.2 Primer design. 42

2.2.1.2.1 The transmembrane isoform of murine IL-4Rα. 42

2.2.1.3 Vector Description. 43

2.2.1.4 Polymerase Chain Reaction (PCR). 43

2.2.1.4.1 Amplification of coding region for the transmembrane isoform of murine IL-4Rα. 43

2.2.1.5 Restriction and ligation of the coding sequence into the pBi-Luc eukaryotic expression vector. 44

2.2.1.6 Agarose gel electrophoresis. 45

2.2.1.7 Gel isolation and purification of DNA. 45

2.2.2 Cell culture. 45

2.2.2.2.1 Hek 293T cells. 45

2.2.2.2.2 Transfection of Hek 293T cells. 46

2.2.3 *In vitro* and *in vivo* determination of transgene functionality**.** 46

2.2.3.1 Template preparation for qRT-PCR assays. 46

2.2.3.1.1 RNA Isolation. 46

2.2.3.1.2 DNAseI treatment of isolated RNA. 47

2.2.3.1.3 cDNA Synthesis. 48

2.2.3.2 Transcription assays. 48

2.2.3.2.1 Primers designed for expression assays. 48

2.2.3.2.2 qRT-PCR. 49

2.2.3.3 Translation assays. 49

2.2.3.3.1 Luciferase assay. 49

2.2.3.3.2 FACS analysis. 50

2.2.4 Generation of chimeras. 51

2.2.4.1 Generation of pBi-IL-4Rα Tg chimeras. 51

2.2.4.2 Genotyping of pBi- IL-4Rα Tg and pVav-tTa Tg. 51

2.2.4.2.1 Genomic DNA extraction. 51

2.2.4.2.2 Genotyping PCR. 51

2.3 Results. 53
2.3.2.1 Transgenic Construct design and cloning. 53
2.3.2.2 *In vitro* expression studies. 57
2.3.2.2.1 Establishment of bi-directional promoter activity. 58
2.3.2.2.2 Establishment of effective doxycycline concentration and repression over time. 60
2.3.2.2.3 Establishment of efficient pTet-Off: pBi-IL-4Rα plasmid ratio. 62
2.3.2.3 *In vitro* inducible repression of IL-4Rα expression. 62
2.3.2.3.1 Transcription efficiency of mIL-4Rα transgene. 64
2.3.2.3.2 Translation efficiency of mIL-4Rα transgene 66
2.3.2.3.3 *In vitro* inducible repression of mIL-4Rα expression. 68
2.3.2.4 Generation and analysis of single transgenic chimeras. 70
2.3.2.4.1 Generation of pBi-IL-4Rα Tg chimeras. 70
2.3.2.4.2 Breeding program. 72
2.3.2.4.4 Stringent control of IL-4Rα expression in pBi-IL-4RαTg / IL-4Rα $^{-/-}$ BALB/c mice. 74
2.3.2.4.3 Genotyping of pBi-IL-4RαTg / IL-4Rα $^{-/-}$ BALB/c and pVav-tTaTg / IL-4Rα $^{-/-}$ BALB/c. 76
2.3.2.5 Analysis of pBi-IL-4RαTg / IL-4Rα $^{-/-}$ BALB/c / pVav-tTaTg/ IL-4Rα $^{-/-}$ BALB/c. 79
2.3.2.5.1 Transcriptional analysis 79
2.3.2.5.2 Translational analysis 82
2.4 Chapter Conclusions. 85

Chapter 3: Dendritic Cell Specific Expression of Cre Recombinase **87**

3.1 Introduction. 88
3.2 Methods and Materials. 88
3.2.1 Cloning of the constructs. 88
3.2.1.1 Plasmid purification. 91
3.2.1.2 Primer design. 91
3.2.1.3 Modified Cre recombinase primers. 91
3.2.1.4 Polymerase Chain Reaction (PCR). 91
3.2.1.4.1 Amplification of Cre cDNA. 91
3.2.1.5 Restriction and ligation of Cre, GFP and CD11c into a eukaryotic expression vector. 91

3.2.1.5.1 Sub-cloning of Cre into the pDrive PCR cloning vector. 92
3.2.1.5.2 Sub-cloning of CD11c into the pGFP-N1 expression vector. 92
3.2.1.5.3 Cloning of the CD11c driven Cre expression vector. 93
3.2.1.6 Agarose gel electrophoresis. 94
3.2.1.7 Gel isolation and purification of DNA. 94
3.2.2 Cell culture**.** 94
3.2.2.1 Hek 293T cells. 95
3.2.2.2 Transfection of Hek 293T cells. 95
3.2.2.3 D25/sc dendritic cell line. 95
3.2.2.4 Transfection of D25/sc cells. 96
3.2.3 *In vitro* studies. 96
3.2.3.1 D25/sc Cell line characterisation. 96
3.2.3.2 CMV promoter activity. 97
3.2.3.3 Cell specific transcription. 97
3.2.3.3.1 Template preparation - RNA isolation. 97
3.2.3.3.2 DNAseI treatment. 98
3.2.3.3.3 cDNA synthesis. 98
3.2.3.3.4 cDNA amplification. 98
3.2.3.4 Cell specific translation. 98
3.2.3.4.1 CD11c driven GFP expression. 99
3.2.3.4.2 Immunofluorescence. 100

3.3 Results.

3.3.1 Vector design and construction. 101
3.3.1.1 Generation of the Cre cDNA fragment. 103
3.3.1.2 Cloning of the CD11c fragment. 104
3.3.1.3 Generation of the CD11c driven Cre vector. 107
3.3.1.4 pCD11c-Cre vector sequence analysis. 109
3.3.2. Preliminary in vitro expression studies. 109
3.2.2.1 Influence of CMV promoter. 111
3.3.3 Characterisation and Transfection of the D25/sc Cell Line. 111
3.3.3.1 Cell line characterisation. 113
3.3.3.2 D25/sc Transfection. 115
3.3.4 In vitro expression studies. 115
3.3.4.1 Cell specific transcription. 117
3.3.4.2 Cell specific translation 119

3.4 Chapter Conclusions. 122

Chapter 4: Generation of molecular tools for the neutralization of signalling via IL-4Rα and IL-13Rα$_2$. 123

4.1 Introduction. 124

4.2 Methods and Materials. 127

4.2.1 Cloning of the constructs. 127

4.2.1.1 Plasmid purification. 127

4.2.1.2 Primer design. 127

4.2.1.2.1 The extracellular domains of IL-4Rα , IL-13Rα$_2$ and IL-2Rγ. 127

4.2.1.3 Template preparation for PCR of IL-13Rα$_2$ and IL-2Rγ extracellular domains. 127

4.2.1.3.1 RNA Isolation. 127

4.2.1.3.2 DNAseI treatment and removal of digested DNA fragments. 128

4.2.1.3.3 cDNA Synthesis. 128

4.2.1.4 Polymerase Chain Reaction (PCR). 129

4.2.1.4.1 Amplification of extracellular domains of IL-4Rα, IL-13Rα and IL-2Rγ. 129

4.2.1.5 Cloning of the coding sequences into eukaryotic expression vectors. 129

4.2.1.5.1 Extracellular domains of IL-4Rα and IL-13Rα$_2$. 129

4.2.1.5.2 Extracellular domain of IL-2Rγ. 130

4.2.1.6 Agarose gel electrophoresis. 131

4.2.1.7 Gel isolation and purification of DNA. 131

4.2.2 Cell culture. 131

4.2.2.1 Hek 293T cells. 131

4.2.2.2 Transfection of Hek 293T cells. 132

4.2.3 Purification and detection of recombinant proteins. 132

4.2.3.1 Large scale protein expression. 132

4.2.3.2 Cell lysate preparation for Hek 293T / pSecTag-sIL13Rα$_2$F$_c$ cultures. 133

4.2.3.3 IgG Protein purification. 133

4.2.3.4 Protein quantification. 133

4.2.3.5 SDS-PAGE. 134

4.2.3.6 Western blot analysis. 134

4.2.4 *In vitro* assays. 135

. 4.2.4.1 Cytokine binding assay. 135

4.2.4.2 Cell proliferation assay. 135

4.2.4.3 T cell differentiation assay. 136

4.2.4.4 Cytokine ELISA. 137
4.2.4.5 Generation of bone marrow derived macrophages (BMDMs). 138
4.2.4.5.1 L929 conditioned medium. 139
4.2.4.6 Measurement of nitric oxide. 139
4.2.4.7 Measurement of arginase activity. 139
4.2.4.8 FACS analysis of BMDMs. 140
4.3 Results. 141
4.3.1 Vector design and construction. 141
4.3.1.2.Molecular cloning and characterisation of F_c-tagged soluble. 141
4.3.1.2.1 The F_c-tagged soluble IL-4Rα eukaryotic expression vector. 145
4.3.1.2.2 The F_c-tagged soluble IL-13Rα_2 eukaryotic expression vector. 148
4.3.1.2.3 The inline F_c-tagged soluble IL-4Rα / soluble IL-2Rγ cytokine trap eukaryotic expression vector. 151
4.3.3 Recombinant fusion protein expression and purification 154
4.3.4 Biochemical protein characterisation. 154
4.3.4.1 Cytokine Binding assays. 157
4.3.4.1.1 sIL-4Rα and sIL-13Rα_2. 158
4.3.4.1.2 sIL-2Rγ– sIL-4Rα cytokine trap. 160
4.3.5 *In vitro* functional assays. 161
4.3.5.1 T cell Proliferation. 161
4.3.5.2 T cell Differentiation. 163
4.3.5.3 Influence of sIL-4RαF_c and sIL-13R$\alpha_2 F_c$ on macrophage responsiveness to mIL-4 and mIL-13. 165
4.3.5.3.1 Bone marrow derived macrophage differentiation. 165
4.3.5.3.2 Macrophage mannose receptor expression. 167
4.4 Chapter Conclusions. 169

Chapter 5: Discussion. 171

References.

Appendix A. 211
A.1 Plasmid Maps. 212
A.2 Reagents and Suppliers. 215
A.3 Software Resources 217
A.4 Specialized Equipment. 217

A.5 Recipes. 218
A.5.1 General Lab Solutions. 218
A.5.2 Bacterial Solutions. 220
A.5.3 Cell Culture Solutions. 221
A.5.4 Immunology Solutions. 223
A.5.5 RNA Solutions. 225
A.6 Generation of pBi-IL-4Rα chimeras. 227
(Find PDF file attached.)

Abstract

List of figures and tables.

Page

Chapter 1: General Introduction. 1

Figure 1.1 Immune system cell development. 3
Figure 1.2 B lymphocyte development. 7
Figure 1.3 Antigen presentation and T lymphocyte activation. 9
Figure 1.4 T cell differentiation. 11
Figure 1.5 Influence of cytokines on immune response. 13
Figure 1.6 IL-4, IL-2 and IL-13 receptor complexes. 18
Figure 1.7 IL-4 and IL-13 Jak/Stat signalling pathway. 21
Figure 1.8 Gene targeting via homologous recombination in ES cells. 25
Figure 1.9 The model of Cre and Flp site-specific recombinase inactivation. 27
Figure 1.10 Combining gene targeting and the Cre-*lox*P recombination system to inactivate a gene in a desired cell type. 30
Figure 1.11 Induced expression via the Tet-Off and Tet-On Systems. 32
Figure 1.12 Inducible transcription via the bi-directional pBI-L Tet vector. 34

Chapter 2: Inducible deletion of IL-4Rα expression. 38

Figure 2.1 Tet-Off inducible system. 41
Table 2.1 Sequences of oligonucleotides used for the amplification of IL-4Rα. 42
Table 2.2 Sequences of oligonucleotides used for the expression studies. 48
Table 2.3 Sequences of oligonucleotides used genotyping Tg mice. 52
Figure 2.2 Flow Diagram of pBi-IL-4Rα Cloning Strategy. 54
Figure 2.3 Amplification of transmembrane IL-4Rα cDNA fragment. 56
Figure 2.4 Restriction enzyme screening and sequence verification of the pBi-IL-4Rα transgenic construct. 56
Figure 2.5 Optimization and assessment of Hek 293T cells transfection efficiency. 57
Figure 2.6 Induced luciferase expression in Hek 293T cells containing both response and regulatory vectors. 59
Figure 2.7 Doxycycline induced suppression of luciferase expression. 61
Figure 2.8 Effect of regulatory and response plasmid ratios on transgene expression. 63

Figure 2.9 Transgene mRNA levels in stable pTet-Off-pBi-IL-4Rα Hek 293T cell line. 65
Figure 2.10 IL-4Rα transgene expression in Hek 293T cells. 67
Figure 2.11 Inducible IL-4Rα transgene expression in Hek 293T cells. 69
Figure 2.12 Flow diagram of generation of pBi-IL-4Rα chimeric mice. 71
Figure 2.13 Breeding scheme for the generation of the final inducible model. 73
Figure 2.15 IL-4Rα transgene leakiness via the CMV promoter. 75
Figure 2.14 Genotyping of generated transgenic lines. 77
Figure 2.14 Genotyping of generated transgenic lines. 78
Figure 2.16 Transgene mRNA levels in pBi-IL-4RαTg / IL-4Rα $^{-/-}$ BALB/c / pVav-tTaTg/ IL-4Rα $^{-/-}$ BALB/c line. 80
Figure 2.16 Transgene mRNA levels in pBi-IL-4RαTg / IL-4Rα $^{-/-}$ BALB/c / pVav-tTaTg/ IL-4Rα $^{-/-}$ BALB/c line. 81
Figure 2.17 pBi-IL-4Rα Tg /pVav-tTa Tg translational analysis. 84

Chapter 3: Dendritic Cell Specific Expression of Cre Recombinase. 87

Figure 3.1. The generation of the CD11c-IL-4Rα$^{-/-}$ model. 90
Table 3.1 Sequences of oligonucleotides used for the amplification of Cre. 91
Figure 3.2 Flow Diagram of pCD11c-GFP and pCD11c-Cre Cloning Strategy. 102
Figure 3.3 Amplification of Cre cDNA fragment. 104
Figure 3.4 Vector construction scheme for pCD11c-GFP. 105
Figure 3.5 Partial *Pst I* Restriction Enzyme Digestion of pBS-CD11c. 106
Figure 3.6. Cloning of CD11c driven expression vectors. 108
Figure 3.7 Sequence Verification of pCD11c-Cre. 110
Figure 3.8 Effect of CMV promoter presence on GFP expression in CD11c vectors. 112
Figure 3.9. D25/sc Cell Phenotype Characterisation. 114
Figure 3.10. Transfection efficiency of D25/sc cells. 116
Figure 3.11. Dendritic cell specific transcription of Cre Recombinase. 118
Figure 3.12. Dendritic cell specific CD11c driven transgene expression. 120
Figure 3.13. Dendritic cell specific CD11c driven Cre expression. 121

Chapter 4: Generation of molecular tools for the neutralization of signalling via IL-4Rα and IL-13Rα$_2$. 123

Figure 4.1. IL-13 and IL-4 receptor combinations and binding. 124
Table 4.1 Sequences of oligonucleotides used for the amplification of the extracellular domains of IL-4Rα , IL-13 Rα$_2$ and IL-2Rγ. 127
Figure 4.2.A Flow Diagram of pSecTag-F$_c^{Mut}$-sIL-4Rα Cloning Strategy. 142
Figure 4.2.B Flow Diagram of pSecTag-F$_c^{Mut}$-sIL-13Rα$_2$ Cloning Strategy. 143
Figure 4.2.C Flow Diagram of pSecTag-F$_c^{Mut}$-sIL-2Rγ–sIL-4Rα Cloning Strategy. 144
Figure 4.3 Amplification of extracellular IL-4Rα cDNA fragment. 144
Figure 4.4 Restriction enzyme screening and sequence verification of the sIL-4RαF$_c$ expression vector. 146
Figure 4.4 Restriction enzyme screening and sequence verification of the sIL-4RαF$_c$ expression vector. 147
Figure 4.5 Amplification of the IL-13Rα$_2$ extracellular cDNA fragment. 147
Figure 4.6 Restriction enzyme screening and sequence verification of the sIL-13Rα$_2$F$_c$ expression vector. 149
Figure 4.7 Insert orientation and sequence verification of the sIL-13Rα$_2$F$_c$ expression vector. 150
Figure 4.8 Amplification of the IL-2Rγ extracellular cDNA fragment.
Figure 4.9 Restriction enzyme screening of sIL-2γ-sIL-4RαF$_c$ clones. 152
Figure 4.10 Insert orientation of sIL-2Rγ-sIL-4RαF$_c$ expression vector. 153
Figure 4.11 SDS-PAGE analyses of IL-4 and IL-13 soluble receptor blockers. 155
Figure 4.12 SDS-PAGE analysis of sIL-2Rγ-sIL-4RαF$_c$ cytokine trap. 156
Figure 4.13 Western Blot detection of secreted proteins. 156
Figure 4.14 Diagram of F$_c$-tagged Soluble Receptor Elisa ProtocoL. 157
Figure 4.15 Cytokine Binding analyses of sIL-4RαF$_c$ and sIL-13Rα$_2$F$_c$. 158
Figure 4.15 Cytokine Binding analyses of sIL-4RαF$_c$ and sIL-13Rα$_2$F$_c$ blockers. 159
Figure 4.16 Cytokine Binding analysis of sIL-2Rγ-sIL-4RαF$_c$ cytokine trap. 160
Figure 4.17 CD4$^+$T Cell proliferation after stimulation with mIL-4, mIL-2, or mIL-4 with sIL-4RαF$_c$. 162
Figure 4.18 Effect by sIL-4RαF$_c$ and sIL-13Rα$_2$F$_c$ on *in vitro* Th1/Th2 differentiation of CD4$^+$ T cells from BALB/c mice. 164
Figure 4.19 Suppression of IL-4 and IL-13 function in BMDM cultures. 166
Figure 4.20 sIL-4RαF$_c$ and sIL-13Rα$_2$F$_c$ dependant suppression of MMR expression. 168

Abbreviations

A_{260}: absorbance at 260 nm

A_{280}: absorbance at 280 nm

A: adenine or adenosine; one-letter code for alanine

Ab: antibody

Ag: antigen

anti-Ig: anti-immunoglobulin antibody

AP: alkaline phosphatase

APC: antigen-presenting cell(s)

ATP: adenosine 5′-triphosphate

BCIP: 5-bromo-4-chloro-3-indolyl phosphate

bis,bisacrylamide: *N,N′*-methylene-bisacrylamide

Bis-Tris: bix-(2-hydroxyethyl)imino-tris-(hydroxymethyl)methane

bp: base pair

BrdU: bromodeoxyuridine

BSA: bovine serum albumin

cDNA: complementary deoxyribonucleic acid

CMV: cytomegalovirus

Da: Dalton

dATP: deoxyadenosine triphosphate

dCTP: deoxycytidine triphosphate

DEPC: diethylpyrocarbonate

dGTP: deoxyguanosine triphosphate

DMEM: Dulbeccos minimum essential medium

DMSO: dimethyl sulfoxide

DNA: deoxyribonucleic acid

DNase: deoxyribonuclease

dNTP: deoxynucleoside triphosphate

DTT: dithiothreitol

dTTP: deoxythymidine triphosphate

EDTA: ethylenediaminetetraacetic acid

ELISA: enzyme-linked immunosorbent assay

EtBr: ethidium bromide

Fab: antigen-binding fragment

FACS: fluorescence-activated cell sorting

Fc: region of IgMs

FCS: fetal calf serum

FITC: fluorescein isothiocyanate

FSC: forward scatter

G: guanine or guanosine; one-letter code for glycine

G-CSF: granulocyte colony-stimulating factor

GM-CSF: granulocyte/macrophage colony-stimulating factor

GTP: guanosine 5′-triphosphate

hr: hours

HRPO: horseradish peroxidase

IFN: interferon

Ig: immunoglobulin

IgA, IgG, IgM, IgD, IgE: five classes of immunoglobulins

IgMs: IgM subset

IL: interleukin

IMDM: Iscoves modified Dulbeccos medium

kb: kilobase

kDa: kilodalton

LPS: lipopolysaccharide

LT: lymphotoxin; TNF-β

MAb: monoclonal antibody

MHC: major histocompatibility complex

min: minutes

MOPS: morpholinepropanesulfonic acid

mp: melting point

***M*$_r$:** relative molecular weight

mRNA: messenger ribonucleic acid

MWCO: molecular weight cutoff

NBT: nitroblue tetrazolium

NK: natural killer (cells)

OD$_{260}$: optical density at 260 nm

OD$_{280}$: optical density at 280 nm

***ori*:** origin of replication

OVA: ovalbumin

PAGE: polyacrylamide gel electrophoresis

PBMC: peripheral blood mononuclear cell(s)

PBS: phosphate-buffered saline

PCR: polymerase chain reaction

PEG: polyethylene glycol

PIPES: piperazine-*N,N'*-bis(2-ethanesulfonic acid)

PMA: phorbol myristate acetate

PMSF: phenylmethylsulfonyl fluoride

Poly(A^+) RNA: polyadenylated ribonucleic acid

r: recombinant (e.g., rIL-2)

R: receptor (e.g., FcR)

RBC: red blood cell(s)

RNA: ribonucleic acid

RNase: ribonuclease

rRNA: ribosomal ribonucleic acid

SDS: sodium dodecyl sulfate

SDS-PAGE: sodium dodecyl sulfate polyacrylamide gel electrophoresis

sec: seconds

S-S: disulfide bonds

SSC: side scatter; sodium chloride/sodium citrate (buffer)

T: thymine or thymidine; one-letter code for threonine

***T_m*:** melting (or midpoint) temperature; thermal denaturation

***t* ½:** half life

TAE: Tris/acetate/EDTA (buffer)

TBE: Tris/borate/EDTA (buffer)

TBS: Tris-buffered saline

TBST: Tris-buffered saline containing Tween-20

TCA: trichloroacetic acid

TCR: T cell receptor

TE buffer: Tris-EDTA buffer

TEMED: *N,N,N′,N′*-tetramethyl-ethylenediamine

TFA: trifluoroacetic acid

Th cells: T helper cells T_H

TNF: tumor necrosis factor

Tris: tris(hydroxymethyl)aminomethane

Tris·Cl: Tris hydrochloride

tRNA: transfer ribonucleic acid

TTE: Triton X-100/Tris/EDTA (buffer)

TTP: thymidine 5'-triphosphate

U: unit (enzyme); uracil or uridine

UV: ultraviolet

Abbreviations

A_{260}: absorbance at 260 nm

A_{280}: absorbance at 280 nm

A: adenine or adenosine; one-letter code for alanine

Ab: antibody

Ag: antigen

anti-Ig: anti-immunoglobulin antibody

AP: alkaline phosphatase

APC: antigen-presenting cell(s)

ATP: adenosine 5′-triphosphate

BCIP: 5-bromo-4-chloro-3-indolyl phosphate

bis,bisacrylamide: *N,N′*-methylene-bisacrylamide

Bis-Tris: bix-(2-hydroxyethyl)imino-tris-(hydroxymethyl)methane

bp: base pair

BrdU: bromodeoxyuridine

BSA: bovine serum albumin

cDNA: complementary deoxyribonucleic acid

CMV: cytomegalovirus

Da: Dalton

dATP: deoxyadenosine triphosphate

dCTP: deoxycytidine triphosphate

DEPC: diethylpyrocarbonate

dGTP: deoxyguanosine triphosphate

DMEM: Dulbeccos minimum essential medium

DMSO: dimethyl sulfoxide

DNA: deoxyribonucleic acid

DNase: deoxyribonuclease

dNTP: deoxynucleoside triphosphate

DTT: dithiothreitol

dTTP: deoxythymidine triphosphate

EDTA: ethylenediaminetetraacetic acid

ELISA: enzyme-linked immunosorbent assay

EtBr: ethidium bromide

Fab: antigen-binding fragment

FACS: fluorescence-activated cell sorting

Fc: region of IgMs

FCS: fetal calf serum

FITC: fluorescein isothiocyanate

FSC: forward scatter

G: guanine or guanosine; one-letter code for glycine

G-CSF: granulocyte colony-stimulating factor

GM-CSF: granulocyte/macrophage colony-stimulating factor

GTP: guanosine 5′-triphosphate

hr: hours

HRPO: horseradish peroxidase

IFN: interferon

Ig: immunoglobulin

IgA, IgG, IgM, IgD, IgE: five classes of immunoglobulins

IgMs: IgM subset

IL: interleukin

IMDM: Iscoves modified Dulbeccos medium

kb: kilobase

kDa: kilodalton

LPS: lipopolysaccharide

LT: lymphotoxin; TNF-β

MAb: monoclonal antibody

MHC: major histocompatibility complex

min: minutes

MOPS: morpholinepropanesulfonic acid

mp: melting point

***M*$_r$:** relative molecular weight

mRNA: messenger ribonucleic acid

MWCO: molecular weight cutoff

NBT: nitroblue tetrazolium

NK: natural killer (cells)

OD$_{260}$: optical density at 260 nm

OD$_{280}$: optical density at 280 nm

***ori*:** origin of replication

OVA: ovalbumin

PAGE: polyacrylamide gel electrophoresis

PBMC: peripheral blood mononuclear cell(s)

PBS: phosphate-buffered saline

PCR: polymerase chain reaction

PEG: polyethylene glycol

PIPES: piperazine-*N,N'*-bis(2-ethanesulfonic acid)

PMA: phorbol myristate acetate

PMSF: phenylmethylsulfonyl fluoride

Poly(A^+) RNA: polyadenylated ribonucleic acid

r: recombinant (e.g., rIL-2)

R: receptor (e.g., FcR)

RBC: red blood cell(s)

RNA: ribonucleic acid

RNase: ribonuclease

rRNA: ribosomal ribonucleic acid

SDS: sodium dodecyl sulfate

SDS-PAGE: sodium dodecyl sulfate polyacrylamide gel electrophoresis

sec: seconds

S-S: disulfide bonds

SSC: side scatter; sodium chloride/sodium citrate (buffer)

T: thymine or thymidine; one-letter code for threonine

T_m: melting (or midpoint) temperature; thermal denaturation

t ½: half life

TAE: Tris/acetate/EDTA (buffer)

TBE: Tris/borate/EDTA (buffer)

TBS: Tris-buffered saline

TBST: Tris-buffered saline containing Tween-20

TCA: trichloroacetic acid

TCR: T cell receptor

TE buffer: Tris-EDTA buffer

TEMED: *N,N,N′,N′*-tetramethyl-ethylenediamine

TFA: trifluoroacetic acid

Th cells: T helper cells T_H

TNF: tumor necrosis factor

Tris: tris(hydroxymethyl)aminomethane

Tris·Cl: Tris hydrochloride

tRNA: transfer ribonucleic acid

TTE: Triton X-100/Tris/EDTA (buffer)

TTP: thymidine 5'-triphosphate

U: unit (enzyme); uracil or uridine

UV: ultraviolet

List of figures and tables.

Page

Chapter 1: General Introduction. 1

Figure 1.1 Immune system cell development. 3
Figure 1.2 B lymphocyte development. 7
Figure 1.3 Antigen presentation and T lymphocyte activation. 9
Figure 1.4 T cell differentiation. 11
Figure 1.5 Influence of cytokines on immune response. 13
Figure 1.6 IL-4, IL-2 and IL-13 receptor complexes. 18
Figure 1.7 IL-4 and IL-13 Jak/Stat signalling pathway. 21
Figure 1.8 Gene targeting via homologous recombination in ES cells. 25
Figure 1.9 The model of Cre and Flp site-specific recombinase inactivation. 27
Figure 1.10 Combining gene targeting and the Cre-*lox*P recombination system to inactivate a gene in a desired cell type. 30
Figure 1.11 Induced expression via the Tet-Off and Tet-On Systems. 32
Figure 1.12 Inducible transcription via the bi-directional pBI-L Tet vector. 34

Chapter 2: Inducible deletion of IL-4Rα expression. 38

Figure 2.1 Tet-Off inducible system. 41
Table 2.1 Sequences of oligonucleotides used for the amplification of IL-4Rα. 42
Table 2.2 Sequences of oligonucleotides used for the expression studies. 48
Table 2.3 Sequences of oligonucleotides used genotyping Tg mice. 52
Figure 2.2 Flow Diagram of pBi-IL-4Rα Cloning Strategy. 54
Figure 2.3 Amplification of transmembrane IL-4Rα cDNA fragment. 56
Figure 2.4 Restriction enzyme screening and sequence verification of the pBi-IL-4Rα transgenic construct. 56
Figure 2.5 Optimization and assessment of Hek 293T cells transfection efficiency. 57
Figure 2.6 Induced luciferase expression in Hek 293T cells containing both response and regulatory vectors. 59
Figure 2.7 Doxycycline induced suppression of luciferase expression. 61
Figure 2.8 Effect of regulatory and response plasmid ratios on transgene expression. 63

Figure 2.9 Transgene mRNA levels in stable pTet-Off-pBi-IL-4Rα Hek 293T cell line. 65
Figure 2.10 IL-4Rα transgene expression in Hek 293T cells. 67
Figure 2.11 Inducible IL-4Rα transgene expression in Hek 293T cells. 69
Figure 2.12 Flow diagram of generation of pBi-IL-4Rα chimeric mice. 71
Figure 2.13 Breeding scheme for the generation of the final inducible model. 73
Figure 2.15 IL-4Rα transgene leakiness via the CMV promoter. 75
Figure 2.14 Genotyping of generated transgenic lines. 77
Figure 2.14 Genotyping of generated transgenic lines. 78
Figure 2.16 Transgene mRNA levels in pBi-IL-4RαTg / IL-4Rα $^{-/-}$ BALB/c / pVav-tTaTg/ IL-4Rα $^{-/-}$ BALB/c line. 80
Figure 2.16 Transgene mRNA levels in pBi-IL-4RαTg / IL-4Rα $^{-/-}$ BALB/c / pVav-tTaTg/ IL-4Rα $^{-/-}$ BALB/c line. 81
Figure 2.17 pBi-IL-4Rα Tg /pVav-tTa Tg translational analysis. 84

Chapter 3: Dendritic Cell Specific Expression of Cre Recombinase. 87

Figure 3.1. The generation of the CD11c-IL-4Rα$^{-/-}$ model. 90
Table 3.1 Sequences of oligonucleotides used for the amplification of Cre. 91
Figure 3.2 Flow Diagram of pCD11c-GFP and pCD11c-Cre Cloning Strategy. 102
Figure 3.3 Amplification of Cre cDNA fragment. 104
Figure 3.4 Vector construction scheme for pCD11c-GFP. 105
Figure 3.5 Partial *Pst I* Restriction Enzyme Digestion of pBS-CD11c. 106
Figure 3.6. Cloning of CD11c driven expression vectors. 108
Figure 3.7 Sequence Verification of pCD11c-Cre. 110
Figure 3.8 Effect of CMV promoter presence on GFP expression in CD11c vectors. 112
Figure 3.9. D25/sc Cell Phenotype Characterisation. 114
Figure 3.10. Transfection efficiency of D25/sc cells. 116
Figure 3.11. Dendritic cell specific transcription of Cre Recombinase. 118
Figure 3.12. Dendritic cell specific CD11c driven transgene expression. 120
Figure 3.13. Dendritic cell specific CD11c driven Cre expression. 121

Chapter 4: Generation of molecular tools for the neutralization of signalling via IL-4Rα and IL-13Rα$_2$. 123

Figure 4.1. IL-13 and IL-4 receptor combinations and binding. 124
Table 4.1 Sequences of oligonucleotides used for the amplification of the extracellular domains of IL-4Rα , IL-13 Rα$_2$ and IL-2Rγ. 127
Figure 4.2.A Flow Diagram of pSecTag-F$_c^{Mut}$-sIL-4Rα Cloning Strategy. 142
Figure 4.2.B Flow Diagram of pSecTag-F$_c^{Mut}$-sIL-13Rα$_2$ Cloning Strategy. 143
Figure 4.2.C Flow Diagram of pSecTag-F$_c^{Mut}$-sIL-2Rγ–sIL-4Rα Cloning Strategy. 144
Figure 4.3 Amplification of extracellular IL-4Rα cDNA fragment. 144
Figure 4.4 Restriction enzyme screening and sequence verification of the sIL-4RαF$_c$ expression vector. 146
Figure 4.4 Restriction enzyme screening and sequence verification of the sIL-4RαF$_c$ expression vector. 147
Figure 4.5 Amplification of the IL-13Rα$_2$ extracellular cDNA fragment. 147
Figure 4.6 Restriction enzyme screening and sequence verification of the sIL-13Rα$_2$F$_c$ expression vector. 149
Figure 4.7 Insert orientation and sequence verification of the sIL-13Rα$_2$F$_c$ expression vector. 150
Figure 4.8 Amplification of the IL-2Rγ extracellular cDNA fragment.
Figure 4.9 Restriction enzyme screening of sIL-2γ-sIL-4RαF$_c$ clones. 152
Figure 4.10 Insert orientation of sIL-2Rγ-sIL-4RαF$_c$ expression vector. 153
Figure 4.11 SDS-PAGE analyses of IL-4 and IL-13 soluble receptor blockers. 155
Figure 4.12 SDS-PAGE analysis of sIL-2Rγ-sIL-4RαF$_c$ cytokine trap. 156
Figure 4.13 Western Blot detection of secreted proteins. 156
Figure 4.14 Diagram of F$_c$-tagged Soluble Receptor Elisa ProtocoL. 157
Figure 4.15 Cytokine Binding analyses of sIL-4RαF$_c$ and sIL-13Rα$_2$F$_c$. 158
Figure 4.15 Cytokine Binding analyses of sIL-4RαF$_c$ and sIL-13Rα$_2$F$_c$ blockers. 159
Figure 4.16 Cytokine Binding analysis of sIL-2Rγ-sIL-4RαF$_c$ cytokine trap. 160
Figure 4.17 CD4$^+$T Cell proliferation after stimulation with mIL-4, mIL-2, or mIL-4 with sIL-4RαF$_c$. 162
Figure 4.18 Effect by sIL-4RαF$_c$ and sIL-13Rα$_2$F$_c$ on *in vitro* Th1/Th2 differentiation of CD4$^+$ T cells from BALB/c mice. 164
Figure 4.19 Suppression of IL-4 and IL-13 function in BMDM cultures. 166
Figure 4.20 sIL-4RαF$_c$ and sIL-13Rα$_2$F$_c$ dependant suppression of MMR expression. 168

Contents

	Page
Abstract.	*viii*
List of figures and tables.	*x*
Abbreviations.	*xiii*
Chapter 1: General Introduction.	**2**
1.1 The immune system.	2
1.1.1 Innate Immunity.	4
1.1.2 Adaptive Immunity.	6
1.1.2.1 B lymphocytes.	6
1.1.2.2 T lymphocytes.	8
1.1.2.3 T lymphocytes and Th1/Th2 differentiation.	10
1.2 Cytokines and immune system communication.	13
1.3 Interleukin-4 and Interleukin-13.	14
1.3.1 Interleukin-4.	15
1.3.2 Interleukin-13.	15
1.4 IL-4Rα.	17
1.4.1 Soluble receptors.	19
1.4.2 IL-4Rα and cytokine signalling pathways.	20
1.5 Molecular manipulation of gene function.	22
1.5.1 Conventional transgenics.	23
1.5.2 Gene targeting using embryonic stem cells.	24
1.5.3 Conditional transgenics.	26
1.5.3.1 Site-specific recombinase systems.	27
1.5.3.2 Tissue specific knockouts.	28
1.5.4 Conditional control of transcription.	31
1.6 Molecular manipulation of IL-4Rα.	35
1.6.1 *Leishmania donovani*.	35
1.6.2 *Nippostrongylus Brasiliensis*.	36
1.6.3 *Schistosoma mansoni*.	37

Chapter 2: Inducible deletion of IL-4Rα expression. **38**

2.1 Introduction. 39

2.2. Methods and Materials. 42

2.2.1 Cloning of the construct.

2.2.1.2 Primer design. 42

2.2.1.2.1 The transmembrane isoform of murine IL-4Rα. 42

2.2.1.3 Vector Description. 43

2.2.1.4 Polymerase Chain Reaction (PCR). 43

2.2.1.4.1 Amplification of coding region for the transmembrane isoform of murine IL-4Rα. 43

2.2.1.5 Restriction and ligation of the coding sequence into the pBi-Luc eukaryotic expression vector. 44

2.2.1.6 Agarose gel electrophoresis. 45

2.2.1.7 Gel isolation and purification of DNA. 45

2.2.2 Cell culture. 45

2.2.2.2.1 Hek 293T cells. 45

2.2.2.2.2 Transfection of Hek 293T cells. 46

2.2.3 *In vitro* and *in vivo* determination of transgene functionality**.** 46

2.2.3.1 Template preparation for qRT-PCR assays. 46

2.2.3.1.1 RNA Isolation. 46

2.2.3.1.2 DNAseI treatment of isolated RNA. 47

2.2.3.1.3 cDNA Synthesis. 48

2.2.3.2 Transcription assays. 48

2.2.3.2.1 Primers designed for expression assays. 48

2.2.3.2.2 qRT-PCR. 49

2.2.3.3 Translation assays. 49

2.2.3.3.1 Luciferase assay. 49

2.2.3.3.2 FACS analysis. 50

2.2.4 Generation of chimeras. 51

2.2.4.1 Generation of pBi-IL-4Rα Tg chimeras. 51

2.2.4.2 Genotyping of pBi- IL-4Rα Tg and pVav-tTa Tg. 51

2.2.4.2.1 Genomic DNA extraction. 51

2.2.4.2.2 Genotyping PCR. 51

2.3 Results. 53
2.3.2.1 Transgenic Construct design and cloning. 53
2.3.2.2 *In vitro* expression studies. 57
2.3.2.2.1 Establishment of bi-directional promoter activity. 58
2.3.2.2.2 Establishment of effective doxycycline concentration and repression over time. 60
2.3.2.2.3 Establishment of efficient pTet-Off: pBi-IL-4Rα plasmid ratio. 62
2.3.2.3 *In vitro* inducible repression of IL-4Rα expression. 62
2.3.2.3.1 Transcription efficiency of mIL-4Rα transgene. 64
2.3.2.3.2 Translation efficiency of mIL-4Rα transgene 66
2.3.2.3.3 *In vitro* inducible repression of mIL-4Rα expression. 68
2.3.2.4 Generation and analysis of single transgenic chimeras. 70
2.3.2.4.1 Generation of pBi-IL-4Rα Tg chimeras. 70
2.3.2.4.2 Breeding program. 72
2.3.2.4.4 Stringent control of IL-4Rα expression in pBi-IL-4RαTg / IL-4Rα $^{-/-}$ BALB/c mice. 74
2.3.2.4.3 Genotyping of pBi-IL-4RαTg / IL-4Rα $^{-/-}$ BALB/c and pVav-tTaTg / IL-4Rα $^{-/-}$ BALB/c. 76
2.3.2.5 Analysis of pBi-IL-4RαTg / IL-4Rα $^{-/-}$ BALB/c / pVav-tTaTg/ IL-4Rα $^{-/-}$ BALB/c. 79
2.3.2.5.1 Transcriptional analysis 79
2.3.2.5.2 Translational analysis 82
2.4 Chapter Conclusions. 85

Chapter 3: Dendritic Cell Specific Expression of Cre Recombinase **87**

3.1 Introduction. 88
3.2 Methods and Materials. 88
3.2.1 Cloning of the constructs. 88
3.2.1.1 Plasmid purification. 91
3.2.1.2 Primer design. 91
3.2.1.3 Modified Cre recombinase primers. 91
3.2.1.4 Polymerase Chain Reaction (PCR). 91
3.2.1.4.1 Amplification of Cre cDNA. 91
3.2.1.5 Restriction and ligation of Cre, GFP and CD11c into a eukaryotic expression vector. 91

3.2.1.5.1 Sub-cloning of Cre into the pDrive PCR cloning vector. 92
3.2.1.5.2 Sub-cloning of CD11c into the pGFP-N1 expression vector. 92
3.2.1.5.3 Cloning of the CD11c driven Cre expression vector. 93
3.2.1.6 Agarose gel electrophoresis. 94
3.2.1.7 Gel isolation and purification of DNA. 94
3.2.2 Cell culture**.** 94
3.2.2.1 Hek 293T cells. 95
3.2.2.2 Transfection of Hek 293T cells. 95
3.2.2.3 D25/sc dendritic cell line. 95
3.2.2.4 Transfection of D25/sc cells. 96
3.2.3 *In vitro* studies. 96
3.2.3.1 D25/sc Cell line characterisation. 96
3.2.3.2 CMV promoter activity. 97
3.2.3.3 Cell specific transcription. 97
3.2.3.3.1 Template preparation - RNA isolation. 97
3.2.3.3.2 DNAseI treatment. 98
3.2.3.3.3 cDNA synthesis. 98
3.2.3.3.4 cDNA amplification. 98
3.2.3.4 Cell specific translation. 98
3.2.3.4.1 CD11c driven GFP expression. 99
3.2.3.4.2 Immunofluorescence. 100

3.3 Results.

3.3.1 Vector design and construction. 101
3.3.1.1 Generation of the Cre cDNA fragment. 103
3.3.1.2 Cloning of the CD11c fragment. 104
3.3.1.3 Generation of the CD11c driven Cre vector. 107
3.3.1.4 pCD11c-Cre vector sequence analysis. 109
3.3.2. Preliminary in vitro expression studies. 109
3.2.2.1 Influence of CMV promoter. 111
3.3.3 Characterisation and Transfection of the D25/sc Cell Line. 111
3.3.3.1 Cell line characterisation. 113
3.3.3.2 D25/sc Transfection. 115
3.3.4 In vitro expression studies. 115
3.3.4.1 Cell specific transcription. 117
3.3.4.2 Cell specific translation 119

3.4 Chapter Conclusions. 122

Chapter 4: Generation of molecular tools for the neutralization of signalling via IL-4Rα and IL-13Rα$_2$. 123

4.1 Introduction. 124

4.2 Methods and Materials. 127

4.2.1 Cloning of the constructs. 127

4.2.1.1 Plasmid purification. 127

4.2.1.2 Primer design. 127

4.2.1.2.1 The extracellular domains of IL-4Rα , IL-13Rα$_2$ and IL-2Rγ. 127

4.2.1.3 Template preparation for PCR of IL-13Rα$_2$ and IL-2Rγ extracellular domains. 127

4.2.1.3.1 RNA Isolation. 127

4.2.1.3.2 DNAseI treatment and removal of digested DNA fragments. 128

4.2.1.3.3 cDNA Synthesis. 128

4.2.1.4 Polymerase Chain Reaction (PCR). 129

4.2.1.4.1 Amplification of extracellular domains of IL-4Rα, IL-13Rα and IL-2Rγ. 129

4.2.1.5 Cloning of the coding sequences into eukaryotic expression vectors. 129

4.2.1.5.1 Extracellular domains of IL-4Rα and IL-13Rα$_2$. 129

4.2.1.5.2 Extracellular domain of IL-2Rγ. 130

4.2.1.6 Agarose gel electrophoresis. 131

4.2.1.7 Gel isolation and purification of DNA. 131

4.2.2 Cell culture. 131

4.2.2.1 Hek 293T cells. 131

4.2.2.2 Transfection of Hek 293T cells. 132

4.2.3 Purification and detection of recombinant proteins. 132

4.2.3.1 Large scale protein expression. 132

4.2.3.2 Cell lysate preparation for Hek 293T / pSecTag-sIL13Rα$_2$F$_c$ cultures. 133

4.2.3.3 IgG Protein purification. 133

4.2.3.4 Protein quantification. 133

4.2.3.5 SDS-PAGE. 134

4.2.3.6 Western blot analysis. 134

4.2.4 *In vitro* assays. 135

. 4.2.4.1 Cytokine binding assay. 135

4.2.4.2 Cell proliferation assay. 135

4.2.4.3 T cell differentiation assay. 136

4.2.4.4 Cytokine ELISA. 137
4.2.4.5 Generation of bone marrow derived macrophages (BMDMs). 138
4.2.4.5.1 L929 conditioned medium. 139
4.2.4.6 Measurement of nitric oxide. 139
4.2.4.7 Measurement of arginase activity. 139
4.2.4.8 FACS analysis of BMDMs. 140
4.3 Results. 141
4.3.1 Vector design and construction. 141
4.3.1.2.Molecular cloning and characterisation of F_c-tagged soluble. 141
4.3.1.2.1 The F_c-tagged soluble IL-4Rα eukaryotic expression vector. 145
4.3.1.2.2 The F_c-tagged soluble IL-13Rα_2 eukaryotic expression vector. 148
4.3.1.2.3 The inline F_c-tagged soluble IL-4Rα / soluble IL-2Rγ cytokine trap eukaryotic expression vector. 151
4.3.3 Recombinant fusion protein expression and purification 154
4.3.4 Biochemical protein characterisation. 154
4.3.4.1 Cytokine Binding assays. 157
4.3.4.1.1 sIL-4Rα and sIL-13Rα_2. 158
4.3.4.1.2 sIL-2Rγ– sIL-4Rα cytokine trap. 160
4.3.5 *In vitro* functional assays. 161
4.3.5.1 T cell Proliferation. 161
4.3.5.2 T cell Differentiation. 163
4.3.5.3 Influence of sIL-4RαF_c and sIL-13R$\alpha_2 F_c$ on macrophage responsiveness to mIL-4 and mIL-13. 165
4.3.5.3.1 Bone marrow derived macrophage differentiation. 165
4.3.5.3.2 Macrophage mannose receptor expression. 167
4.4 Chapter Conclusions. 169

Chapter 5: Discussion. **171**

5.1 Conclusions drawn from this study. 171
5.1.1 Chapter 2: Inducible deletion of IL-4Rα expression. 171
5.1.2 Chapter 3: Dendritic Cell Specific Expression of Cre Recombinase. 174
5.1.3 Chapter 4: Generation of molecular tools for the neutralization of signalling via IL-4Rα and IL-13Rα_2. 175
5.2 Conclusion. 178

References. **180**

Appendix A. **211**

A.1 Plasmid Maps. 212
A.2 Reagents and Suppliers. 215
A.3 Software Resources 217
A.4 Specialized Equipment. 217
A.5 Recipes. 218
A.5.1 General Lab Solutions. 218
A.5.2 Bacterial Solutions. 220
A.5.3 Cell Culture Solutions. 221
A.5.4 Immunology Solutions. 223
A.5.5 RNA Solutions. 225
A.6 Generation of pBi-IL-4Rα chimeras. 227
(Find PDF file attached.)

Chapter 1: General Introduction.

1.1 The immune system.

Immunology is the study of the systems involved in host protection from foreign macromolecules or invading organisms and the ensuing host defense responses. The immune system can be divided into the innate and adaptive responses. The host immune response, being either innate or adaptive, depends on the ability to distinguish between *self* and *non-self* molecules (summarized in Janeway *et al.,* 2002). *Self* molecules are those components of the host body that can be distinguished from foreign substances by the immune system (Smith, 1997). In contrast, *non-self* molecules are those recognized as foreign molecules.

All cells in the immune system have a common origin in the bone marrow. These include the myeloid (neutrophils, basophils, eosinpophils, macrophages and dendritic cells) and lymphoid (B lymphocyte, T lymphocyte and Natural Killer) cells (Kondo *et al.,* 2003). Both groups differentiate along distinct pathways (Figure 1.1). The myeloid stem cell gives rise to erythrocytes, platelets, neutrophils, monocytes/macrophages and dendritic cells (Akashi *et al.,* 2000), in contrast the lymphoid stem cell gives rise to the Natural Killer, T cells and B cells (Igarashi *et al.,* 2002; Kondo *et al.,* 1997; Kouro *et al.,* 2002). T cell development initiates with the precursor T cells migrating to the thymus. In the thymus these cells differentiate into two distinct types of T cells, the $CD4^+$ T helper (Th) cell and the $CD8^+$ pre-cytotoxic T cell. Furthermore, two types of Th cells are produced in the thymus the Th1 cells, which assist the $CD8^+$ pre-cytotoxic cells to differentiate into cytotoxic T cells, and Th2 cells, which facilitate in B cell differentiation into plasma cells, which subsequently secrete antibodies.

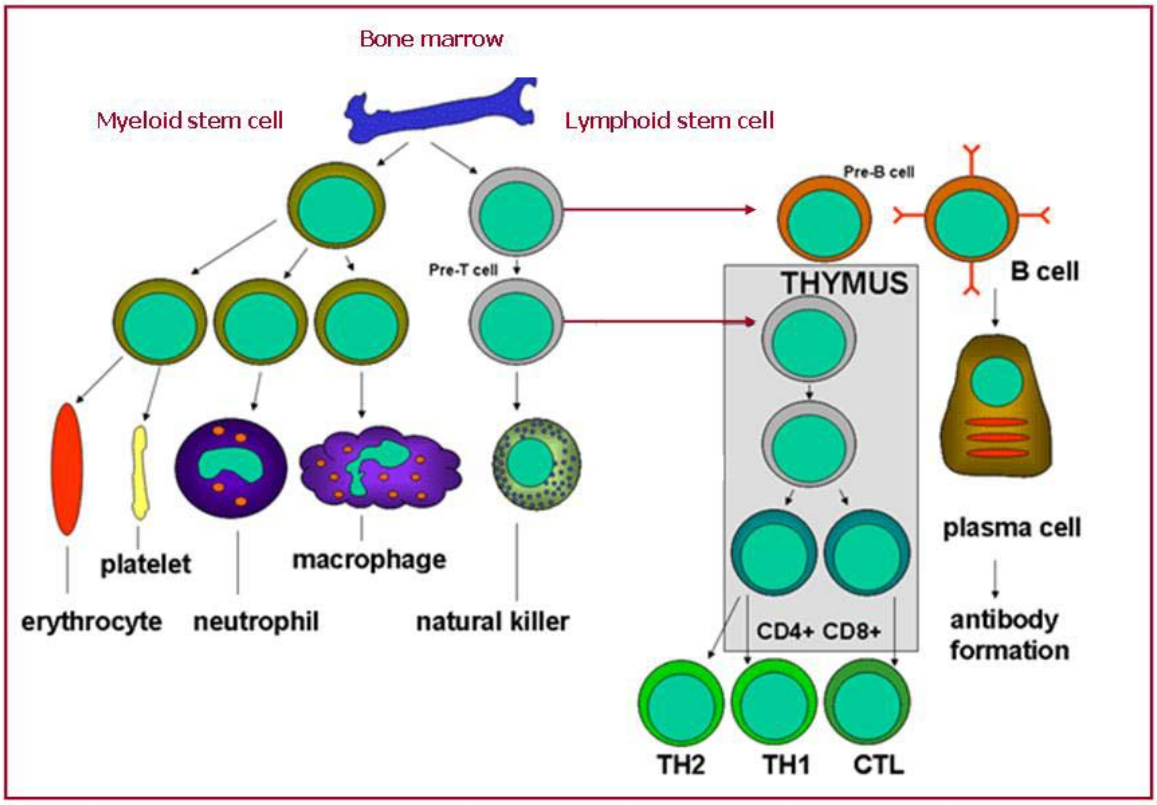

Figure 1.1 Immune system cell development.

All hematopoietic cells are derived from pluripotent stem cells. These cells branch into two main lineages, one specific for lymphoid cell development and the other specific for the myeloid cells. The lymphoid stem cell differentiates into either T cells or B cells depending on the immediate microenvironment. T cell development takes place in the thymus and B cells develop in the foetal liver and bone marrow. The plasma cells which develop from the precursor B cells are characterised as the most differentiated antibody-forming cell. The natural killer (NK) cells are also derived from the common lymphoid stem cell. The myeloid cells differentiate into the committed cells shown on the left. Figure adapted from Microbiology & Immunology On-Line, http://pathmicro.med.sc.edu/ghaffar/innate.htm.

1.1.1 Innate Immunity.

The innate immune system consists of the cells and mechanisms that provide the host immediate, non-specific defence against infection by other organisms. The innate system therefore recognizes, and reacts to pathogen or antigen presence in a generic way (Kapetanovic and Cavaillon, 2007). The key elements of innate immunity include anatomical barriers, secretory molecules and cellular components. The physical anatomical barriers include the skin and internal epithelial layers, movement associated with the gastro-intestinal tracts and the oscillation of broncho-pulmonary cilia. Additionally, these protective surfaces are associated with chemical agents. Consequently, the first lines of defence against foreign organisms are the physical and chemical barriers being the skin and molecules such as the low molecular weight proteins the defensins (Yang *et al.,* 2007), found in the lung and gastrointestinal tract displaying antimicrobial activity and the surfactants in the lung which act as opsonins (Peng *et al.,* 2007).

Upon penetration of these barrier layers the main effector immune cells involved in the subsequent response are phagocytic cells that respond rapidly by engulfing microbial pathogens and killing them independently from antibodies (Alberts *et al.,* 2002; Janeway *et al.,* 2002). Amongst the phagocytic cells are:

- Neutrophils: Characteristically neutrophils are the first cells recruited to acute inflammatory sites and are the most highly adherent, motile, phagocytic leukocytes (Kansas, 1996).
- Antigen presenting cells characteristically lack antigen-specific receptors. Instead, they capture, process and present antigens to T cell receptors. APCs include macrophages, dendritic cells and B cells.
- Monocytes/Macrophages: Macrophages process protein antigens and present antigen peptides to T cells. Monocytes/macrophages are highly adherent, motile and phagocytic; involved in assembly and regulation of other cells of the immune system, such as T lymphocytes. They serve as antigen processing-presenting cells; and act as cytotoxic cells when armed with specific IgG antibodies. Macrophages, differentiated monocytes, are recruited to sites of inflammation and are capable of becoming further specialized through cytokine stimulation (Gordon, 1986; Savill *et al.,* 2002; Ziegler-Heitbrock, 1989).

- Dendritic cells: Amongst the most important antigen-presenting cells are the highly specialized dendritic cells. Tissue dendritic cells consume antigen at infection sites and are activated by the innate immune response. Subsequently, these cells migrate to local lymphoid tissue and mature into cells that are highly effective at presenting antigen to re-circulating T cells. These mature dendritic cells are distinguished by surface molecules, known as co-stimulatory molecules that synergize with antigen in the activation of naive T cells (Janeway *et al.,* 2001; Savina and Amigorena, 2007). Dendritic cells are in constant communication with other components of the host immune system. This interaction can be at a distance via cytokines, for example, the stimulation of dendritic cells *in vivo* with microbial extracts stimulates the dendritic cells to rapidly produce IL-12 (Reis e Sousa *et al.,* 1997). Subsequent signaling via the secreted IL-12 directs the naive CD4 T cells towards a Th1 phenotype. The ultimate consequence is priming and activation of the immune system for attack against the antigens presented on the dendritic cell surface. The type of dendritic cell also dictates the profile of the cytokines produced. The lymphoid dendritic cell has the ability to produce huge amounts of IFNα, in quantities exceeding production by any of the other blood cells (Siegel *et al.,* 1999). Dendritic cell communication can also be via direct cell-to-cell contact based on the interaction of cell-surface proteins, illustrated in the interaction of the DC receptor CD40 with CD40L present on the lymphocyte (Lefrançois *et al.,* 1999). Dendritic cells thus serve as an important link between the innate and adaptive immune systems, by their antigen presentation to one of the key effector cell types of the adaptive immune system; the T cells (Guermonprez *et al.,* 2002).

In addition to the phagocytic cells, mast cells, basophils and eosinophils, natural killer cells and γδ T cells also play important roles in the innate response (Beutler, 2004). For example:

- Eosinophils: The eosinophils participate in hypersensitivity reactions via cytotoxicity, which is mediated by large cytoplasmic granules. These granules contain the eosinophilic basic and cationic proteins (Gleich *et al.,* 1995).
- Basophils and mast cells are involved in the production of cytokines that have roles in host defense against antigens and stimulation of allergic inflammation. These cells present surface membrane receptors for IgE antibodies and contain numerous large cytoplasmic granules, containing heparin and histamine. When cell-bound IgE antibodies cross-link to antigens, the cells degranulate and

produce low-molecular weight vasoactive mediators, like histamine through which they exercise immune effector functions (Galli *et al.,* 1999; Metcalfe *et al.,* 1997).

- Natural Killer Cells: NK cells are large circulating granular lymphocytes that nonspecifically kill certain types of tumor cells and pathogen or virus-infected cells. This killing function is enhanced by cytokines such as IL-2 and IFN-γ. Additionally microorganisms stimulate NK cells to produce a number of cytokines such as, IL-2, IFN-γ, IFN-α, and TNF-α. (Alberts *et al.,* 2002; Baron *et al.,* 1996; Janeway *et al.,* 2002).

Although both innate and adaptive immune systems function to protect against antigens the response elicited by the two systems differ and one of the most distinguishing factors between the adaptive and innate systems is the immunological memory demonstrated by the adaptive system (Mayer, 2006). This enables a swift response upon subsequent exposure to the same antigen. Yet it is important to recognize that most immune responses rely on the combined interplay between the various components of both the innate and adaptive immune systems.

1.1.2 Adaptive Immunity.

Adaptive immunity can be described as antigen or pathogen specific. This specificity is conferred on the system by pre exposure to the pathogenic target. These specific responses are typically rapid and effective. A range of cells that include the B lymphocytes, T cells and dendritic cells orchestrates the response.

1.1.2.1 B lymphocytes.

The antibody producing B cells confer the humoral immunity; these cells differentiate into plasma cells to secrete antibodies (figure 1.2). Antibodies circulate the host blood and tissue fluids binding specifically to their antigen and are involved in processing antigenic proteins and presenting the peptide antigen fragments, some of which are complexed with MHC class II molecules and then presented on the cell surface to $CD4^+$ T cells.

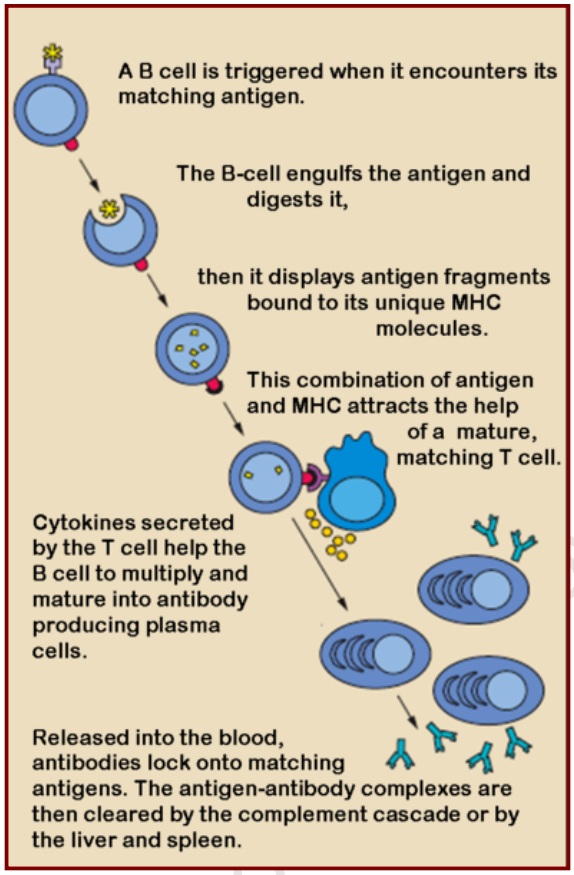

Figure 1.2 B lymphocyte development.
The figure illustrates the development of the B cell subsequent to antigen presentation. Figure obtained from The Immune System. NIH Publication No. 03–5423.

B cell development is characterized by recombination of immunoglobulin H and L chain genes and expression of specific surface monomeric IgM molecules. At this stage of development, B cells are highly susceptible to the induction of tolerance. This specific tolerance being the process whereby B lymphocytes recognizing self antigens are deleted before they develop into fully immunocompetent cells. Mature B cells are characterized by surface IgD molecules; these mature cells are capable of differentiation into antibody-producing plasma cells subsequent to antigen exposure (Dal Porto *et al.,* 2004; Raghaven and Bjorkman, 1996).

B cell activation into antibodies capable of producing and secreting cells is antigen-dependent. Specific antigens bind to surface Ig molecule, this leads to the B cell differentiating into plasma cells that produce and secrete antibodies of the same antigen-binding specificity. B cell interaction with T helper cells leads to their proliferation and

isotype class switching of the immunoglobulin that is produced, yet retaining the same antigen-binding specificity.

Following binding to the antigen the antibody can function in one of the following ways; 1) neutralization of the pathogenic features of the antigen (e.g. toxins), 2) facilitation of the ingestion by the phagocytic cells, 3) adherence to and stimulation of complement molecules to produce opsonins or 4) contributing to antibody-dependent cellular cytotoxicity. Hence, antibody interaction with other parts of the immune system, allows the recognition and elimination of antibody-antigen complex (Hofer *et al.,* 2006). The receptor to which antigen epitopes bind on T-lymphocytes is the T-cell receptor (TCR) (Rudolph *et al.,* 2006). TCR only recognizes the antigen when it is presented by host cells in combination with major histocompatibility complex (MHC) molecules (Cresswell *et al.,* 2005). This recognition leads to the release of cytokines or the elimination of the presenting cell-antigen complex (Janeway *et al.,* 2001).

1.1.2.2 T lymphocytes.

T cells that have not encountered antigens are described as naïve T cells, these are activated to produce armed effector T cells when they encounter their specific antigen which presents in the form of a peptide:MHC complex on the surface of an activated antigen-presenting cell (Hughes *et al.,* 2006).

T lymphocytes fall into three functional classes that detect antigens derived from different types of pathogen (Figure 1.3). Antigens from intracellular pathogens that multiply in the cytoplasm are passed to the cell surface by MHC class I molecules and presented to CD8 T cells. These differentiate into cytotoxic T cells that eliminate the infected target cells (Luther and Cyster, 2001). This process is mediated by the release of cytotoxic proteins such as perforin and granzyme, or the induction of apoptosis due to Fas ligand binding (Wong and Pamer, 2003).

Antigen peptides from pathogens multiplying in intracellular vesicles, and those derived from ingested extracellular bacteria and toxins, are carried to the cell surface by MHC class II molecules and presented to CD4 T cells. Following this activation, characteristic cytokine and chemokine secretion profiles permit the classification of $CD4^+$ T helper (Th) cells into two major subpopulations (Paul and Seder, 1994). These two types of effector T cell are the Th1 and Th2 cells. Typically antigens presented via macrophages and dendritic cells to T cells are inclined to stimulate the differentiation of Th1 cells which are associated with intracellular pathogens.

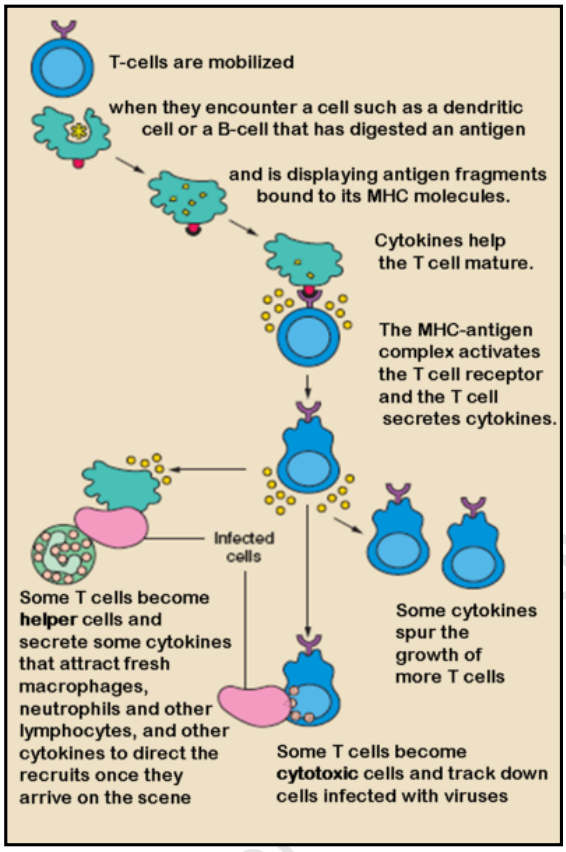

Figure 1.3 Antigen presentation and T lymphocyte activation.

Subsequent to antigen presentation naïve T cells differentiate into helper T cells or cytotoxic T cells. Each group has distinct cytokine profiles and functions in either humoral or cellular immunity. Figure adapted from The Immune System. NIH Pub No. 03–5423.

Conversely, extracellular soluble antigens, associated with nematode infections, tend to stimulate the production of Th2 cells (Figure 1.4) (Mosmann *et al.,* 1986; Swain *et al.,* 1988). Both Th1 and Th2 cells originate from the same naïve IL-2 producing $CD4^+$ T cell precursors. (Kondo *et al.,* 1997; Kondo *et al.,* 2003)

1.1.2.3 T lymphocytes and Th1/Th2 differentiation.

Th1 cells are involved in cell-mediated immunity; these cells are characterized by the production of pro-inflammatory cytokines like IFN-γ, IL-2, and TNF-β. Pro-inflammatory cytokines stimulate the microbial properties of macrophages, and leads to increased B cell production of IgG antibodies effective at opsonising extracellular pathogens for uptake by phagocytic cells. Thus cytokines secreted by Th1 cells activate cytotoxic T cells and macrophages to stimulate cellular immunity and inflammation (Stevens *et al.,* 1988). Additionally Th1 cells also secrete IL-3 and GM-CSF, which leads to increased leukocyte production by the bone marrow. Th2 cells initiate the humoral immune response by activating naïve antigen-specific B cells to produce IgM antibodies. Th2 cells secrete IL-4, IL-5, IL-6, and IL-10, cytokines that are involved in the induction of antibody production by B cells (Katona *et al*., 1988).

The transcription factors, T-bet and GATA-3, play a critical role in the differentiation to either a Th1 or a Th2 cell. T-bet transcriptional activity has been shown to be beneficial for the development of Th1 cells (Szabo *et al.,* 2000). In contrast, GATA-3 activity promotes the differentiation to Th2 cells (Zheng and Flavell, 1997). T-bet increases the production of Th1 cells by activation of cytokine gene transcription, like *IFN-γ* which is required for Th1 function (Szabo *et al.,* 2002). In parallel, it blocks the activity of GATA-3 (Usui *et al.,* 2006).

Th1 and Th2 cytokines are antagonistic in activity; the secretion of IL-4 stimulates Th2 activity and suppresses Th1 activity, while IL-12 promotes Th1 activities. The Th1 cytokines IL-12 and IFN-γ inhibits proliferation of Th2 cells. IFN-γ and IL-2 stimulate B cells to secrete IgG_{2a} and inhibit secretion of IgG_1 and IgE whereas IL-4 stimulates B cells to secrete IgE and IgG_1 (Hsieh *et al*., 1993). In contrast, the Th2 cytokine IL-10 inhibits Th1 secretion of IFN-γ and IL-2; additionally it suppresses MHC II expression (Alberts *et al.,* 2002). The balance between Th1 and Th2 activity may manoeuvre the immune response on the path of cell-mediated or humoral immunity.

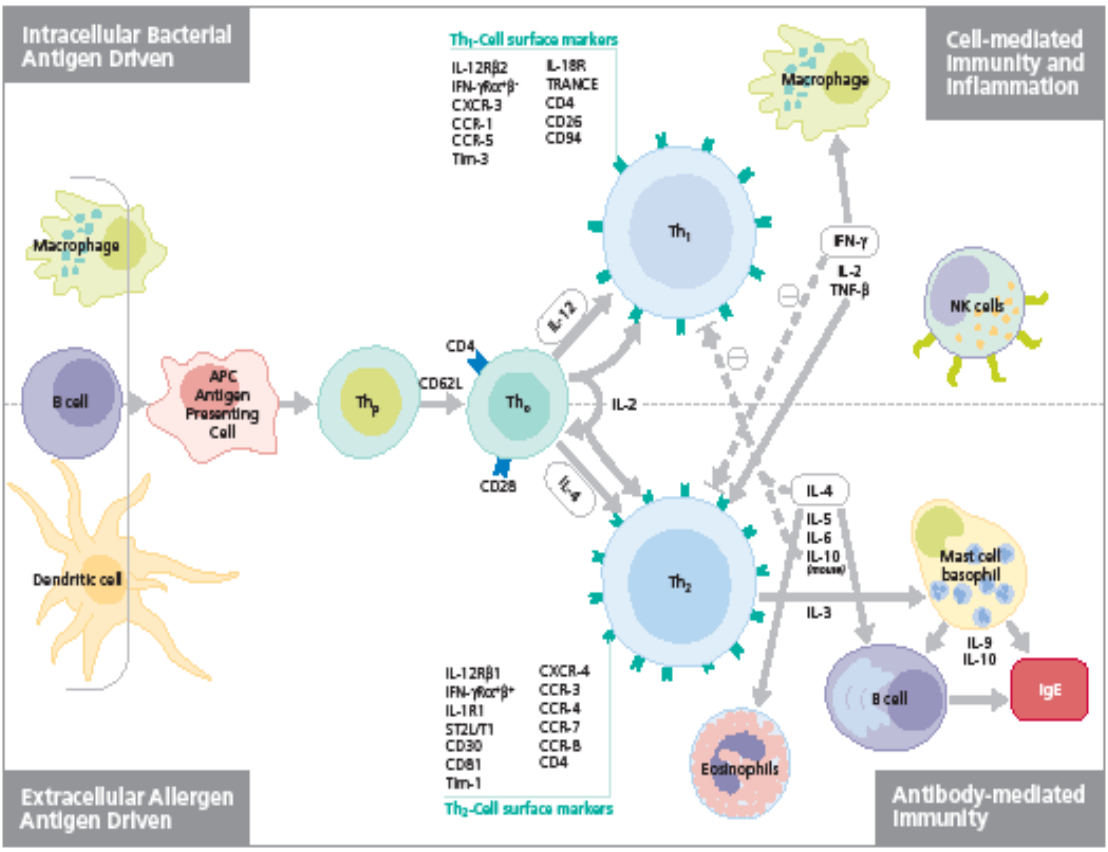

Figure 1.4 T cell differentiation.

Antigen presenting cells initiates the process of naïve $CD4^+$ T helper cell differentiation along the Th1 or Th2 pathway. The cytokines IL-12 and IFN-γ promote Th1 cell development and IL-4 promotes the differentiation to Th2. Upon differentiation, the Th1 and Th2 cells produce cytokines leading to different and often opposing responses ranging from stimulation of B cells and antibody production to phagocytosis.

Other T cell subsets include Tr1, Th3 and natural $CD4^+CD25^+$ regulatory T cells (Tregs), these cells are involved in the regulation of immune responses and have important functions in prevention of autoimmunity and excessive effector responses to pathogens. Tr1 and Th3 cells produce and secrete immunosuppressive cytokines including IL-10 and TGF-β (McGruirk and Mills, 2002; O'Garra *et al.,* 2004; Sakaguchi *et al.,* 1995).

Regulatory T cells (TRegs) are a key subset of $CD4^+$ T cells. TRegs are characterized by the expression of the transcription factor FOXP3 (Forkhead box P3) and the IL-2 receptor and unlike activated effector T cells low levels of CD127 (Seddiki *et al.,* 2006; Wing *et al.,* 2006). Studies in mouse models have implicated TRegs in the inhibition of allergic responses and it has been suggested that they control Th2-cell responses in humans. This inhibition is achieved through the inhibitory cytokines IL-10 and TGFβ leading to atopy that is a result of an imbalance between Th2 cells and TRegs (Bacchetta *et al.,* 2007; Larche *et al.,* 2007).

Th17 cells are another newly identified type of $CD4^+$ T cell. These cells secrete IL-17A and IL-17F, which are associated with neutrophilic inflammation(Stockinger *et al.,* 2007) It has been shown that IL-17A is over expressed in asthmatic airways in association with neutrophil influx (Bullens *et al.,* 2006), additionally it stimulates the production of the IL-8, a neutrophil chemo attractant, by airway smooth muscle cells (Dragon *et al.,* 2007). Furthermore, these cells have demonstrated functions in autoimmunity and it has been suggested that they may function in the clearance of pathogens not recognized by the Th1 and Th2 cells (Bettelli *et al.,* 2006)

Despite the means in which the antigen co-stimulatory signals are presented, the main factors affecting the development of Th subpopulations are the cytokines and chemokines present in the immediate T cell environment. New advances in the use of knockout mice and inducible systems may lead to a better understanding of the properties and interactions of the individual cytokines and chemokines that play a role in Th cell activation.

1.2 Cytokines and immune system communication.

Both the innate and adaptive immune responses can be characterised by their cytokine responses. The cytokine super family of proteins forms an integral part of the signaling network between cells and is essential in generating and regulating the immune response (Figure 1.5). Cytokines are small soluble proteins that are produced in response to an immune stimulus. They act at the cellular level by binding to membrane receptors, and inducing a cellular response. This response is activated by altering the gene expression profiles of cytokine-regulated genes (Taniguchi, 1995).

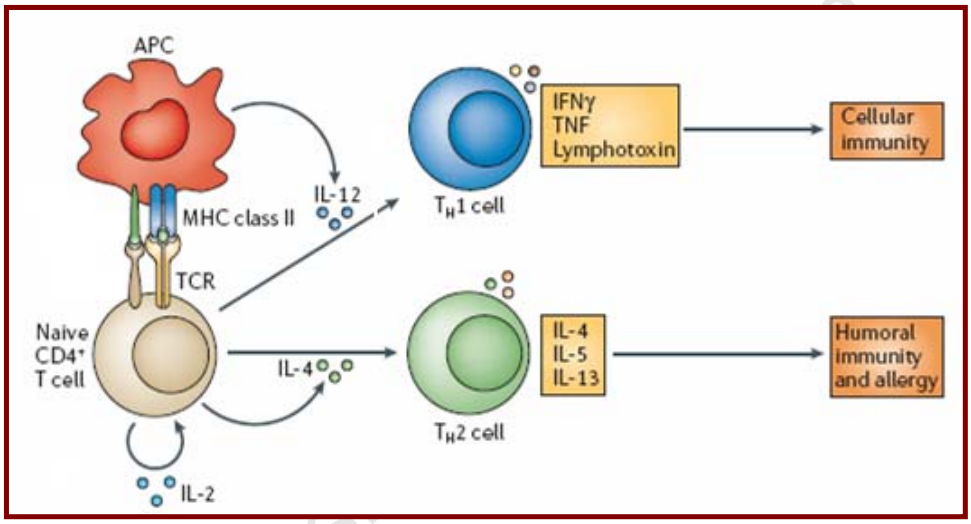

Figure 1.5 Influence of cytokines on immune response.

Upon T cell activation IL-2 is secreted leading to proliferation of these activated T cells. With IL-4 secretionTh2 cells are produced secreting IL-4, IL-5 and IL-13, thus supporting an innate or humoral immune environment. Conversely, IL-12 secreted by antigen presenting cells skews the response to an adaptive immune response associated with the production of IFN-γ, TFN-α and lymphotoxin.

Numerous cytokines have been identified and are characterized by their diverse functions. Responses to cytokines include modulation of membrane protein expression, proliferation, effector molecule secretion and differentiation of B and T lymphocytes (O'Shea *et al.,* 2002).

Cytokines are referred to as interleukins, growth factors, colony-stimulating factors, tumor necrosis factors, interferons and chemokines. Important examples of these include the following:

- Interferons. IFNα and IFNβ are produced by virally infected cells. They are mainly involved in inhibition of virus replication in the infected cells and induction of resistance to viral infection in uninfected cells (Bogdan, 2000). IFNγ, which is produced by T cells, stimulates antigen-presenting cell MHC expression.
- Chemokines. MIP-1α, MIP-1β, MCP-1α, and RANTES are involved in the attraction and migration of leukocytes to sites of infection (Pestka *et al.,* 2004).
- TGF, the transforming growth factor promotes growth of fibroblasts while colony-stimulating factors mediate proliferation and differentiation of macrophages, monocytes, bone-marrow stem cells and leukocyte precursors (Janeway *et al.,* 2002).

The major groups of interleukins are responsible for the stimulation of immune cell proliferation and differentiation. This group includes Interleukin 1 (IL-1), which is produced by T cells (Nakae *et al.,* 2001), and IL-2, which stimulates proliferation of antigen-activated T and B cells. Additionally, IL-4, IL-5, and IL-6 stimulate proliferation and differentiation of B cells and Granulocyte Monocyte Colony-Stimulating Factor (GM-CSF), which stimulate hematopoiesis (Aria *et al.,* 1990).

1.3 Interleukin-4 and Interleukin-13.

The hematopoietin family of cytokines, namely; IL-3, IL-4, IL-5, IL-13, and GM-CSF are a group of soluble proteins produced by effector Th cells. Similarity in cytokine structure lead to this grouping (Alberts *et al.,* 2002). The genes of the cytokines in this group are also closely linked in the genome and all are produced by Th2 cells. Furthermore, these cytokines bind related receptors known as the class I cytokine receptors. All are to some degree involved in lymphocyte activation and differentiation, the apparent overlapping biological functions can be attributed to the shared receptor subunits (Malabarba *et al.,* 1996).

Of particular importance in the current study are the roles of IL-4 and IL-13 and their associated receptor complexes in Th2 immunity, therefore these cytokines are further discussed in the following section.

1.3.1 Interleukin-4.

The Interleukin-4 (IL-4) gene is located on human chromosome 5 and murine chromosome 11. Alternative splicing events, shown to be tissue-specific, leads to the transcription and translation of different isoforms of IL-4 (Yatsenko *et al.,* 2004). IL-4, originally named B-lymphocyte stimulating factor-1, was identified due to its ability to induce proliferation of resting B-cells co-stimulated with anti-IgM antibodies (Howard *et al.,* 1982). Roles for IL-4 have now been described in a wide range of cells.

IL-4 is produced and secreted by activated T cells, mast cells, eosinophils and basophils. IL-4 function has effects on, amongst others, B cells, T cells, macrophages, mast cells, fibroblasts and endothelial cells are diverse (Delespesses *et al.,* 1989; Monroe *et al.,* 1988; Spits *et al.,* 1987; Yoshimoto and Paul, 1994). These include the induction of expression of immune receptors such as of MHC II molecules on resting B cells (Noelle *et al.,* 1984), IL-4R (Ohara and Paul, 1988), CD80 and CD86 (Stack *et al.,* 1994).

Additionally, IL-4 increases cell surface expression and secretion and of IgE and IgG1 (Pene *et al.,* 1988) and regulates heavy chain class switching of these immunoglobins (Lebman *et al.,* 1988), while suppressing production of IgM, IgG2a, IgG2b and IgG3 (Snapper et al., 1988). Such effects have important consequences in inducing immediate hypersensitivity (allergic) reactions while producing protection against helminth infections (Haas *et al.,* 1999; Maizels and Yazdanbakhsh, 2003).

Mast cell proliferation and the production of G-CSF and M-CSF (Essner *et al.,* 1989, Standiford *et al.,* 1990) can also be driven by IL-4, while it exerts an inhibitory effect on monocyte production of IL-1, IL-6, IL-8 and TNF (Miossec *et al.,* 1992).

Furthermore, IL-4 plays critical roles in T-cell function: these effects include stimulation of T cell proliferation (Mitchell *et al.,* 1989), the development of antigen-specific cytotoxic T cells (Horohov *et al.,* 1988; Widmer *et al.,* 1987), and differentiation of naïve CD T cells to the Th2 phenotype. These IL-4 driven responses are associated with the down regulation of the inflammatory actions of Th1 cells, thus supporting humoral immunity (Le Gros *et al.,* 1990).

1.3.2 Interleukin-13.

IL-13 shares various structural characteristics with IL-4 and belongs to the same α-helix protein family. Similar to IL-4, the IL-13 gene is also located on human chromosome 5 and murine chromosome 11. Of great importance is the shared receptor α subunits between IL-4 and IL-13(McKenzie *et al.,* 1993). Furthermore IL-13 functions can frequently be similar to those driven by IL-4, but key differences are apparent.

IL-13 is produced by T cells, mast cells, NK cells, basophils and dendritic cells (de Waal Malefyt *et al.,* 1995). The requirement of the IL-4Rα chain in IL-13 signal transduction explains in part the shared biological functions of IL-4 and IL-13. Similar to IL-4, IL-13 up regulates MHC class II molecules and it also induces the expression of surface IgM, CD23, CD71 and CD72 (de Waal Malefyt *et al.,* 1995; McKenzie *et al*, 1993). On monocytes IL-13 up regulates the expression of the adhesion molecules CD11b and CD11c (de Waal Malefyt *et al.,* 1993).
IL-13 also has important anti-inflammatory activities. Examples are the inhibition of the synthesis of TNF-α and the macrophage inflammatory protein-1α (MIP-1α), cytokines involved in the inhibition of nitric oxide production by LPS-activated murine macrophages and superoxide anion production by human monocytes (Doherty *et al.,* 1993; Doyle *et al.,* 1994). The inhibition of nitric oxide production by murine macrophages leads to increased uptake of iron and diminishing effector function (Weiss *et al.,* 1997). Furthermore IL-13 increases the expression of the mannose receptors on both human and murine monocytes and macrophages (Doyle *et al.,* 1994). It induces vascular cell adhesion molecule (VCAM)-1 on vascular epithelium which then directs lymphocyte, monocyte, basophil and eosinophil migration to sites of inflammation (Ying *et al.,* 1997).

These IL4 / IL13 shared functional similarities lead to the view that IL-13 was functionally redundant from IL-4. However, IL-13 exerts effector functions that distinguish it from IL-4 (Wynn, 2003). Host resistance to the *N.brasilienis* and *T.muris* gastrointestinal nematodes is mediated by Th2 cytokine responses and IL-13 has an essential role (Urban *et al.,* 1998). IL-13 is also the central mediator of allergic asthma, regulating eosinophilic inflammation, alveolar mucus secretion, and airway hyper responsiveness to a greater degree than IL-4 (Willis-Karp *et al.,* 1998).
Despite this and in contrast to IL-4 it fails to have any biological effect on T cells (Zurawski *et al.,* 1993), including lack of activation of T cell proliferation (de Waal Malefyt *et al.,* 1995).

1.4 IL-4Rα.

Functional effects of cytokines are dependent on their initiation of intracellular signaling through binding to their specific receptors. In the case of IL-2, IL-4 and IL-13 this signaling event begins with the dimerization of the appropriate receptor chains subsequent to receptor binding. IL-2, IL-4 and IL-13 all require IL-4Rα as part of their heterodimeric receptor complexes and subsequent signaling (Figure 1.6).

The type I receptor consists of the 140 kDa IL-4Rα and the common IL-2Rγ chain (Mosley *et al.,* 1989). This complex binds IL-4 with high affinity (Kd~50-100pM), however physiological signaling depends upon IL-4-mediated heterodimerization of the IL-4Rα with an additional chain (Lai *et al.,* 1996). In most cells the dominant chain involved in this heterodimerization is the common γ chain which was first identified as part of the IL-2 receptor (Russell *et al.,* 1993). The IL-13 receptor complex does not use the common γ chain; however the IL-4Rα chain is a component of the IL-13R complex (Obiri *et al.,* 1997). IL-4Rα chain alone can bind IL-4 but not IL-13. The other cell surface polypeptides involved in the IL-13 receptor complex are IL-13Rα$_1$ (Aman *et al.,* 1996; Hilton *et al.,* 1996) and IL-13Rα$_2$.

The type II receptor consists of IL-4Rα chain and the 70 kDa IL-13Rα$_1$ chain. This complex binds both IL-4 and IL-13 with high affinity (Hilton *et al.,* 1996). The IL-13Rα$_1$ chain exclusively binds IL-13 but with low affinity (Zuwarski *et al.,* 1993). IL-13Rα$_1$ is expressed on the cell surface of a broad range of cells yet no expression has been shown on mouse T or B cells. This could explain the lack of IL-13 responsiveness in these cells (Murata *et al.,* 1998 and Vita *et al.,* 1995).

The third receptor chain is the 60 kDa IL-13Rα$_2$, which binds IL-13 with high affinity in the absence of IL-4Rα (Caput *et al.,* 1996). Importantly, the majority of lymphoid cells show a lack of IL-13Rα$_2$ expression (Guo *et al.,* 1997). The IL-13R complexes function as secondary receptors for IL-4. This is in contrast to the IL-4R complex, which consisting of the IL-4Rα chain and the common γ chain, is only specific for IL-4, despite the fact that the common γ chain is a shared component of IL-2, IL-4, IL-5, IL-7 and IL-9. This was shown by competitive binding studies where IL-4 displayed preferential binding when compared to IL-13. Furthermore, blocking access to the IL-4Rα chain, by means of monoclonal antibody binding, lead to a lack of IL-4 / IL-13 functionality (Feng *et al.,* 1995).

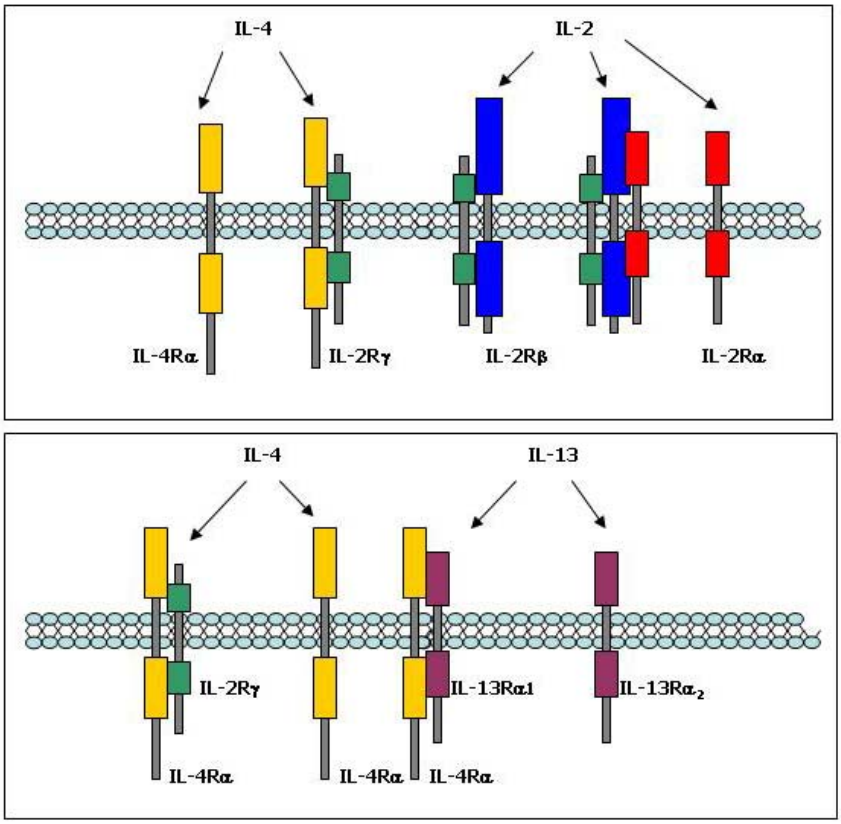

Figure 1.6 IL-4, IL-2 and IL-13 receptor complexes

IL-4 binds with IL-4Rα subunit in combination with either Type I receptor, the common γ chain or with the Type II receptor, IL-13Rα$_1$. IL-13 interacts with IL-13Rα$_1$ in combination with IL-4Rα or with IL-13Rα$_2$. IL-2 binds to either IL-4Rα in combination with γc, with γc in combination with IL-2Rβ, IL-2Rβ with IL-2 chains α and γc or with IL-2Rα.

The cytoplasmic domain of IL-13Rα$_2$ differs from that of IL-13Rα$_1$ in that it does not possess either signaling motifs or signaling molecule binding sequences; it was thus proposed that IL-13Rα$_2$ acts like a decoy receptor similar to the properties shown by the IL-1 type II receptor (Colotta *et al.,* 1994) and subsequent studies with IL-13Rα$_2$ knockout mice indicated this lack of signaling (Rahaman *et al.,* 2002). Yet, this view of the IL-13Rα$_2$ function was shown to be incorrect with data demonstrating IL-13 signaling via IL-13Rα$_2$ (Fichtner-Feigl *et al.,* 2006; Wilson *et al.,* 2007). Additionally it was shown that IL-13Rα$_2$ expression was regulated by IL-13 and that the absence of this receptor chain leads to an elevation in IL-13-dependent liver fibrosis during *Schistosoma mansoni* infection (Chiaramonte *et al.,* 2003).

1.4.1 Soluble receptors.

The membrane-bound IL-13 and IL-4 receptors both have soluble isoforms. These secreted receptor molecules have bee identified as physiological regulators of IL-13 and Il-4 involved in modulation of the immune responses normally controlled by IL-4 and IL-13 cytokines (Maliszewski and Fanslow, 1990).

The secreted form of IL-13Rα_2 was identified as a 45-50 kDa protein in the serum and urine of mice. This protein bound IL-13 with a 300-fold higher affinity than that shown by a recombinant IL-13Rα_2 protein. It displayed structural differences to the cell surface receptor and was antigenically distinctive from the IL-13Rα_2. Additionally it acted as a potent inhibitor of IL-13 cytokine binding to its cell surface receptor (Zhang *et al.,* 1997). The soluble IL-4R is a 30-40 kDa truncated form of the membrane bound receptor that results from alternative mRNA splicing of transcript from the gene which encodes both the membrane-bound and secreted isoforms (Wrighton *et al.,* 1992). It displays comparable IL-4 binding affinity to that shown by the membrane IL-4Rα and functions by neutralizing the biological effects of IL-4 *in vitro* (Fanslow *et al.,* 1990; Keegan *et al.,* 1991; Mosley *et al.,* 1989). The soluble IL-4R isoform also functions as an IL-4 antagonist with a characteristic role in IL-4 ligand-receptor interaction *in vivo*. This was demonstrated by treatment of *Leishmania major* infected mice with this isoform. A surplus of the soluble receptor protein rendered the mice clinically resistant to *L. major* and shifted the pattern of cytokines towards a Th1 type, in this way provided long-lasting resistance against re-infection (Gessner *et al.,* 1994).

It is recognized that recombinant soluble receptors can interfere with the biological functions of cytokines and this makes them appropriate candidate molecules for the future treatment of certain pathological conditions where cytokine activity needs to be modulated.

1.4.2 IL-4Rα and cytokine signaling pathways.

As mentioned IL-4Rα is the receptor for both IL-4 and IL-13, belonging to the type I cytokine receptor family. IL-4Rα is expressed in low numbers (100-5 000/cell) on a variety of both Th1 and Th2 cells (Lowenthal *et al.,* 1988). IL-4R expression in a majority of cells is in association with the common γ chain, which is required for IL-4 signal transduction (Kondo *et al.,* 1993).

Subsequent to cytokine-receptor binding there are four main cytokine signaling pathways. These are the Ras/mitogen-activated protein kinase (Ras/MAPK) and phosphoinositide-3-kinase (PI-3-kinase) pathways which are important for cellular proliferation (Deane and Fruman, 2004), the signal transducer and activator of transcription (STAT) pathways which stimulate gene transcription, the pathways originating from activation of the receptor associated kinases like Janus kinases (JAKs) and lastly the pathways involved in apoptosis which are activated by amongst others Ligand and TRAIL (Aggarwal, 2003).

The major mechanisms by which hematopoietin cytokine receptors (amongst them IL-4Rα) transduce intracellular signals (Figure 1.7) are virtually identical and can be attributed to the fact that these receptors lack endogenous kinase activity (Nelms *et al.,* 1999). This leads to the requirement for receptor-associated kinases for the initiation of signaling. The main signaling molecules involved in this pathway are members of the Janus family of cytoplasmic tyrosine kinases (JAKs) (Ihle, 1995; Taniguichi, 1995). IL-4 receptor binding leads to heterodimerization of the IL-4Rα chain with the γc chain (Kammer *et al.,* 1996), this initiates Jak-1 association with the IL-4Rα chain and Jak-3 with the γc chain. In parallel binding of IL-13 to IL-13Rα leads to the association with Jak-2 (Murata *et al.,* 1996; Miyazaki *et al.,* 1994).

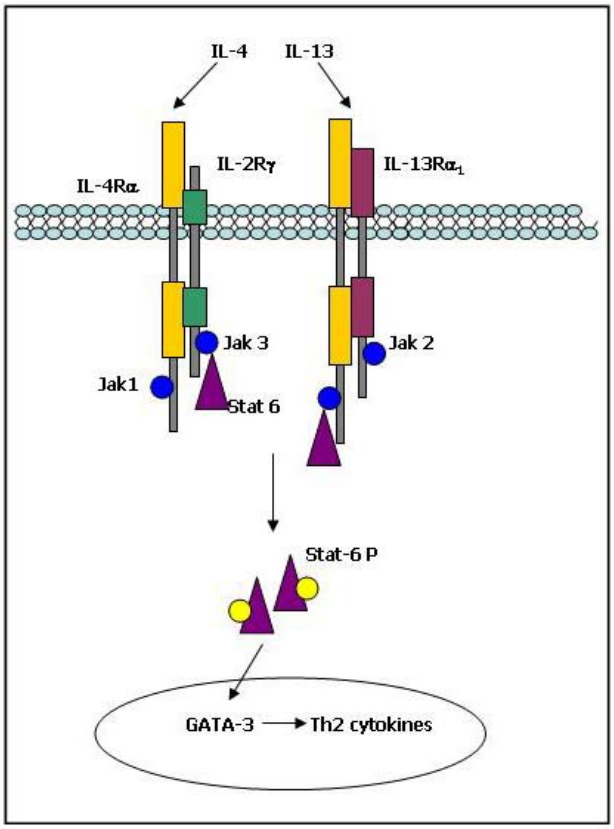

Figure 1.7 IL-4 and IL-13 Jak/Stat signaling pathway.

After receptor heterodimerization Jak tyrosine kinases are phosphorylated leading to the association of the Stat signal transducing proteins. These proteins are phosphorylated by the Jak kinases and proceed to form homodimmers. Subsequent to translocation into the nucleus these complexes activate GATA-3 which initiates Th2 cytokine transcription.

With the activation of these signal transducers tyrosine residues in the cytoplasmic domain of the IL-4Rα chain are phosphorylated, these phosphorylated chains act as docking sites for signalling molecules (Smerz-Bertling and Duschl, 1995). Subsequently, the signal transducing activators of transcription (STATs) bind to the phosphorylated receptor via a conserved SH2 domain. Bound STAT6 is then phosphorylated by the activated kinases (Darnell, 1997). These phosphorylated STAT6 molecules form homodimmers followed by the translocation to the nucleus and subsequent stimulation of target gene transcription (Ivashkiv, 1995; Murphy *et al.,* 2000). IL-4-mediated STAT6 activation regulates the expression of transcription factors GATA-3, which result in the production of Th2 cytokines and chromatin remodelling at the IL-4 locus (Ouyang *et al.,* 2000).

STAT6 activation after IL-4 stimulation is selectively impaired in Th1 cells (Kudo *et al.,* 1997), indicating the status of IL-4 receptor (IL-4R)-mediated signaling during initial activation. In Th1 cells, the phosphorlyated IL-4Rα chain binds the N-terminal 50 amino acids of SOCS5 (suppressor of cytokine signaling-5) leading to a reduction of the association of Jak-1 with the IL-4R, decreased STAT6 activation and Th2 cell differentiation. SOCS5 interaction is independent of tyrosine phosphorylation (Seki *et al.,* 2002). In certain cell types, signalling is initiated by activation of insulin receptor substrates, IRS1/IRS2. Phosphorylation of the IRS molecules leads to interaction with cytoplasmic signalling molecules phosphatidylinositol 3-kinase (PIK3C3).These molecules form a link between IL-4R and signalling pathways involved in cellular proliferation (Izuhara and Harada, 1996).

1.5 Molecular manipulation of gene function.

Mice have become important tools in biomedical research and are the most widely used laboratory animals in transgenic studies. This is due to the genetic similarity between humans and mice including the conservation of most human genes in the mouse genome. The accessibility of numerous genetically homogeneous inbred strains (Silver, 1995), the opportunity for germline gene modification (Isola and Gordon, 1991) and the availability of embryonic stem (ES) cells offer flexibility when establishing new technologies (Camper *et al.,* 1995). It has become feasible to produce mice with genetic alterations ranging from simple gene disruptions to the more complex cell-specific inducible systems (Goosen and Bujard, 2002). Transgenic mice are produced in order to investigate the role of genetic mutation with the potential to then lead to studies questioning the molecular and biochemical mechanisms involved. Furthermore, transgenic models can help in designing novel therapeutic strategies for the investigated disease. Studies with these transgenic models are unique in offering the opportunity to investigate genotype-phenotype relationships relevant for unravelling the biologic role of human genes (Hofker and van Deursen, 2003; Muller, 1999).

Landmarks in the development of mouse technology include; the generation of transgenic mice, via the stable introduction of genes into the germline of the experimental model (Palmiter *et al.,* 1982). This allowed the generation of mice with virtually any genotype and the analysis of the consequences of these mutations in the milieu of a developing and intact model. Secondly, the development of pluirpotent embryonic stem (ES) cell cultures which lead to gene targeting via homologous

recombination in these cells, permitting the precise modification of the gene of interest. Developing from this was the generation of gene knockout (Mansour *et al.,* 1988) and tissue-specific knockout models. Lastly the systems for inducible transcriptional activation in mice (Goosen *et al.,* 1993), which afford the researcher with the most flexibility in terms of modification of gene function.

1.5.1 Conventional transgenics.

Transgenic technology, referred to as the techniques involved in the stable introduction of genes into the germline of the mouse (Gordon *et al.,* 1980), can be split into two experimental categories; the "gain-of-function" mutations and the "loss-of-function" mutations.

The generation of transgenic mice characterised with "gain-of-function" mutations is associated with the microinjection of the gene of interest into the one-celled zygote. This technology was developed from the direct microinjection of a DNA fragment consisting of the promoter of the mouse metallothionein-I gene linked to the cDNA of rat growth hormone into the pronuclei of fertilized mouse eggs (Bronson and Smithies, 1994; Palmiter *et al.,* 1982). The technique of DNA microinjection results in random integration of the injected DNA fragment or transgene which gives rise to founder lines which have to undergo extensive characterisation, many of which then display variable expression of the integrated gene (Muller, 1999). Conventional transgenic as a science has not changed a great deal and is often limiting, since it represents "gain-of-function" models and genetic disease is more likely characterized by "loss-of-function" which is beyond the scope of this conventional transgenic technology (Moreadith and Radford, 1997).

1.5.2 Gene targeting using embryonic stem cells.

The generation of transgenic mice characterised with "loss-of-function" mutations employs embryonic stem cells. Some of the initial limitations in transgenic research were overcome with strategies combining embryonic stem cells and gene targeting technology.

Pluripotential embryonic stem cell lines were derived from mouse blastocytes (Evans and Kaufmann, 1981; Martin, 1981), and subsequently, it was shown that these cultures were able to develop into functional germ-line chimeras after blastocysts injection. These cells showed germline competence and transmission of genetic material to the next

generation, thus introduction of mutations in these cells could allow for the generation of mice with a predetermined genotype (Bradley *et al.,* 1984).

The principles of homologous recombination were developed in yeast and homologous recombination in mammalian cells, between an artificial targeting vector and an endogenous gene, was first demonstrated for the β-globin locus (Smithies *et al.,* 1985). Subsequently, gene targeting via homologous recombination in murine embryonic stem cells (Thomas and Capecchi, 1987) was achieved for the selectable hypoxanthine phosphoribosyl transferase (HPRT) gene locus. In a seminal study (Mansour *et al.,* 1988) the gene of interest was interrupted by the homologous recombination of a neomycin selection cassette in a position that would disrupt transcription, in this way generating a "loss-of-function" mutation (Figure 1.8). Gene targeting allows the precise modification of the target gene where, in principle and has been used to generate numerous knockout models (see http://www.jax.org). This constitutive inactivation of gene function leads to models which are always deficient in the deleted gene product.

Embryonic stem cells can also be used for the targeted insertion or "knock-in" of transgenic sequences. Here the DNA sequence can be placed under the control of the regulatory elements of the particular endogenous locus. The transgene can be inserted, leaving the target locus functional or conversely, the transgene can replace a region of the target gene, thereby disrupting the functionality of the endogenous gene (Ledermann, 2000). This was illustrated by the disruption of the murine *Int-2* gene via the insertion of the *lacZ* gene, thus enabling transgene transcription driven by the endogenous promoter and subsequent *in situ* expression studies (Mansour *et al.,* 1988). This approach has also been employed to study the role of cytokines and their receptors in determining hematopoietic cell fate (Stoffel *et al.,* 1999). The thrombopoietin receptor gene, *Mpl*, was replaced with a chimeric construct encoding the extracellular domain of *Mpl* and the cytoplasmic domain of the granulocyte colony-stimulating factor (*Gcsfr*). This lead to chimeric receptor binding to thrombopoietin and subsequent signalling via the *Gcsfr* intracellular domain. This study illustrated, *in vivo,* that the cytoplasmic domain of *Gcsfr* can functionally replace *Mpl* signalling, in this way supporting normal megakaryopoiesis and platelet formation.

.

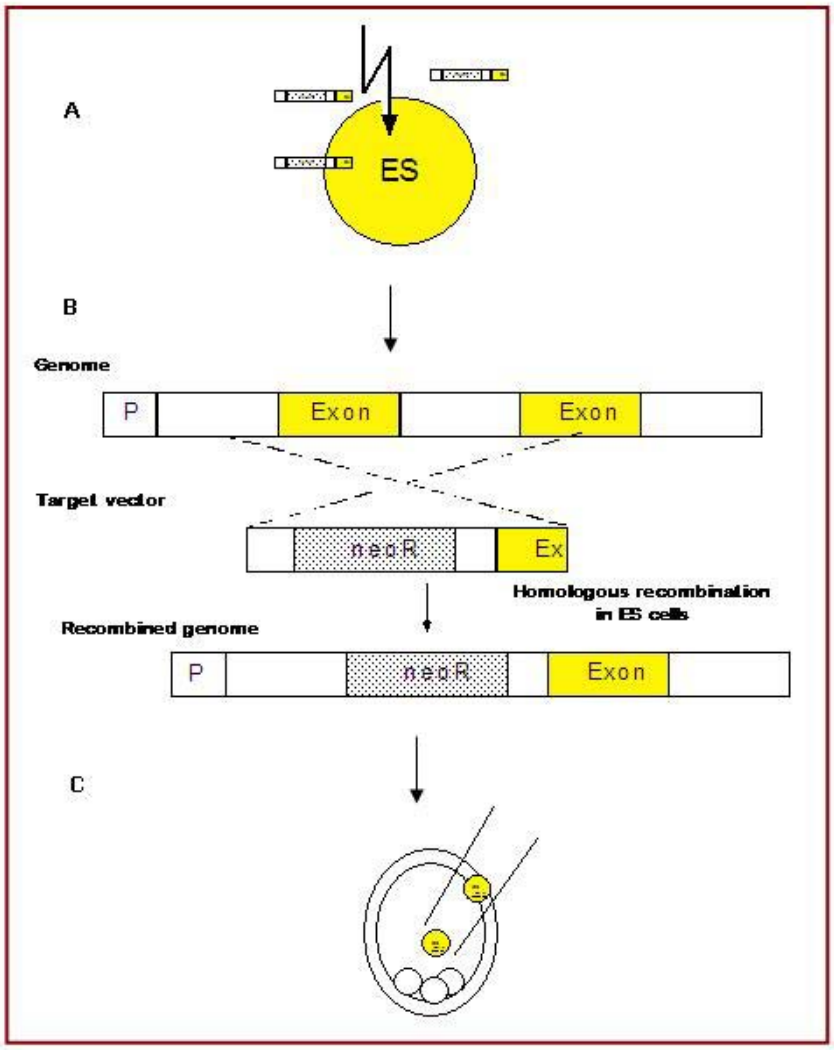

Figure 1.8 Gene targeting via homologous recombination in ES cells.

This technique disrupts the target gene in the murine germline by insertion of a selectable marker. In principle every gene can be silenced in this way, which has lead to the mouse being the species of choice for biomedical research. **A**. The target vector containing the neo cassette is electroporated in to ES cells. **B.** The selectable marker is inserted into the genome via homologous recombination. **C**. Following clone selection the ES cells are microinjected into blastocysts and transferred to pseudo pregnant females.

The drawbacks in this approach include potential embryonic lethality if the gene product is essential for development (Fortschegger *et al.,* 2007). Conventional knockout methods also affect every cell in the animal which makes distinguishing between primary and secondary changes in phenotype difficult. Additionally, the constitutively deficient animal may compensate for the loss of gene product consequently rendering the resulting phenotype comparable to a wild-type animal even if the gene product has an important function (Guidi *et al.,* 2004). These problems can be avoided by tissue-specific and inducible gene disruption techniques.

1.5.3 Conditional transgenics.

Conditional gene targeting builds on the conventional transgenic strategies and allows for control of the gene targeting event both in a tissue-specific and temporal manner. Here gene function modulation is conditional to a certain stimulus. The conditional manipulation of individual gene activities can be divided into two basic strategies; the first of these targets the genes directly by site-specific recombination resulting in activation, inactivation or modification of target gene function and the second quantitatively and reversibly controls the gene's function, in most part leaving the endogenous gene function untouched within its genetic context (Gossen and Bujard, 2002; Lebermann, 2000; Ryding *et al.,* 2001;).

1.5.3.1 Site-specific recombinase systems.

The most widely employed method to achieve tissue-specific gene targeting is the use of site-specific recombinase systems. These systems consist of two elements namely the recombinase enzyme and the DNA sequence it recognizes. Recognition is by a consensus sequence and the recombinase catalyzes recombination between two of its recognition sites to bring about the modification of the associated DNA. Modifications can range from DNA deletion (Figure 1.9) and insertion to inversion or translocation (Hofker and van Deursen, 2003). DNA segments can be inverted or deleted in *cis* or can be connected in *trans*. This broadens the scope of function from basic deletion of DNA segments to applications like chromosome engineering and recycling of selectable markers (Aduin and Bradley, 1996; Yu and Bradley, 2001). The type of modification depends on the orientation and location of the recognition sites.

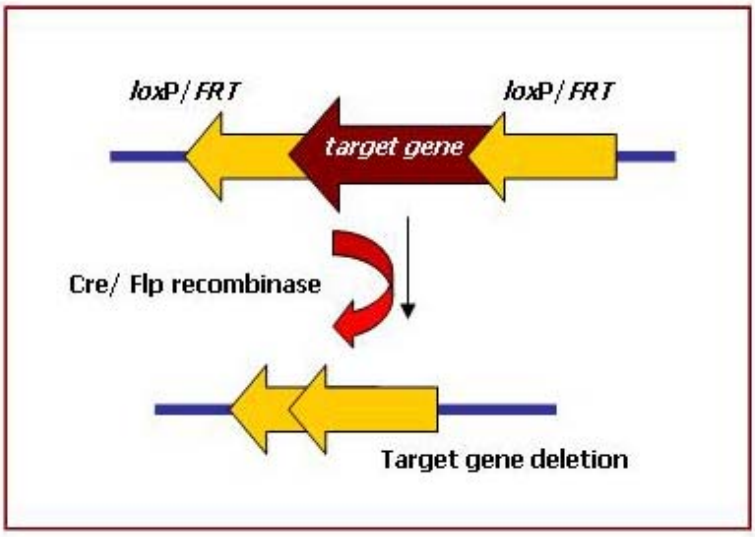

Figure 1.9 The model of Cre and Flp site-specific recombinase inactivation.

The figure illustrates the most generally applied approach whereby gene function is inactivated by the deletion of DNA fragments located between the repeated recombination sites. The *lox*P or *FRT* sites are recognized by recombinases Cre or Flp and excised from the genome.

Presently, there are two members of the integrase family of site-specific recombinases; the Cre-*lox*P system from the bacteriophage P1 (Lakso *et al.,* 1992; Orban *et al.,* 1992; Sauer and Henderson, 1989) and the Flp-*FRT* system from the budding yeast *Saccharomyces cerevisiae* (Dymecki, 1996; O'Gorman *et al*., 1991) being applied in conditional control of gene expression via site-specific DNA recombination. Both Cre and Flp recognize a 34bp consensus sequence consisting of two 13bp inverted repeats flanking an 8bp nonpalindromic core defining the orientation of the of the recognition site. These systems are both derived from evolutionary distant species and this and the recognition site length of 34bp make them remarkably specific (Gossen and Bujard, 2002; Nagy, 2000). Additionally no accessory proteins or high-energy cofactors are required for activity and both Cre and Flp recombination functions have been shown to function in mice, with Flp needing a temperature optimum of 37°C (Buchholz *et al.,* 1998).

Of these two recombinase systems the Cre-*lox*P system is most widely used and one of the most impressive applications of this system in mice is its use in the inactivation of gene expression in a temporally and spatially controlled manner (Lewandoski, 2001; Lobe and Nagy, 1998, Nagy, 2000).

Limitations of gene-targeting that can be circumvented with this approach include; embryonic lethality and problems that arise if the gene phenotype affects multiple tissues. Certain biological questions can also be addressed in a manner not afforded with gene targeted models alone (Gossen and Bujard, 2002).

1.*5.3.2* *Tissue specific knockouts.*

One of the most powerful strategies developed in mouse technology was the combination of conventional gene targeting techniques and the conditional site-specific recombination systems to achieve cell type-specific knockouts.

Here standard gene targeting techniques are used to produce a model in which an essential region of the target gene is floxed (flanked by the *lox*P sequences); in this way tissue-specific *cre* expression will lead to inactivation of the floxed allele. Before the recombination event this conditional allele usually displays a wild-type phenotype since, in most cases, the *lox*P sites are placed in the introns. The mouse line carrying this conditional allele is then crossed with an effector mouse line that expresses *cre* in a tissue-specific manner. Cre expression leads to Cre catalysing the site-specific recombination between the *lox*P sites in this manner deleting the sequences flanked by the *lox*P sites and resulting in gene silencing (Kwan, 2002; Muller, 1999). Therefore the progeny from this cross will only display inactivation of the conditional allele in the cells expresses *cre* (Gu *et al.,* 2001; Takeda *et al.,* 1998).

The cDNA encoding the site-specific Cre recombinase in the effector mouse line is either introduced as a regulated transgene driven by a tissue-specific promoter or the gene is inserted by "knock-in" gene targeting adjacent to a suitable endogenous promoter (Ledermann, 2000). An example of this is the "knock-in" of *cre* behind the *Cd19* locus which enabled B-cell specific expression (Rickert *et al.,* 1997). Since the lox*P* sites are generally placed in introns and the target gene displays a wild-type phenotype until the expression of Cre and the ensuing recombination event occurs, an advantage of this approach is the elimination of potential embryonic lethality caused by the target gene inactivation (Gossen and Bujard, 2002).

Figure 1.10 illustrates the approach starting with the gene targeting and the recombination events in ES cells, leading up to the inter crossing of the mouse lines and generation of the subsequent cell-specific knockout model.

The two primary disadvantages of the Cre/*lox* system are that not all tissue specific promoters display complete specificity (Sauer, 1998) where basal levels of expression in other cell types can sometimes cause unintended gene expression. Secondly, Cre-induced recombination is an irreversible genetic modification. These limitations can be overcome by systems that would allow the control of gene transcriptional events from the "outside" at will.

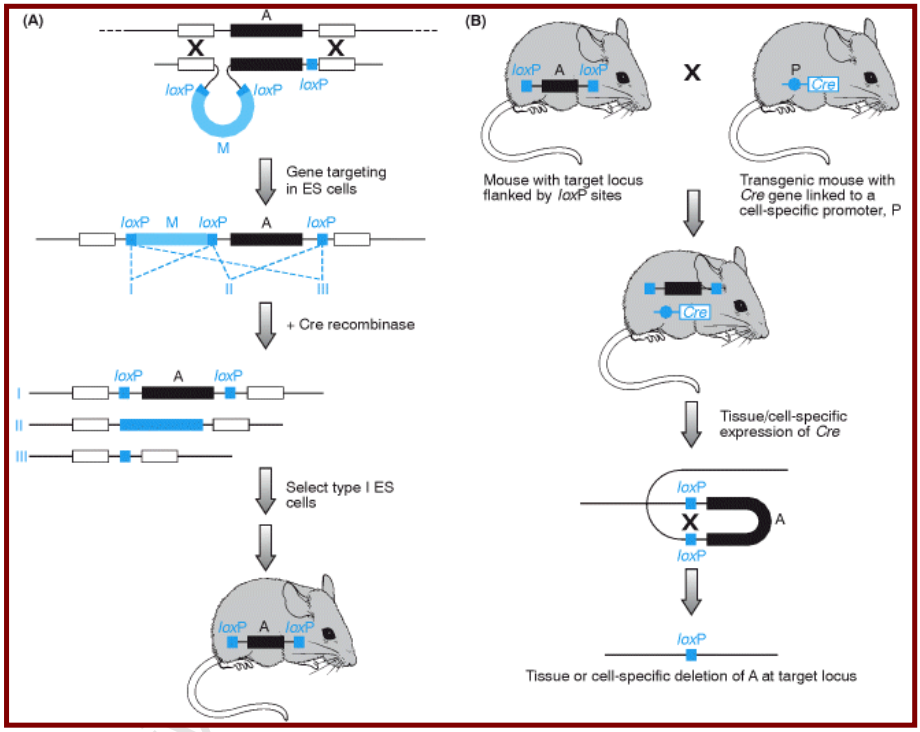

(Strachan and Read, 1999)

Figure 1.10 Combining gene targeting and the Cre-*lox*P recombination system to inactivate a gene in a desired cell type.

A. The standard homologous recombination method using mouse ES cells, in which three *lox*P sites are introduced along with a marker M at a target locus A. The *Cre* recombinase is transfected and transient expression leads to the recombination between the introduced *lox*P sites resulting in different products. Type I recombinants are used to generate mice in which the target locus is flanked by *lox*P sites. These mice can then be inter crossed with previously constructed transgenic mice (**B**) carrying an integrated construct consisting of the *Cre* recombinase gene linked to a tissue-specific promoter. Offspring which contain both the *lox*P-flanked target locus plus the *Cre* gene will express the *Cre* gene tissue-specific manner resulting in recombination between the *lox*P sites and inactivation of the target locus A.

1.5.4 Conditional control of transcription.

Ideally and perfect genetic transcriptional switch would result in low basal gene expression in the "off" mode and high levels of gene transcription in the "on" mode. Additionally the switch should be specific but reversible for the target gene and show no interference with other cellular components. This criteria was achieved by the binary transgenic systems where the gene expression is controlled by the interaction between two components, namely an effector transcribed from the regulatory element and the target transgene on which it acts which is located on the response element (Gossen and Bujard, 2002; Lewandoski, 2001). The most widely used transcription activation systems are those controlled by tetracyclines. These systems have been applied to cultured cells of plant, avian, insect and mammalian origin but also on whole organisms like *Drosophila* and mice (Bello *et al.,* 1998; Love *et al.,* 2000).

Two key characteristics of the Tet regulatory system (Goosen *et al.,* 1995) distinguishes it from other transcription activation systems, firstly the binding specificity and affinity displayed between the Tet repressor (Tet R) and the tet operon (*tet*O), its specific binding site, and additionally between the Tet repressor and the inducing agent being tetracycline or doxycycline. Secondly, the inducing agents, some of which have been used in human medical field for years, have been well characterized in terms of their chemical and physiological properties (Gossen and Bujard, 2002; Hofker and van Deursen, 2003). In terms of transgenic studies the tetracycline analogues, doxycycline and anhydrotetracycline are used in preference to tetracycline owing to the higher tTA binding affinities and lower toxicities shown by these analogous (A-Mohammadi *et al.,* 1997; Gossen and Bujard, 1993)

There are two basic complementary tetracycline-inducible expression systems, namely the tTA or Tet-Off system (Gossen and Bujard, 1992) and the rtTA or Tet-On system (Gossen *et al.,* 1995). Both systems require two building blocks: the ligand dependent transactivator (r)tTA as the effector and a *tet*O^{CMV} minimal promoter cassette, which regulates the expression of the target transgene. The effector is a fusion of sequences that encode the VP16 transactivation domain and the *Escherichia coli* tetracycline repressor (TetR) protein, which specifically binds to both doxycycline or tetracycline and the 19bp operator sequence (*tet*O) of the *tet* operon in the target gene. This binding results in the activation of transcription. In the Tet-Off system, the inducing agent doxycycline prevents binding of the transactivator tTa to the *tet*O, in this way inactivating transcription. In contrast, the presence of doxycycline is required for the binding of the

rtTa (reverse tetracycline controlled transactivator) to *tet*O and the subsequent activation of gene expression in the Tet-On system (Gossen *et al.,* 1995) (Figure 1.11).

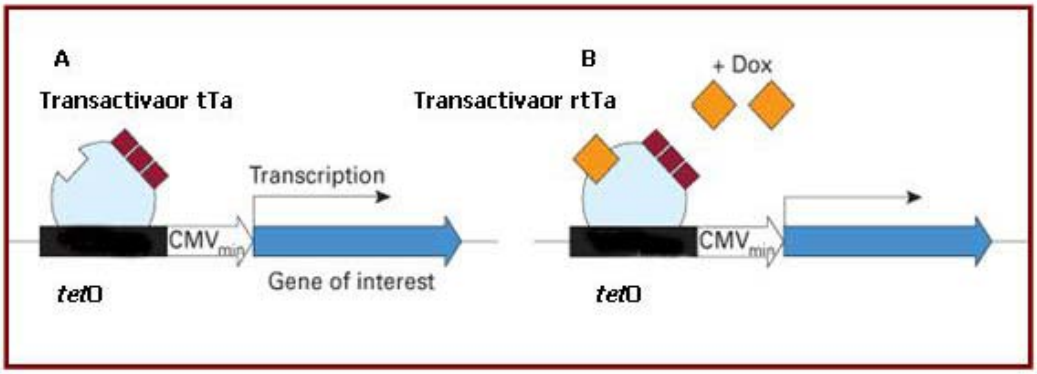

Figure 1.11 Induced expression via the Tet-Off and Tet-On Systems.

A. In the Tet-Off system, the basal state is maintained in the presence of doxycycline, which prevents binding of the tTa protein to *tet*O, and induced, by Dox removal. **B**. In the Tet-On system transcription is activated in the presence of Dox, which permits binding of the rtTa transactivator protein to the *tet*O.

The main distinction between the Tet-Off and Tet-On systems is the kinetics of target gene activation. In the Tet-Off system the transgene is only fully inactivated by the continuous administration of doxycycline. Activation occurs with doxycycline removal and is thus dependent on the rate of doxycycline clearance. It has been shown that this clearance can range from 24 hours up to 1 week in mice depending on the tissue type of interest. In contrast with the addition of doxycycline in the Tet-On system there is a rapid activation of target gene transcription, as fast as 1 hour, whereas the subsequent inactivation depends on the doxycycline clearance form the tissues of interest (Kistner *et al.,* 1996; Hasan *et al.,* 2001). However, the rtTA in the Tet-Off system retains some affinity for the *tet*O sequences even in the absence of doxycycline. This retains affinity results in a continuous low level of basal expression, unacceptable in most systems, an example be the regulated expression of toxins (Keyvani *et al.,* 1999).

The Tet-inducible expression systems are continually being modified (Baron and Bujard, 2000; Goosen and Bujard, 2001) with different transactivator domains, trans-repression domains, codon-usage modifications and variations to the configuration of *tet*O sequences (Baron *et al.,* 1997; Urlinger *et al.,* 2000; Wells *et al.,* 1999). One of these modifications now allows for the simultaneous expression of two target transgenes. This was achieved by flanking the *tet*O sequences with two minimal promoters (Baron *et al.,* 1995) (Figure 1.12). This system enables the transcriptional activation in cultured cells and transgenic mice to be examined by means of one promoter driving the expression of both the target gene and a reporter gene such as green fluorescent protein or luciferase (Krueger *et al.,* 2006; Lavon *et al.,* 2000)

Strategies are also being developed as an alternative to the use of Cre transgenic lines. Thus circumventing the need to generate and characterize the Cre transgenic lines. Recombinant adenoviral vectors are being used to deliver Cre to somatic tissues in mice carrying floxed alleles (Chang *et al.,* 1999; Wang *et al.,* 1996). Additionally, to achieve temporal regulation and promoter specificity Cre variants that only function in the presence of an exogenous inducer have been generated. In this combined system expression of *cre*, from the Cre variants occurs only when the drug tetracycline is administered, allowing researchers to start and stop expression of the gene at any time. This was achieved by fusing the Cre coding region with a mutated ligand-binding domain (LBD) from either the progesterone (Kellendonk *et al.,* 1996) or the estrogen receptor (Feil *et al.,* 1996). These mutated forms of the LBD will only bind and localize to the nucleus in the presence of synthetic steroids, RU486 and tamoxifen respectively. No binding is shown in the presence of endogenous steroids. Another advancement in the pursuit for controlling gene expression spatially and temporally was by combining the Cre/*lox*P and the tetracycline-regulated transcriptional systems (Belteki *et al.,* 2005; Mao *et al.,* 2005; Utomo *et. al.,* 1999; Yu *et al.,* 2005). Here transcription is activated by the administration of doxycycline, as the Tet-On system is utilized, this induction of *cre* expression with doxycycline in the rtTa system results in tight regulation of the translational and subsequent recombination event.

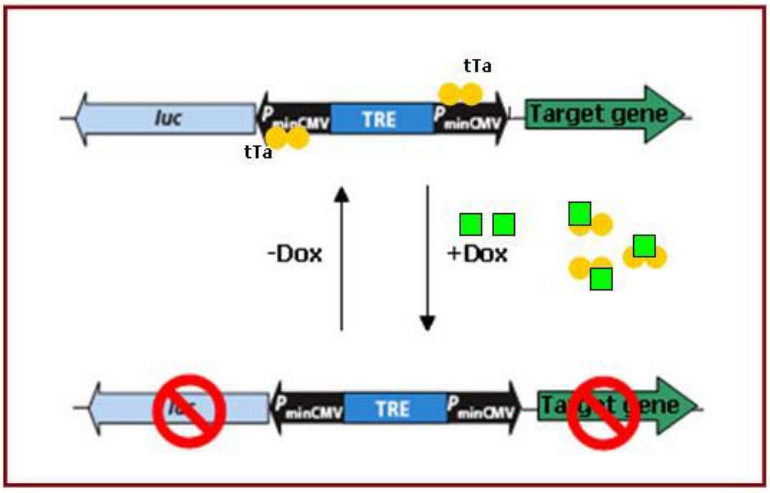

Figure 1.12 Inducible transcription via the bi-directional pBI-L Tet vector.

The vector expresses a gene of interest and luciferase, GFP or any other reporter from a bidirectional *tet*O promoter. In the presence of doxycycline, the tTa is prevented form binding to the *tet*O operon. With the removal and subsequent clearance of the doxycycline the Dox, induced suppression is lifted and transcription of both the target gene and the reporter is activated.

1.6 Molecular manipulation of IL-4Rα.

Conventional gene targeting and site-specific recombination techniques have also been employed to produce a model where IL-4Rα is transcriptionally inactivated. The floxed IL-4Rα model was generated using homologous and site-specific recombination in embryonic stem cells, the targeting strategy yielded a silent mutation whereby the lox*P* sites were placed in introns and 5'and 3' ends of exons. The IL-4Rα $^{lox/lox}$ mice thus display a wild-type phenotype in the absence of Cre/lox*P* recombination. With recombination the IL-4Rα expression is eliminated in all cells of the resulting model (IL-4Rα $^{-/-}$). The IL-4Rα $^{-/-}$ mice are ineffective in functions associated with the IL-4 and IL-13 cytokine binding to this receptor. Use of this model established that the IL-4Rα chain is a vital component of both the IL-4 and the IL-13 receptor complexes and thus the associated receptor complex signaling (Mohrs *et al.,* 1999).
Infectious disease studies with IL-4$^{-/-}$ and the above mentioned IL-4Rα$^{-/-}$ mice have lead to novel findings, as illustrated below.

1.6.1 Leishmania donovani.

Amongst the infectious diseases, studies using *Leishmania major* as a model have contributed a great deal of the determining data on the role of IL-4 in the host protective response. The first evidence of a role for IL-4 in infection was shown by studies with this intracellular prorozoan parasite, when it was established that host protection is mediated by Th1 cytokines and inhibited by the Th2 cytokines (Scott *et al.,* 1988). It was shown that apart from MHC molecule antigen presentation, mediation between cytokines determines the developmental immune skewing to either the Th1 or Th2 effector phenotype (Reiner. and Locksley, 1993). Researchers were given the opportunity to further dissect the role of IL4 in *Leishmania donovani* infection by the development of IL-4$^{-/-}$ and IL-4Ra$^{-/-}$ mice. Studies with these mice have provided invaluable information including demonstrating that IL-4 is vital for the optimal resolution of the primary *L.donovani* infection and that both IL-4 and IL-13 play important roles as positive regulators of immunity to *L. donovani*. Furthermore that the absence of the functional IL-4Rα through which both IL-4 and IL-13 signal resulted in delayed maturation of the associated granuloma formation (Stäger *et al.,* 2003). This dissection of cytokine function could be facilitated greatly by the use of mice where IL-4Rα gene expression is spatially and temporally controlled. They have the potential to broaden the scope of analysis into the IL-4 and IL-13 effects at both the onset and later stages of the granulomatous response thus determining the precise role of IL-4Rα signalling in the induction of anti-

leishmanial responses. The IL-4Rα $^{lox/lox}$ model was also used as backbone to generate a conditional tissue-specific IL-4Rα $^{-/-}$ by inter crossing these with mice with mice where the expression of *cre* recombinase is restricted to the $CD4^+$T cells. Tissue specificity was gained by the use of Lck driven *cre* expression (Radwanska *et al.,* 2007). Studies using *L.major* and this model showed that the infected mice deficient in IL-4Rα expression on $CD4^+$T cells developed the disease phenotype associated with mice that are genetically resistant to *L.major* infection, in this way confirming the importance of this receptor in *L.major* disease progression.

1.6.2 Nippostrongylus Brasiliensis.

Initial analysis of the host response against *Nippostrongylus brasiliensis* showed that the Th2 cytokines IL-4 and IL-13 have a protective role in the host response against the intestinal nematode parasites (Finkelman et al., 2004). But the use of IL-$4^{-/-}$ and IL-$13^{-/-}$ mice greatly elucidated the cytokine roles and demonstrated that IL-13 is more important than IL-4 as an inducer signalling pathway that stimulates parasite expulsion (Urban *et al.,* 1998). Furthermore, knockout mice were also instrumental in the finding that worm expulsion requires IL-4Rα espression by non-bone marrow (goblet cells, intestinal epithelium, smooth muscle, vascular endothelium) derived cells but not by marrow-derived cells (T cells, B cells, mast cells dendritic cells or macrophages) (Katona *et al.,* 1988; Urban *et al.,* 2001) and that both IL-4 and IL-13 effect these cells in ways that contribute to expulsion (Urban *et al.,* 1998; Urban *et al.,* 2000).

Yet, evidence is lacking as to whether any of these effects or cell types are sufficient and/or essential for expulsion. Thus generating mice that selectively express IL-4Rα would contribute to the identification of the cell types participating in worm expulsion and could also elucidate the IL-4/IL-13/IL-4Rα-dependent mechanism of host protection via worm expulsion. An example of this is the conditional model where the mice are deficient in IL-4Rα expression exclusively in smooth muscle cells. This model has been used to study the role of the receptor, on these cells, in functions mediated in response to *Nippostrongylus brasiliensis* infection (Horsnell *et al.,* 2007).

1.6.3 Schistosoma mansoni.

Investigation in to host immune response to *Schistosoma mansoni* showed that both IL-4 and IL-13 are necessary for the induction Th2 inflammatory response which is a prerequisite for granuloma formation (Chiaramonte *et al.,* 1999; Wynn *et al.,* 1999). However, as above , the use of IL-$4^{-/-}$ mice led to the finding that IL-13, in contrast to IL-4, was more important in the regulation of collagen synthesis in parasite egg-induced granuloma formation (Chiaramonte *et al.,* 1999(b)). Macrophage/neutrophil-specific IL-4 receptor deficient mice were generated to investigate the role of the receptor and signaling via IL-4/IL-13 on myeloid cells during Th2 immune responses using *Schistosoma mansoni* infection of these mice (Herbert *et al.,* 2004). Results from the studies demonstrated that host survival was dependent on IL-4Rα signaling in macrophages.

The use of cell-specific IL4R$\alpha^{-/-}$ mice further demonstrated that subsequent to exposure to *S. mansoni* eggs T-cell-specific IL-4Rα signaling is essential for Th cell polarization. Furthermore using these mice enabled the differentiation between the role of the T cells and cells like macrophages in host survival (Leeto *et al.,* 2006).

It would thus be beneficial to combine the IL-4R$\alpha^{-/-}$ model with models where the IL-4Rα expression can be spatially and temporally deleted and reconstituted in certain cell populations. This could be achieved by combining the IL-4R$\alpha^{-/-}$ model with a model where the Tet system is used to induce expression in a cell-specific manner. Such strategies have the potential to overcome limitations inherent in conventional gene targeted mice, in addition such models could provide the tools necessary to investigate the precise role of IL-4Rα signalling in the generation and maintenance of organ specific immune responses, potentially providing a design paradigm for future analysis of the role for cytokines in immune-mediated regulation of infectious disease. Lastly, the resulting disease models could facilitate the design of novel therapeutic strategies to potentiate protection against debilitating infectious organisms.

Chapter 2: Inducible deletion of IL-4Rα expression.

Aim: Generation of new transgenic line, which would allow the inducible cell-specific reconstitution of IL-4Rα.

2.1 Introduction.

Studies with IL-4 knockout (IL-$4^{-/-}$) and IL-4Rα knock out (IL-$4R\alpha^{-/-}$) models have lead to novel findings. In the case of intestinal nematode parasites, such as *Nippostrongylus Brasiliensis*, the Th2 cytokines IL-4 and IL-13 were shown to have a distinct role in protection against these parasites. Additionally, IL-13 was shown to be more important than IL-4 as an inducer in the signalling pathway that stimulates the parasite's expulsion (Urban *et al.,* 1998 and Finkelman *et al*., 1999). Using *Schistosoma mansoni*, with these models, led to the findings that both IL-4 and IL-13 are required for the induction of the Th2 inflammatory response necessary for granuloma formation (Chiaramonte *et al*., 1999 a, b). However, there are weaknesses with the current knock out models. The existing models fail to discriminate between effects exerted during certain stages of the immune response and give no clear definition of exact cellular targets of cytokine action. Recent advances have made it possible to improve on the conventional IL-$4R\alpha^{-/-}$ mice using genetic manipulation and generating inducible cell-specific models allowing deletion as well as gene reconstitution. This will enable the investigation of the role of IL-4Rα signaling in the initiation and maintenance of organ-specific and non-polarized immune responses during infection.

The current chapter deals with the generation of a mouse model, which will enable the inducible and cell-specific deletion or reconstitution of IL-4Rα expression. The model described here has the potential to provide the means to analyze and define the role of IL-4Rα signalling and cytokine/cytokine receptor pathways in various murine infectious disease models. In order to achieve this, the Tet System, developed by Gossen and Bujard (1992), is being utilized (Figure 2.1). The end goal being to generate a model which would allow for the cell-specific, here hemapoeitic, and inducible reconstitution or deletion of IL-4Rα. Briefly, two transgenic (Tg) mouse lines were involved in the generation of the final double transgenic model. The first line expresses the transactivator, tTA, from the Tet-Off expression cassette. For the purposes of this study, we obtained the previously generated and characterised Vav-tTa transgenic line. In this line the expression of tTa is driven by the Vav hemapoeitic specific promoter (Wiesner *et*

al., 2005). The second mouse line expresses the IL-4Rα cDNA under the dictates of a cytomegalovirus (P^{CMV}) minimal promoter supplemented with seven tet operon (Tet_O) sequences. The operon serves as a binding site for the transactivator. After backcrossing both these lines to the IL-4Rα$^{-/-}$ BALB/c genetic background, the two transgenic lines will be crossed to generate a double transgenic mouse on the IL-4Rα$^{-/-}$ backbone. In these double transgenic mice, the transactivator will be synthesized in a cell specific manner leading to cell specific IL-4Rα reconstitution in the IL-4Rα$^{-/-}$ background. As this binding of the transactivator to the Tet_O is inhibited by tetracycline, oral administration of tetracycline will extinguish IL-4Rα expression. Ultimately, having this system on the IL-4Rα$^{-/-}$ background will allow for the reconstitution of the IL-4Rα gene in a cell specific and tetracycline-repressible manner.

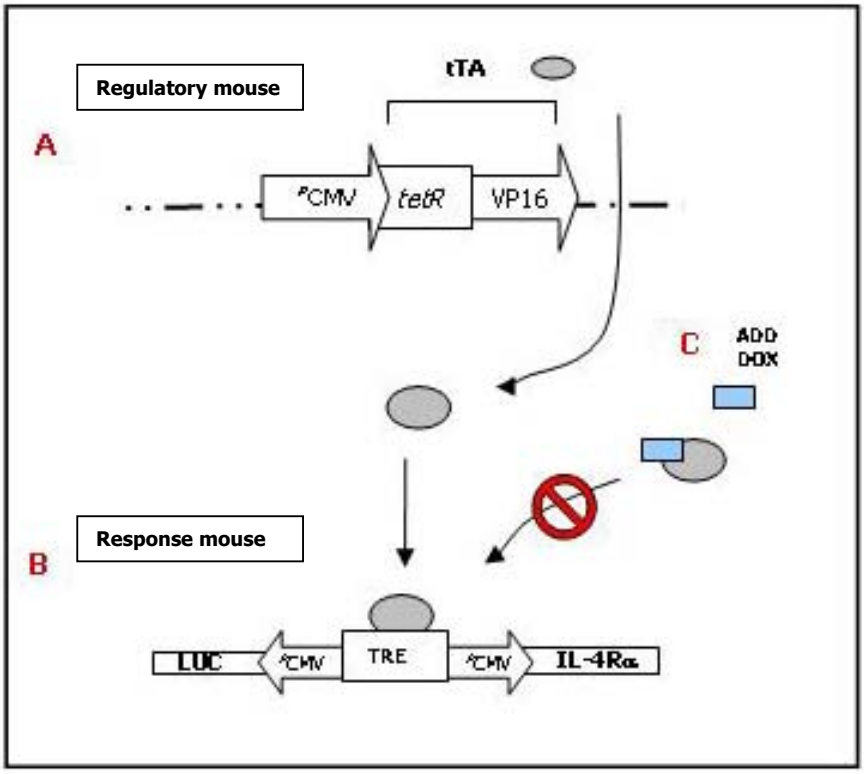

Figure 2.1 Tet-Off inducible systems.

In the Tet-Off system, the uninduced basal level of transcriptional activation is maintained in the presence of doxycycline. This prevents the binding of the tTa effector protein to the Tet_O sequences in the pBi-Luc / pBi-IL-4Rα vector. Tight binding is permitted with the removal of doxycycline, this induces high-level transcription. **Panel A**, The regulatory mouse, where the pTet-Off vector expresses the tTa transactivator protein. **Panel B**, The response mouse, where, if crossed with the regulatory mouse, tTa binds to Tet_O inducing target gene expression via the P^{CMV} bi-directional promoter. **Panel C**, Addition of doxycycline. The doxycycline binds to the tTA in this way preventing tTa binding to Tet_O and subsequent target gene expression. With the removal of the doxycycline the tTa binding is restored and target gene expression reactivated.

2.2 Methods and Materials.

2.2.1 Cloning of the constructs.

2.2.1.1 Plasmid purification.

All molecular biological manipulations were performed according to established protocols (Ausubel *et al.,* 1995). Chemicals and reagents were Molecular Biology Grade. Small-scale plasmid purifications were performed using a SV Wizard Plasmid Purification preps and a Wizard Maxiprep kit (Promega Corp., Madison, USA) was used for large-scale purifications, using protocols supplied with each kit.

2.2.1.2 Primer design.

Synthetic oligonucleotide primers were supplied by the Oligonucleotide Synthesis Facility, Department of Molecular and Cell Biology, University of Cape Town.

The template used for the primer design was the 2501bp cDNA encoding the transmembrane IL-4Rα (as described by Schulte *et al.,* 1997, and cloned into the pM5neo eukaryotic expression vector obtained from Prof. A. Gessner). For cloning and subsequent expression using the pBi-L vector (Baron *et al.,* 1995, CLONTECH Laboratories, Inc) the Kozak ribosomal binding sequence (Kozak, 1987) was included to improve subsequent expression. In order to do this the original primer used (in the above mentioned publication) was modified as follows; the sense primer used in this paper was discarded and a new one designed which included this Kozak consensus sequence and the *Mlu I* restriction enzyme sequence. The reverse primer sequence was modified by the addition of the *Eco RV* restriction site.

2.2.1.2.1 The transmembrane isoform of murine IL-4Rα.

Table 2.1 Sequences of oligonucleotides used for the amplification of IL-4Rα.

Name	Sequence
IL-4Rα reverse	5′ GGG **GATATC** CCCTGGCCTCAGCACAGACCTC ‘3 #
IL-4Rα forward	5′ GGG **ACGCGT** **ACCATGG** GGCGGCTTTGCACCAAGTTCCTGAC ‘3*

* The sequence corresponding to the *Mlu I* RE site is **bold** and the Kozak sequence is underlined.
\# The sequence corresponding to the *Eco RV* restriction site is in **bold**.

2.2.1.3 Vector Description.

The pBi-L vector, into which the IL-4Rα cDNA was subsequently cloned, is a response plasmid used to express both the gene of interest and luciferase from a bidirectional tet-responsive promoter (Baron *et al.,* 1995) in CLONTECH's Tet-Off™ Gene Expression Systems (CLONTECHniques XI(3):2–5). This system was used in order to utilize the tetracycline-regulated expression systems described by Gossen & Bujard (1992). The pBi-L vector contains the bidirectional promoter Pbi-1 which is responsive to the tTA regulatory protein in the Tet-Off systems. This promoter contains the Tet-responsive element (TRE), which consists of seven copies of the 42-bp tet operator sequence (tetO). The TRE element is between two minimal CMV promoters (P_{min}^{CMV}), which lack the enhancer that is part of the complete CMV promoter. This leads to, Pbi-1 being silent in the absence of binding by the tTA regulatory protein. P_{min}^{CMV1}controls the expression of the gene of interest while P_{min}^{CMV2}controls the expression of luciferase. Gene expression can thus be monitored indirectly via the luciferase reporter function.

2.2.1.4 Polymerase Chain Reaction (PCR).

2.2.1.4.1 Amplification of coding region for the transmembrane isoform of murine IL-4Rα.

The amplification of the coding region for the transmembrane isoform of the murine IL-4Rα cDNA fragment was performed by the Polymerase Chain Reaction (PCR) using the BD Advantage™ 2 PCR Kit (BD Biosciences Clontech) and 1ng pM5neo plasmid (obtained from Prof. A. Gessner) as template. This eukaryotic expression vector contains the 2501bp cDNA encoding the transmembrane isoform of IL-4Rα (Schulte *et al.,* 1997). The coding region was generated from RNA isolated from a BALB/c mouse. The choice of polymerase was based on the 2501bp length of the desired product. The BD Advantage™ 2 PCR Kit allows efficient and accurate amplification of DNA templates using long PCR. The PCR mix contains the TITANIUM Taq polymerase which allows automatic hot-start PCR and proofreading activity.The reaction was preformed in a 50µl volume containing 10 × BD Advantage 2 PCR Buffer, 50 × dNTP Mix (10mM each), 50 × BD Advantage 2 Polymerase Mix (all from BD Biosciences Clontech) and 0.75µM of each primer. For the target size of 2501bp the following cycling parameters were used: an initial denaturation step at 95°C for 1min, followed by 30 cycles consisting of 95°C incubation for 30s, an annealing step at 65°C for 2min, and an extension step at 72°C for 3min. A final step of 72°C for 5min was included to complete partial extension reactions.

2.2.1.5 Restriction and ligation of the coding sequence into the pBi-Luc eukaryotic expression vector.

The amplified fragments corresponding to IL-4Rα were recovered from a 1% (w/v) low melting agarose gel (section 2.1.7) and purified with the Wizard SV Gel Extraction Kit (Promega). The procedure was performed according to the manufacturer's recommendations. The isolated fragments were then digested with 10U of the restriction enzymes *Mlu I* and *Eco RV* (Roche Diagnostics GmbH, Mannheim, Germany) for 6h at 37°C. The digested fragments were recovered from a 1% (w/v) low melting agarose gel, and purified with the Wizard SV Gel Extraction Kit (Promega). A plasmid linearized by *Mlu I* / *Eco RV* cleavage was dephosphorylated in a 30µl reaction volume consisting of 1 × Shrimp Alkaline Phosphatase reaction buffer (Promega), 300ng pBi-Luc (Clontech) and 0.3U of Shrimp Alkaline Phosphatase (SAP). The mixture was incubated at 37°C for 15min, and the enzyme inactivated by incubation of the reaction at 65°C for 15min. Approximately 61ng of the purified fragment (in three-fold molar excess to vector) was mixed with 50ng dephosphorylated of pBi-Luc (Clontech), 1µl 10 × Ligation Buffer (Promega) and 1µl of T4 DNA Ligase (Promega, 3 Weiss U/µl) in a total volume of 10µl. An experimental control (background control) was included where the digested IL-4Rα insert fragment was omitted. The ligation reaction was allowed to proceed overnight at 4°C. Following ligation, 5µl of the ligation mix was added to 50µl of calcium chloride competent DH5α *E.coli* cells (Invitrogen, Gibco BRL, U.S.A.). The suspension was incubated on ice for 30min after which the cells were heat-shocked, according to the methodology of Inoue and co-workers (1990) at 42°C for 45sec. The transformed cells were immediately placed on ice (4°C) for a further 2min and 900µl of room temperature SOC medium [0.5% (w/v) yeast extract, 2% (w/v) tryptone, 10mM $NaCl_2$, 2.5mM KCl, 10mM $MgCl_2$, 20mM $MgSO_4$ and 20mM glucose] was added. Cells were incubated with shaking (200rpm) at 37°C for 1h. Following incubation, 100µl of the transformed cells were plated onto LB agar plates containing 50µg/ml ampicillin. Plates were incubated for 14h at 37°C. Plasmid DNA was isolated (see section 2.1.1) from overnight cultures containing 5ml LB medium supplemented with 50µg/ml ampicillin and colonies chosen randomly from the incubated plates. Positive constructs were identified by restriction enzyme screening with the restriction enzymes *Mlu I* and *Eco RV* (Roche), and verified by a secondary PCR screening with the oligonucleotide primers initially used to amplify the inserts. The correct fragments from both procedures were verified by electrophoresis on a 1% (w/v) agarose gel stained with ethidium bromide (0.5µg/ml*)* as described below (section 2.1.6). Plasmids found to contain correct inserts were sequenced by automated nucleotide sequencing pBi-IL-4Rα. Glycerol stocks were prepared of the *E.coli* DH5α cells

containing the pBi-IL-4Rα plasmids with the coding regions for IL-4Rα and stored at -70 °C.

2.2.1.6 Agarose gel electrophoresis.

All DNA samples including PCR products, restriction enzyme (RE) digestion and RE screening products, were verified by agarose gel electrophoresis through a 0.8 or 1% (w/v) agarose gels (gel percentage was dependant on fragment size) in 1 × TAE electrophoresis buffer. Samples were electrophoresed at constant voltage of 150V for 45min at room temperature. Gels were stained with ethidium bromide (0.5µg/ml). DNA was visualised by short wavelength UV transillumination (A_{254nm}).

2.2.1.7 Gel isolation and purification of DNA.

DNA samples including PCR products and samples from RE digestions of fragments to be used in ligation were electrophoresed on a 1% low melting point agarose gel in 1 × TAE electrophoresis buffer (containing 0.5µg ethidium bromide/ml) at 90V for 1h. DNA was visualised by brief exposure to low wavelength UV (A_{320nm}). The appropriate bands were excised from the gels with a sterile blade. Gel slices were melted by incubation at 65°C in heating block and DNA purified using the Wizard SV Gel Extraction kit (Promega), according to the manufactures instructions. DNA concentrations were determined from the absorbance of samples at A_{260nm} using the conversion factor for double stranded DNA (1OD unit = 50µg/ml).

2.2.2 Cell culture.

2.2.2.2.1 Hek 293T cells.

The human embryonic kidney 293 cell line (Hek 293T) (obtained from Gordon Brown, IIDMM, UCT Medical School) was used for all *in vitro* transfection and expression studies. The cells were cultured in DMEM medium pH7.4, supplemented with 10% Foetal Calf Serum (Gibco Life Technologies, Paisely, UK) 10mg/ml streptomycin and 10U/ml penicillin at 37°C and 5% CO2. Cells were passaged when cell monolayer reached ~70% confluence. Cells were split at a 1:10 ratio by aspirated the growth media from the cells and rinsing once with 1 x PBS. The adherent cells were then dislodged from the tissue culture flasks (Nalge Nunc International, Naperville, IL, USA) by addition of Trypsin-EDTA solution (0.53mM EDTA, 0.05% trypsin) (Gibco) and incubation for 1min at room temperature. After gentle tapping of the flask the suspension was diluted in DMEM supplemented with 10% FCS to inactivate the trypsin. This suspension was centrifuged at 1 200rpm for 8min and the supernatant carefully aspirated from cell pellet. Cells were

then resuspended in DMEM / 10% FCS and transferred to the appropriate size tissue culture flask.

2.2.2.2.2 Transfection of Hek 293T cells.

Unless otherwise stated, sub confluent Hek 293T cells (cell monolayer at ~70% confluence) were transfected in serum-free conditions using Lipofectamine Reagent (Invitrogen Corporation, Carlsbad, CA, USA). Lipofectamine Reagent (Invitrogen) employs a lipid-mediated (Felgner and Ringold, 1989) method; the transfection was preformed with optimization of the manufacture's instructions. Briefly, cells were plated at $2x10^5$cell/well in a 6 well tissue culture plate (Nalge Nunc International) and incubated at 37°C in a humidified 5% CO_2 for 18-24h. Subsequently, two tubes with 0.75ml DMEM media/well were prepared. 1ug isolated plasmid DNA, diluted to a working concentration of 1ug/ml in distilled H_2O, was added to one tube and to the other 5ul of Lipofectamine Transfection Reagent (Invitrogen). The reaction mixtures from the two tubes were combined and incubated at room temperature for 20min. The adherent Hek 293T cells were washed twice with 3ml/well serum-free DMEM media. The 1.5ml reaction mixture was then carefully plated onto the cells. The cells were incubated at 37°C in a humidified 5% CO_2 incubator for 24h. After over night incubation the serum-free media was aspirated from the cells and cells were re-incubated after the addition of 3ml DMEM supplemented with 10% Foetal Calf Serum (Gibco Life Technologies). The antibiotic 800µg/ml G418 (Sigma) was used to select (maintainace concentration of 400µg/ml) stable eukaryotic cell lines that have been transfected with the pTet-Off vector which contains the gene for neomycin resistance. With co-transfection with either the pBi-IL-4Rα or the control pBi-Gl vector 200µg/ml Hygromycin B was also added to the media as these vectors contain the hygromycin resistance gene.

2.2.3 *In vitro* and *in vivo* determination of transgene functionality.

2.2.3.1 Template preparation for qRT-PCR assays.

2.2.3.1.1 RNA Isolation.

Total RNA was extracted from transfected Hek 293T cells or splenocytes of transgenic mice using TriReagent (Molecular Research Company, Cincinnati, USA) as per the manufacture's instructions. The collected tissue was homogenized on ice in 2ml TriReagent for every 100mg of tissue. 200µl of chloroform was added for every 1ml of lysate and vortexed thoroughly. The samples were incubated at room temperature for 15min and centrifuged at 13 500rpm for 15min at 4°C. The top aqueous layer was

transferred to a new tube and an equal volume of 100% isopropanol added and mixed. The RNA was precipitated out of solution by incubating overnight at –80°C and centrifuging at 13 500rpm for 30min at 4°C. The RNA pellet was washed twice in 800µl 70% ethanol, air-dried and resuspended in 50µl-100µl of DEPC-treated water. All purified RNA samples were DNAseI treated and stored at -80°C. The quality of the RNA was checked by determining the ratio of the absorbance at A_{260}/A_{280} and by running 1µg of RNA on a 1% agarose gel that contained 2.2M formaldehyde. The concentration of the RNA was determined by measuring the A_{260}. All solutions, except TRIS-containing buffers, used for the RNA work were treated with DEPC to destroy any endogenous RNAses. To each solution, DEPC was added to a final concentration of 0.1% and gently shaken overnight at 37°C. The solutions were then autoclaved for 30min to remove any traces of DEPC. For TRIS-containing buffers, solutions were prepared using DEPC-treated water and an ultra-pure TRIS stock designated for RNA work only.

2.2.3.1.2 DNAseI treatment of isolated RNA.

The RNA was DNAseI treated to remove contaminating genomic DNA, proteins, residual phenol and salts. 1-10µg of total RNA was incubated with DNAseI cocktail (1 X DNAse1 buffer (Promega, Madison, WI, USA), 10U/µl DNAse1 (Roche Diagnostics GmbH, Mannheim, Germany), 1U/µl RNAsin (Promega, Madison, WI, USA) for 60min at 37°C. The DNAseI-treated RNA was purified from the digested DNA fragments and concentrated using the Qiagen MiniElute RNA cleanup kit (Qiagen, Valencia, CA, USA) as per the manufacturer's instructions. Briefly, the volume of the total RNA was adjusted to 100 µl by adding RNAse-free water. β-mercaptoethanol was added to Buffer RLT before use as per the manufacturer's instructions. 350µl of Buffer RLT was added to the RNA and vortexed. 250µl of 96% ethanol was added and vigorously vortexed to precipitate the RNA out of solution. Each sample was then applied to a single RNeasy mini-column and centrifuged at 10 000rpm for 15sec at room temperature. The flow-through was discarded and the RNeasy mini-column transferred to a new 2ml collection tube. The mini-column was washed with 500µl Buffer RPE and centrifuged at 10,000 rpm for 15sec at room temperature. The wash step was repeated and the mini-column centrifuged at 10,000rpm for 2min. The mini-column was then transferred to a new 2ml collection tube and centrifuged at 10,000rpm for 2min at room temperature to dry the membrane. After transfer to a new 1.5ml elution tube, 30µl RNAse-free water was added directly on to the membrane and incubated for 5min at room temperature. To elute the RNA the mini-column was then centrifuged at 10,000rpm for 1min at room temperature. This step was repeated and both 30µl RNA elutes pooled. The elimination of contaminating genomic DNA was confirmed by RT-PCR using primers that bound to genomic DNA. The quality

and quantity of the RNA was checked by spectroscopy and denaturing gel electrophoresis using standard methods (Sambrook and Russell, 2001). The A_{260}/A_{280} ratio was measured and an aliquot was run on a 1% agarose gel containing 2.2M formaldehyde. The RNA was stored at –80°C until used.

2.2.3.1.3 cDNA Synthesis.

The genomic DNA free RNA was reverse transcribed into cDNA using the ImProm-II™ Reverse Transcription System (Promega, Madison, WI, USA) as per the manufacturer's instructions. 0.5µg of Oligo (dT)15 primer was added to 1-10µg of genomic DNA free RNA in a final volume of 20µl. The sample was denatured at 70°C for 10min then immediately cooled on ice (4°C) for 5min. 20µl of cDNA synthesis cocktail (ImProm-II™ 5X Reaction Buffer, 4mM $MgCl_2$, 0.5mM each dNTP, 1U/µl RNAsin, 2.0µl ImProm-II™ Reverse Transcriptase) was added to the sample and samples then incubated at 25°C for 5min to anneal the primers. cDNA synthesis was extended at 55°C for 90min. The reaction was heat deactivated at 75°C for 5min and cooled at 4°C. The cDNA concentrations were determined from the absorbance of samples at A_{260nm} using the conversion factor for double stranded DNA (1OD unit = 50µg/ml). The samples were diluted to a 100ng/µl in PCR water, divided into aliquots and stored at –20°C.

2.2.3.2 Transcription assays.

2.2.3.2.1 Primers designed for expression assays.

Table 2.2 Sequences of oligonucleotides used for the expression studies

Name	Sequence	Product Size
Exon 8 forward	5′ GTA CAG CGC ACA TTG TTT TT '3	194bp
Exon 8 reverse	5′ CTC GGC GCA CTG ACC CAT CT '3	
β-actin forward	5′ TGG AAT CCT GTG GCA TCC AGA AAC '3	210bp
β-actin reverse	5′ TAA AAC GCA GCT CAG TAA CAG TCC '3	
IL-4Rα Tg forward	5′ TGA CCT ACA AGG AAC CCA GGC '3	168bp
IL-4Rα Tg reverse	5′ GAA CAG GCA AAA CAA CGG GAT '3	
Luc forward	5′ AAT CTG ACG CAG GCA GTT CT '3	186bp
Luc reverse	5′ CCA GGG ATT TCA GTC GAT GT '3	
tTa forward	5′ GGA CGA GCT CCA CTT AGA CG '3	183bp
tTa reverse	5′ GGC ATC GGT AAA CAT CTG CT '3	

2.2.3.2.2 qRT-PCR

The 2µl of the cDNA, at a final concentration of 10ng/reaction, was added to 18µl PCR cocktail (1 X Sensimix d(T) (Quantace, Neutral Bay, NSW, Australia) containing 1 X SYBR GreenI, 4.0mM $MgCl_2$, 0.5µM forward primer, 0.5µM reverse primer, 0.1mg/ml molecular grade BSA). PCR products were amplified on the Lightcycler (Roche) using the generic programme:1 cycle at 95°C for 10 minutes, 50 cycles of 95°C for 5 seconds, 62°C for 15 seconds, 72°C for 10-60 seconds depending on PCR product size. Extension time was calculated based on the fact that DNA Taq Polymerase can cover 25 base pairs (bp) per second: $Temperature_{extend}$ = (PCR product size in bp) / (25bp/second). Data was acquired at 80°C for 1sec. A melting curve analysis was performed at the end of the amplification program: 95°C for 0 sec, 75°C for 15sec, 65°C for 15sec and 95°C for 0sec with a ramping time of 0.1°C/sec. The β-actin gene was used as the housekeeping gene for data normalization. The levels of mRNA transcription relative to mRNA levels of a housekeeping gene (β-actin) were determined. For quantitative analysis data was analysed using the "Fit Points" and "Standard Curve Method". Primer sequences and product sizes are given in Table 2.2.

2.2.3.3 Translation assays.

2.2.3.3.1 Luciferase assay.

To determine the levels of luciferase expression the Luciferase Assay System was utilised (Promega). Prior to performing the assay the Luciferase Assay Reagent (LAR) was prepared by adding 10ml of the Luciferase Assay Buffer to a vial of lyophilized Luciferase Assay Substrate. To avoid freeze-thaw cycles the reconstituted reagent was dispensed into 100µl working aliquots (the reaction requires this volume to initiate enzyme activity) and stored at -70°C. 1 x Luciferase Cell Culture Lysis Reagent (CCRL, Promega) was prepared by adding 4 volumes of water to 1 volume of the 5 x lysis buffer supplemented with 1mg/ml BSA (the addition of BSA ensures that luciferase is not lost from solution by absorption). This buffer and the LAR were allowed to equilibrate at room temperature before use. Cell lysates were prepared for the both the adherent Hek 293T cells and the nonadherent splenocytes by lysis via resuspension with1 x lysis reagent. The suspensions were incubated at 4°C for 10min, vortexed for 10-15sec and centrifuged at 12,000 x g for 10min at 4°C. The supernatant was transferred to sterile eppendorf tubes and either stored at -70°C or used in the assay. 20µl of the cell lysate was dispensed in a 96 well half area black plate with clear bottom. Prior to assay the plate reading luminometer (Fluroscan Ascent FL, Thermo Scientific, USA) was programmed for a 10sec integration time, 2sec lag time and 100µl dispensing volume. The dispensing and aspirating tubing was primed with LAR and the dispensing head placed in the appropriate dispensing

position. The plate was placed into the luminometer which injected the 100ul LAR per well and read wells immediately after injection. The plate was then advanced to the next well and the process repeated. The results are given as relative light units (RLU). All values obtained from the luminometer indicating luciferase activity were normalized to total cell protein content.

2.2.3.3.2 FACS analysis.

Hek 293T cells were removed from tissue culture well plates (Nalge Nunc) using Trypsin/EDTA buffer (Gibco) and incubation for 1min at room temperature. After gentle tapping of the flask the suspension was diluted in DMEM / 10% FCS to inactivate the trypsin. The suspension was centrifuged at 1,200rpm at 4°C for 8min and the supernatant carefully aspirated from cell pellet. The cells were resuspended in 5ml DMEM / 10% FCS. Transgenic mice were sacrificed by cervical dislocation. Spleens were removed aseptically and placed in ice cold RPMI 1640 supplemented with 10% FCS (Gibco). Single cell suspensions were prepared and filtered through 70µm nylon cell strainers (Becton-Dickinson, New Jersey). Cells contaminated with red blood cells were resuspended in 5ml Red cell lysis buffer (0.15M NH4Cl, 1.0M NaHCO3, 0.1M Na2 EDTA) and underlayed carefully with 2ml heat inactivated FCS. The cells were centrifuged at 1 200rpm at 4°C for 10min and resuspended in 5ml RPMI 1640 / 10% FCS. Aliquots of cells (10µl) were diluted in Trypan Blue and counted on a Neubauer haemocytometer to determine concentrations of viable cells. For each staining $1x10^5$ cells were blocked for 25min in 100µl FACS buffer containing 1% heat inactivated rat serum and 4µg/ml 2.4G2 (anti-$F_c\gamma$RII and –III). The cells were washed in 500µl FACS buffer (PBS supplemented with 0.1% BSA and 0.05% Sodium Azide) and resuspended in 100µl FACS buffer containing one of the following antibodies to cell surface markers: $CD11^b$-Fitc , B220-Fitc, CD4-Fitc, CD124-PE, CD-45-biotin (BD Bioscience, Pharmigen, San Diego, CA). Cells were also stained in parallel for the isotype control for CD124: Rat $IgG_{2a\kappa}$. Cells were stained by incubation in the dark for 30min at 4°C after which the cells were washed with 500µl FACS buffer and centrifugation at 1,200rpm for 10min. Pelleted cells were resuspended and incubated for a further 15min on ice with 100µl of a saturating amount of streptavidin-APC (BD Biosciences) in FACS buffer. Cells were washed with 500µl FACS buffer and centrifugation at 1,200rpm for 10min. After this final wash, cells were resuspended in 300µl FACS buffer supplemented with 7-AAD (Sigma, St. Louis, USA). Dead cells stained with 7-AAD were excluded from analysis. Stained cell acquisition was preformed using a FACSCalibur flow cytometer (BD Biosciences) and data analyzed using CellQuest software (Becton-Dickinson, Ferndale, South Africa). 100,000 cells were acquired for analysis.

2.2.4 Generation of chimeras.

2.2.4.1 Generation of pBi-IL-4Rα Tg chimeras.

For protocol see Appendix A.

2.2.4.2 Genotyping of pBi- IL-4Rα Tg and pVav-tTa Tg.

2.2.4.2.1 Genomic DNA extraction.

Mouse-tail cuttings, approximately 1cm, were digested overnight in digestion buffer (50mM Tris-HCl, pH8; 100mM EDTA; 100mM NaCl, 1% SDS, 0.5mg/ml Proteinase K) at 56°C with gentle shaking. The samples were centrifuged at 14,000 rpm for 15min and the clear supernatant transferred to a clean microcentrifuge tube. An equal volume isopropanol was added and thoroughly mixed. The genomic DNA was allowed to precipitate out of solution by incubating at room temperature for 30min and centrifuged at 14,000 rpm at 4°C for 30min. The genomic DNA pellet was washed in 1ml 70% ethanol, air-dried and resuspended in 500µl sterile water. The quantity and quality of the genomic DNA was checked by spectroscopy by reading the absorbance at A_{260} and A_{280}.

2.2.4.2.2 Genotyping PCR.

All mice were genotyped prior to experiments to confirm their genotype using gene specific primers. 2µl of genomic DNA was added to 48µl of PCR cocktail (1 X Supertherm PCR Buffer, 1.5mM $MgCl_2$, 0.2mM dNTPs, 0.125U/µl Supertherm Taq, 0.25µM forward primer and 0.25µM reverse primer). Control reactions included a (i) no template/water control, (ii) positive control and (iii) negative control. The PCR products were amplified on a MJ thermocycler (Biozym, Hessisch Oldendorf, Frankfurt, Germany). The PCR cycle for the *pBi-IL-4Rα Tg*: 1 cycle at 94°C for 1min; 25 cycles of 94°C for 1min, 58°C for 1min, 72°C for 1.5min; 1 cycle at 72°C for 5min. The PCR cycle for the *pVav-tTa Tg*: 1 cycle at 94°C for 10min (hot start); 30 cycles of 94°C for 30sec, 55°C for 30sec, 72°C for 1min; 1 cycle at 72°C for 7min. The PCR cycles for the *Wild-type* and *Knock-out alleles*: 1 cycle at 94°C for 1min; 40 cycles of 94°C for 30sec, 57°C for 30sec, 72°C for 1 min; 1 cycle at 72°C for 5min. The PCR products were analysed by gel electrophoresis. Primers used are listed in Table 2.3.

Table 2.3 Sequences of oligonucleotides used genotyping Tg mice.	
Name	**Sequence**
Glob forward	5′ TGA GTG TGC TGT TGT TGC TG ‘3 #
Glob reverse	5′ GGG TCC ATG GTG ATA CAA GG ‘3*
Vav forward	5′ CTC TCT TGC CTG CCT GTG ‘3 #
Vav reverse	5′ GTA AAC TTC TGA CCC ACT GGA AT ‘3*
Wild-type allele forward	5′ GTA CAG CGC ACA TTG TTT TT ‘3 #
WT reverse	5′ CTG GGC GCA CTG ACC CAT CT ‘3*
Knockout allele forward	5′ GGC TGC TGA CCT GGA ATA ACC ‘3 #
KO reverse	5′ CCT TTG AGAACT GCG GGC T ‘3*

2.3 Results.

The following is a brief outline of the steps involved in the generation of the new transgenic model:

1. Transgene design and cloning, including sequence verification.
2. *In vitro* determination of transgene functionality.
3. Generation of chimeras.
4. Breeding and genotyping.
5. *In vivo* functionality assays.

2.3.2.1 Transgenic Construct design and cloning.

In order to generate the pBi-IL-4Rα inducible mouse model, cloning of the pBi-IL-4Rα response vector was required (illustrated in Figure 2.2). To sub-clone, and ultimately express the transmembrane isoform of mIL-4Rα the corresponding coding region was amplified using the pM5neo plasmid (Prof. A. Gessner) as template. The pM5neo eukaryotic expression vector contains the 2501bp cDNA encoding the transmembrane isoform of IL-4Rα (Schulte *et al.,* 1997). The cDNA was generated from RNA isolated from a BALB/c mouse.

Primers were designed to incorporate *Mlu I* and *Eco RV* restriction enzyme sites, to allow subsequent ligation into pBi-Luc expression vectors digested with the same set of enzymes. In order to improve translation, via an optimized transcription start site, the Kozak consensus sequence was incorporated in the forward primer sequence. The sequence is contiguous with the ATG start codon and greatly increases the efficiency of translation and hence overall expression of the product gene (Kozak, 1986). Primers were designed to generate this consensus sequence, at the 5' end of the amplified IL-4Rα cDNA fragment, by the addition of 3 extra bases.

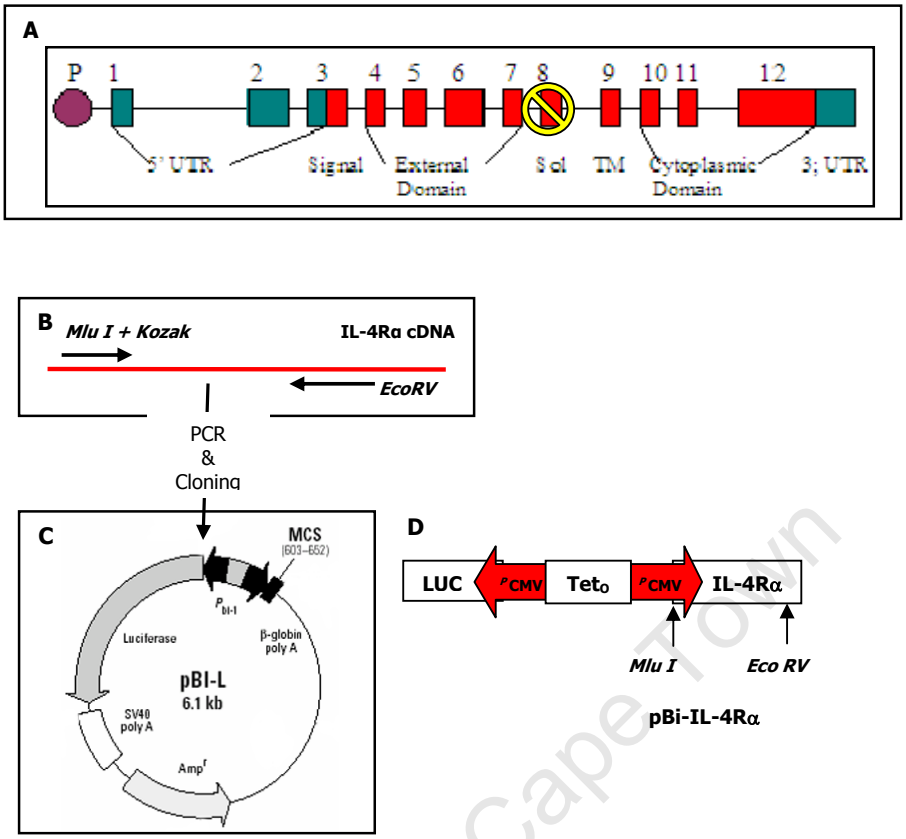

Figure 2.2 Flow Diagram of pBi-IL-4Rα Cloning Strategy.

Transgene design for the inducible reconstitution of IL-4Rα in IL-4Rα$^{-/-}$ mice. The expression construct is comprised of the IL-4Rα cDNA fragment cloned into the multi-cloning site of the pBi-Luc vector (Baron *et al.*, 1995). The bi-directional vector allows for the simultaneous expression of the IL-4Rα gene and the reporter gene luciferase driven by the minimal tet operon. **Panel A**, *IL-4Rα* map. Transmembrane isoform indicated. The transmembrane isoform coding region is 2501bp in length and codes for 831 amino acids. **Panel B**, Primer design and PCR of mIL-4Rα transgene using pM5neo as template. **Panel C**, RE digestion of amplified IL-4Rα cDNA and ligation into pBi-Luc. **Panel D**, The bi-directional mIL-4Rα expression cassette. The *Mlu I – Eco RV* ligation junctions are indicated.

Amplification produced the desired 2501bp mIL-4Rα cDNA fragment (Figure 2.3). The fragments were isolated from a low melting agarose gel and digested with the *Mlu I* and *Eco RV* enzymes. The digested fragments were isolated in the same manner as the PCR products and subsequently ligated into the pBi-Luc vector digested with the same restriction enzyme set as those used on the amplified mIL-4Rα cDNA fragment (see Figure 2.2 for vector construction scheme).

The construct was transformed into DH5α *E. coli* cells, and colonies screened by restriction enzyme digestion. The restriction enzyme combination of *Mlu I* / *Acc I* was used to identify the pBi-IL-4Rα colonies into which IL-4Rα had been ligated in-frame (Figure 2.4, Panel A). Using these enzymes, which have single recognition sites in the insert sequence (Fig.2.4.B), confirmed the orientation of the ligated cDNA fragment in the vector, which is important for the in-frame expression of the cloned cDNA. Furthermore, insert presence was confirmed with the *Mlu I* and *Eco RV*; both enzyme recognition sites were present at the ligation junction of positive clones. This digestion product, the 2501bp cDNA insert fragment is shown in lane 3. The sequences of inserts in positive constructs were subsequently verified by automated nucleotide sequencing after which the construct was referred to as pBi-IL-4Rα.

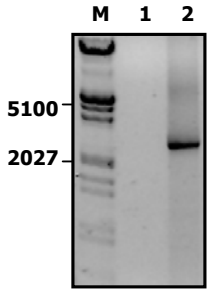

Figure 2.3 Amplification of transmembrane IL-4Rα cDNA fragment.

PCR was performed to amplify the coding region of the transmembrane isoform of mIL-4Rα using oligonucleotides specific for the sequence and pM5neo as template. A negative, no DNA control was included where no DNA template was added to the reaction mixture. 0.7% (w/v) agarose gel in 1 × TAE containing ethidium bromide and visualized using short wavelength UV transillumination. **Lane M**, DNA molecular weight marker. **Lane 1**, Amplified 2501bp IL-4Rα cDNA fragment.

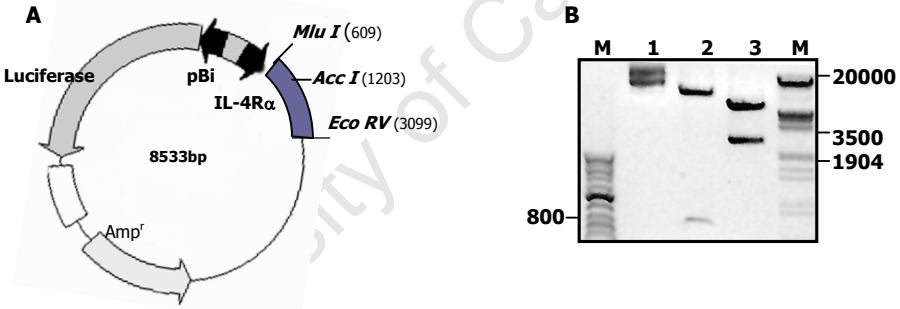

Figure 2.4 Restriction enzyme screening and sequence verification of the pBi-IL-4Rα transgenic construct.

Panel A, pBi-IL4Rα vector map. Enzymes used in RE screening indicated. The cDNA insert was ligated into pBi-Luc. Following transformation and plasmid isolation the colonies were screened via RE digestion. The illustration shows the theoretical recognition sites in colonies positive for the insert. **Panel B**, 0.7% (w/v) agarose gel in 1 × TAE containing ethidium bromide and visualized using short wavelength UV transillumination. **Lanes M**, DNA molecular weight marker. **Lane 1**, undigested pBi-IL4Rα. **Lane 2**, *Mlu I* | *Acc I* digestion products. **Lane 3**, *Mlu I* | *Eco RV* digestion products.

2.3.2.2 In vitro expression studies.

Prior to the generation of the chimera mice the functionality of the bi-directional mIL-4Rα construct under the control of the Tet system was assessed. All the functionality assays were performed in Hek 293T cells. Transfection efficiency was determined qualitatively via GFP UV fluorescence using the pGFP-N1 reporter constructs. In this reporter construct GFP expression is driven by the constitutively active CMV promoter (Figure 2.5.A). Vector transfection was optimized for the reagent used and the efficacy of Lipofectamine proved higher than Effectene (Figure 2.5, Panel C and B respectively). Transfection efficiency was additionally confirmed via FACS analysis of the fluorescence (GFP).

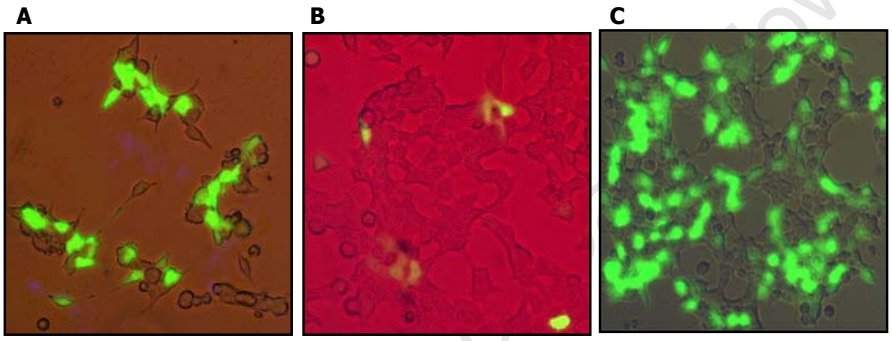

Figure 2.5 Optimization and assessment of Hek 293T cells transfection efficiency.

Panel A, **B** and **C**; UV fluorescent images of pGFP-N1 transfected Hek 293T cells. 24h Post transfection cells were analysed to assess transfection efficiency. **Panel A**, GFP fluorescing Hek 293T cells. **Panel B**, Hek 293T cells transfected with Effectene transfection reagent. **Panel C**, Hek 293T cells transfected with Lipofectamine transfection reagent. Images observed under 20X magnification.

2.3.2.2.1 Establishment of bi-directional promoter activity.

Binding of the tTA transactivator protein to the Tet_O operon, an element of the generated pBi-IL-4Rα response vector, leads to the simultaneous expression of the luciferase reporter and the gene of interest (in this case IL-4Rα). Thus, the chemiluminscent luciferase assay was used to confirm:

1. Efficient tTA expression;
2. Tet_O operon binding and
3. Bi-directional promoter functionality.

Western blots were performed to illustrate tTA expression but this assay proved unsuccessful. This could be attributed to the tTA expression being below detectable levels, as the transactivator is only needed in very low doses for successful promoter activation (Tet Systems Manual). Western Blots would also not have been sufficient since these only verify the presence of the tTa protein and does not reveal the functional role of the transactivator binding to the bi-directional promoter.

The Tet system functionality in Hek 293T cells is illustrated Figure 2.6. In the cell only and cells transfected with the response, pBi-IL-4Rα / pBi-Luc or the regulatory, pTet-Off, vectors only (first 4 bars in graph) background levels of chemiluminscence and thus luciferase expression was detected. These control experiments also served as an indication of the bi-directional promoter leakiness *in vitro*, as is observed by the background levels of luciferase expression shown by the response, pBi-IL-4Rα or pBi-Luc transfected cells only (bar 3 and 4 respectively). In the cells transfected with both the response, pBi-IL-4Rα or pBi-Luc, and the regulatory pTet-Off vectors an increased level of chemiluminscence and consequently luciferase expression was shown (bars 5 and 7). Accordingly, in the presence of doxycycline (bar 6 and 8) basal expression was undetectable and similar to that detected in the cell only control (bar 1).

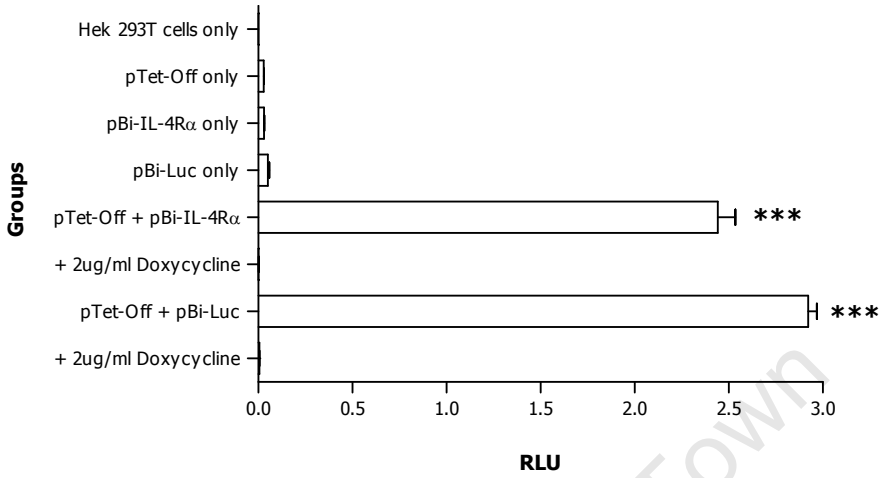

Figure 2.6 Induced luciferase expression in Hek 293T cells containing both response and regulatory vectors.

All experimental groups were transiently transfected with the vectors indicated. Luciferase induction levels were assayed 24h post transfection. Cells were incubated with 2υg/ml doxycycline 12h post transfection. The results represent 1 of 4 independent experiments and show the average ±_SEM of triplicate values. Statistical differences between groups calculated using unpaired Student's *t* test defining differences to untransfected Hek 293T cells as significant (***, p ≤0.0001). RLU refers to relative light units.

2.3.2.2.2 Establishment of effective doxycycline concentration and repression over time.

In the presence of doxycycline (Dox) the tTa effector protein, expressed via the Tet-Off regulatory vector, is unable to bind to the Tet_O operon sequences, thus suppressing target gene expression. Previously shown data suggests that the optimal concentration may vary between different cell lines (Tet Systems Manual). Additionally that full repression of gene expression in Tet-Off cell lines can be obtained with 10ng–1µg/ml Dox. Thus for the subsequent *in vitro* assays, using Hek 293T cells, it was necessary to determine the concentration of doxycycline which would lead to full suppression of tTa binding and transcriptional activation from the bi-directional promoter. For both the pBi-IL-4Rα and the control pBi-Luc vectors co-transfected with the pTet-Off regulatory vector, complete suppression was obtained with a concentration of 0.01µg/ml Dox present in the culture media (Figure 2.7, Panel A.1 and A.2 respectively).

Furthermore, when determining the decrease in luciferase expression with cells co-transfected with the pBi-IL-4Rα and pTet-Off vectors and cultured with 1µg/ml Dox efficient suppression was obtained after 12h of culture (Fig.2.7.B). Subsequently, a Dox concentration of 0.01µg/ml was used for suppression of target gene expression and analyzed 12h after addition of the Dox.

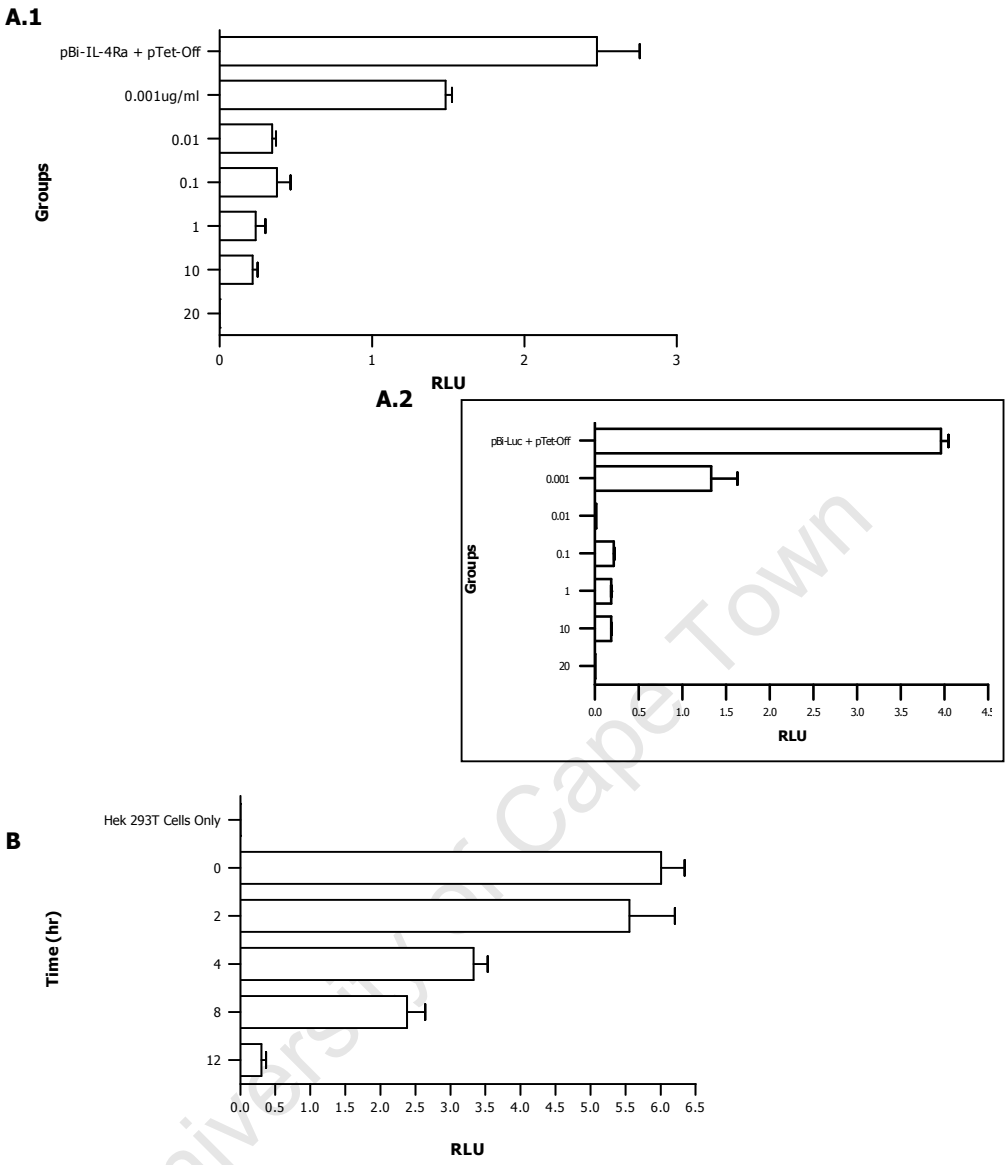

Figure 2.7 Doxycycline induced suppression of luciferase expression.

All experimental groups were transiently transfected with the vectors indicated. **Panel A.1** and **A.2**, Dose dependent suppression. Doxycycline, at the concentrations indicated, was added 6h post transfection and luciferase expression levels assayed 24h post transfection. **Panel B**, Time dependent suppression. Cells were incubated with 1ug/ml doxycycline. Luciferase induction levels were assayed at times indicated post transfection. The results represent 1 of 3 independent experiments and show the average ± SEM of triplicate values. RLU refers to relative light units.

2.3.2.2.3 Establishment of efficient pTet-Off: pBi-IL-4Rα plasmid ratio.

It has previously been shown that the ratio of the regulatory plasmid (pTet-Off) vs. the response plasmid is critical in transient expression studies. From these data, the suggested ratio is up to a 100-fold excess of regulatory plasmid over the response plasmid. These conditions assure high intracellular concentrations of the tTA effector protein and subsequent increased binding to the Tet_O operon on the response plasmid. Furthermore, these plasmid ratios give low background while maintaining a high expression potential. It was shown that in the presence of Dox, the background synthesis of reporter enzymes decreases proportionally when the amount of the response plasmid is lowered. This is in contrast to unsuppressed levels (i.e. Dox absent for media) which are affected less by the relative amount of the plasmid (Prof. H Bujard website).

Thus, in order to assess the IL-4Rα transgene expression accurately the ratio at which to transfect the regulatory pTet-Off and response pBi-IL-4Rα plasmid was determined quantitatively via qRT-PCR expression analysis of the luciferase reporter, tTa effector and IL-4Rα transgene. Hek 293T cells were transfected with the regulatory pTet-Off and response pBi-IL-4Rα vectors at plasmid ratios of 1:1, 1:10 and 10:1 respectively. Additionally cells were transfected with single vectors as control and with control pBi-Luc with pTet-Off at the same ratios as above. The control experiments (Figure 3.8, Panel A and A.1) determined the background expression and also the basal level of luciferase expression in the absence of doxycycline. With an response vector, pBi-Luc or pBi-IL-4Rα to regulatory vector, pTet-Off, ratio of 1:10 there was a significant increase (when compared to cells transfected with the single vectors values of $p < 0.05$ were obtained) to in luciferase expression in the cells transfected with the control plasmid (pBi-Luc) (A) and the generated pBi-IL4Rα plasmid (Panel A.1). This increased reporter expression was verified with qRT-PCR (Fig.2.8.A.2) which also indicated a significant difference when compared to cells transfected with single vectors only ($p < 0.0001$). Furthermore, with the tTa effector expression ($p=0.0033$) and the IL-4Rα transgene expression ($p < 0.0001$) was similarly elevated in cells containing a 10-fold excess of the regulatory plasmid (Fig.2.8.B and C respectively). These results are in agreement with the expected outcomes given by Prof. H.Bujard.

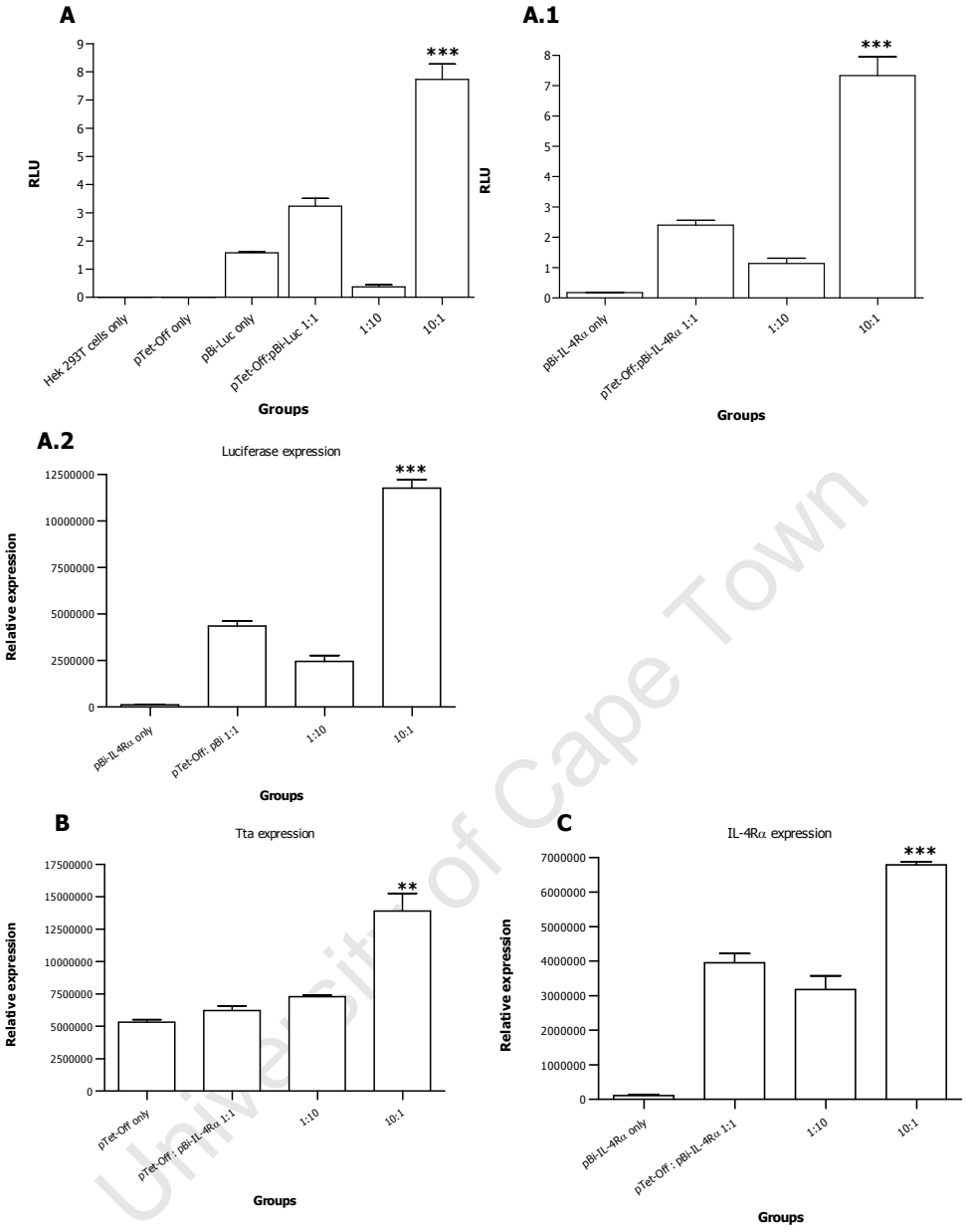

Figure 2.8 Effect of regulatory and response plasmid ratios on transgene expression.

All experimental groups were transiently transfected with the vectors and ratios indicated. **Panel A.1**, Control experiments. Luciferase expression levels assayed 24h post transfection via chemiluminscent assay. RLU refers to relative light units **Panel A.2**, Luciferase expression levels assayed 24h post transfection. Levels of luciferase mRNA relative to mRNA levels of a housekeeping gene (actin) were determined by real-time PCR. For both **Panel B** and **C;** Levels of tTa and IL-4Rα mRNA relative to mRNA levels of actin were determined by real-time PCR. **Panel B**, tTa effector protein expression levels 24h post transfection **Panel C**, IL-4Rα transgene expression levels 24h post transfection. Statistical differences between groups calculated using unpaired Student's *t* test defining differences to cells transfected with single vectors as significant (***, p ≤0.0001, **p=0.0033).The results represent 1 of 3 independent experiments and show the average ± SEM of triplicate values.

2.3.2.3 *In vitro* inducible repression of IL-4Rα expression.

2.3.2.3.1 Transcription efficiency of mIL-4Rα transgene.

Subsequent to the completion of the pilot studies (section 2.2.2) stable cell lines were generated and clones tested for relevant gene expression via quantitative RT-PCR.
As expected a higher level of tTa mRNA correlated with an increase in transcription from the bi-directional promoter, leading to increased levels of the IL-4Rα transgene mRNA (Figure 2.9, Panel A and B respectively).
In Panel A, no transcription was observed in the untransfected Hek 293T cells. In contrast, when compared to the untransfected cells, there was a significant ($p < 0.05$) increase in the levels of transcribed tTa mRNA in both the single and double cell lines. This clearly indicated the transcriptional activity of the regulatory plasmid. IL-4Rα transcription was also significantly elevated, but only in the double cell line containing both the response and regulatory vectors (Fig 2.9.B). This confirmed the transcriptional activity of the response vector.

2.3.2.3.2 Translation efficiency of mIL-4Rα transgene.

To asses the *in vitro* functionality of the IL-4Rα transgene further FACS analysis was utilised to determine the translational levels of the transgene. In this, and subsequent expression studies, the untransfected Hek 293T cell line was used as control. The IL-4Rα cell surface expression was analyzed using four colour FACS analysis where different cell populations were identified by cellular staining with fluorescence labelled antibodies. The choice of antibody was based on specificity to the murine IL-4Rα markers which would be present on the double stable expressing cell line only. Isotype controls for the antibodies were employed to ensure antibody specificity and additionally functioned as negative controls for the staining. To isolate the viable cells, the cells were incubated with 7-AAD or propidium iodide which is a marker for non-viable cells.
The stained pTet-Off-pBi-IL-4Rα Hek 293T cell line, showed a positive shift in murine IL-4Rα surface expression when compared to the controls, namely, untransfected cells and cells containing the single vector only (Figure 2.10, Panel A). Similarly, the untransfected and transfected cell isotype controls also lacked a shift indicating positive murine IL-4Rα surface staining (Fig.2.10, Panel B.1 and B.2 respectively).

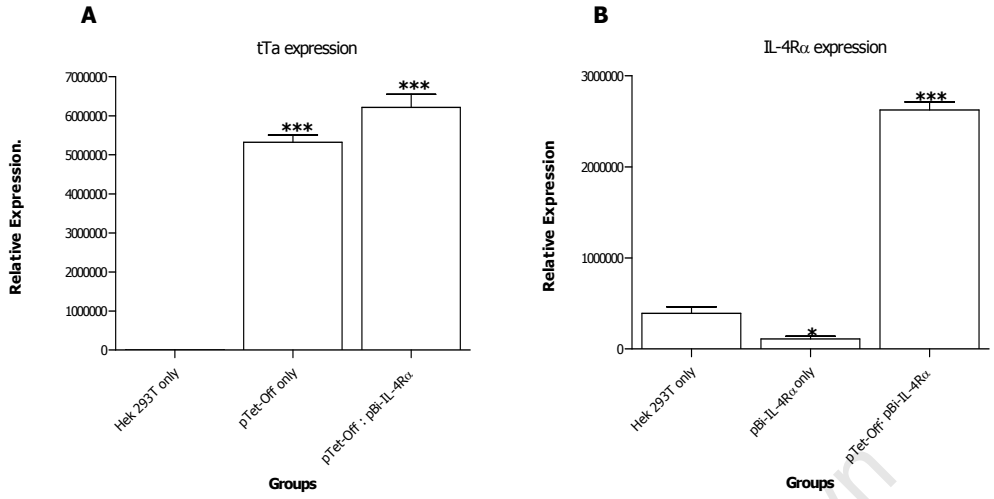

Figure 2.9 Transgene mRNA levels in stable pTet-Off-pBi-IL-4Rα Hek 293T cell line.

Single stable and double stable cell lines indicated. Cells were harvested and cDNA synthesized from transfected and untransfected Hek 293T cells. **Panel A**, Regulatory plasmid, pTet-Off expression. Levels of tTa effector mRNA relative to mRNA levels of a housekeeping gene (actin) were determined by real-time PCR. **Panel B**, Response plasmid, pBi-IL-4Rα expression. Levels of IL-4Rα mRNA relative to mRNA levels of actin. Statistical differences between groups were calculated using unpaired Student's *t* test defining differences against untransfected Hek 293T cells as significant (***, p ≤0.0001, *p=0.05).The results represent 1 of 3 independent experiments and show the average ± SEM of triplicate values.

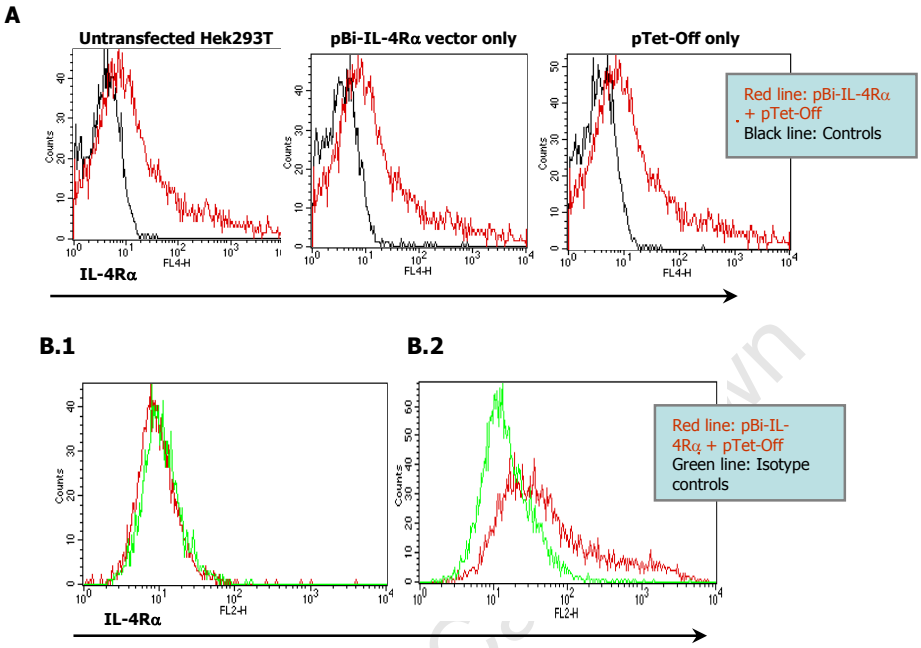

Figure 2.10 IL-4Rα transgene expression in Hek 293T cells.

Panel A and **B**, Histograms indicating the shift in fluorescence due to positive murine IL-4Rα surface expression. **Panel A**, The cell and vector controls. Hek 293T cells untransfected, and transfected with the single vectors only, and stained for murine IL-4Rα expression. **Panel B.1 and B.2**, Isotype controls. Untransfected and double stable Hek 293T cells stained for murine IL-4Rα. Lines representing differently stained cells are indicated in the legend. Histograms are representative of populations gated for viable cells. Results shown are for 1 of 4 independent experiments.

2.3.2.3.3 In vitro inducible repression of mIL-4Rα expression.

In the absence of Dox the tTa effector protein expressed via the pTet-Off regulatory vector binds uninhibited to the Tet_O operon located on the pBi-IL-4Ra response vector. In this way, target gene expression is initiated from the bi-directional promoter element. We had previously established the optimal Dox concentration and the time necessary for efficient suppression of target gene expression (see section 2.2.2.2). To proceed with the *in vitro* studies to establish the IL-4Rα transgene functionality, the inducibility of the transgene expression, as opposed to the luciferase reporter studied previously, was investigated. The pTet-Off-pBi-IL-4Rα Hek 293T cell line was incubated with Dox (1µg/ml) and as with the luciferase studies; cells were harvested at certain time points, and analyzed for IL-4Rα transgene surface expression via FACS analysis. The stained pTet-Off-pBi-IL-4Rα Hek 293T cell line, showed a positive shift in murine IL-4Rα surface expression when compared to the controls, namely, untransfected cells and the antibody isotype control showed the desired lack of a positive fluorescent shift in the lower right quadrant of the illustrated dot plot (Figure 2.11, Panel A and B respectively). At 0h, time indicating addition of Dox, ~18% of the cells stained positive for murine IL-4Rα surface markers (Fig.2.11.C). This percentage decreased to that of ~1.8% at 24h of Dox incubation. This confirmed the *in vitro* functionality and inducibility of the generated pBi-IL-4Rα transgenic construct.

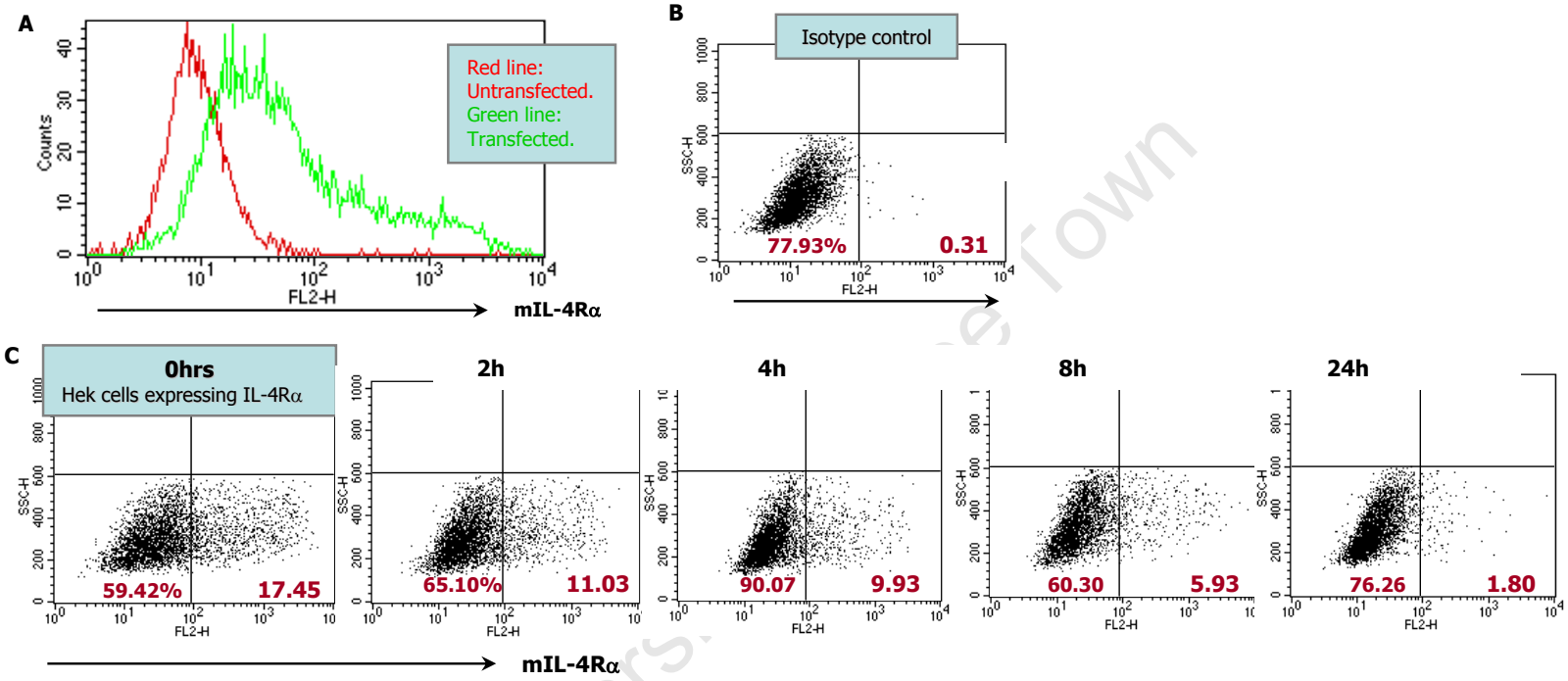

Figure 2.11 Inducible IL-4Rα transgene repression in Hek 293T cells.

Panel A, Untransfected cell control. Histogram indicating the shift in fluorescence due to positive murine IL-4Rα surface expression on pTet-Off-pBi-IL-4Rα Hek 293T cells. Lines representing different cells are indicated in the legend. **Panel B**, The antibody isotype control. Dot plot of pTet-Off-pBi-IL-4Rα cells stained for Rat IgG2a, K expression. **Panel C**, Time dependant suppression of expression, hours represent time after addition of doxycycline. Double stable Hek 293T cells stained for murine IL-4Rα. Percentage values in the lower right quadrant indicating positive mIL-4Rα surface expression. Histogram and dot plots are representative of populations gated for viable cells. Results shown are for 1 of 3 independent experiments.

2.3.2.4 Generation and analysis of single transgenic chimeras.

2.3.2.4.1 Generation of pBi-IL-4Rα Tg chimeras.

Following the *in vitro* functional analysis of the pBi-IL-4Rα vector, chimeric mice were generated, by Nucleis in France, in a process (complete protocols as supplement to Methods section) that involved the following steps (illustrated in Figure 2.12):

- Targeted insertion of the modified transgene into the *hprt* docking sites via homologous recombination (Panel A).
- Electroporation of transgene into embryonic stem cells recombinant clones (B). Positive clones are identified by HAT selection.
- Positive cells were microinjected (C) into blastocysts, derived from pseudo pregnant females, and implanted into pseudo pregnant mice.

The advantages of this targeted insertion of the transgene into the *hprt* docking site are two-fold, firstly, the locus demonstrates no intrinsic enhancer activity and secondly it provides a permissive chromatin environment that supports promoter dependent transgene expression. The inserted transgene is X chromosome-linked. 7 male pBi-IL-4Rα chimeric were successfully generated (Fig.2.12.D).

In order to generate the desired model where IL-4Rα is expressed in cell-specific and inducible manner, the chimeric mice needed to be with an additional transgenic line, the regulatory line, which would contribute the transgene to express the tTa effector Due to the particular immunoregulatory roles of IL-4 and IL-4Rα we were interested to achieve hematopoietic tissue specific inducible IL-4Rα expression and it is to this end that we obtained the tTA-Vav transgenic line (Prof. D. Largaespada). In this line the tetracycline transactivator (tTA) expression is driven by the Vav hematopoietic promoter (Wiesner *et al.*, 2005).

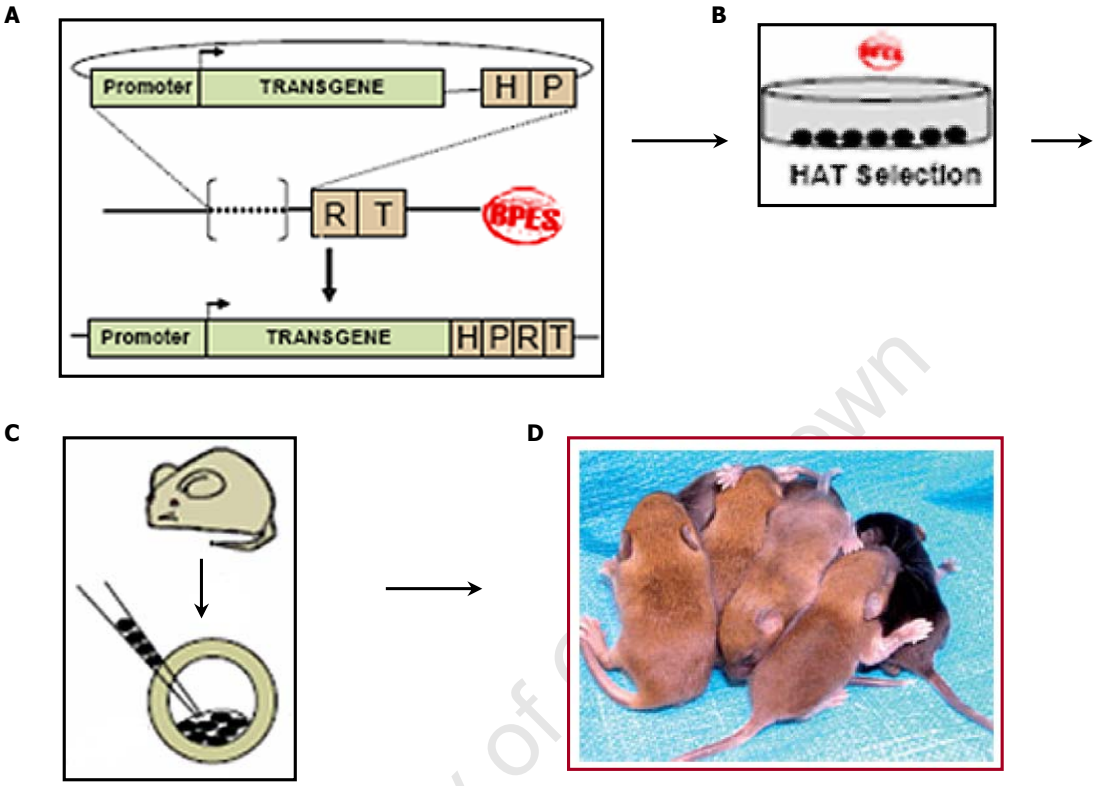

Figure 2.12 Flow diagram of generation of pBi-IL-4Rα chimeric mice.

Panel A, The targeted insertion of the pBi-IL-4Rα into the *hprt* docking site. **Panel B**, Electroporation of the modified pBi-IL-4Rα transgene into BPES cells. **Panel C**, Microinjection of the recombinant ES clones into blastocysts. Blastocysts were derived from pseudo pregnant female. **Panel D**, Birth of pBi-IL-4RαTg chimeric mice.

2.3.2.4.2 Breeding program.

Subsequently, both the pBi-IL-4RαTg and pVav-tTavTg founder lines underwent an extensive breeding program (illustrated in Figure 2.13). Briefly, the two separate lines (pBi-IL-4RαTg and pVav-tTaTg) were crossed into the IL-4Rα$^{-/-}$ BALB/c mouse line (Fig.2.13.A). Using the IL-4Rα$^{-/-}$ background is required for the tissue specific reconstitution and deletion of the receptor. Additionally, a BALB/c genetic background would be ideal when studying the role of IL-4Rα in immunity when working with for example allergy and nematode parasites, as this genotype skews to a Th2 response. This genetic background responds in a highly Th2 biased way, while still being able to produce a Th1 response. Another reason for the use of BALB/c mice is also breeding convenience, as all IL-4Rα$^{-/-}$ and cell specific IL-4Rα$^{-/-}$ models available and in use in the laboratory are on a BALB/c background and are thus relevant for the Th2 pathologies studied here.

After positive genotyping analysis confirming genetic background, transgene presence and IL-4Rα$^{-/-}$ knockout status the progeny, of the above-mentioned cross, were inter-crossed (Fig.2.13.B) to create the final model. This line consisted of a double transgenic, pBi-IL-4RαTg and pVav-tTaTg, on an IL-4Rα$^{-/-}$ BALB/c background.

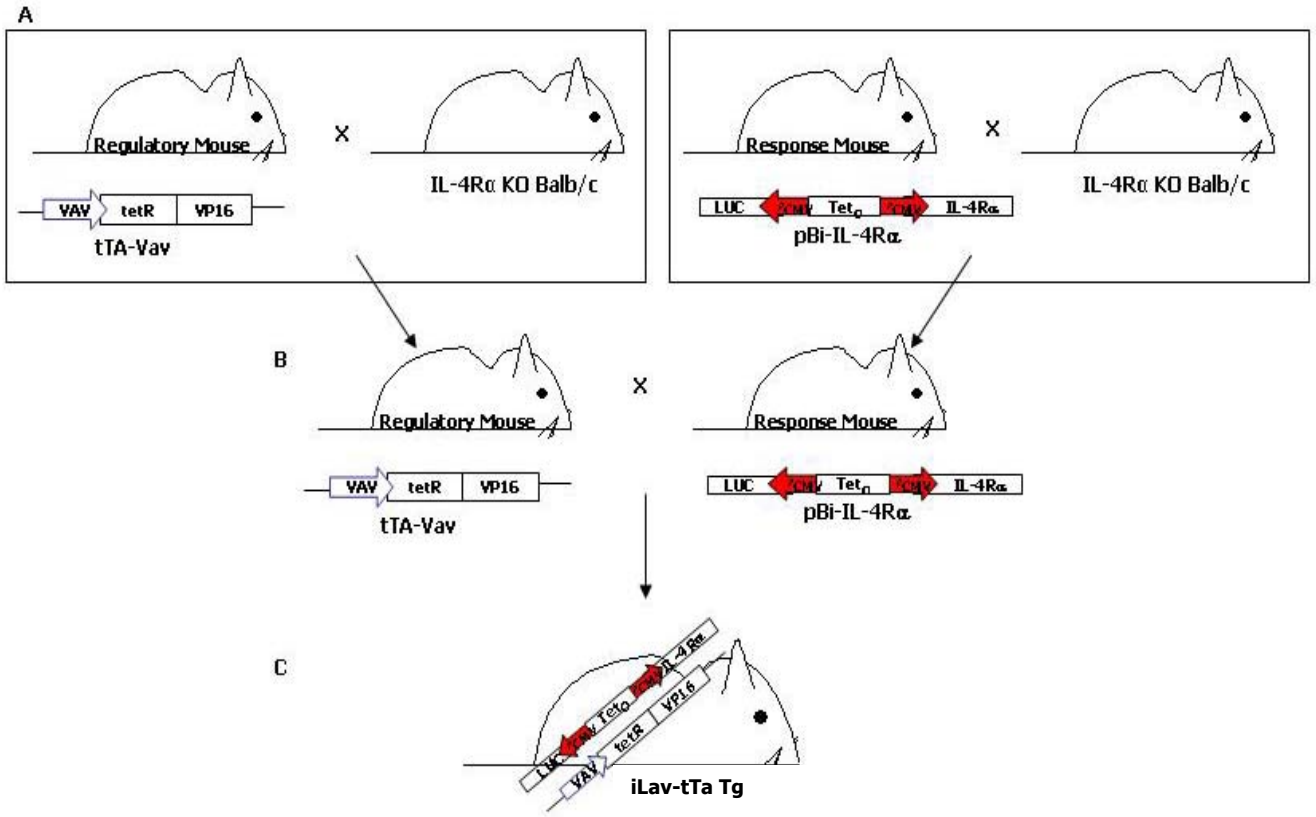

Figure 2.13 Breeding scheme for the generation of the final inducible model.

Panel A, Separate mating schemes for the crossing of pBi-IL-4RαTg and pVav-tTaTg founder lines into the IL-4Rα$^{-/-}$ BALB/c background. **Panel B**, Inter-crossing of the pBi-IL-4RαTg IL-4Rα$^{-/-}$ BALB/c and pVav-tTaTg IL-4Rα$^{-/-}$ BALB/c progeny from the two separate crossings in **A**. **Panel C**, Progeny of **B** result in the final inducible model. With a pBi-IL-4RαTg / pVav-tTaTg / IL-4Rα$^{-/-}$ BALB/c genotype.

2.3.2.4.3 Stringent control of IL-4Rα expression in pBi-IL-4RαTg / IL-4Rα $^{-/-}$ BALB/c mice.

The modified CMV minimal promoter driving expression of both the luciferase and IL-4Rα genes, in pBi-IL-4RαTg / IL-4Rα $^{-/-}$ BALB/c mice, lacks the strong enhancer elements typically associated with CMV immediate early promoters (Tet System Manual). Furthermore, due to the absence of these enhancer elements, there should theoretically be extremely low background expression of luciferase and IL-4Rα, from the Tet_O, in the absence of binding and activation by the TetR domain of transactivator protein tTA.

In order to test the stringency of the CMV driven target gene expression, FACS analysis was employed to establish the extent of the transgene leakiness, and thus non-specific expression, in the generated pBi-IL-4RαTg / IL-4Rα $^{-/-}$ BALB/c single transgenic model. Following positive genotyping verification, splenocytes from BALB/c, IL-4Rα $^{-/-}$ BALB/c and pBi-IL-4RαTg / IL-4Rα $^{-/-}$ BALB/c mice were analyzed for IL-4Rα expression. The IL-4Rα $^{-/-}$ and BALB/c models were included as controls for negative and positive IL-4Rα expression. Expression was specifically analyzed in granulocytes, T cells and B cells. As expected, IL-4Rα staining was clearly apparent in BALB/c mice and absent in IL-4Rα $^{-/-}$ mice in all the cell populations. No IL-4Rα surface expression was found in the pBi-IL-4RαTg / IL-4Rα $^{-/-}$ BALB/c mice. Staining results are indicative of the stringency of expression via the Tet system and confirm the lack of transgene leakiness in the generated pBi-IL-4RαTg / IL-4Rα $^{-/-}$ BALB/c mice single transgenic line.

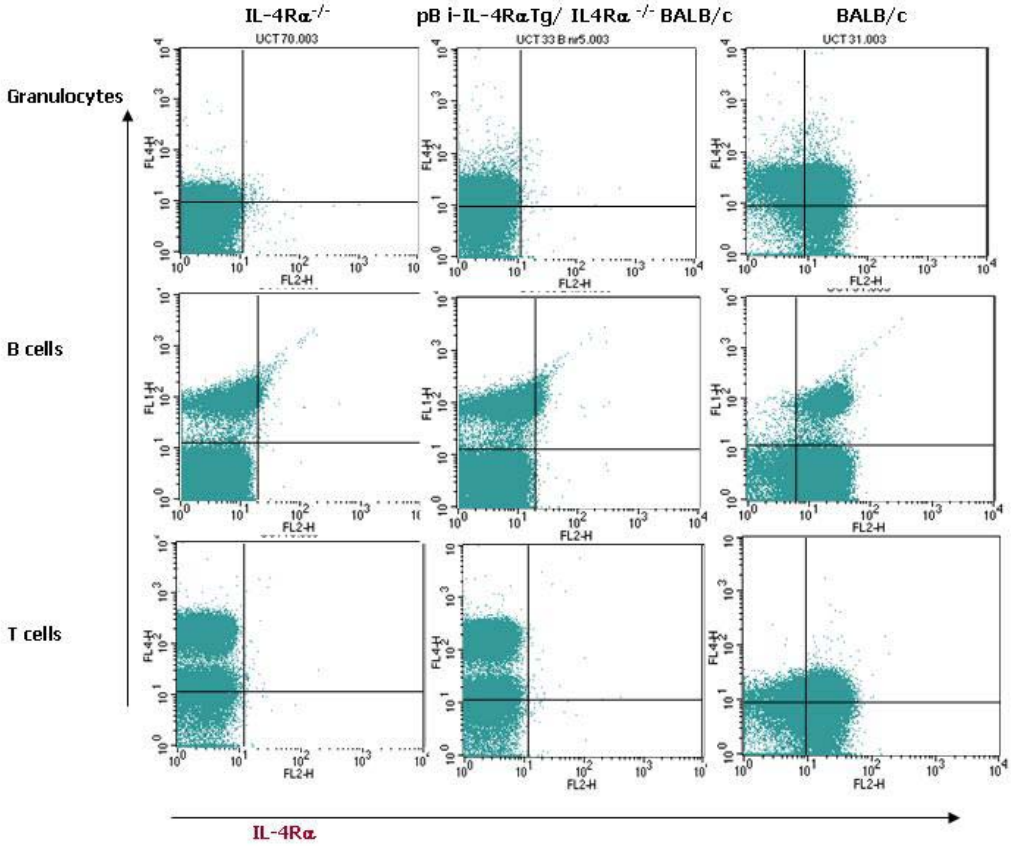

Figure 2.15 IL-4Rα transgene leakiness via the CMV promoter.

The IL-4Rα cell surface expression was analyzed using four colour FACS analysis where different cell populations, namely granulocytes, B cells and T cells, were identified by cellular staining with fluorescence labelled antibodies. To isolate the viable cells, the cells were incubated with 7-AAD which is a marker for non-viable cells. Dot plots indicating the shift in fluorescence due to positive murine IL-4Rα surface expression. The three experimental groups are indicated. Positive staining for all groups indicated in the upper right quadrant. Dot plots are representative of populations gated for viable cells. Results shown are for 1 of 4 independent experiments.

2.3.2.4.4 Genotyping of pBi-IL-4RαTg / IL-4Rα $^{-/-}$ BALB/c and pVav-tTaTg / IL-4Rα $^{-/-}$ BALB/c.

The genotypes of the genetically modified mice were confirmed via PCR analysis. For the pBi-IL-4RαTg / IL-4Rα $^{-/-}$ BALB/c transgenic model the presence of the transgene was determined by using a set of primers (Glob R & F) binding to and amplifying a region that includes 43bp of IL-4Rα coding region and 92bp of b-globin ploy A signal (illustrated in Figure 2.14, Panel A). The primers were designed to be specific for the transgene and stringent PCR conditions allow for the amplification of a 193bp fragment only in mice where the transgene is present. For the identification of mice with the pVav-tTaTg transgene PCR primers and conditions were obtained from the researchers involved in the generation of this model. The primers, specific for the pVav-tTa transgene, were used in combination with primers designed to amplify the endogenous Tsh1 locus as a reaction control (Fig.2.14.B).

To discern between mice with a IL-4Rα$^{-/-}$ genotype and those still containing the IL-4Rα gene two sets of primers were used, one amplifies the wild-type allele and another that amplifies the "knockout allele". In an IL-4Rα$^{-/-}$ mouse exons 7, 8 and 9 of the IL-4Rα gene are deleted. The forward primer to the wild-type allele binds in exon 7 and the reverse primer in exon 8 resulting in the amplification of a 600bp fragment from DNA of a wild-type mouse where these are present (Fig.2.14.C). For the knock-out genotype, the forward primer of the knockout allele binds in exon 6 and the reverse primer in exon 10. Using DNA from a KO mouse, these primers would amplify 471bp fragment, but the ~3000bp region between exon 6 and 10 in a wild-type mouse is too vast to amplify. Therefore, only BALB/c wild-type mice would contain the 600bp wild-type fragment and the 471bp knockout allele would only be present in DNA from mIL-4Rα$^{-/-}$ mice (Fig.2.14.D).

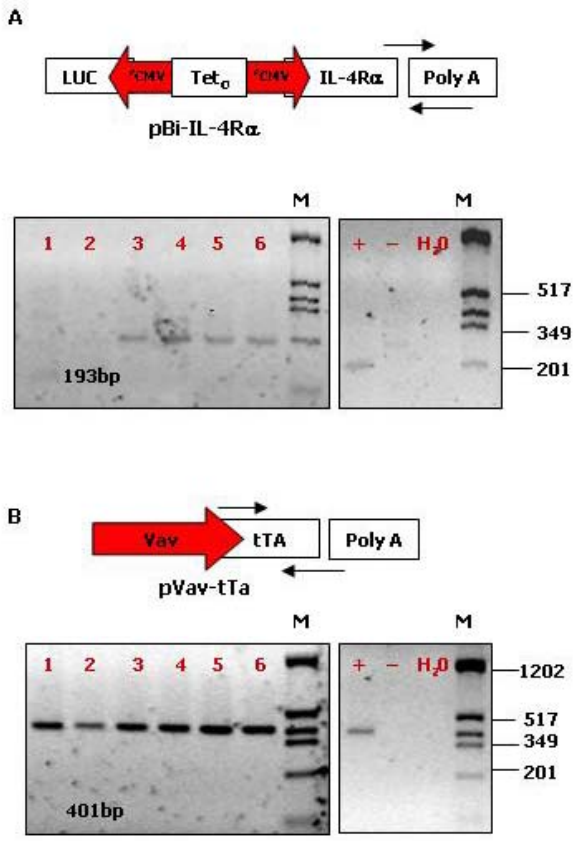

Figure 2.14 Genotyping of generated transgenic lines.

Four separate PCRs were used to identify pBi-IL-4RαTg / IL-4Rα $^{-/-}$ BALB/c / pVav-tTaTg/ IL-4Rα $^{-/-}$ BALB/c. In all panels; 1.2% (w/v) agarose gel in 1 × TAE containing ethidium bromide and visualized using short wavelength UV transillumination. A negative (H_2O), no DNA control was included where no DNA template was added to the reaction mixture. The second negative control (-) uses DNA extracted from a BALB/c wild-type mouse. Positive (+) controls using previously identified templates positively amplified with the reaction primer set. **Panel A**, Lanes 1-6, amplification products using glob F and R on DNA extracted from 6 pBi-IL-4RαTg / IL-4Rα $^{-/-}$ BALB/c / pVav-tTaTg/ IL-4Rα $^{-/-}$ BALB/c littermates. The 193bp fragment indicates the presence of the transgene in lanes 3-6. **Panel B**, Products using tTa R and F on the same samples as in **A.** The 401bp fragment in lanes 1-6 indicates the presence of the transgene.

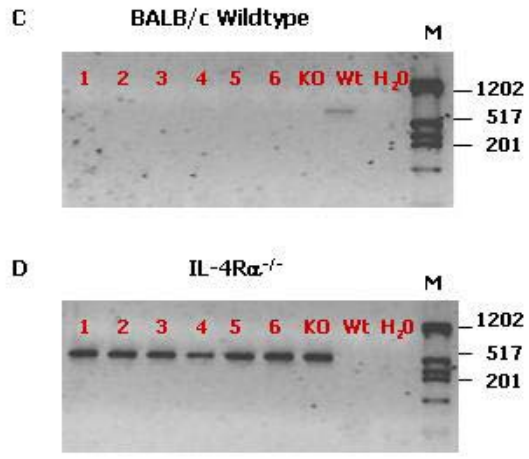

Figure 2.14 Genotyping of generated transgenic lines.

Four separate PCRs were used to identify pBi-IL-4RαTg / IL-4Rα $^{-/-}$ BALB/c / pVav-tTaTg/ IL-4Rα $^{-/-}$ BALB/c. In all panels; 1.2% (w/v) agarose gel in 1 × TAE containing ethidium bromide and visualized using short wavelength UV transillumination. A negative (H_2O), no DNA control was included where no DNA template was added to the reaction mixture. The second negative control (-) uses DNA extracted from a BALB/c wild-type mouse. Positive (+) controls using previously identified templates positively amplified with the reaction primer set. **Panel C**, Amplification for the BALB/c wild-type allele, the 600bp fragment is only present in the Wt control sample. **Panel D**, The reaction products from the knock out amplification where the 471bp fragment in lanes 1-6 and the KO control indicates the IL-4Rα$^{-/-}$ genotype.

2.3.2.5 Analysis of pBi-IL-4RαTg / IL-4Rα $^{-/-}$ BALB/c / pVav-tTaTg/ IL-4Rα $^{-/-}$ BALB/c.

Following the breeding and establishment of the final pBi-IL-4RαTg / pVav-tTaTg / IL-4Rα$^{-/-}$ BALB/c double transgenic line, the *in vivo* functionality of the transgenes and the Tet system was established. Analysis on a transcriptional and translational level was performed to show IL-4Rα reconstitution confined to hemopoeitic cells.

2.3.2.5.1 Transcriptional analysis.

To assess the transcriptional activity of the incorporated transgenes, namely the murine IL-4Rα (from pBi-IL-4RαTg) and the tTA transactivator (from pVav-tTaTg), quantitative real time-PCR was performed. In addition to transcriptional levels, this analysis confirmed the bi-directional promoter activity via analysis of the luciferase reporter expression. The choice of experimental groups was based on the positive genotyping results, which verified transgene presence and the IL-4Rα $^{-/-}$ BALB/c background. Groups analyzed included; the single transgenic lines, namely pVav-tTaTg/ IL-4Rα $^{-/-}$ BALB/c and pBi-IL-4RαTg / IL-4Rα $^{-/-}$ BALB/c and three of the pBi-IL-4RαTg / IL-4Rα $^{-/-}$ BALB/c / pVav-tTaTg / IL-4Rα $^{-/-}$ BALB/c lines which had been generated from three different pBi-IL-4RαTg / IL-4Rα $^{-/-}$ BALB/c founder lines.

tTA transactivator transcription (Figure 2.16, Panel A) was present in all three lines at varying degrees, although the founder line D showed a level below that of the single transgenic line (pVav-tTaTg/ IL-4Rα $^{-/-}$ BALB/c only). As expected, the luciferase mRNA was present in all lines (Panel B), the transcription profile reflected that shown by the tTA transcripts, with founder line B showing decreased levels when compared to lines D and C. pBi-IL-4RαTg transcripts (Fig.2.16.C) were present in all three pBi-IL-4RαTg / IL-4Rα $^{-/-}$ BALB/c / pVav-tTaTg/ IL-4Rα $^{-/-}$ BALB/c lines, with the line derived from pBi-IL-4RαTg-B displaying the highest level of transcription, as it had with tTA and luciferase. These results lead to subsequent analysis being confined to the pBi-IL-4RαTg / IL-4Rα $^{-/-}$ BALB/c / pVav-tTaTg / IL-4Rα $^{-/-}$ BALB/c line derived from pBi-IL-4RαTg-B.

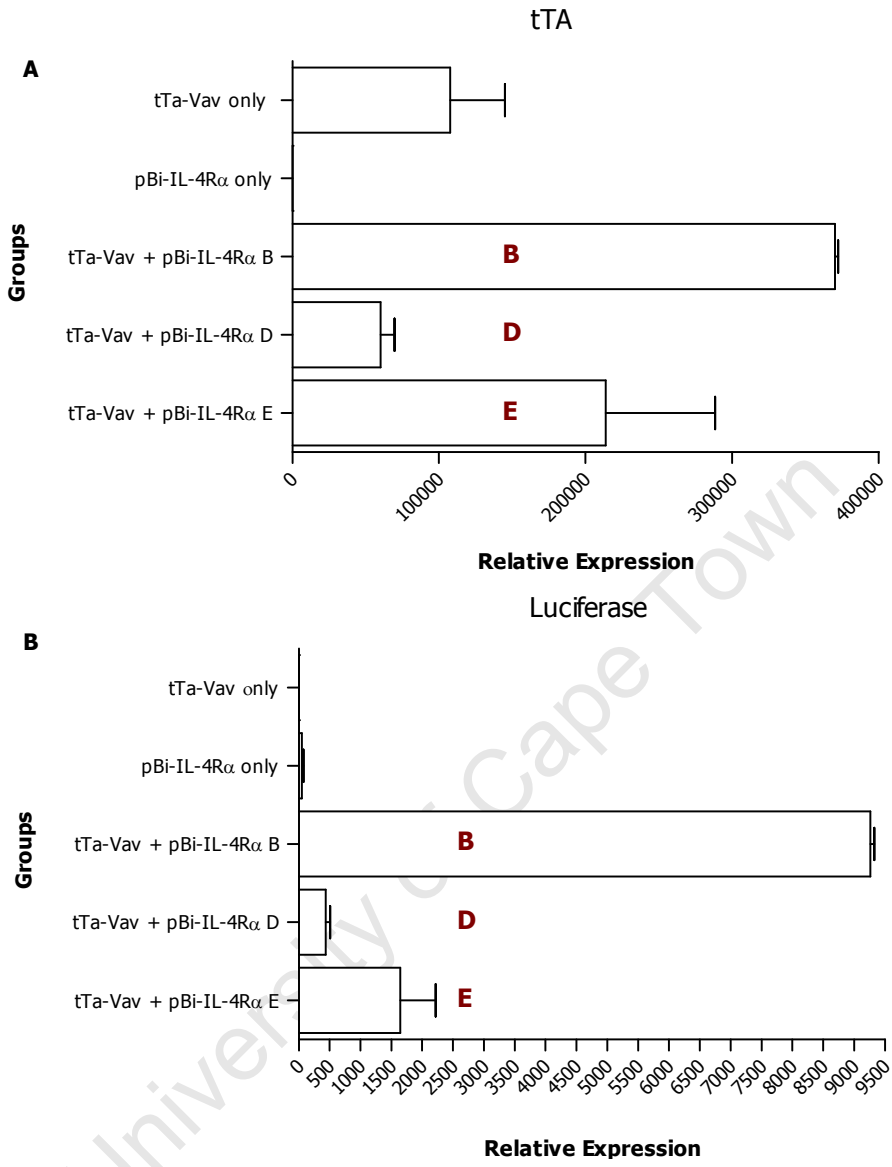

Figure 2.16 Transgene mRNA levels in pBi-IL-4RαTg / IL-4Rα $^{-/-}$ BALB/c / pVav-tTaTg/ IL-4Rα $^{-/-}$ BALB/c line.

cDNA was synthesised from mRNA extracted from the splenocytes. Different transgenic lines are indicated. **Panel A**, Transactivator tTa transcription. Levels of tTa mRNA relative to mRNA levels of a housekeeping gene (actin) were determined by real-time PCR. **Panel B**, Levels of luciferase mRNA relative to mRNA levels of actin. The results represent 1 of 3 independent experiments and show the average ± SEM of triplicate values.

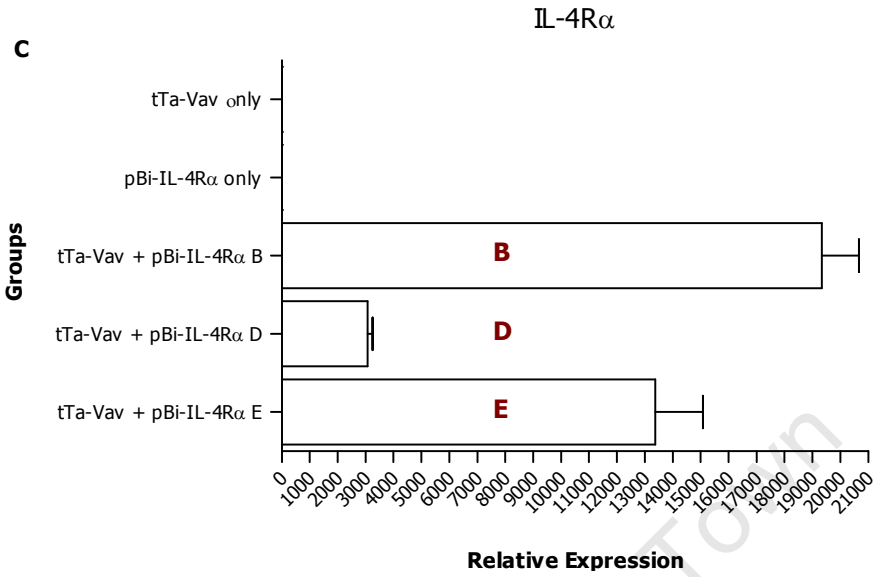

Figure 2.16 Transgene mRNA levels in pBi-IL-4RαTg / IL-4Rα $^{-/-}$ BALB/c / pVav-tTaTg/ IL-4Rα $^{-/-}$ BALB/c line.

Different transgenic lines are indicated. **Panel C**, mRNA transcription, driven by the bi-directional promoter. mRNA levels for IL-4Rα, relative to mRNA levels of the housekeeping gene actin. The results represent 1 of 3 independent experiments and show the average ± SEM of triplicate values. 3-4 mice / group were used per experiment.

2.3.2.5.2 Translational analysis.

Subsequently transgene functionality was investigated on the translational level. The level of IL-4Rα expression was assessed in hemapoeitic cells only, in this way the inducibility of the bi-directional promoter and functioning of the cell specific Vav promoter was verified.

Following genotyping results which confirmed transgene presence or absence and IL-4Rα$^{-/-}$ BALB/c background, the IL-4Rα cell surface expression was analyzed with FACS. For the experimental control (Figure 3.17, Panel A) the following groups were analyzed; IL-4Rα$^{-/-}$, BALB/c, pBi-IL-4RαTg / IL-4Rα $^{-/-}$ BALB/c and pVav-tTaTg / IL-4Rα $^{-/-}$ BALB/c. As expected, only the cells from BALB/c mice showed a positive shift in fluorescence indicative of IL-4Rα expression. There was a clear difference in the IL-4Rα surface staining, on hemapoeitic cells, for the male and female pBi-IL-4RαTg / IL-4Rα $^{-/-}$ BALB/c / pVav-tTaTg / IL-4Rα $^{-/-}$ BALB/c mice from the B transgenic line (Fig.2.17.B). Both showed increased expression when compared to IL-4Rα$^{-/-}$ mice yet, the male had an improved level to that shown by the female cells. This difference in expression was further verified by the chemiluminscent luciferase assay where the luciferase expression in the male mouse vastly exceeded that in the female mouse (Fig.2.17.C).

This difference could be attributed to the fact that the pBI-IL-4RαTg is an X chromosome-linked transgene or possible even variability in transgene expression. Further analysis of the pBi-IL-4RαTg / IL-4Rα $^{-/-}$ BALB/c / pVav-tTaTg / IL-4Rα $^{-/-}$ BALB/c mice is needed to address the differences in transcription and translation shown between the different lines and sexes.

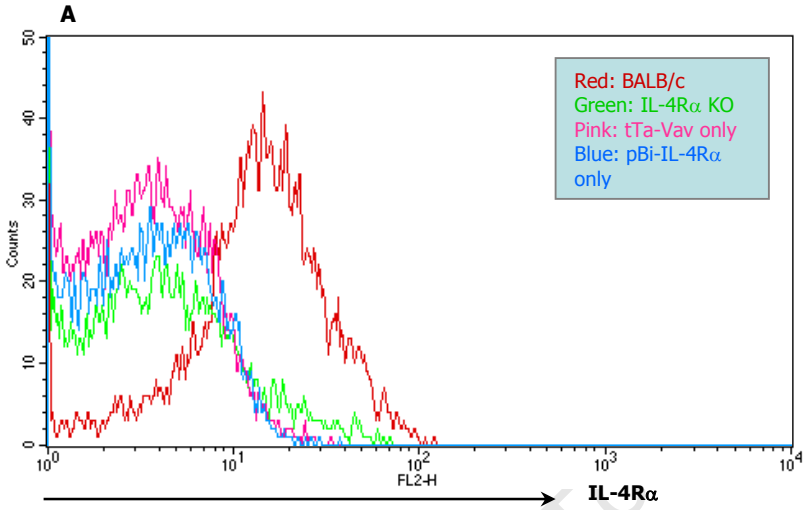

Figure 2.17 pBi-IL-4Rα Tg /pVav-tTa Tg translational analysis.

The IL-4Rα cell surface expression was analyzed using four colour FACS analysis FACS was preformed on cell suspensions obtained splenocytes. The groups analyzed are indicated. Cells were gated for the hemapoeitic marker and viable cells were isolated by incubation with 7-AAD, a marker for non-viable cells. **Panel A** and **B**, Histograms indicating the shift in fluorescence due to positive murine IL-4Rα surface expression. Histograms are representative of populations gated for viable hemapoeitic cells. **Panel A**, The control FACS using the groups indicated. IL-4Rα expression shown in the BALB/c group only.

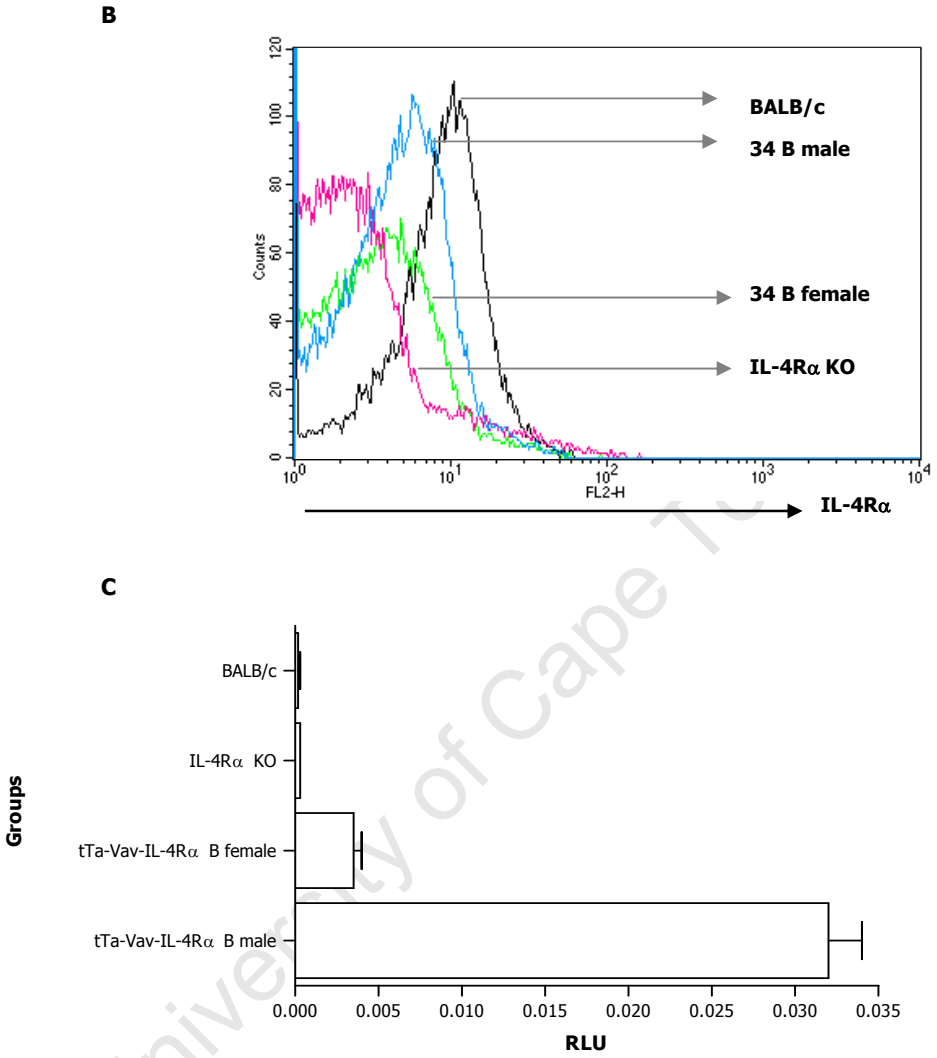

Figure 2.17 pBi-IL-4Rα Tg /pVav-tTa Tg translational analysis.

Panel A and **B**, Histograms indicating the shift in fluorescence due to positive murine IL-4Rα surface expression. Histograms are representative of populations gated for viable hemapoeitic cells. **Panel B**, The experimental groups indicated. **Panel C**, Chemiluminscent assay indicating luciferase induction levels of the groups indicated.

2.4 Chapter Conclusions.

Subsequent to pBi-IL-4Rα transgenic construct cloning, the clones were successfully verified via restriction enzyme screening followed by sequence verification (section 2.3.2.1, pBi-IL-4Rα vector map in Appendix A). This was followed by the pilot studies to establish the construct and Tet System functionality. These were performed *in vitro* using Hek 293T cells and the results lead to the following conclusions:

1. The efficient functioning of the Tet system as assessed by the bi-directional promoter activity (2.3.2.2.1), via the expression of the reporter luciferase. The results of this chemiluminscent luciferase assay confirmed both efficient tTA expression and Tet_O operon binding.
2. Inducibility of the system shown by the repression of reporter expression over time (2.3.2.2.2). These assays also established an effective doxycycline concentration for the complete suppression of target gene expression after ~12h (Figure 2.7).
3. Lastly, the pilot studies determined the efficient pTet-Off: pBi-IL-4Rα plasmid ratio to be used in the generation of stable lines and expression studies using transient transfection (2.3.2.2.3). This showed increased luciferase reporter and tTa effector expression in cells containing a 10-fold excess of the regulatory plasmid, which was in agreement with previous studies.

The pilot studies, using the reporter expression for most of the assays, lead on to the *in vitro* studies demonstrating inducible repression of the generated pBi-IL-4Rα transgenic construct (section 2.3.2.3). These confirmed:

1. Transcription efficiency of mIL-4Rα transgene (2.3.2.3.1), these results indirectly confirmed tTa effector transcription.
2. Translation efficiency of mIL-4Rα transgene (2.3.2.3.2) and inducible repression of mIL-4Rα expression (2.3.2.3.3).

Following the *in vitro* studies which illustrated functionality of the generated pBi-IL-4Rα construct, the construct, primers and PCR protocols were sent to *Nucleis* in France where the pBi-IL-4Rα chimeras were generated (2.3.2.4.1). After the successfully birth and delivery of 7 male chimeras, the extensive and sometimes complicated breeding program commenced (2.3.2.4.2). The aim here was firstly to cross the pBi-IL-4Rα Tg with the IL-4Rα$^{-/-}$ and in this way to generate a line deficient of IL-4Rα, yet carrying the transcriptionally silent pBi-IL-4Rα transgene in all tissues. The next cross was using the progeny and breeding these with the pVav-tTa Tg, also on an IL-4Rα$^{-/-}$ background. In this way generating an inducible model where IL-4Rα could only be reconstituted in

hemapoeitic cells. After successful genotyping of pBi-IL-4Rα Tg /pVav-tTa Tg IL-4Rα$^{-/-}$ BALB/c line (2.3.2.4.3) the *in vivo* characterisation confirmed functionality of both transgenes and thus the Tet system on a transcriptional (2.3.2.5.1) and translational level (2.3.2.5.2).

Although we describe here the successful generation of an inducible and cell specific model, it is essential to establish the final line lacking variability in translation before studies using this model can commence.

Chapter 3: Dendritic Cell Specific Expression of Cre Recombinase.

Aim: Cloning and *in vitro* functional analysis of constructs designed to express Cre recombinase and Green Fluorescent Protein (GFP) under the control of the murine dendritic cell specific promoter, CD11c.

3.1 Introduction.

Dendritic cells (DCs) consist of a group of antigen presenting cells which function by patrolling the tissues of the body, recognising, processing and presenting antigens to T cells in the secondary lymphoid tissues (Arpinati *et al.,* 2000; Banchereau *et al.,* 1998). Following antigen recognition, immature (naïve) DCs become activated to mature DCs, which are characterized by the enhanced expression of MHC II and other co-stimulatory molecules. Additionally the secretion of proinflammatory cytokines allows DCs to activate naïve and memory T cells, thereby modulating the immune response (Moser and Murphy, 2000). DCs serve as a vital link between the adaptive and innate immune systems and promote both primary and secondary immune responses (Palucka and Banchereau, 1999). Furthermore, DC functions are required for the homeostatic maintenance of T cells and for the development of tolerance to self antigens (Lanzavecchia and Sallusto, 2004). Important concepts that have emerged from dendritic cell research include the following, firstly, that the dendritic cell system comprises of a large collection of subpopulations with different functions. This functional diversity is associated to their differentiation state as well as their specific location and is a consequence of differential interactions with antigens and immune system effector cells (Banchereau *et al.,* 2000). Secondly, and more importantly, dendritic cells have emerged as promising alternative tools for vaccination and immunotherapy of cancer autoimmunity and allergy (Fong and Engelman, 2000; Jonuliet *et al.,* 2001).

It has been suggested that a candidate cytokine for the enhancement of the immunoregulatory capacities of dendritic cells is IL-4 (Morita *et al.,* 2001). Even though IL-4Rα is expressed on the DC cell surface (Fisher *et al.,* 1999), IL-4 was not acknowledged as a DC product or seen as important in the maturation of DCs as T cells were seen as the main producers of IL-4 during the development of Th2 responses. It has been accepted that DCs are generally associated with being IL-12 producers and responders. In deed it has been suggested that IL-4 is of minor importance in their function (Haas *et al.,* 1999).

However, recent studies have shown that immature DC exposure to IL-4 drives DC, to become net producers of IL-4 as opposed to IL-12. Thus, IL-4 presence, during the early stages of development of DC, could influence the production of cytokines in those cells and lead to the production of this Th2-polarizing cytokine in DC (Maroof *et al.,* 2005). A recent study also demonstrated IL-4 suppression of type I IFN-induced DC activation and their expression of cytokines and antiviral genes via the inhibition of STAT-1 and STAT-2 phosphorylation. In this way, IL-4 reduced the autocrine loop that is associated with the increase in the effects of type I IFNs (Sriram *et al.,* 2007).

It is thus of great interest to investigate more specifically the interaction and importance of IL-4Rα on DCs, especially pertaining to Th2 immune response modulation. In order to address such questions we describe here the generation of a dendritic cell (DC) specific IL-4Rα deficient mouse model (CD11c-Cre-IL-4Rα$^{lox/-}$). This will be achieved by inter-crossing newly generated CD11c-CreTg mice with floxed IL-4Rα and global IL-4Rα$^{-/-}$ mice (Figure 3.1). In this model, Cre recombinase transgene expression will be directed exclusively to DCs due to the incorporation of the appropriate cell specific promoter. Cre expression will lead to the inactivation of the lox P flanked IL-4Rα gene.

The present study deals with the:

1. Molecular cloning and characterisation of eukaryotic expression vectors containing the mouse dendritic cell specific promoter (CD11c). Vectors were designed for optimal expression, directed via CD11c, of the Cre Recombinase and Green Fluorescent Protein (GFP) transgenes.
2. *In vitro* functional analysis of these constructs to show cell specific transcription and translation of the transgenes.

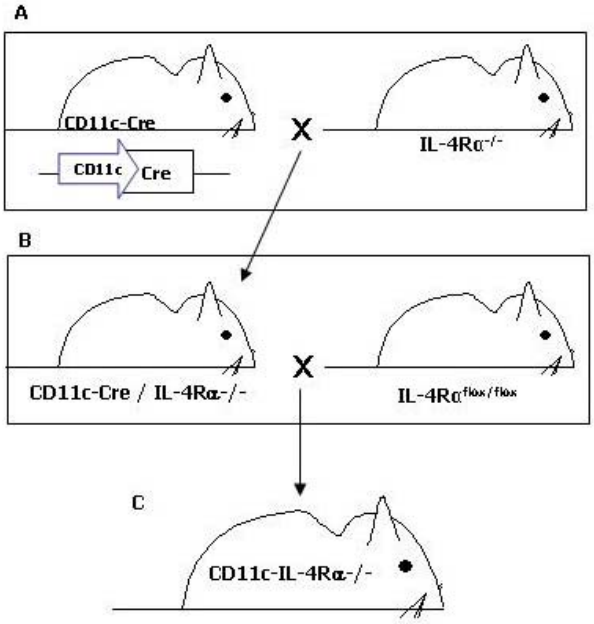

Figure 3.1 The generation of the CD11c-IL-4Rα$^{-/-}$ model.

Panel A, Breeding scheme for the crossing of the newly generated pCD11c-CreTg and the existing IL-4Rα$^{-/-}$ line. **Panel B,** Inter-crossing of the CD11c-Cre / IL-4Rα$^{-/-}$ progeny from **A** with the IL-4Rα$^{flox/flox-}$ line. **Panel C,** Progeny of **B** result in the model. With the genotype of: CD11c-IL-4Rα$^{-/-}$ BALB/c.

3.2 Methods and Materials.

3.2.1 Cloning of the constructs.

3.2.1.1 Plasmid purification.

All molecular biological manipulations were performed according to established protocols (Ausubel *et al.,* 1995). Chemicals and reagents were Molecular Biology Grade. Small-scale plasmid purifications were performed using a SV Wizard Plasmid Purification preps and a Wizard Maxiprep kit (Promega Corp., Madison, USA) was used for large-scale purifications, using protocols supplied with each kit.

3.2.1.2 Primer design.

Synthetic oligonucleotide primers were supplied by the Oligonucleotide Synthesis Facility, Department of Molecular and Cell Biology, University of Cape Town.

3.2.1.3 Modified Cre recombinase primers.

Table 3.1 Sequences of oligonucleotides used for the amplification of Cre.

Name	Sequence
Cre reverse	5′ ATATAT GCGGCCGC**CTA-**TGTCCTGATAGCGG ‘3*
Cre forward	5′ TA GTCGACCCGCC**GCCATGG-**CACCCAAGAAGAAG ‘3′#

* The sequence corresponding to the *Not I* restriction site is underlined and the Stop codon is in **bold**.

The sequence corresponding to the *Sal I* restriction site is underlined and the modified Kozak sequence is in **bold**.

3.2.1.4 Polymerase Chain Reaction (PCR).

3.2.1.4.1 Amplification of Cre cDNA.

The amplification of the coding region for the Cre Recombinase cDNA fragment was performed by the Polymerase Chain Reaction using 5ng of the pMC-Cre (Gu *et al.,* 1993) as template. The reaction was preformed in a 50µl volume containing 1 × SuperTherm PCR Buffer, 1.5mM $MgCl_2$, 0.2mM dNTPs, 0.125U/µl Supertherm Taq (Medox Biotech India Pvt. Ltd. Chennai, India) and 0.5µM of each primer. The following cycling parameters were used: an initial denaturation step at 95°C for 1min, followed by 35 cycles consisting of 95°C incubation for 1min, an annealing step at 58°C for 1min, and an extension step at 72°C for 1.5min. A final step of 72°C for 5min was included to complete partial extension reactions.

3.2.1.5 Restriction and ligation of Cre, GFP and CD11c into a eukaryotic expression vector.

3.2.1.5.1 Sub-cloning of Cre into the pDrive PCR cloning vector.

The amplified fragments corresponding to Cre were recovered from a 1% (w/v) low melting agarose gel (section 3.1.6) and purified with the Wizard SV Gel Extraction Kit (Promega). The procedure was performed according to the manufacturer's recommendations. Approximately 73ng of the purified fragment (in five-fold molar excess to 3.85kb vector) was mixed with 50ng of pDrive, 1µl 10 × Ligation Buffer (Promega) and 1µl of T4 DNA Ligase (Promega, 3 Weiss Units/µl) in a total volume of 10µl. A background control was included where the Cre insert fragment was omitted. The ligation reaction was allowed to proceed overnight at 4°C. Following ligation, 5µl of the ligation mix was added to 200µl of calcium chloride competent JM109 *E.coli* cells (Invitrogen Corporation, Carlsbad, CA, USA). The suspension was incubated on ice for 30min after which the cells were heat-shocked, according to the methodology of Inoue and co-workers (1990) at 42°C for 45sec. The transformed cells were immediately placed on ice (4°C) for 2min and supplemented with 800µl of room temperature SOC medium. Cells were incubated with shaking (200rpm) at 37°C for 1h. Following incubation, 50µl of the transformed cells were plated onto LB agar plates containing 50µg/ml ampicillin. Plates were incubated for 14h at 37°C. Plasmid DNA was isolated (see section 3.1.1) from overnight cultures containing 5ml LB medium supplemented with 50µg/ml ampicillin and colonies chosen randomly from the incubated plates. Positive constructs for Cre were identified by restriction enzyme screening with the restriction enzymes *Not I* and *Sma I* (Roche Diagnostics GmbH, Mannheim, Germany). The correct fragments were verified by electrophoresis on a 0.8% (w/v) agarose gel stained with ethidium bromide (0.5µg/ml*)* as described (section 3.1.5). Plasmids found to contain correct inserts were sequenced by automated nucleotide sequencing (DNA Sequencing Unit, Department of Molecular and Cell Biology, University of Cape Town) and denoted pDrive-Cre. Glycerol stocks were prepared from the *E.coli* JM109 cells containing the pDrive plasmids with the coding regions for Cre recombinase and stored at -70°C.

3.2.1.5.2 Sub-cloning of CD11c into the pGFP-N1 expression vector.

The 5,5kb DNA fragment containing the regulatory elements of the mouse CD11c promoter (Agger *et al.,* 1990) was digested from the pBS-CD11c vector (obtained from Prof. Karjalainen). The fragment was digested with 10U *Sst I* (Roche) at 37°C for 18h. The digested fragments were recovered from a 1% (w/v) low melting agarose gel (section 3.1.6) and purified with the Wizard SV Gel Extraction Kit (Promega). The purified fragment was partially digested with *Pst I* (Roche) as follows. Six eppendorf tubes were

placed and ice, the first tube received double the concentration of purified fragment and 2U of *Pst I.* Half of the volume from tube 1 was removed and the aliquot added to tube 2 from which the serial dilution was continued to tube 6. All 6 tubes were then incubated at 37°C for 1h. The pGFP-N1 vector was digested with the same set of enzymes and both the *Sst I / Pst I* digested CD11c fragment and *Sst I / Pst I* digested pGFP-N1 vector were recovered from a 1% (w/v) low melting agarose gel (section 3.1.6) and purified with the Wizard SV Gel Extraction Kit (Promega). The procedure was performed according to the manufacturer's recommendations. Approximately 100ng of the purified fragment was mixed with 50ng of pGFP-N1, 1µl 10 × Ligation Buffer (Promega) and 1µl of T4 DNA Ligase (Promega, 3 Weiss Units/µl) in a total volume of 10µl. A background control was included where the CD11c insert fragment was omitted. The ligation reaction was allowed to proceed overnight at 4°C. Following ligation, 5µl of the ligation mix was added to 200µl of calcium chloride competent DH5α *E.coli* cells (Invitrogen). The suspension was incubated on ice for 30min after which the cells were heat-shocked (as described by Inoue and co-workers, 1990) at 42°C for 45sec. The transformed cells were immediately placed on ice (4°C) for a further 2min and 800µl of room temperature SOC medium was added. Cells were incubated with shaking (200rpm) at 37°C for 1h. Following incubation, 50µl of the transformed cells were plated onto LB agar plates containing 100µg/ml kanamycin. Plates were incubated for 14h at 37°C. Plasmid DNA was isolated (see section 3.1.1) from overnight cultures containing 5ml LB medium supplemented with 100µg/ml kanamycin and colonies chosen randomly from the incubated plates. Positive constructs for Cre were identified by restriction enzyme screening with the restriction enzymes *Pst I* and *Sst I* (Roche). The correct fragments were verified by electrophoresis on a 0.8% (w/v) agarose gel stained with ethidium bromide (0.5µg/ml) as described (section 3.1.5). Plasmids found to contain correct inserts were sequenced by automated nucleotide sequencing (DNA Sequencing Unit, Department of Molecular and Cell Biology, University of Cape Town) and denoted pCD11c-GFP. Glycerol stocks were prepared from the *E.coli* DH5α cells containing the pGFP-N1 plasmids containing the CD11c promoter and stored at -70°C.

3.2.1.5.3 Cloning of the CD11c driven Cre expression vector.

The *Not I* and *Sal I* digestion of pCD11c-GFP separates the GFP fragment from the vector sequence when electrophoresed. Thus, the cloning of the Cre insert into the pCD11c-GFP is a replacement of GFP open reading frame with that of the Cre cDNA. For this cloning, 5ug of the pCD11c-GFP and pDrive-Cre constructs were digested separately with a restriction enzyme mixture of 6U of *Sal I* and 6U *Not I* (Roche). The reaction was incubated at 37°C for 6h. The digested products corresponding to Cre insert fragment

and the pCD11c-GFP vector were recovered from a 0.7% (w/v) low melting agarose gel (section 3.1.6) and purified with the Wizard SV Gel Extraction Kit (Promega), as per manufacturer's recommendations. Approximately 18ng of the purified fragment (in five-fold molar excess to 8.283kb vector) was mixed with 50ng of digested pCD11c-GFP, 1µl 10 × Ligation Buffer (Promega) and 1µl of T4 DNA Ligase (Promega, 3 Weiss U/µl) in a total volume of 10µl. A background control was included where the Cre insert fragment was omitted. The ligation reaction was allowed to proceed overnight at 4°C. Following ligation, 5µl of the ligation mix was added to 200µl of calcium chloride competent JM109 *E. coli* cells (Invitrogen). The suspension was incubated on ice for 30min after which the cells were heat-shocked (Inoue *et al.,* 1990) at 42°C for 45sec. The transformed cells were immediately placed on ice (4°C) for a further 2min and 800µl of room temperature SOC medium was added. Cells were incubated with shaking (180rpm) at 37°C for 1h. Following incubation, 50µl of the transformed cells were plated onto LB agar plates containing 100µg/ml kanamycin. Plates were incubated for 14h at 37°C. Plasmid DNA was isolated (see section 3.1.1) from overnight cultures containing 5ml LB medium supplemented with 100µg/ml kanamycin and colonies chosen randomly from the incubated plates. Positive constructs containing the Cre fragment were identified by restriction enzyme screening with the restriction enzymes *Not I* and *Sal I* (Roche). The correct fragments were verified by electrophoresis on a 0.8% (w/v) agarose gel stained with ethidium bromide (0.5µg/ml*)* as described (section 3.1.5). Plasmids found to contain correct inserts were sequenced by automated nucleotide sequencing (DNA Sequencing Unit, Department of Molecular and Cell Biology, U.C.T) and denoted pCD11c-Cre. Glycerol stocks were prepared from the *E.coli* JM109 cells containing the pCD11c-GFP plasmids with the newly cloned pCD11c-Cre recombinase and stored at -70°C.

3.2.1.6 Agarose gel electrophoresis.

All DNA samples including PCR products, restriction enzyme (RE) digestion and RE screening products, were verified by agarose gel electrophoresis through a 0.8 or 1% (w/v) agarose gels (gel percentage was dependant on fragment size) in 1 × TAE electrophoresis buffer. Samples were electrophoresed at constant voltage of 150V for 45min at room temperature. Gels were stained with ethidium bromide (0.5µg/ml). DNA was visualised by short wavelength UV transillumination (A_{254nm}).

3.2.1.7 Gel isolation and purification of DNA.

DNA samples including PCR products and samples from RE digestions of fragments to be used in ligation were electrophoresed on a 1% low melting point agarose gel in 1 × TAE electrophoresis buffer (containing 0.5µg ethidium bromide/ml) at 90V for 1h. DNA was

visualised by brief exposure to low wavelength UV (A_{320nm}). The appropriate bands were excised from the gels with a sterile blade. Gel slices were melted by incubation at 65°C in heating block and DNA purified using the Wizard SV Gel Extraction kit (Promega), according to the manufactures instructions. DNA concentrations were determined from the absorbance of samples at A_{260nm} using the conversion factor for double stranded DNA (1OD unit = 50µg/ml).

3.2.2 Cell culture.

3.2.2.1 Hek 293T cells.

The human embryonic kidney 293 cell line (Hek 293T) (obtained from Gordon Brown, IIDMM, UCT Medical School) was used for as a control cell line in all transfection and expression assays. The cells were cultured in DMEM medium pH7.4, supplemented with 10% Foetal Calf Serum (Gibco Life Technologies, Paisely, UK) 10mg/ml streptomycin and 10U/ml penicillin at 37°C and 5% CO2. Cells were passaged when cell monolayer reached ~70% confluence. To split cells to a 1:10 ratio the media was aspirated from the cells and cells then washed once with 1 x PBS. The adherent cells were dislodged from the tissue culture flasks (Nalge Nunc International, Naperville, IL, USA) by addition of Trypsin-EDTA solution (0.53mM EDTA, 0.05% trypsin) (Gibco) and incubation for 1min at room temperature. After gentle tapping of the flask the suspension was diluted in DMEM supplemented with 10% FCS to inactivate the trypsin. Cell suspension was pelleted at 1 200rpm for 8min and the supernatant carefully aspirated. Cells were then resuspended in DMEM supplemented with 10% FCS and transferred to the appropriate size tissue culture flask.

3.2.2.2 Transfection of Hek 293T cells.

Hek 293T cells were transfected using Lipofectamine Transfection Reagent (Invitrogen Corporation, Carlsbad, CA, USA).which employs a lipid-mediated (Felgner and Ringold, 1989) method, with optimization of the manufactures instructions. Briefly, to achieve a cell monolayer of ~70% confluence the cells were plated at $2x10^5$cell/well in a 6 well tissue culture plate (Nalge Nunc International) and incubated at 37°C in a humidified 5% CO_2 for 18-24h. Subsequently, two tubes with 0.75ml DMEM media/well were prepared. 1ug isolated plasmid DNA, diluted to a working concentration of 1ug/ml in distilled H_2O, was added to one tube and 5ul of Lipofectamine Reagent (Invitrogen) to the other. The reaction mixtures from the two tubes were combined and incubated at room temperature for 20min. The adherent Hek 293T cells were washed twice with 3ml/well serum-free DMEM media. The 1.5ml reaction mixture was then carefully plated onto the cells. The

cells were incubated at 37°C in a humidified 5% CO_2 incubator for 24h. Following over night incubation the serum-free media was aspirated from the cells and cells were re-incubated after the addition of 3ml DMEM supplemented with 10% Foetal Calf Serum (Gibco). Clone selection was achieved by the addition of 300µg/ml Zeocin (Invitrogen) and 250µg/ml was used for maintenance.

3.2.2.3 D25/sc dendritic cell line.

The mouse dendritic cell line, D25/sc (obtained from Ulrich Schaible, Germany. Winzler *et al.,* 1997) was used to assess the CD11c driven expression. The cells were cultured in RPMI 1640 supplemented with 10% FCS (Gibco) 10mg/ml streptomycin and 10U/ml penicillin at 37°C and 5% CO2. The adherent cells were passaged when cell confluence reached ~60%. To split cells to a 1:10 ratio the media was aspirated from the cells and cells then washed once with 1 x PBS. The adherent cells were dislodged from the tissue culture flasks (Nalge Nunc International) by addition of Trypsin-EDTA solution (Gibco) and incubation for 5min at 4°C. After gentle tapping of the flask the suspension was diluted in RPMI / 10% FCS to inactivate the trypsin. Cell suspensions were pelleted at 800rpm for 8min and supernatants removed. Cells were then resuspended in RPMI / 10% FCS and transferred to the appropriate size tissue culture flask. Unless otherwise stated, sub confluent D25/sc cells (cell monolayer at ~60-70% confluence) were used for transfection studies.

3.2.2.4 Transfection of D25/sc cells.

To optimize transfection efficiency two transfection reagents and electroporation was tested. The reagents were; the liposome based reagent, Lipofectamine (Invitrogen) and the non-liposomal lipid reagent, Effectene (Qiagen, Valencia, CA, U.S.A). The procedures for transfection with these reagents were performed according to the manufacturer's recommendations. For electroporation, the cells were dislodged from the flask by addition of Trypsin-EDTA solution (Gibco), as described in section 3.2.1.3. After centrifugation the cell pellet was resuspended in RPMI / 20% FCS. 20µg of isolated DNA was mixed into $5x10^6$ cells in a final volume of 200µl per electroporation cuvette (Gene Pulser® Cuvettes, 0.2 cm gap, Biorad). The cuvette was incubated on ice for 10min. The chilled cuvette was placed in the electroporation machine and two different sets of conditions were tested; firstly 320kV, 125µF, and 260kV, 975µF. After electroporation the cuvettes were placed on ice for 10min. 800µl RPMI / 10% FCS was added to the cuvettes and the final volume aliquoted into 5 wells of a 24 well tissue culture plate (Nalge Nunc International). The cells were incubated at 37°C and 5% CO_2 for 24-48h and subsequently assayed for expression.

3.2.3 *In vitro* studies.

3.2.3.1 D25/sc Cell line characterisation.

Media was aspirated from both Hek 293T and D25/sc cells after which the cells were washed once with 1 x PBS. The adherent cells were dislodged from the flask by incubation for 1min at room temperature with Trypsin-EDTA solution (Gibco). After gentle tapping of the flasks the cell suspensions were diluted in DMEM supplemented with 10% FCS in order to inactivate the trypsin. This cell suspension was pelleted by centrifugation at 1 000rpm for 8min and the supernatant carefully aspirated from the cell pellet. Cells were resuspended in 2ml complete DMEM / 10% FCS, 100U/ml penicillin and 100µg/ml streptomycin (all reagents supplied by Gibco). Aliquots of cells (10µl) were diluted in Trypan Blue and counted on a Neubauer haemocytometer to determine concentrations of viable cells. For each staining $1x10^5$ cells were blocked for 25min in 100µl FACS buffer containing 1% heat inactivated rat serum and 4µg/ml 2.4G2 (anti-$F_{c\gamma}$RII and –III). The cells were washed in 500µl FACS buffer (PBS supplemented with 0.1% BSA and 0.05% Sodium Azide) and resuspended in 100µl FACS buffer containing one of the following antibodies to cell surface markers: MHC class II-FITC and CD11c-PE labelled (BD Bioscience, Pharmigen, San Diego, CA). Cells were also stained in parallel for the isotype controls for these antibodies: Hamster IgG and Rat $IgG_{2a\kappa}$. Staining was preformed by cell incubation in the dark for 30min at 4°C after which the cells were washed with 500µl FACS buffer and centrifugation at 1,200rpm for 10min. After this final wash cells were resuspended in 300µl FACS buffer supplemented with 7-AAD (Sigma, St. Louis, USA). Dead cells stained with 7-AAD were excluded from analysis. Stained cell acquisition was preformed using a FACSCalibur flow cytometer (BD Biosciences) and data analyzed using CellQuest software (Becton-Dickinson, Ferndale, South Africa). 100,000 cells were acquired for analysis.

3.2.3.2 CMV promoter activity.

Transfected Hek 293T cells were harvested by dislodging the cells from the tissue culture plates with 1 x Trypsin/EDTA Solution (Gibco). The cells were pelleted from this suspension by centrifugation at 1,200rpm for 10min. Aliquots of cells (10µl) were diluted in Trypan Blue and counted on a Neubauer haemocytometer to determine concentrations of viable cells. $5x10^5$cells/ml were pooled for each experimental group and washed in 500µl FACS buffer by centrifugation at 1,200rpm for 5min. Cell pellets were resuspended in 500µl FACS buffer supplemented with 7-AAD (Sigma). Dead cells stained with 7-AAD were excluded from analysis. Acquisition was preformed using a FACSCalibur flow

cytometer (BD Biosciences) and data analyzed using CellQuest software (Becton-Dickinson). 100 000 cells were acquired for analysis.

3.2.3.3 Cell specific transcription.

3.2.3.3.1 Template preparation - RNA isolation.

Total RNA was extracted from lymph nodes of a Cre Tg BALB/c mouse using TriReagent (Molecular Research Company, Cincinnati, USA) as per the manufacture's instructions. The collected nodes were homogenized on ice in 2ml TriReagent for every 100mg of tissue. 200µl of chloroform was added for every 1ml of lysate and vortexed thoroughly. The samples were incubated at room temperature for 15min and centrifuged at 13,500rpm for 15min at 4°C. The top aqueous layer was transferred to a new tube and an equal volume of 100% isopropanol added and mixed. The RNA was precipitated out of solution by incubating overnight at –80°C and subsequent centrifugation at 13,500rpm for 30min at 4°C. The RNA pellet was washed twice in 800µl 70% ethanol, air-dried and resuspended in 50µl-100µl DEPC-treated water. All purified RNA samples were DNAseI treated and stored at -80°C. The quality of the RNA was checked by determining the ratio of the absorbance at A_{260}/A_{280} and by electrophoresis of 1µg RNA on a 1% agarose gel that contained 2.2M formaldehyde. The concentration of the RNA was determined by measuring the A_{260}. All solutions used for the RNA work, except TRIS-containing buffers, were treated with DEPC to destroy any endogenous RNAses. To each solution, DEPC was added to a final concentration of 0.1% and gently shaken overnight at 37°C. The solutions were then autoclaved for 30min to remove any residual DEPC. For TRIS-containing buffers, solutions were prepared using DEPC-treated water and an ultra-pure TRIS stock designated for RNA work only.

3.2.3.3.2 DNAseI treatment.

The RNA was DNAse I treated to remove contaminating genomic DNA, proteins, residual phenol and salts. 1-10µg of total RNA was incubated with DNAseI cocktail (1 x DNAse1 buffer (Promega, Madison, WI, USA), 10U/µl DNAse1 (Roche), 1U/µl RNAsin (Promega) for 60min at 37°C. The DNAse I treated RNA was purified and concentrated using the Qiagen MiniElute RNA cleanup kit (Qiagen) as per the manufacturer's instructions (see Methods and Materials section 3.3.1.2 for detailed protocol). The elimination of contaminating genomic DNA was confirmed by RT-PCR using primers that bound to genomic DNA. The quality and quantity of the RNA was checked by spectroscopy and denaturing gel electrophoresis using standard methods (Sambrook *et al.,* 2001). The A_{260}/A_{280} ratio was measured and an aliquot was run on a 1% agarose gel containing 2.2M formaldehyde. The RNA was stored at –80°C until used.

3.2.3.3.3 cDNA synthesis.

The genomic DNA free RNA was reverse transcribed into cDNA using the ImProm-II™ Reverse Transcription System (Promega) as per the manufacturer's instructions. Briefly, 0.5µg of Oligo (dT)15 primer was added to 1-10µg of DNAse I treated RNA in a final volume of 20µl. The sample was denaturing at 70^{o}C for 10min and then cooled on ice for 5min. 20µl of cDNA synthesis cocktail (ImProm-II™ 5 x Reaction Buffer, 4mM $MgCl_2$, 0.5mM each dNTP, 1U/µl RNAsin, 2.0µl ImProm-II™ Reverse Transcriptase) was added and the samples incubated at 25^{o}C for 5min to anneal the primers. cDNA synthesis was extended at 45^{o}C for 90min. The reaction was heat deactivated at 75^{o}C for 5min and cooled on ice. The samples were divided into aliquots and stored at –20^{o}C.

3.2.3.3.4 cDNA amplification.

The amplification of the mRNA transcripts was performed by the PCR using 5ng of the synthesized cDNA as template. The reaction was preformed in a 25µl volume containing 1 × SuperTherm PCR Buffer, 2.5mM $MgCl_2$, 0.2mM dNTPs, 0.25U/µl Supertherm Taq (Medox Biotech) and 0.5µM of each primer. The following cycling parameters were used: an initial denaturation step at 95°C for 1.5min, followed by 30 cycles consisting of 95°C incubation for 1min, an annealing step at 62°C for 1min, and an extension step at 72°C for 1.5min. A final step of 72°C for 5min was included to complete partial extension reactions.

3.2.3.4 Cell specific translation.

3.2.3.4.1 CD11c driven GFP expression.

24h Post transfection media was aspirated from the transfected Hek 293T and D25/sc cells after which the cells were washed once with 1 x PBS. The adherent cells were dislodged from the plates by incubation for 2min at room temperature with Trypsin-EDTA solution (Gibco). Plates were tapped gently and cell suspensions diluted in DMEM / 10% FCS in order to inactivate the trypsin. This suspension was pelleted at 1 200rpm for 8min and the supernatant carefully aspirated from the cell pellet. Cells were resuspended in 2ml complete DMEM / 10% FCS (Gibco). Aliquots of cells (10µl) were diluted in Trypan Blue and counted on a Neubauer haemocytometer to determine concentrations of viable cells. The cells were washed in 500µl FACS and resuspended in 300µl FACS buffer supplemented with 7-AAD (Sigma). Dead cells stained with 7-AAD were excluded from analysis. Acquisition was preformed with a FACSCalibur flow cytometer (BD Biosciences) and data analyzed using CellQuest software (Becton-Dickinson). 100 000 cells were acquired for analysis.

3.2.3.4.2 Immunofluorescence.

$5x10^4$cells transfected cells were grown on sterile slides overnight in DMEM / 10% FCS (Gibco) containing 10mg/ml streptomycin and 10U/ml penicillin at 37°C and 5% CO2. The media was removed by aspiration and the cells briefly rinsed with 1 x PBS. Cells were fixed by incubation with ice-cold methanol:acetone (1:1, v/v) in the dark for 2min. The slides were rinsed 3 times with 1 x PBS, each rinsed lasting 5min. The slides were blocked by incubation for 20min with 5% (w/v) PBS-BSA (Sigma). The blocking solution was aspirated from slides and slides washed with 1 x PBS. The FITC-labeled Cre antibody (Sigma) was diluted 1:200 (v/v) in PBS-BSA and a sufficient volume used to cover the glass. Cells were incubated for 30min in the dark at room temperature. The antibody solution was aspirated off the cells and slides washed three times with 1 x PBS for 5min each wash. The APES coated coverslips were mounted with mounting medium. Slides were dried and examined using a fluorescence microscope.

3.3 Results.

3.3.1 Vector design and construction.

Separate cloning steps were involved in the generation of the transgenic constructs where Cre Recombinase and Green Fluorescent protein (GFP) transcription is driven by the dendritic cell specific promoter, CD11c (refer to Figure 3.2). The mouse CD11c promoter represents the best marker available for mouse DC. The 5.5kb fragment of the CD11c 5' region provides the regulatory elements required to drive expression of transgenes specifically in DC and not in other cell types (Brocker *et al.,* 1997 and Metlay *et al.,* 1990). The promoter sequence had previously been cloned (Agger *et al.,* 1990) into in a pBSbluescript vector as a 5,5 kb fragment containing the 5' region of the mouse *CD11c* gene (received from K. Karjalainen, Switzerland).

This vector, pBS-CD11c, was digested with restriction enzymes that would separate the promoter sequence from the vector sequence. The isolated CD11c promoter sequence was sub-cloned into the pGFP-N1 eukaryotic expression vector (refer to section 3.1.2) which served as the vector backbone. The pGFP-N1 expression vector contains a fragment from the rabbit β-globin gene. This DNA segment provides the cloned transgenes with an intron as well as a polyadenylation signal, which has shown to be valuable in the efficient export of the transcripts from the nucleus (Minvielle-Sebastia and Keller, 1999; Neugebauer, 2002).

The Cre and GFP transgenes were present as cDNA fragments in the eukaryotic expression vectors pMC-Cre and pGFP-N1, respectively. The Cre transgene was PCR amplified, sequenced and cloned into a PCR cloning vector (pDrive) subsequent to being sub-cloned into the newly generated CD11c vector (section 3.1.1). The GFP transgene was present in the pGFP-N1 vector backbone into which the CD11c promoter sequence was cloned. The complete cloned CD11c gene transcript was sequence verified using nucleotide sequencing in conjunction with primer walking. The detailed cloning description of the pCD11c-GFP and pCD11c-Cre expression vectors follow.

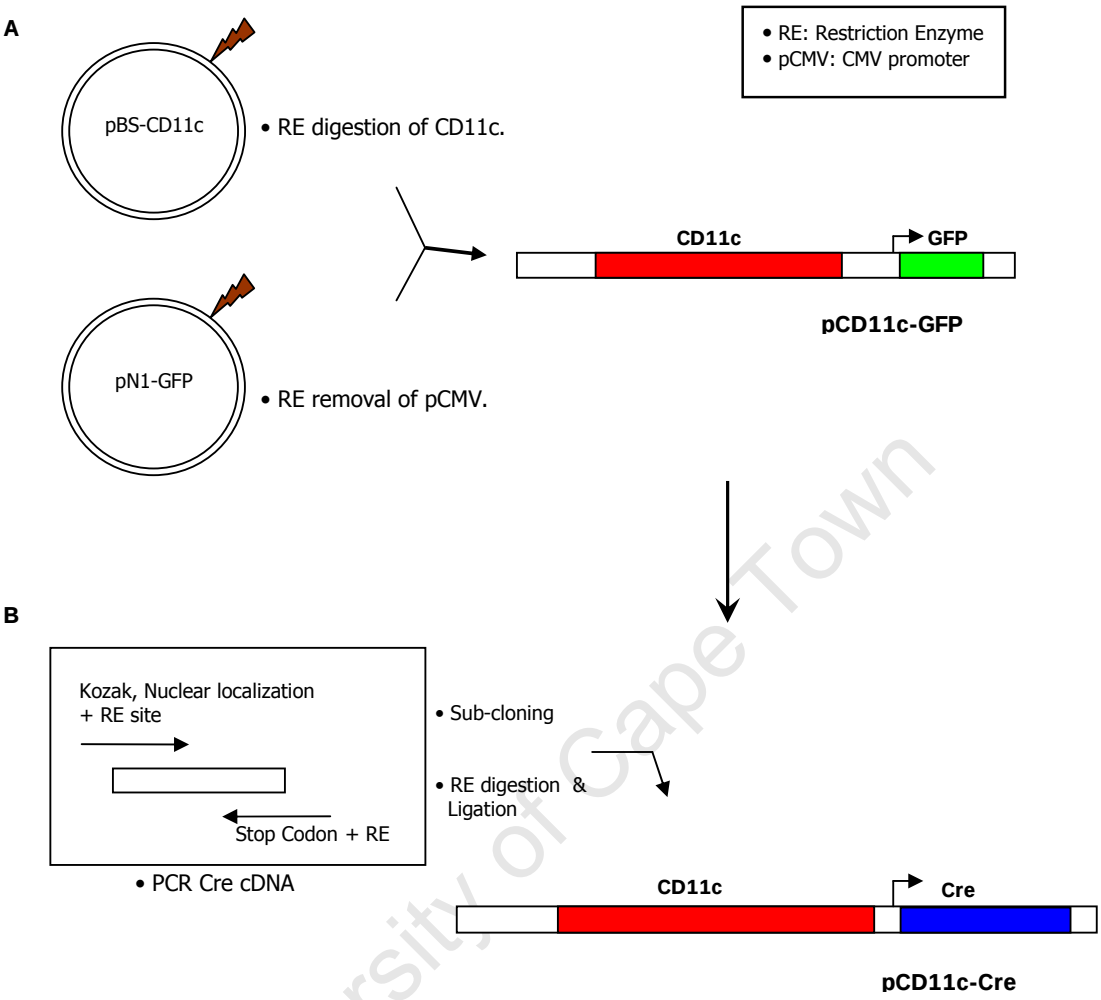

Figure 3.2 Flow Diagram of pCD11c-GFP and pCD11c-Cre Cloning Strategy.

Panel A, Cloning of pCD11c-GFP by restriction enzyme removal of the CMV promoter and CD11c ligation into pGFP-N1, serving as the vector backbone. **Panel B**, Primer design and PCR of Cre recombinase transgene DNA. RE digestion of Cre cDNA and pCD11c-GFP, followed by ligation to generate pCD11c-Cre.

3.3.1.1 Generation of the Cre cDNA fragment.

In order to sub-clone and express Cre recombinase, the corresponding coding region for the protein was amplified by PCR using primer pairs that introduce *Sal I* and *Not I* restriction enzyme sites (refer to Figure 3.2). These restriction enzyme recognition sites are absent from the Cre sequence. They were incorporated to allow for the subsequent ligation into the CD11c directed expression vector, pCD11c-GFP, which having been digested with the same enzymes, generates complementary sticky ends for the directed ligation. The primer set was designed to amplify the Cre sequence using the eukaryotic expression vector pMC-Cre as PCR template. This eukaryotic expression vector contains a nuclear localization signal in the first 27 bases of the Cre sequence (Kalderon *et al.*, 1984). The nuclear localization signal targets the expressed protein to the cell nucleus through the Nuclear Pore Complex, directing the newly synthesized protein into the nucleus via its recognition by cytosolic nuclear transport receptors (Kozak, 1984). In order to improve translation, via an optimized transcription start site, the Kozak consensus sequence was incorporated in the forward primer sequence. The sequence is contiguous with the ATG start codon and greatly increases the efficiency of translation and hence overall expression of the product gene (Kozak, 1986). The primers were designed to generate this consensus sequence, at the 5' end of the amplified Cre fragment, by the addition of 3 extra bases. A stop codon (TGA) was included in the reverse primer sequence, in this way eliminating any additional amino acid expression from the template, pMC-Cre vector sequence.

The amplification produced the desired 1292bp Cre recombinase transgene DNA, and both amplification and fragment size was confirmed via gel electrophoresis (Figure 3.3). The amplified fragments were gel isolated and subsequently cloned into, pDrive, a PCR cloning vector. This type of cloning, namely, T/A cloning takes advantage of the terminal transferase activity of Taq DNA polymerases, which adds a single 3'-A overhang to each end of the PCR product. The resulting PCR product is then ligated into a linear vector with a 3' terminal 'T' at both ends. The construct was transformed into DH5α *E.coli* cells, and colonies screened by restriction enzyme digestion. The sequences of inserts in positive constructs were subsequently verified by automated nucleotide sequencing after which the construct was referred to as pDrive-Cre.

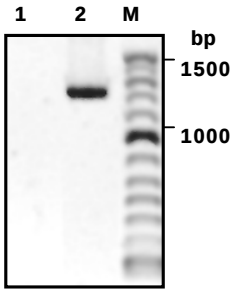

Figure 3.3 Amplification of Cre cDNA fragment.

1 % (w/v) agarose gel in 1 × TAE containing ethidium bromide and visualized using short wavelength UV transillumination. **Lane M**, DNA molecular weight marker. **Lane 2**, Amplified 1292bp Cre DNA fragment. **Lane 1**, Positive No DNA control

3.3.1.2 Cloning of the CD11c fragment.

To obtain dendritic cell specific expression of the Cre recombinase the previously characterized CD11c promoter (Agger *et al.,* 1990) fragment was used. The pBS-CD11c vector, containing the regulatory elements of the CD11c promoter, was manipulated via *Sst I* restriction enzyme (see Figure 3.4 Panel A & B for vector construction scheme). The CD11c promoter sequence has two *Pst I* restriction enzyme recognition sites. To prevent the removal of any promoter sequence a partial digestion was required (Fig.3.5). To facilitate this, the former *Sst I* digestion was followed by a partial *Pst I* digestion. Subsequently, the digested promoter DNA was separated from the vector sequences by electrophoresis and extracted from the agarose slices. These *Sst I* / *Pst I* digested fragments were then ligated into complementary restriction enzyme sticky ends on the pGFP-N1 vector. The ligated construct was transformed into JM109 *E.coli* cells, and colonies screened by restriction enzyme digestion. This screening confirmed insert size and correct orientation for the in-frame expression of the cloned cDNA. The construct was referred to as pCD11c-GFP.

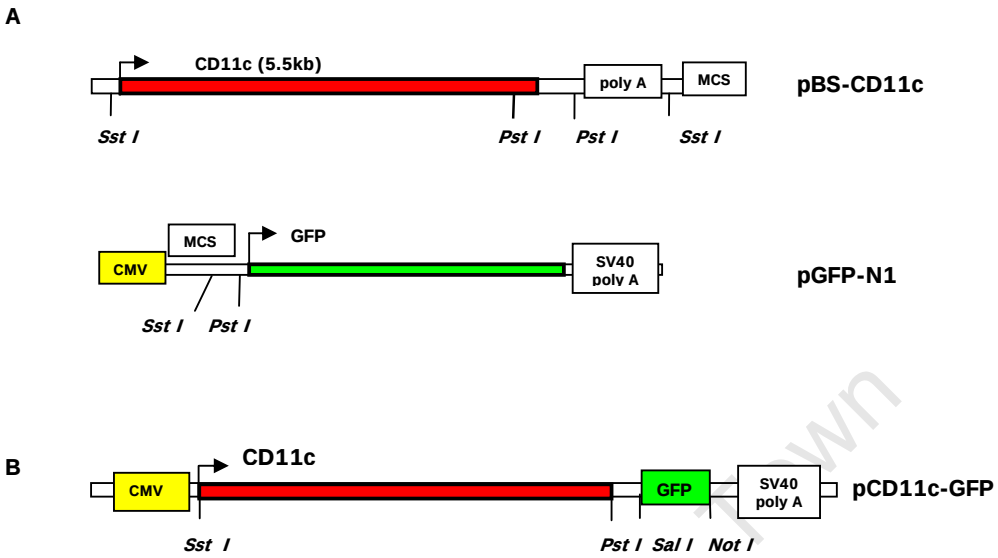

Figure 3.4 Vector construction scheme for pCD11c-GFP.

Panel A, Vector maps of pBS-CD11c and pGFP-N1, indicating restriction enzyme sites used in cloning pCD11c-GFP. The pGFP-N1 expression vector served as backbone for the resulting pCD11c-GFP vector. **Panel B**, The pCD11c-GFP vector which served as backbone for the pCD11c-Cre expression vector. pCD11c-GFP also served as a control for CD11c driven expression due to the GFP element.

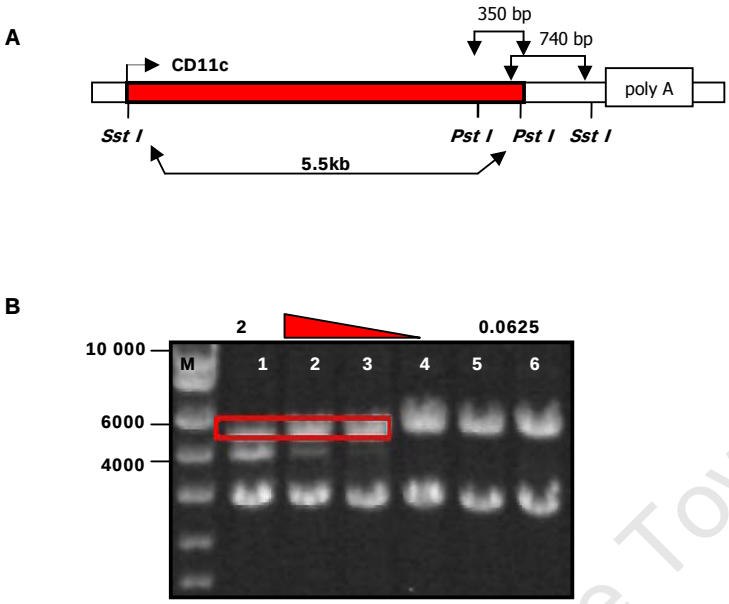

Figure 3.5 Partial *Pst I* Restriction Enzyme Digestion of pBS-CD11c.

Panel A, pBS-CD11c vector map showing *Pst I* and *Sst I* RE sites and the fragment sizes generated by digestion with theses enzymes. **Panel B**, 0.8 % (w/v) agarose gel in 1 × TAE containing ethidium bromide and visualized using short wavelength UV transillumination. **Lane M**, DNA molecular weight marker. **Lanes 1 - 6**, pBS-CD11c vector digestion with decreasing amounts of *Pst I* enzyme. Units of enzyme per reaction decreased from 2 - 0.0625 U. The 5.5 kb CD11c digested promoter fragment isolated from the agarose gel is indicated.

3.3.1.3 Generation of the CD11c driven Cre vector.

With the aim of the molecular cloning and subsequent cell specific expression, of Cre recombinase, the corresponding cDNA coding sequence for the protein was digested with *Sal I* / *Not I* from the pDrive-Cre cloning vector. The pCD11c-GFP expression vector was digested with the same set of enzymes (Figure 3.6, Panel A). Following digestion, the GFP transgene DNA was separated from the vector sequences by electrophoresis, in this way removing this transgene from the final construct. The digested fragments were isolated from a low melting agarose gel and subsequently ligated (Fig.3.6.B). The ligated construct was transformed into JM109 *E.coli* cells. To verify the presence of the Cre transgene insert, plasmid DNA isolated from the resulting colonies, were screened by *Sal I* / *Not I* restriction enzyme digestion (Fig.3.6.C). With this screening, both insert size and correct orientation was confirmed via agarose gel electrophoresis. The construct was referred to as pCD11c-Cre and pCD11c-GFP.

3.3.1.4 pCD11c-Cre vector sequence analysis.

The automated sequence analysis was employed to sequence verify the cloned CD11c expression vectors, pCD11c-Cre and pCD11-GFP. Due to the 5.5 kb CD11c promoter size, primer walking was used to sequence the entire promoter from 5' to 3' end. With this sequence data theoretical vector maps were constructed and possible restriction sites identified. To confirm the sequencing data restriction enzyme screening was preformed using enzymes based on these maps. Figure 3.7 illustrates this for the pCD11-Cre vector. Panel A shows the theoretical vector map, with enzyme positions, that was constructed in DNAssist with the sequence data. The program allows the displayed sequence files to be edited and analyzed. Subsequently the vector was digested with the indicated enzymes. The products of these RE digestion reactions were analyzed via agarose gel electrophoresis (Panel B). The expected fragment sizes, as predicted by the sequence data and constructed maps, were observed. These assays established the cloned vector sequence.

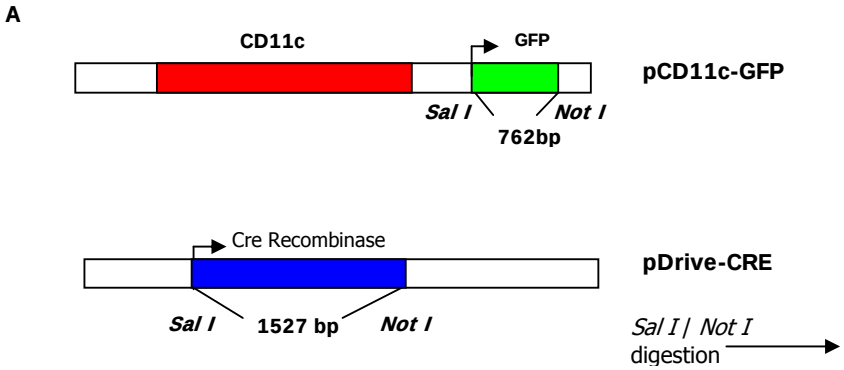

Figure 3.6. Cloning of CD11c driven expression vectors.

Panel A, Vector maps of vectors used for sub-cloning pCD11c-Cre. RE sites and fragment sizes generated by digestion are indicated.

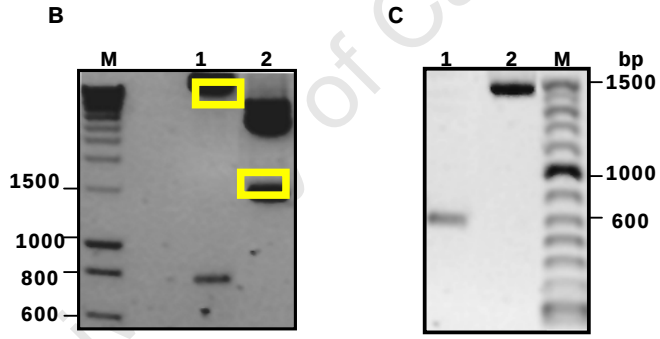

Figure 3.6. Cloning of CD11c driven expression vectors.

Panel B & **C** both display 0.8 % (w/v) agarose gel in 1 × TAE containing ethidium bromide and visualized using short wavelength UV transillumination. For both **Panel B** & **C**, **Lane M**, DNA molecular weight marker. **Panel B**, Vector digestion followed by separation and isolation from agarose gel. Fragments isolated are indicated. **Lane 1**, 765 bp *Not I* / *Sal I* digested GFP fragment separated from pCD11c-GFP backbone vector. **Lane 2**, 1492 bp *Not I* / *Sal I* digested Cre fragment from the digestion of pDrive-Cre. **Panel C**, Restriction enzyme screening of cloned pCD11c-Cre and pCD11c-GFP. **Lane 1**, 765 bp GFP fragment from the digestion of pCD11c-GFP with *Not I* and *Sal I*. **Lane 2**, 1492 bp Cre fragment from the digestion of pCD11c-Cre with *Not I* and *Sal I*.

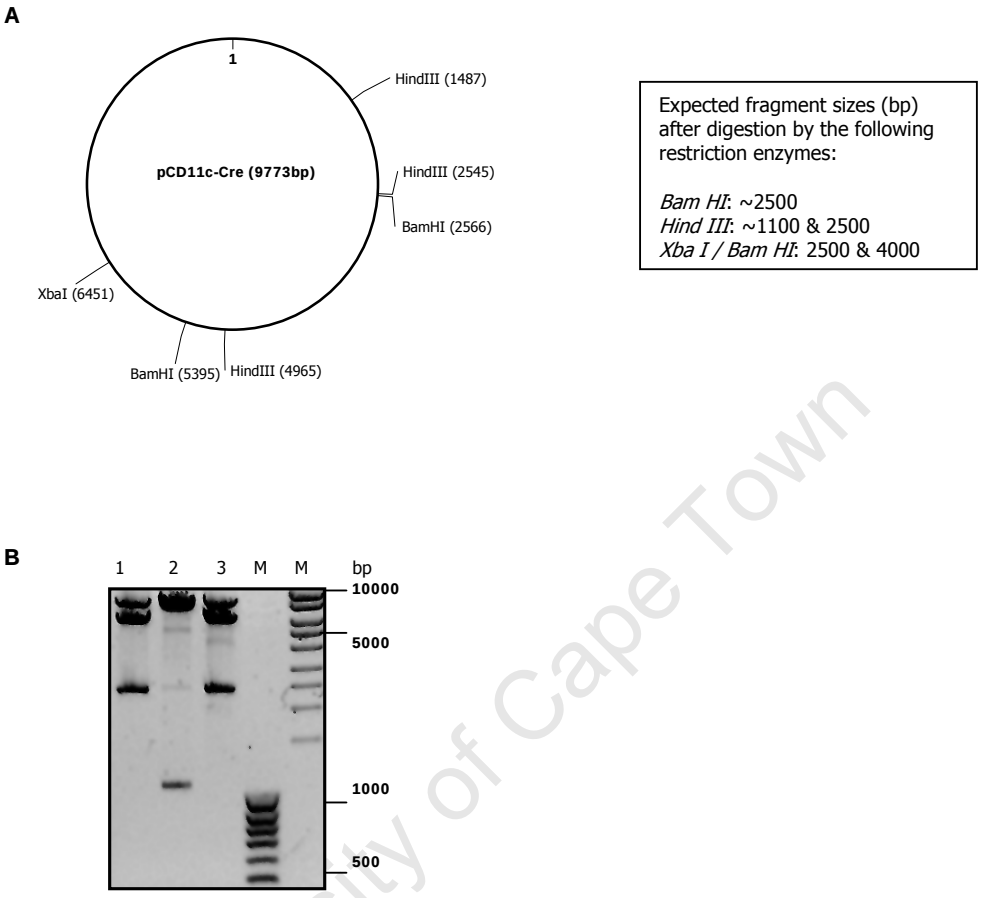

Figure 3.7 Sequence Verification of pCD11c-Cre.

Panel A, Theoretical vector map, based on sequence data, indicating possible enzyme sites. The inset lists these enzymes with the expected fragment sizes generated after digestion of the pCD11c-Cre. **Panel B**, 0.8 % (w/v) agarose gel in 1 × TAE containing ethidium bromide and visualized using short wavelength UV transillumination. **Lane M**, DNA molecular weight marker. **Lane 1**, 2500 bp fragment generated by *Bam HI* digestion. **Lane 2**, 1100 and 2500 bp fragments from *Hind III* digestion. **Lane 3**, 2500 and 4000 bp fragments generated after digestion with *Bam HI / Hind III*.

3.3.2. Preliminary *in vitro* expression studies.

3.2.2.1 Influence of CMV promoter.

The CMV (Human Cytomegalovirus Immediate-Early) promoter drives GFP expression in the pGFP-N1 eukaryotic expression vector. This promoter has previously been shown to be constitutively active in multiple cell types (Schmidt *et al.,* 1990; Fitzsimons *et al.,* 2002) and is routinely used in vector construction and expression studies. As illustrated (Figure 3.6), pGFP-N1 served as the vector backbone for the CD11c expression constructs. As a component of the pGFP-N1 vector, the CMV promoter sequence was still present in the cloned pCD11c-GFP and pCD11c-Cre expression vectors (Figure 3.6). The cloned CD11c promoter has an approximate size of 5500bp. This could prevent any read through from the CMV promoter thus eliminating CMV influence on the CD11c driven Cre and GFP transgene expression. To validate that the CMV promoter was transcriptionally inactive, the expression of GFP was characterized in Hek 293T cells using three different GFP expression vectors:

- Firstly, pGFP-N1 was used as the positive control for CMV driven GFP transcription.
- Secondly, the cloned pCD11c-GFP vector, with the CMV promoter preceding the CD11c sequence, namely p_{CMV}CD11c-GFP. The level of GFP expression in the Hek 293T cells transfected with this vector would indicate if the CMV promoter is still active in this construct.
- Thirdly, a duplicate to the second vector with the exception of the lack of the CMV promoter, pCD11c-GFP. It was expected that cells with this vector would be deficient in GFP expression, due to the lack of CMV promoter. This result would also indicate cell specificity by the CD11c promoter.

  For the construction of the pCD11c-GFP vector an additional cloning step was included. Briefly, the CMV element was removed from the vector sequence via restriction enzyme digestion. The enzymes used were unique to the CMV element only, thus not recognising and digesting other sites of the vector backbone or the cloned CD11c promoter sequence. Following agarose gel separation and isolation of the CMV and vector sequences the vector was re-ligated generating the CD11c expression vector, pCD11c-GFP. Subsequently, the three expression vectors were transfected into Hek 293T cells and GFP expression assessed using FACS analysis. The choice of cell line was based on the transcriptional inactivity of the dendritic cell promoter, CD11c, in Hek 293T cells (section 3.2.3.1). Thus, the observed GFP expression was exclusively a function of the CMV promoter activity. A significant decrease in the GFP expression was observed with the FACS analysis of the Hek 293T cells transfected with the CD11c expression vectors

lacking the CMV promoter (Figure 3.8). The FACS dot plot quadrant percentages, for the upper light quadrant represent the viable cells expressing GFP. As shown, this percentage declined from 42.46% for control pGFP-N1 vector to 23.32% in the p_{CMV}CD11c-GFP. Lastly, of the viable cells transfected with pCD11c-GFP, only 5.19% expressed the GF protein. These results indicated the strength of the CMV promoter and that it still had an influence on transgene transcription when present in the vectors containing the 5,5 kb CD11c promoter. Therefore, it would be transcriptionally active in dendritic cells leading to false positive CD11c driven expression results. These results lead to the exclusive use of the pCD11-GFP and pCD11c-Cre vectors, lacking the CMV promoter, for all subsequent *in vitro* functional assays.

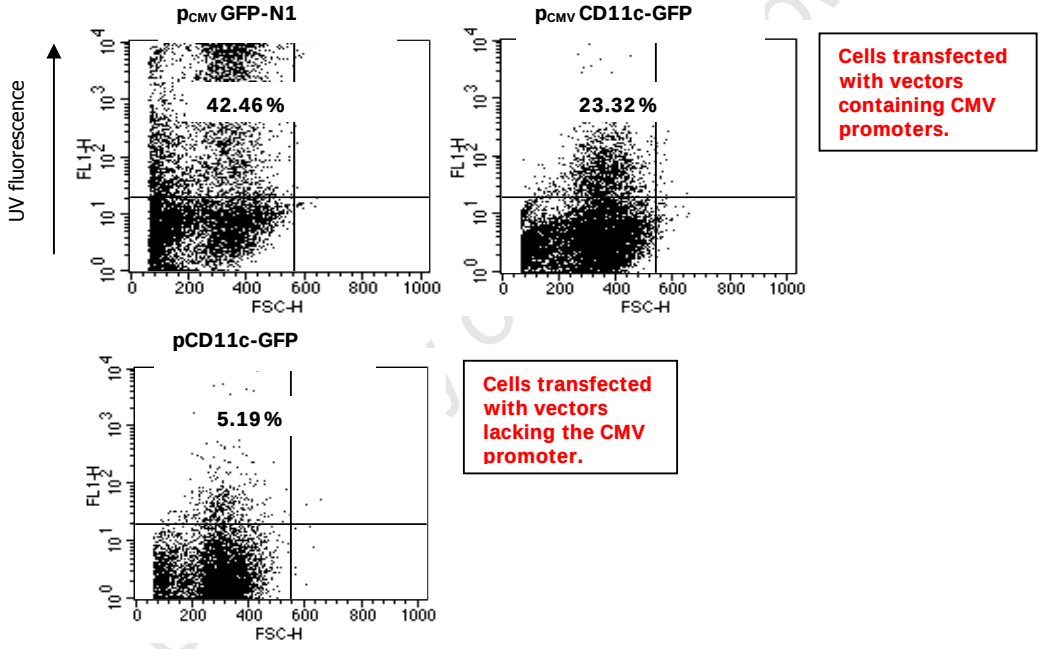

Figure 3.8 Effect of CMV promoter presence on GFP expression in CD11c vectors.

FACS analysis of GFP fluorescence from Hek 293T cells transfected with 3 vectors carrying different promoter elements. 24h post transfection cells were harvested and incubated with 7AAD. Dot plots representing 1 of 4 independent experiments. The upper left quadrant percentage indicates the viable GFP expressing cells.

3.3.3 Characterisation and Transfection of the D25/sc Cell Line.

3.3.3.1 Cell line characterisation.

To asses the *in vitro* functionality of the CD11c driven expression vectors the dendritic cell line, D25/sc (Gift from Ulrich Schaible, Germany. Winzler *et al.,* 1997) was used. Prior to the expression studies the cell line was characterised to confirm the dendritic cell phenotype. Cell phenotype characterisation was based on the surface expression of MHC II and CD11c. Both MHC II and CD11c are established markers for dendritic cell populations (Lui *et al.,* 2001). In this, and subsequent expression studies, the Hek 293T cell line was used as control. Using this cell line, transfected with the control pCD11c-GFP vector, generated a tool for determining transfection efficiency, promoter activity and cell type specific expression via the CD11c.

The D25/sc cell surface expression was analyzed using FACS analysis (Figure 3.9). The choice of antibody was based on specificity to the CD11c and MHC II markers present on the cell. Isotype controls for these antibodies were employed to ensure antibody specificity and additionally functioned as negative controls for the staining. The stained D25/sc cells, showed a positive shift in CD11c surface expression when compared to the controls, namely, unstained cells and antibody isotype staining (Fig.3.9.A). In comparison no CD11c expression was observed on the Hek 293T cells, indicated by the lack of fluorescent shift between the stained and unstained cells. Both cell lines stained positively for the MHC II marker (Fig.3.9.B). This data established the D25/sc cell phenotype as being similar to primary dendritic cells via the positive staining for CD11c and MHC II surface markers. Additionally, Hek 293T cell could be used as a control for assessing cell specific expression via the CD11c promoter.

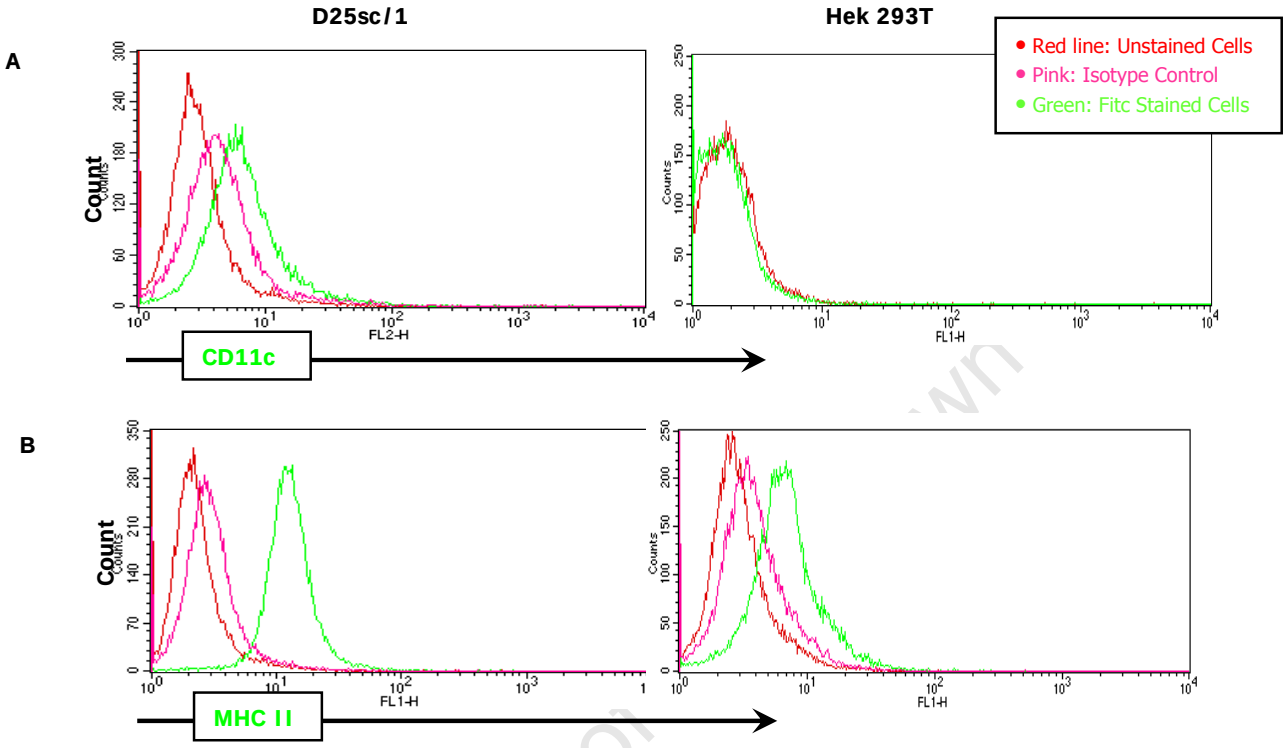

Figure 3.9. D25/sc Cell Phenotype Characterisation

$5x10^5$ cells from Hek 293T and D25/sc cell lines were stained with labelled antibodies. Subsequently, 4 colour FACS analyses were employed to identify surface markers present on the two cell lines. To isolate the viable cells, the cells were incubated with 7-AAD which is a marker for non-viable cells, these cells were excluded from analysis. **Panel A** and **B**, Histograms indicating the shift in fluorescence in due to positive CD11c and MHC II surface expression. **Panel A**, D25/sc and Hek 293 T cells stained for CD11c expression. **Panel B**, D25/sc and Hek 293 T cells stained for MHC II. Lines representing differently stained cells are indicated in the legend. Histograms are representative of populations gated for viable cells. Results shown are for 1 of 3 independent experiments.

3.3.3.2 D25/sc Transfection.

The expression studies were initiated with the establishment of a transfection method for the D25/sc cells. Primary dendritic cells display low transfection efficiency and to avoid any efficiency problems three different transfection methods were tested. These were:

1) The liposome based reagent, Lipofectamine. The general principle behind this method is the use of a liposome formulation that interacts spontaneously with DNA to form lipid-DNA complexes with complete DNA condensation. These liposomes fuse with cell membranes mediating efficient uptake and subsequent expression of the DNA.

2) The non-liposomal lipid reagent, Effectene. The reagent is used in conjunction with a special DNA-condensing enhancer and optimized buffer. The enhancer first condenses the DNA molecules and Effectene Reagent subsequently coats them with cationic lipids. These coated particles then transfer the DNA into the cells.

3) Lastly, electroporation, employing two different sets of parameters. The parameters were voltage (V) and resistance (Ω). The two combinations were high voltage, 320kV, and low resistance, 125µF, and low voltage, 260kV, high resistance, 975µF.

GFP expression was used to determine the transfection efficiency by each method. In all methods the cells were transfected with the pGFP-N1 control vector. 24h post transfection UV fluorescence was quantified with FACS analysis. Figure 3.10 illustrates the transfection efficiency by each method as a function of the viable UV positive cells. The highest level of transfection efficiency was observed for both the electroporation experiments. The percentage viable cells showing GFP expression was at ~10% and ~5% for the two respective experiments. This was unexpected since the cell death using this mechanical technique was very high at ~40%. The transfection reagents showed low, ~2% for cells transfected with Lipofectamine, or no (immeasurable) for the Effectene transfected cells, UV positive cells after 24h. These results lead to electroporation being employed for transfection of the D25/sc cell line.

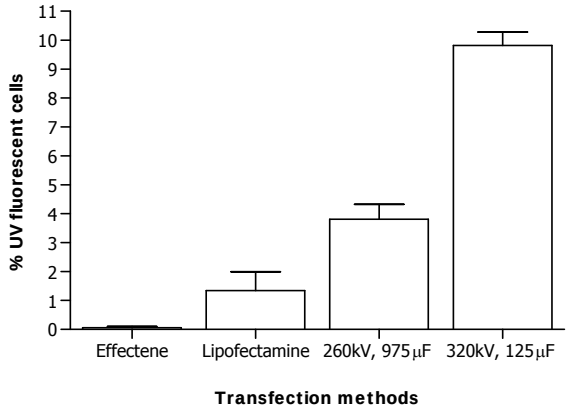

Figure 3.10. Transfection efficiency of D25/sc cells.

D25/sc cells were grown to the mid-log phase after which the cells were seeded and transfected using the different transfection methods indicated in the legend. 24h post transfection viable GFP expressing cells were determined and quantified using FACS. Results shown represent 3 independent experiments.

3.3.4 *In vitro* expression studies.

3.3.4.1 Cell specific transcription.

To assess the cell specific transgene expression from pCD11c-Cre, mRNA expression levels were analyzed. Having established that Hek 293T cells do not express CD11c (Section 3.2.1, Fig. 3.9) these cells, transfected with the pCD11c-Cre construct, were used as a positive control for CD11c cell specific driven transcription. D25/sc cells were electroporated with the construct and for both cell types untransfected cell controls were included. Cells were harvested 24h post transfection and cellular RNA isolated. Following cDNA synthesis transgene mRNA transcription levels were assayed with real-time PCR. Nested PCR primers which were specific for the Cre transcript were used.

Analysis of the RT-PCR (Figure 3.11) showed no transcription of the Cre transgene in the transfected Hek 293T cells. This was based on the lack of amplification product using the Cre specific primers. In contrast, the expected 243bp fragment was observed in the pCD11c-Cre transfected D25/sc cells, indicating that these cells were transcribing transgenic Cre mRNA. Additionally, this mRNA transcription was shown to be dendritic cell specific.

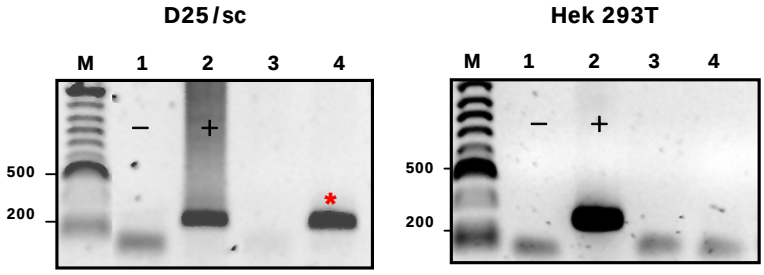

Figure 3.11. Dendritic cell specific transcription of Cre Recombinase.

RT-PCR of cDNA synthesized from pCD11c-Cre transfected and untransfected Hek 293T and D25/sc cells. Amplification products electrophoresised in 1.2 % (w/v) agarose gel in 1 × TAE containing ethidium bromide and visualized using short wavelength UV transillumination. In both figures: **Lane M**, DNA molecular marker. **Lane 1**, No DNA negative control. **Lane 2**, Positive control using cDNA synthesized from spleen cells isolated from a Cre transgenic mouse. **Lane 3**, Amplification products using cDNA from untransfected cells. **Lane 4**, Amplification products using cDNA from pCD11c-Cre transfected cells. The 243bp Cre product is indicated in the agarose figure labeled as D25/sc

3.3.4.2 Cell specific translation.

To further characterise the cell specific transgene expression from the pCD11c-Cre and pCD11c-GFP constructs, protein expression levels were analyzed. Transgene translation was determined using FACS analysis and immunohistological staining of the transfected cells.

For the FACS analysis the pCD11c-GFP construct and control pGFP-N1 vector were used and translation determined as a function of the GFP transgene expression. As with the transcription studies, transfected Hek 293T cells were used as a positive control for CD11c cell specific driven expression. pGFP-N1 was used as control of GFP expression via the CMV promoter. Both the D25/sc cells and Hek 293T cells were transfected with pCD11c-GFP and pGFP-N1. Cells were incubated with 7-AAD to isolate the viable cell populations. Untransfected cell controls, for both cell types, were also incubated with this fluorescent dye and functioned as the negative control for GFP expression. Hek 293T cells transfected with pGFP-N1, showed increased expression of GFP when compared to the untransfected cell control (Figure 3.12, Panel A). In contrast, the expression levels obtained for the pCD11c-GFP transfected Hek 293T cells were similar to the untransfected cell control. This observed lack of GFP expression via the CD11c promoter, in the Hek 293 T cells, indicated cell specificity of the CD11c promoter. This was confirmed in Panel B, where GFP expression was at comparatively the same levels for the pCD11c-GFP and pGFP-N1 transfected D25/sc cells. These expression levels were additionally reflected in the UV fluorescent images captured for the D25/sc cells transfected with pCD11c-GFP and pGFP-N1 constructs (Panel C).

Subsequently, protein expression was also analyzed with immunohistological staining of pCD11c-Cre transfected D25/sc cells. Transfected and untransfected cellular preparations were incubated with a FITC-labelled antibody recognising the expressed Cre protein. The immunohistological analysis of the cell preparations is shown in Figure 3.13. It was observed, Panel B, that staining by the antibody recognising Cre recombinase was confined to the transfected cells only. This result suggests that the expression of the Cre transgene, driven by the CD11c promoter, is restricted to the transfected cells, thus confirming the RT-PCR and FACS data.

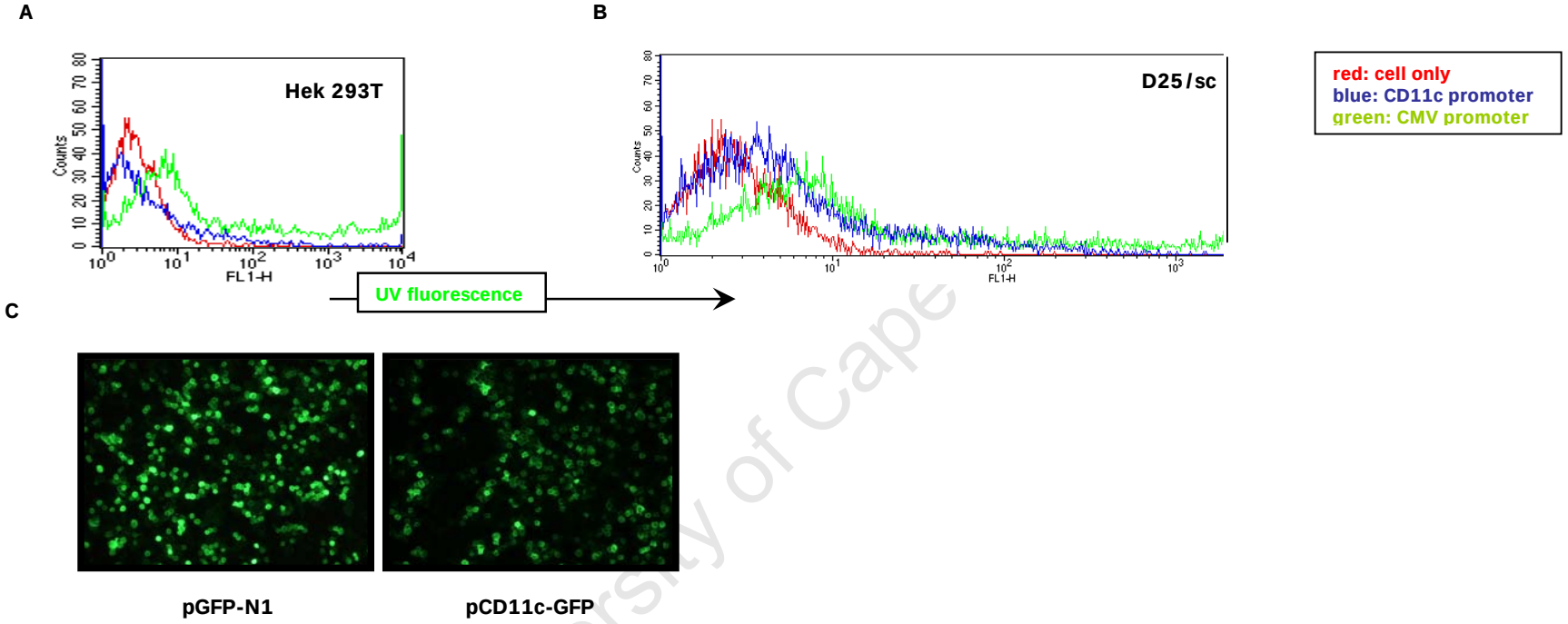

Figure 3.12. Dendritic cell specific CD11c driven transgene expression.

Panel A and **B**; Histograms indicating the shift in UV fluorescence in due to GFP expression. **Panel A**, Hek 293 T cells and **Panel B**, D25/sc cells. 24h Post transfection, Hek 293T and D25/sc cells were harvested and incubated with 7AAD. Cells were then assessed for GFP expression driven by the CD11c or CMV promoters of the pCD11c-GFP and pGFP-N1 expression vectors, respectively. Lines representing untransfected and transfected cells are indicated in the legend. Histograms are representative of populations gated for viable cells. Results sown are for 1 of 3 independent experiments. **Panel C**, UV fluorescent images of pGFP-N1 and pCD11c-GFP transfected D25/sc cells. 24h Post transfection D25/sc cells were harvested and equal amounts seeded on histological slides. Cells were air-dried overnight and images observed under 20 X magnification

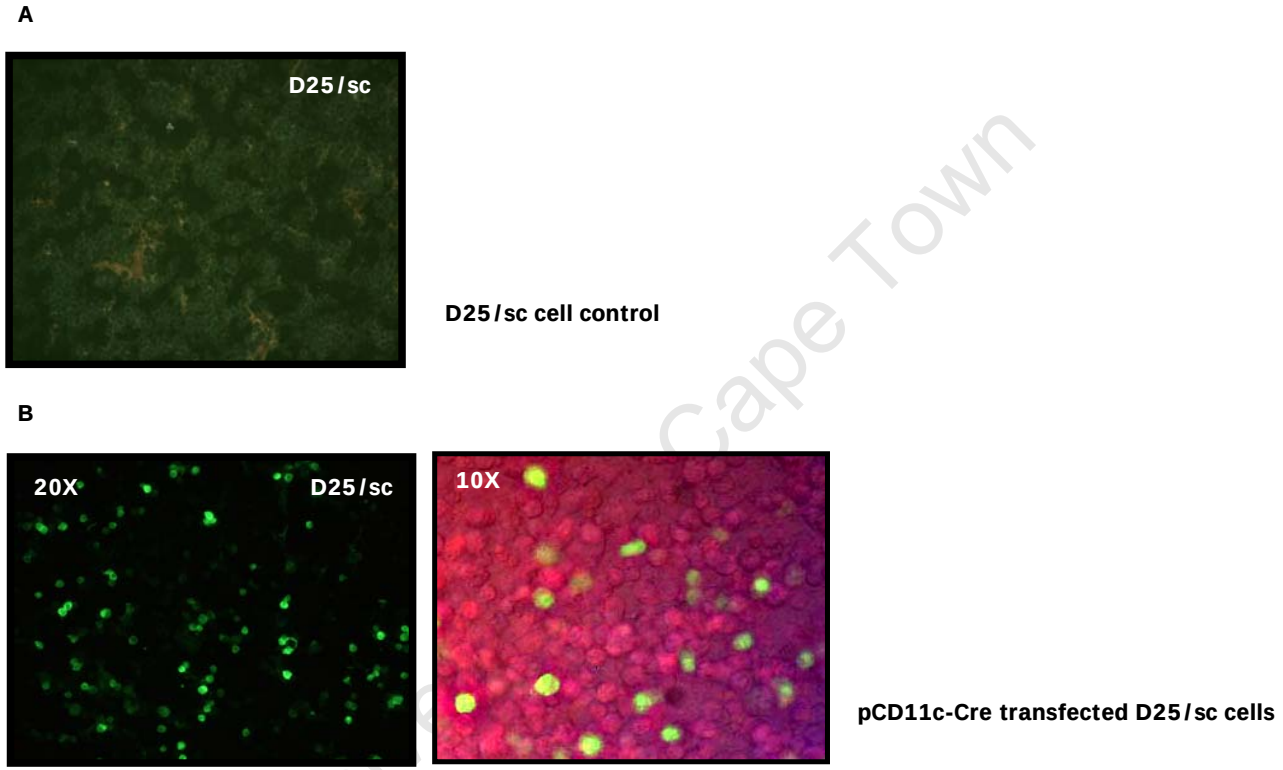

Figure 3.13. Dendritic cell specific CD11c driven Cre expression.

Panel A & **B**, UV fluorescent images of the staining of D25/sc cells with the FITC labelled anti-Cre. **Panel A**, Negative control, showing untransfected cells which were stained in parallel to transfected cells. **Panel B**, Stained pCD11c-Cre transfected cells. Magnification is indicated.

3.4 Chapter Conclusions.

Following the multistep expression vector cloning strategy the pCD11c-Cre and pCD11c-GFP constructs were successfully characterised via RE screening and automated nucleotide sequencing, including primer walking owing to the size of the CD11c promoter (section 3.3.1).

The subsequent pilot studies included D25/sc phenotype characterisation and establishment of an efficient transfection method for this cell line (3.3.3.1. and 3.3.3.2). Data on DC cell lines is scarce and having received the line without any protocols pertaining to culture or transfection these were established preceding any functionality assays. Fortunately the cells stained for the surface markers present on immature dendritic cells (CD11c and MHC II) and with the increased transfection efficiency employing an optimised electroporation protocol, as opposed to reagents, the *in vitro* functionality of the CD11c promoter and the Cre recombinase and GFP transgenes could be assessed.

The CD11c driven Cre and GFP expressing vectors were transfected into both the Hek 293T, which served as a control cell line, and into the D25/sc cell lines. Utilising the GFP reporter function the CD11c promoter activity in D25/sc cells had previously been established in the pilot studies (3.3.2), where cells transfected with the pCD11c-GFP construct were used. With the mRNA transcripts isolated from these cells it was possible to investigate Cre recombinase transgene transcription, and as expected Cre specific cDNA was present only in the D25/sc cells but not in the transfected Hek 293T cells (3.3.4.1). Translational activity of the GFP and Cre transgenes was confirmed via FACS analysis which was positive for GFP expression and by staining of the transfected cells with an antibody against Cre. As with the transcriptional and FACS data the antibody only stained in the D25/sc cells transfected with the pCD11-Cre construct (3.3.4.2)

In conclusion, we have successfully generated 2 functional transgenic constructs: the pCD11c-GFP that could potentially be utilised as a reporter for the CD11c activity in generated transgenic models and the pCD11c-Cre construct that after generation of the transgenic mouse and breeding into the IL-4R$^{flox/flox}$ line will lead to the DC specific disruption of IL-4Rα expression.

Chapter 4: Generation of molecular tools for the neutralization of signalling via IL-4Rα and IL-13Rα$_2$.

Aim: Cloning and *in vitro* functional analysis of expression vectors for F_c-tagged IL-4Rα and IL-13Rα$_2$ soluble receptors and the IL-4Rα-IL-2γ cytokine trap.

4.1 Introduction.

Host protection against parasites and induction of allergic disease is largely dependant on the prominent role played by the related Th2 cytokines IL-4 and IL-13. Both bind to cell membrane receptors that contain the IL-4Rα chain (Chiaramonte *et al.*, 2003; Fallon *et al.*, 2000;; Madden *et al.*, 1991; Urban *et al.*, 1998; Wills-Karp *et al.*, 1998). IL-13 and IL-4 signalling pathways are illustrated in Figure 1. Cytokine binding leads to the activation of a signalling cascade starting with Stat6 and ultimately leading to the cellular response (Kaplan *et al.*, 1996). IL-13 and IL-4 do however exert diverse biological effects which have partly been contributed to the lack of IL-13 signalling through the type 1 IL-4 receptor (Chomarat and Banchereau, 1998). Thus far, these IL-4 / IL-13 signalling pathways have been shown to be complex and as yet not fully understood (Lin *et al.*, 1995; Zuwarski *et al.*, 1993).

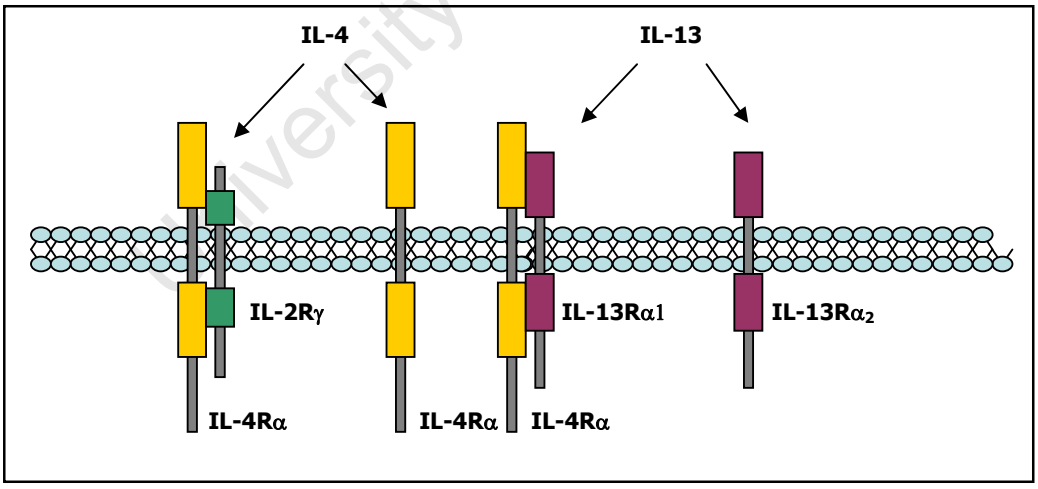

Figure 4.1. IL-13 and IL-4 receptor combinations and binding.

IL-4 binds and interacts with the IL-4Rα subunit in combination with the Type I IL-4R – γc or alternately with IL-13Rα1. IL-13 interacts with IL-13Rα1 in combination with IL-4Rα or with IL-13Rα$_2$.

Cytokine blockers with the potential to inhibit the cytokine – receptor interaction have proven to be powerful tools in the pursuit to an enhanced understanding of cytokine function during certain disease states. Of these the TNF-α blocker (Enbrel) is a prime example which has lead to clinical trails in patients suffering from rheumatoid arthritis (Goldenberg, 1999). Previously, an IL-13 blocker consisting of the extracellular domain of murine IL-13Rα_2 fused to the hinge-CH2-CH3 regions of hIg-γ1 had been generated (Donaldson *et al.*, 1998). This soluble form of the IL-13 binding protein demonstrated high affinity binding and specificity for the IL-13 cytokine. Furthermore, it displayed an effective IL-13 antagonistic function (Grunig *et al.*, 1998; Urban *et al.*, 1998). Previous studies also describe the generation of IL-4 cytokine blockers. Examples of these blockers are; recombinant IL-4 soluble proteins, an IL-4 binding antibody (11B11), recombinant mutated IL-4 proteins or IL-4/anti-IL-4mAb complexes (IL-4C) (Finkelman *et al.*, 1999;Grunewald *et al.*,1997; Maliszewski *et al.*, 1990). In addition, the use of heterodimeric receptor complexes, an example being the human soluble IL-2Rγ - soluble IL-4Rα cytokine trap has the potential of being even more potent a blocker of cytokine function (Economides *et al.*, 2003). It was shown that incorporating both receptor components, namely, IL-4Rα and IL-2Rγ, involved in forming the multi-component IL-4 receptor system, resulted in more effective IL-4 cytokine binding.

The soluble IL-13Rα_2F$_c$ fusion protein described in the current study differs from the recombinant mentioned previously, in two ways; firstly the RNA used to generate the coding region for the extracellular domain of IL-13Rα_2 was isolated from a BALB/c mouse strain as opposed to the C3H/HeJ RNA used in the above-mentioned study. For our purposes this represented a more relevant genetic background to study IL-4Rα, as the majority of the IL-4Rα transgenic mice available are on a BALB/c background. Secondly, the fusion of the extracellular domain is to a mutated form of the human IgG1. It is not clear how these differences will be represented in the phenotype, but should be borne in mind when comparing binding affinity and antagonistic/agonistic roles. The IL-4 soluble receptor blocker described in this report was generated from BALB/c cDNA and fused to the human F$_c$ tag, and as with the sIL-13Rα_2F$_c$ blocker it isn't clear how these differences will be represented in the studies. Furthermore, the generation of the sIL-2Rγ-sIL-4Rα cytokine trap the design was based on the molecular design of a previously generated IL-4 cytokine trap (Economides *et al.*, 2003). With differences being in the use of extracellular domains of BALB/c IL-4Rα and IL-2Rγ, as opposed to the human IL-4Rα and IL-2Rγ extracellular domains used in the above-mentioned study.

Finally, we aimed to build on the vast body of knowledge of the previously investigated cytokine blockers to generate F$_c$-tagged soluble receptor blockers for IL-4Rα, IL-13Rα_2

and the IL-2Rγ-IL-4Rα receptor complex. These Fc-tagged blockers would have the ability to block cytokine function *in vitro* and subsequently *in vivo*. The design and generation of these fusion proteins were although analogous to previous described IL-4 and IL-13 cytokine blockers an refinement of these. This optimization was in the construct design where we specifically used cDNA of a BALB/c genetic background (to skew the Th1 / Th2 response), and a mutated human F_c-tag which decreases non-specific binding by these fusion proteins.

4.2 Methods and Materials.

4.2.1 Cloning of the constructs.

4.2.1.1 Plasmid purification.

All molecular biological manipulations were performed according to established protocols (Ausubel *et al.,* 1995). Chemicals and reagents were Molecular Biology Grade. Small-scale plasmid purifications were performed using a SV Wizard Plasmid Purification preps and a Wizard Maxiprep kit (Promega Corp., Madison, USA) was used for large-scale purifications, using protocols supplied with each kit.

4.2.1.2 Primer design.

Synthetic oligonucleotide primers were supplied by the Oligonucleotide Synthesis Facility, Department of Molecular and Cell Biology, University of Cape Town.

4.2.1.2.1 The extracellular domains of IL-4Rα , IL-13Rα$_2$ and IL-2Rγ.

Table 4.1 Sequences of oligonucleotides used for the amplification of the extracellular domains of IL-4Rα , IL-13 Rα$_2$ and IL-2Rγ.

Primer name	Sequence
IL-4Rα F	5′ AT-**GGTACC-**CATCAAGGTCCTGG ‘3*
sIL-4Rα R	5′ TT-GCGGCCGC**-**AGGCGCTGTATCAGG ‘3′#
IL-13 Rα$_2$ F	5′ AA-**GGTACC-**TAACTGGCTATTCTTTGGAG ‘3*
sIL-13 Rα$_2$ R	5′ AA-GCGGCCGC**-**TTTGAGTCTGGCCCTG ‘3′#
IL-2Rγ F	5′ GGG-GCGGCCGC**-**GAAACTATTATTGTCACCTAGATCC ‘3′#
IL-2Rγ R	5′ GGG-GCGGCCGC**-**GAAGGATTCTCCTCTACAGTA ‘3′#

* The sequence corresponding to the *Kpn I* restriction site is in **bold**.
# The sequence corresponding to the *Not I* restriction site is underlined.

4.2.1.3 Template preparation for PCR of IL-13Rα$_2$ and IL-2Rγ extracellular domains.

4.2.1.3.1 RNA Isolation.

Total RNA was extracted from spleen and lymph nodes of BALB/c mice using TriReagent (Molecular Research Company, Cincinnati, USA) as per the manufacture's instructions. Organs were homogenized on ice in 2ml TriReagent for every 100mg of tissue. 200µl Chloroform was added for every 1ml of lysate and vortexed thoroughly. The samples were incubated at room temperature for 15min and centrifuged at 13 500rpm for 15min at 4^{o}C. The top aqueous layer was transferred to a new tube and an equal volume of

100% isopropanol added and mixed. The RNA was precipitated out of solution by overnight incubation at –70°C followed by centrifugation at 13 500rpm for 30min at 4°C. The RNA pellet was washed twice in 800µl 70% ethanol, air-dried and resuspended in 50µl-100µl of DEPC-treated water. All purified RNA samples were DNAseI treated (4.1.4.2) and stored at -70°C. RNA quality was determined by measuring the ratio of the absorbance at A_{260nm}/A_{280nm} and by electrophoresis of 1µg RNA on a 1% agarose gel containing 2.2M formaldehyde. The concentration of the RNA was determined by measuring the A_{260nm}. All solutions, except TRIS-containing buffers, used for the RNA work were treated with DEPC to destroy any endogenous RNAses. To each solution, DEPC was added to a final concentration of 0.1% and gently shaken overnight at 37°C. The solutions were then autoclaved for 30min to remove any traces of DEPC. For TRIS-containing buffers, solutions were prepared using DEPC-treated water and an ultra-pure TRIS stock designated for RNA work only.

4.2.1.3.2 DNAseI treatment and removal of digested DNA fragments.

All isolated RNA preparations were DNAseI treated. 1-10µg of total RNA was incubated with DNAseI cocktail (1 x DNAse1 buffer (Promega), 10U/µl DNAse1 (Roche Diagnostics GmbH, Mannheim, Germany), 1U/µl RNAsin (Promega) for 60min at 37°C. The DNAseI-treated RNA was cleaned using the Qiagen MiniElute RNA cleanup kit (Qiagen, Valencia, CA, USA) as per the manufacturer's instructions (see Methods and Materials section 3.3.1.2 for detailed protocol). This helped remove contaminating genomic DNA, proteins, residual phenol and salts. The elimination of contaminating genomic DNA was confirmed by RT-PCR using primers that bound to genomic DNA. The quality and quantity of the RNA was checked by spectroscopy and denaturing gel electrophoresis using standard methods (Sambrook *et al.,* 2001). The A_{260nm}/A_{280nm} ratio was measured and an aliquot was run on a 1% agarose gel containing 2.2M formaldehyde. The RNA was stored at –70°C until used.

4.2.1.3.3 cDNA Synthesis.

The genomic DNA free RNA was reverse transcribed into cDNA using the ImProm-II™ Reverse Transcription System (Promega) as per the manufacturer's instructions. Briefly, 0.5µg of Oligo (dT)15 primer was added to 1-10µg of genomic DNA free RNA in a final volume of 20µl. The sample was denaturing at 70°C for 10 minutes after which it was cooled on ice for 5min. 20µl of cDNA synthesis cocktail (ImProm-II™ 5 x Reaction Buffer, 4mM $MgCl_2$, 0.5mM each dNTP, 1U/µl RNAsin, 2.0µl ImProm-II™ Reverse Transcriptase was added and the samples incubated at 25°C for 5min to anneal the primers. cDNA

synthesis was extended at 45°C for 90min. The reaction was heat deactivated at 75°C for 5min and cooled on ice. The samples were divided into aliquots and stored at –20°C.

4.2.1.4 Polymerase Chain Reaction (PCR).

4.2.1.4.1 Amplification of extracellular domains of IL-4Rα, IL-13Rα and IL-2Rγ.

The amplification of the coding region of the extracellular domain of IL-4Rα (sIL-4Rα) was performed by PCR using 10ng of the pM5neo as template. This eukaryotic expression vector (obtained from A.Gessner) contains the 2501bp cDNA encoding the transmembrane IL-4Rα (Schulte *et al.,* 1997). The coding regions for the extracellular domains of IL-13Rα_2 (sIL-13Rα_2) and IL-2Rγ (sIL-2Rγ) were amplified using 10ng synthesized cDNA (section 4.1.4) as template. Reactions were preformed in a 50µl volume containing 1 × SuperTherm PCR Buffer, 1.5mM $MgCl_2$, 0.2mM dNTPs, 0.125U/µl Supertherm Taq (Medox Biotech India Pvt. Ltd. Chennai, India) and 0.5µM of each primer. The following cycling parameters were used for all three domains: an initial denaturation step at 94°C for 1min, followed by 30 cycles consisting of 94°C incubation for 1min, an annealing step at 60°C for 1min, and an extension step at 72°C for 1.5min. A final step of 72°C for 5min was included to complete partial extension reactions.

4.2.1.5 Cloning of the coding sequences into eukaryotic expression vectors.

4.2.1.5.1 Extracellular domains of IL-4Rα and IL-13Rα_2.

The amplified fragments corresponding to sIL-4Rα and sIL-13Rα_2 were recovered from a 1% (w/v) low melting agarose gel (section 4.1.7) and purified with the Wizard SV Gel Extraction Kit (Promega). The procedure was performed according to the manufacturer's recommendations. The isolated fragments were then digested with 10U of the restriction enzymes *Kpn I* and *Not I* (Roche) for 6h at 37°C. The digested fragments were recovered from a 1% (w/v) low melting agarose gel, and purified with the Wizard SV Gel Extraction Kit (Promega). The pSecTagF_C^{Mut} plasmid linearized by *Kpn I* / *Not I* cleavage was dephosphorylated in a 30µl reaction volume consisting of 1 × Shrimp Alkaline Phosphatase (SAP) reaction buffer (Promega), 300ng of the plasmid and 0.3U of SAP. The mixture was incubated at 37°C for 15min, and the enzyme inactivated by incubation of the reaction at 65°C for 15min. The purified fragment, in five-fold molar excess to the vector, was mixed with 50ng dephosphorylated pSecTagF_C^{Mut}, 1µl 10 × Ligation Buffer (Promega) and 1µl of T4 DNA Ligase (Promega, 3 WeissU/µl) in a total volume of 10µl. An experimental control (background control) was included where the digested sIL-4Rα or sIL-13Rα_2 insert fragments were omitted. The ligation reaction was allowed to proceed overnight at 4°C. Following ligation, 5µl of the ligation mix was added to 200µl

of calcium chloride competent DH5α *E.coli* cells (Invitrogen, Gibco BRL, USA). The suspension was incubated on ice for 30min after which the cells were heat-shocked, according to established methodology (Inoue *et al.,* 1990) at 42°C for 45sec. The transformed cells were immediately placed on ice (4°C) for a further 2min and then supplemented with 800µl room temperature SOC medium. Cells were incubated with shaking (200rpm) at 37°C for 60min. Following incubation, 100µl of the transformed cells were plated onto LB agar plates containing 50µg/ml ampicillin. Plates were incubated for 14h at 37°C. Plasmid DNA was isolated (see section 4.1.1) from overnight cultures containing 10ml LB medium supplemented with 50µg/ml ampicillin and colonies chosen randomly from the incubated plates. Positive constructs for sIL-4Rα and sIL-13Rα$_2$ were identified by restriction enzyme screening with the restriction enzymes *Not I* and *Kpn I* (Roche), and verified by a secondary PCR screening with the oligonucleotide primers initially used to amplify the respective inserts. The correct fragments from both procedures were verified by electrophoresis on a 1% (w/v) agarose gel stained with ethidium bromide (0.5µg/ml*)* (section 4.1.6). Plasmids found to contain correct inserts were sequenced by automated nucleotide sequencing, and denoted pSecTag-sIL-4RαF$_c$ and pSecTag-sIL-13Rα$_2$F$_c$. Glycerol stocks were prepared of the DH5α *E.coli* cells containing the pSecTagF$_C^{Mut}$ plasmids with the coding regions for sIL-4Rα and sIL-13Rα$_2$ and stored at -70°C.

4.2.1.5.2 Extracellular domain of IL-2Rγ.

The protocol followed was similar to that for the sIL-4Rα and sIL-13Rα$_2$ amplified fragments with a few modifications. Briefly, the amplification fragments were isolated (4.1.7) and digested with 10U of the restriction enzyme *Not I* (Roche) for 6h at 37°C. The digested fragments were recovered from a 1% (w/v) low melting agarose gel, and gel purified. The pSecTag-sIL-4RαF$_c$ plasmid linearized by a *Not I* cleavage was dephosphorylated using SAP (as described in 4.1.5.1) after which the purified amplification fragments, in five-fold molar excess to vector, was mixed with 50ng dephosphorylated pSecTag-sIL-4RαF$_c$, 1µl 10 × Ligation Buffer (Promega) and 1µl of T4 DNA Ligase (Promega, 3 WeissU/µl) in a total volume of 10µl. An experimental control was included where the digested sIL-2Rγ insert fragment was absent. After overnight incubation at 4°C, 7,5µl of the ligation mix was added to 400µl of calcium chloride competent JM109 *E.coli* cells (Invitrogen). The cells were transformed with the ligation mix (as described in 4.1.5.1) (Inoue *et al.,* 1990) and following the final incubation step in the procedure, 100µl of the transformed cells were plated onto LB agar plates containing 50µg/ml ampicillin. Plates were incubated for 16h at 37°C. Plasmid DNA was

isolated (see section 4.1.1) from overnight cultures containing 10ml LB medium supplemented with 50µg/ml ampicillin and colonies chosen randomly from the plates. Positive constructs for sIL-2Rγ were identified by restriction enzyme screening with *Eco RV / Sca I and Pst I* (Roche). The correct fragments were verified by electrophoresis on a 1% (w/v) agarose gel stained with ethidium bromide (0.5µg/ml) (described in 4.1.6). Plasmids found to contain correct inserts were sequenced by automated nucleotide sequencing, and denoted sIL-2Rγ-sIL-4RαF_c. Glycerol stocks were prepared of the JM109 *E.coli* cells containing the pSecTagF_C^{Mut} plasmids with the in-line coding regions for sIL-4Rα and sIL-2Rγ and stored at -70°C.

4.2.1.6 Agarose gel electrophoresis.

All DNA samples including PCR products, restriction enzyme (RE) digestion and RE screening products, were verified by agarose gel electrophoresis through a 0.8 or 1% (w/v) agarose gels (gel percentage was dependant on fragment size) in 1 × TAE electrophoresis buffer. Samples were electrophoresed at constant voltage of 150V for 45min at room temperature. Gels were stained with ethidium bromide (0.5µg/ml). DNA was visualised by short wavelength UV transillumination (A_{254nm}).

4.2.1.7 Gel isolation and purification of DNA.

DNA samples including PCR products and samples from RE digestions of fragments to be used in ligation were electrophoresed on a 1% low melting point agarose gel in 1 × TAE electrophoresis buffer (containing 0.5µg ethidium bromide/ml) at 90V for 1h. DNA was visualised by brief exposure to low wavelength UV (A_{320nm}). The appropriate bands were excised from the gels with a sterile blade. Gel slices were melted by incubation at 65°C in heating block and DNA purified using the Wizard SV Gel Extraction kit (Promega), according to the manufactures instructions. DNA concentrations were determined from the absorbance of samples at A_{260nm} using the conversion factor for double stranded DNA (1OD unit = 50µg/ml).

4.2.2 Cell culture.

4.2.2.1 Hek 293T cells.

The human embryonic kidney 293 cell line (Hek 293T) (obtained from Gordon Brown, IIDMM, UCT Medical School) was used for all transfection and expression assays. The cells were cultured in DMEM medium pH7.4, supplemented with 10% Foetal Calf Serum (FCS)(Gibco Life Technologies, Paisely, UK) 10mg/ml streptomycin and 10U/ml penicillin

at 37°C and 5% CO2. Cells were passaged when cell monolayer reached ~70% confluence. To split cells to a 1:10 ratio the media was aspirated from the cells and cells washed once with 1 x PBS. The adherent cells were dislodged from the flask by addition of Trypsin-EDTA solution (Gibco) and incubation for 1min at room temperature. After gentle tapping of the flask the suspension was diluted in DMEM supplemented with 10% FCS to inactivate the trypsin. This suspension was pelleted at 1 200rpm for 5min and the supernatant carefully decanted. Cells were resuspended in DMEM / 10% FCS and transferred to the appropriate size tissue culture flask (Nalge Nunc International, Naperville, IL, USA). Unless otherwise stated, sub confluent Hek 293T cells (cell monolayer at ~70% confluence) were transfected in serum-free conditions using Lipofectamine Reagent (Invitrogen).

4.2.2.2 Transfection of Hek 293T cells.

Hek 293T cells were transfected using Lipofectamine Reagent (Invitrogen) which employs a lipid-mediated method (Felgner and Ringold, 1989), with optimization of the manufacture's instructions. Briefly, cells were plated at $2x10^5$cell/well in a 6 well plate (Nalge Nunc International) and incubated at 37°C in a humidified 5% CO_2 for 24h. The next day, two tubes each containing 0.75ml DMEM media was prepared. 1ug isolated plasmid DNA, diluted to a working concentration of 1ug/ml in distilled H_2O, was added to one tube and to the other 5ul of Lipofectamine Transfection Reagent (Invitrogen). The reaction mixtures from the two tubes were combined and incubated at room temperature for 20min. The adherent Hek 293T cells were washed twice with 3ml/well serum-free DMEM media. The 1.5ml reaction mixture was then carefully plated onto the cells. The cells were incubated at 37°C in a humidified 5% CO_2 incubator for 24h. Subsequently, the serum-free media was aspirated and cells re-incubated with 3ml DMEM / 10% FCS (Gibco) with selective pressure maintained with the addition of 250µg/ml Zeocin (Invitrogen).

4.2.3 Purification and detection of recombinant proteins.

4.2.3.1 Large scale protein expression.

Large scale protein expression was achieved by increasing the size and number of cell culture flasks used for culture. Cultures were prepared from Hek 293T cells containing pSecTag-sIL13Rα_2F$_c$, sIL-4RαF$_c$ or sIL-2Rγ-sIL-4RαF$_c$ (as described in section 4.2.1) in media supplemented with 250µg/ml Zeocin (Invitrogen). Culture media was collected every 72-96h and cells re-incubated with fresh media and antibiotics for a further 72h. Collected culture media, containing the secreted recombinant proteins, was filter

sterilized through a 0.22μM filter (Millipore Corporation, Bedford, USA). 0.05% Sodium Azide was added to filtered media after which it was stored at 4°C.

4.2.3.2 Cell lysate preparation for Hek 293T / pSecTag-sIL13Rα_2F_c cultures.

Hek 293T cells transfected with sIL13Rα_2F_c were cultured and culture media collected at intervals (4.3.1). Adherent cells were rinsed twice with 10ml ice-cold 1 × PBS. 5ml ice-cold modified RIPA buffer was added to the cells and flasks incubated at 4°C for 10min. Cell suspensions from all flasks were pooled and transferred to a sterile 50ml centrifuge tube. Centrifuge tubes were left on ice for 15min with gently agitation at intervals. Cellular lysates were collected with centrifugation in a JA-14 rotor (Beckman), using a J2-21 centrifuge (Beckman) at 12 000 × g for 20min at 4°C. Lysates were filter sterilized through a 0.22μM filter (Millipore Corporation), supplemented with 0.05% Sodium Azide and stored at 4°C until use.

4.2.3.3 IgG Protein purification.

Protein A Sepharose chromatography was utilised to purify the expressed proteins. All material to be used was equilibrated at room temperature, the temperature at which the chromatography was preformed. The medium slurry, nProtein A Sepharose 4 Fast Flow (Amersham Biosciences) was de-gassed after which the slurry was poured into the column. The settled medium was equilibrated with 10 column volumes of binding buffer [50mM Tris·Cl, pH 7.0]. The collected supernatants were centrifuged in a JA-14 rotor (Beckman), using a J2-21 centrifuge (Beckman) at 12 000 × g for 20min at 4°C. Centrifuged supernatant was diluted with half a volume of binding buffer and applied to the column. The supernatant was re-applied and run through the column for an additional 3 times. The column was washed with 10 column volumes of binding buffer. Fc-tagged soluble receptors were eluted from the column beads with 100mM glycine, pH 2.5. The eluted protein was collected in sterile tubes containing a 25% final fraction volume of 1M Tris·Cl, pH 8.0. Approximately 2 column volumes were collected. The columns were washed with 5 column volumes of binding buffer supplemented with 0.05% Sodium Azide and stored at 4°C. Fractions were measured individually using a spectrophotometer at A_{280nm}. Peak fractions were combined. Eluted protein was desalted and concentrated by addition of 15ml 1 × PBS and centrifugation at 4000 × g for 20min using Amicon Ultra-15 centrifugal filter device (Millipore) as per the manufacture's instructions. 0.05% Sodium Azide was added to the concentrated solute which was then stored at 4°C.

4.2.3.4 Protein quantification.

Protein concentrations were determined using a microassay procedure using Pierce BCA Protein Assay Reagent according to the manufacture's protocol (Pierce Chemical Company, Rockford, Illinois, USA). Briefly, nine dilutions, prepared in the same diluent used for the protein sample, of a BSA standard (Bio-Rad), was used in the linear range from 0.2mg/ml to 1.8mg/ml. Sample was diluted in a 3-fold linear range. Duplicates of10ul of the sample or the standard were pippetted into a micro plate (Nalge Nunc International). The sample diluent was used as a blank control. The BCA working solution was prepared by mixing 50 parts solution A to 1 part solution B. 200ul of this working solution was added to all wells. The plate was incubated at 37°C for 30min. After incubation, the plate was equilibrated at room temperature and the absorbance measured at A_{540nm} in a VersaMax microplate reader (Molecular Devices Corporation, Sunnyvale, CA, U.S.A). Comparison of the test samples to a standard curve provided the protein concentration.

4.2.3.5 SDS-PAGE.

All proteins were analysed by SDS-PAGE electrophoresis as described by Laemmli (1970). Depending on protein size the gels consisted of a 10-15% (w/v) polyacrylamide (acrylamide:bisacryamide 29:1) containing 375mM Tris·Cl (pH 8.8) and 0.1% (w/v) SDS. The stacking gel consisted of 6% (acrylamide:bisacryamide 29:1) (w/v) polyacrylamide containing 125mM Tris·Cl (pH 6.8) and 0.1% (w/v) SDS. Samples were denatured at 95°C in 1 × sample application buffer containing 25% (v/v) β-mercaptoethanol. Gels were electrophoresed at 200V for 1h in a MiniProtean III (Bio-Rad) electrophoresis system. Following electrophoresis, gels were stained with Coomassie Blue stain solution [0.25% (w/v) Coomassie Brilliant Blue in 100% methanol] for 1h and destained overnight in destain solution [7% (v/v) acetic acid, 25% (v/v) ethanol].

4.2.3.6 Western blot analysis.

Following SDS-PAGE electrophoresis proteins were transferred to a PVDF membrane (Amersham-Pharmacia, Tokyo). Prior to transfer all components used in the transfer assembly were soaked in ice-cold 1 x transfer buffer for 30min at 4°C. Proteins were transferred using tank transfer (Mini Trans-Blot Electrophoretic Transfer Cell, BioRad) with the gel/membrane stack completely immersed in the buffer reservoir. Transfer was performed at 375mA for 2h. The membrane was removed from the transfer stack and washed with distilled water. The membrane was blocked with 1 x TBS (Tris-buffered saline) containing 5% nonfat dry milk for 60min at room temperature. In this way blocking unoccupied membrane sites and preventing nonspecific binding of antibodies.

The primary antibody, IgG-AP (goat anti human, Sigma) was diluted 1/5000 in blocking solution containing 0.05% Tween 20 and 3% milk powder and incubated overnight at 4°C with agitation. Unbound primary antibody was removed by washing the membrane 3 times for 3-5min each with 1 x TBS 0.05% Tween 20. Chromogenic detection (Leary, *et al.,* 1983) was performed by incubating the membrane with a solution of 200µl NBT/BCIP substrate (Roche) diluted in 10ml NBT substrate buffer for 2-5min in the dark.

4.2.4 *In vitro* assays.

4.2.4.1 Cytokine binding assay.

The level of cytokine binding by sIL-13Rα_2F$_c$, sIL-4RαF$_c$ and sIL-2RγF$_c$ was measured by ELISA. Maxisorb 96 well ELISA plates (Nalge Nunc) were coated overnight at 4^{o}C with 50µl capturing antibody diluted in coating buffer (1 x PBS, 0.02% Sodium Azide) at the recommended concentration; 0.002mg/ml for ant-IL-4 and 0.02mg/ml anti-IL-13. Or alternatively plates were coated with varying concentrations of purified sIL-13Rα_2F$_c$, sIL-4RαF$_c$ and sIL-2RγF$_c$ (for sIL-4RαF$_c$ 0.025mg/ml, 0.012mg/ml, 0.06mg/ml, 0.025mg/ml was used; for sIL-13Rα_2F$_c$ 0.2mg/ml, 0.1mg/ml, 0.05mg/ml and 0.02mg/ml was used and for sIL-2RγF$_c$ 0.002mg/ml was used) diluted in coating buffer. Coated plates were washed and incubated overnight at 4°C with 200µl blocking buffer. The appropriate recombinant protein standard was diluted to the recommended concentration, then serially diluted three-fold in dilution buffer and 50µl added to wells of washed plates. The plates were incubated overnight at 4^{o}C and washed. 50µl of the appropriate biotinylated antibody was diluted to the recommended concentration in dilution buffer and 50µl was added to each well. The plates were incubated at 37^{o}C for 3h, washed and 50µl of streptavidin-alkaline phosphatase diluted 1:1000 in dilution buffer was added to each well. The plates were incubated for 60min at 37^{o}C, washed and 50µl substrate solution added to each well. The enzymatic reaction was developed at room temperature and stopped when the most concentrated standard reached 1.0 to 1.5 A_{405nm} OD units. The developing reaction was stopped by adding 50µl of 1M NaOH to each well. The plates read at A_{405nm} using a VersaMax microplate reader (Molecular Devices). For the wash steps above, each well was washed 4 times with 300µl of wash buffer. For IL-13 reaction development, streptavidin–horseradish peroxidase and TMB Substrate Solutions (Roche) were used as per the manufacturer's instructions.

4.2.4.2 Cell proliferation assay.

Naïve mice (3/group) were sacrificed by a high anaesthetic dose of CO_2. Lymph nodes were removed aseptically and placed in ice cold IMDM media supplemented with 10% FCS (Gibco). Single cell suspensions were prepared and filtered through 70µm nylon cell strainers (Becton-Dickinson, New Jersey). Cells contaminated with red blood cells were resuspended in 5ml Red cell lysis buffer and underlayed with 1ml heat inactivated FCS. Cells were centrifuged at 1 200rpm for 10min at 4°C and resuspended in 2ml IMDM supplemented with 10% FCS (Gibco). 10µl aliquots of the cell suspension was diluted in Trypan Blue and counted on a Neubauer haemocytometer. Cell concentrations of the unstained viable cells were determined and volumes adjusted to attain a concentration of $5x10^5$cell/ml. PMA (Sigma) was added to cells a 5ng/ml final concentration. 100µl cells from each group were plated out in triplicate in round bottomed 96 well tissue culture plates (Nalge Nunc). Working dilutions of stimulants were prepared in IMDM / 10% FCS as follows: 1) 2000U/ml rIL-2, 2000U/ml rIL-4, (all supplied by BD Pharmingen, San Diego, CA) and 500ng/ml sIL-4RαF_c; 2) 400ng/ml rIL-13 (R&D Systems, Minneapolis, MN) and 1µg/ml sIL-13R$\alpha_2 F_c$. Stimulant dilutions were added to the plated cells at 100µl per well. Included was a medium only control where 100µl IMDM / 10% FCS was added to a row of plated cells. Cells were cultured for 48h at 37°C in a humidified 5% CO_2 incubator. For the quantification of cell proliferation a colorimetric immunoassay (Roche) based on BrdU incorporation during DNA synthesis was used. The protocol was followed as per manufactures instructions. Briefly, 20µl BrdU labelling solution was added to the cells for a final concentration of 10µM BrdU per well. The cells were re-incubated for an additional 24h as above. Cell plates were centrifuged at 1 200rpm at 4°C for 10min cells ad labelling medium removed by aspiration. Cells were dried for 1h at 60°C. 200µl FixDenat Solution was added to each well and cells incubated at room temperature for 30min. FixDenat solution was removed by flicking. After addition of 100µl/well anti-BrdU-POD working solution, cells were incubated at room temperature for 1h. The antibody conjugate was removed by flicking the plate after which cells were rinsed 3 times with 200µl/well washing solution. 100µl Substrate solution was added to each well and cells incubated at room temperature until colour development was sufficient for photometric detection. The reaction was stopped with the addition of 25ul 1M H_2SO_4 per well. The sample absorbance was measured on a Versamax microplate spectrophotometer (Molecular Devices) at A_{450nm} (reference wavelength: A_{690nm}).

4.2.4.3 T cell differentiation assay.

Naïve mice (5/group) were sacrificed by a high anaesthetic dose of CO_2. Lymph nodes were removed aseptically and placed in ice cold RPMI 1640 supplemented with 10% FCS (Gibco). Single cell suspensions were prepared and filtered through 70µm nylon cell strainers (Becton-Dickinson). Cells contaminated with red blood cells were resuspended in 5ml Red cell lysis buffer and underlayed carefully with 1ml heat inactivated FCS. Cells were centrifuged at 1 200rpm at 4°C for 10min and resuspended in 2ml RPMI 1640 / 10% FCS (Gibco). Aliquots of the cell suspension (10µl) was diluted in Trypan Blue and counted on a Neubauer haemocytometer. Viable cell concentrations were determined and volumes adjusted to attain a concentration of $1x10^6$cell/ml. $CD4^+$ T cells were purified by magnetic CD4 microbeads using the MiniMACS system as per manufacture's instructions (Miltenyi Biotec, Auburn, CA). Cell purity determined by FACScan analysis was ~96%. $2x10^5$cells per well in complete RPMI 1640 medium / 10% FCS (Gibco), supplemented with 50uM B2-mercaptoethanol (Sigma, St. Louis, MO), 1mM sodium pyruvate and non-essential amino acids (Gibco), were plated in flat bottom 96 well plates (Nalge Nunc). The wells had been coated overnight at 4°C with 10µg/ml anti-CD3 and 5µg/ml ant-CD28 (both BD Pharmingen) in filter sterilized 1 x PBS. For TH1 polarization cells were incubated with 5ng/ml IL-12 (BD Pharmingen) and 50µg/ml anti-IL-4 (clone 11B11). For Th2 polarization cells were stimulated with 50µg/ml anti-IFN-γ (BD Pharmingen) and either 50ng/ml murine IL-4 (BD Pharmingen) or 100ng/ml IL-13 (R&D System). To asses the ability of the F_c-tagged soluble receptors to block polarization, cells were incubated with either; 1) 50µg/ml anti-IFN-γ, 50ng/ml murine IL-4 and 150ng/ml sIL-4RαF_c or 2) 50µg/ml anti-IFN-γ, 100ng/ml IL-13 and 250ng/ml sIL-13R$\alpha_2 F_c$. Cells incubated with complete media only were included as a control. The cells were incubated in a final volume of 200µl for 72h at 37°C in a humidified 5% CO_2 incubator. Subsequently, cells were transferred to a round bottom 96 well plate (Nalge Nunc) and washed 2 times in RPMI 1640 / 10% FCS. Washed cells were resuspended in complete RPMI 1640 medium supplemented with 20U/ml IL-2 (BD Pharmingen) containing cytokines and antibodies, as above. Cells were further incubated for 48h. Cells were washed with fresh culture medium and re-plated in triplicate at 2x105cells per well in a flat bottom 96 well plate pre-coated overnight with 20µg/ml anti-CD3 (BD Pharmingen). After 48h incubation, supernatants were harvested and frozen at -70°C. Subsequently cytokine analysis was preformed using ELISA.

4.2.4.4 Cytokine ELISA.

Maxisorb 96 well ELISA plates (Nalge Nunc) were coated overnight at 4°C with 50µl of capturing antibody diluted in coating buffer at the recommended concentration. Plates were washed, and blocked for 24h at 4°C with 200µl blocking buffer and subsequently washed. Samples were serially diluted two-fold in dilution buffer and 50µl added to each well. Similarly, the appropriate recombinant protein standard was diluted to the recommended concentration, serially diluted three-fold in dilution buffer and 50µl added to designated control wells. The plates were incubated overnight at 4°C and washed. 50µl of the appropriate biotinylated antibody was diluted to the recommended concentration in dilution buffer and 50µl was added to each well. The plates were incubated at 37°C for 4h, washed and 50µl of streptavidin-alkaline phosphatase diluted 1:1000 in dilution buffer was added to each well. The plates were incubated for 60min at 37°C, washed and 50µl substrate solution added to each well. The enzymatic reactions were developed at room temperature and were stopped when the most concentrated standard reached 1.0 to 1.5 A_{405nm} OD units. The developing reaction was stopped by adding 50µl of 1M NaOH to each well. The plates were read at A_{405nm} using a VersaMax microplate reader (Molecular Devices Corporation). For the wash steps above, each well was washed 4 times with 300µl of wash buffer. For IL-13 ELISA reaction development, streptavidin–horseradish peroxidase and TMB Substrate Solutions (Roche) were used as per the manufacturer's instructions.

4.2.4.5 Generation of bone marrow derived macrophages (BMDMs).

Naïve mice were sacrificed by cervical dislocation and the femur and tibia bones collected. The bone marrow cells were flushed from the bones using DMEM (Gibco) / 10% FCS containing 100U/ml penicillin G and 100µg/ml streptomycin. The cells were washed and pelleted by centrifuging at 1 200rpm at 4°C for 10min. The bone marrow cells were added at a final concentration of $1x10^6$cells/ml in PLUTZNIK media and transferred into a special gas-permeable 15cm x 6cm Teflon coated-bag (Max Planck Institute for Immunobiology, Max Planck, Freiberg, Germany). The L929 conditioned medium contained GM-CSF and M-CSF, which stimulated the differentiation and growth of bone marrow stem cells into macrophages. The open end of the bag was heat-sealed and bone marrow stem cells incubated at 37°C under 5% CO_2 for 10 days. The supernatant was discarded and the adherent cells were massaged from the Teflon-coated bags into DMEM / 10% FCS, 100U/ml penicillin G and 100µg/ml streptomycin. The BMDMs were washed twice in DMEM / 10% FCS, to remove residual GM-CSF from the L929 conditioned medium.

For the subsequent F_c-tagged soluble receptor blocking assays, measuring NO and arginase activity, the BMDMs were plated at a density of $4x10^6$BMDMs/ml in a volume of 100ul in flat bottom 96 well plates (Nalge Nunc) to which the following stimulant mixtures were added; 100ul media only, mIL-4 (1000U/ml, BD Pharmigen), mIL-4 / sIL-4RαF_c (10 X that of mIL-4), mIL-13 (200ng/ml, R&D Systems) and mIL-13 / sIL-13R$\alpha_2 F_c$ (10 X that of mIL-13). Cells were incubated overnight at 37°C under 5% CO_2. Subsequently, IFN-γ (200U/ml, BD Pharmigen) and LPS (20ng/ml, Sigma) was added and cells incubated a further 48h. The plates were centrifuged at 1 200rpm for 10min. Supernatant was removed for nitric oxide (NO) measurements. The remaining cells were washed with 1 x PBS. Cell lyses was achieved by resuspension in 50ul 0.1% Trition X-100 and shaking at 80rpm for 30min at room temperature. After careful resuspension arginase activity was measured (section 4.4.8).

For the subsequent F_c-tagged soluble receptor blocking assays, measuring mannose receptor expression, BMDMs were plated at a density of $2x10^6$ BMDMs cells/well in a 12 well plate and stimulated with mIL-4, mIL-13, mIL-4 / sIL-4RαF_c or mIL-13 / sIL-13R$\alpha_2 F_c$ (as above) for 72h at 37°C under 5% CO_2.

4.2.4.5.1 L929 conditioned medium.

L929 cells were maintained in DMEM (Gibco) / 10% FCS supplemented with 100U/ml penicillin G and 100µg/ml streptomycin until 90% confluence. The growth media was removed and the cells washed in 10ml 1 x PBS. Cells were removed from the plastic surface of the flask by incubation in 5ml Trypsin/EDTA buffer (Gibco) at room temperature for 4min. The cells were washed in 50ml DMEM / 10% FCS and seeded at $2x10^4$cells/ml in 100ml DMEM / 10% FCS, with appropriate antibiotics. The L929 cells were grown in $162cm^2$ tissue culture grade flasks (Corning Costar Corporation, Cambridge, MA, USA) at 37°C under 5% CO_2 for 7 days. The supernatant was harvested and centrifuged at 2 500rpm for 15min at 4°C to get rid of cell debris. The clear supernatants were stored in 50ml aliquots at –20°C.

4.2.4.6 Measurement of nitric oxide.

Cell culture supernatants were analyzed for the production of nitric oxide (NO) using the Griess reaction assay, which measures the concentration of nitrite, a stable product of the reaction of NO with O_2 (Ding *et al.,* 1988). Supernatant samples and standards (1mM NO_2 solution) were serially diluted three-fold in DMEM / 10% FCS supplemented with 100U/ml penicillin G and 100µg/ml streptomycin (all Gibco). 50µl of these dilutions were added to designated wells in a flat-bottomed 96 well plate. 25µl of Griess Reagent 1 and

then 25µl of Griess Reagent 2 were sequentially added to each well. The plate was incubated at room temperature for 5min to allow development of the reaction. The purple-pink colour of the reactions was read at A_{540nm} and the reference at A_{690nm} using VersaMax microplate reader (Molecular Devices Corporation).

4.2.4.7 Measurement of arginase activity.

Arginase I activity in BMDMs was measured as previously described (Corraliza *et al.,* 1994). Subsequent to cell lysis, 50ul of 10mM $MnCl_2$, 50mM Tris·Cl (pH7.5) was added and the enzyme activated for 10min at 55°C. Arginine hydrolysis was carried out in sterile eppendorf tubes by the addition of 25µl 0.5M arginine (pH9.7) to 25µl of the activated cell lysates. The samples were incubated at 37°C for 60min and the reaction stopped by the addition of 400µl of an acid mixture consisting of H_2SO_4, H_3PO_4 and H_2O (1:3:7). Aliquots of 25µl of 9% ISPF (freshly made) dissolved in 100% ethanol was added to each sample and samples heated at 100°C for 45min. After placing the samples in the dark for 10min, 200µl of each was transferred to a 96 well microtiter plate (Nalge Nunc International). A standard curve was prepared by making 3-fold dilutions of 1mg/ml of urea in H_2O. The standards were treated as the samples from the addition of the acid mixture. The absorbance's of samples and standards were measured at A_{540nm} using a Versamax spectrophotometer (Molecular Devices Corporation). The urea concentration measured for each sample was used as a measure of arginase activity.

4.2.4.8 FACS analysis of BMDMs.

BMDMs were removed from the flat bottom 96 well plates (Nalge Nunc) using Trypsin/EDTA buffer (Gibco). Cell suspensions were centrifuged at 1 200rpm for 8min and resuspended in 2ml complete IMDM / 10% FCS supplemented with 100 U/ml penicillin and 100µg/ml streptomycin (all Gibco). Aliquots of cells (10µl) were diluted in Trypan Blue and counted on a Neubauer haemocytometer to determine concentrations of viable cells. $5x10^5$ cells were pooled for each stimulant group and resuspended in 2% paraformaldehyde diluted in 1 x PBS and incubated for 30min on ice. The cell suspension was washed by centrifugation at 1 200rpm for 10min and resuspended in 1 x PBS. Cells were centrifuged as before and resuspended in a mixture consisting of 0.5% saponin diluted in 1 x PBS. The cells were incubated for 10min at 37°C and subsequently transferred to ice for 10min. Cells were pelleted by centrifugation at 1 200rpm for 10min and resuspended in 100µl blocking buffer consisting of 0.5% saponin diluted in 1 x PBS and the following antibodies; αCD8(Ly-2)-biotin (0.7mg/ml) and αCD206-biotin (0.1mg/ml) (all BD Biosciences). These suspensions were stained in the dark on ice for 20min. Cells were centrifuged at 1 200rpm for 10min and resuspended in 100ul blocking

buffer containing αCD11b-PE (10µg/ml) (Integrin$\alpha_m$chain,Mac-1αchain) and incubated on ice for 20min. Cells centrifuged at 1 200rpm for 10min and resuspended in 500ul 1 x PBS containing 0.5% saponin. Pelleted cells were resuspended and incubated for a further 15min on ice with 100µl of a saturating amount of streptavidin-APC (BD Biosciences) in FACS buffer. After the final wash with 300µl FACS buffer, cells were resuspended in 300µl FACS buffer supplemented with 7-AAD (Sigma, St. Louis, USA). Dead cells stained with 7-AAD were excluded from analysis. Stained cell acquisition was preformed using a FACSCalibur flow cytometer (BD Biosciences) and cells analyzed using CellQuest software (Becton-Dickinson, Ferndale, South Africa). 100 000 cells were acquired for analysis.

4.3 **Results**.

4.3.1 Vector design and construction.

To generate soluble chimeric proteins of the IL-4Rα, IL-13Rα_2 and IL-2Rγ-IL-4Rα, the corresponding coding regions for the extracellular domains of the three separate proteins were PCR amplified and cloned into the eukaryotic expression vector, pSecTag-F_c^{Mut}. The cloning strategy for the three constructs are illustrated in Figures 4.2 A, B and C. pSecTag-F_c^{Mut} consists of the pSecTag expression vector which has been modified by the addition of a mutated F_c fragment in the multiple cloning site. The purpose of this F_c fragment mutation is to inhibit F_cR binding and complement fixation (Majeau *et al.*, 1994). Cloning the coding regions into this vector enables the expression of the recombinant proteins fused to the hinge and F_c domains of human IgG1. Furthermore, the F_c tag is utilised in the detection of transfected cells expressing the proteins of interest. This tag is additionally used for protein purification via protein A Sepharose affinity chromatography (Bjork *et al.*, 1972).

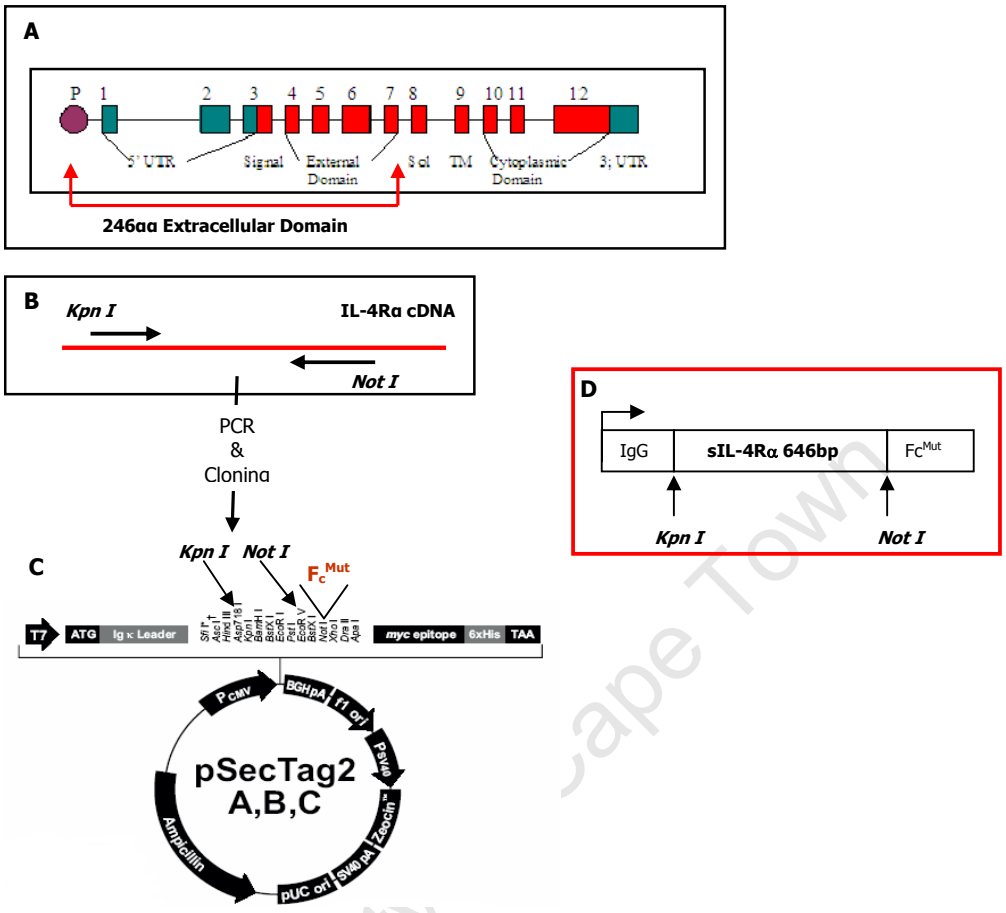

Figure 4.2.A Flow Diagram of pSecTag-F_c^{Mut}-sIL-4Rα Cloning Strategy.

Panel A, *IL-4Rα* map. Extracellular domain indicated. The soluble/secreted isoform coding region is 646bp in length and codes for 246 amino acids. **Panel B**, Primer design and PCR of sIL-4Rα transgene using BALB/c cDNA. **Panel C**, RE digestion of sIL-4Rα cDNA and ligation into pSecTag-F_c^{Mut}. The pSecTag-F_c^{Mut} eukaryotic expression vector modified via the addition of a mutated F_c fragment in the multiple cloning site (MCS). **Panel D**, The sIL-4Rα expression cassette. The IgG1 leader sequence which is followed by the sIL-4Rα coding region and F_c^{Mut} tag. The *Kpn I – Not I* ligation junctions are indicated.

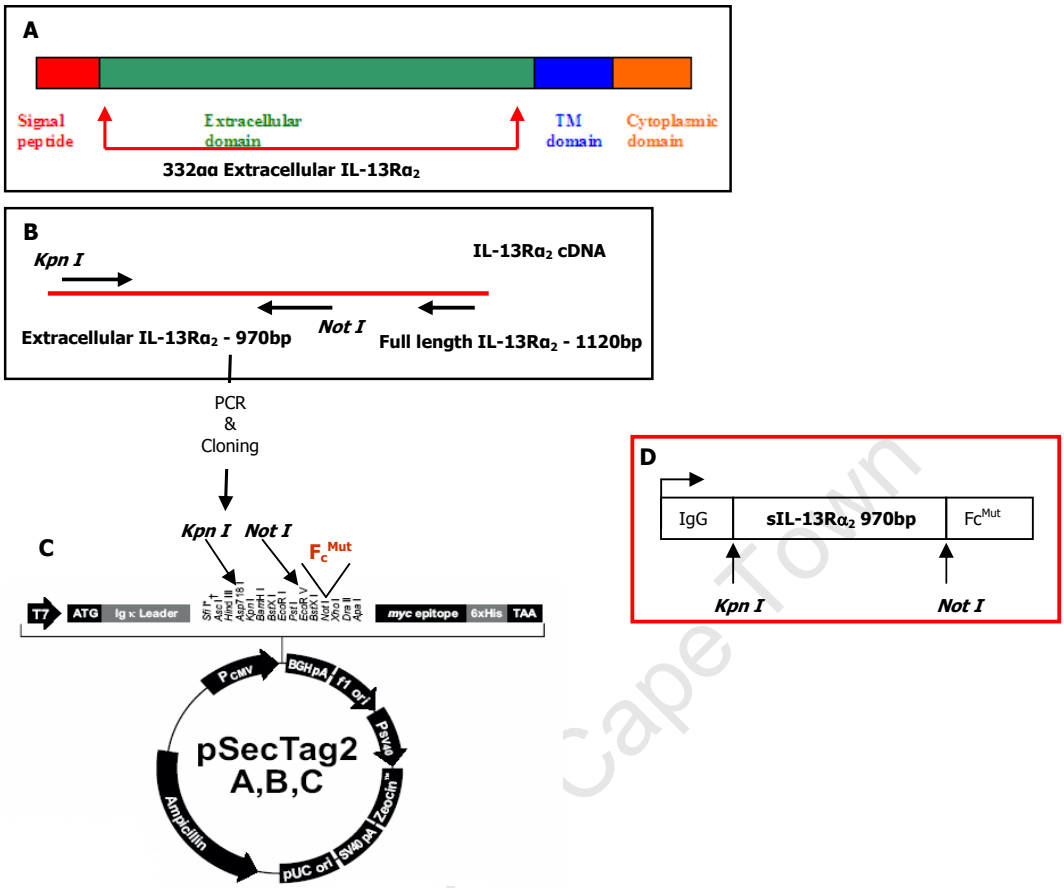

Figure 4.2.B Flow Diagram of pSecTag-F_c^{Mut}-sIL-13Rα_2 Cloning Strategy

Panel A, *IL-13Rα_2* map. Extracellular domain indicated. The soluble/secreted isoform coding region is 970bp in length and codes for 332 amino acids. **Panel B**, Primer design and PCR of both full-length and extracellular sIL-13Rα_2 transgenes using BALB/c cDNA. **Panel C**, RE digestion of sIL-13Rα_2 cDNA and ligation into pSecTag-F_c^{Mut}. The pSecTag-F_c^{Mut} eukaryotic expression vector modified via the addition of a mutated Fc fragment in the multiple cloning site (MCS). **Panel D**, The sIL-13Rα_2 expression cassette. The IgG1 leader sequence which is followed by the sIL-13Rα_2 coding region and F_c^{Mut} tag. The *Kpn I – Not I* ligation junctions are indicated.

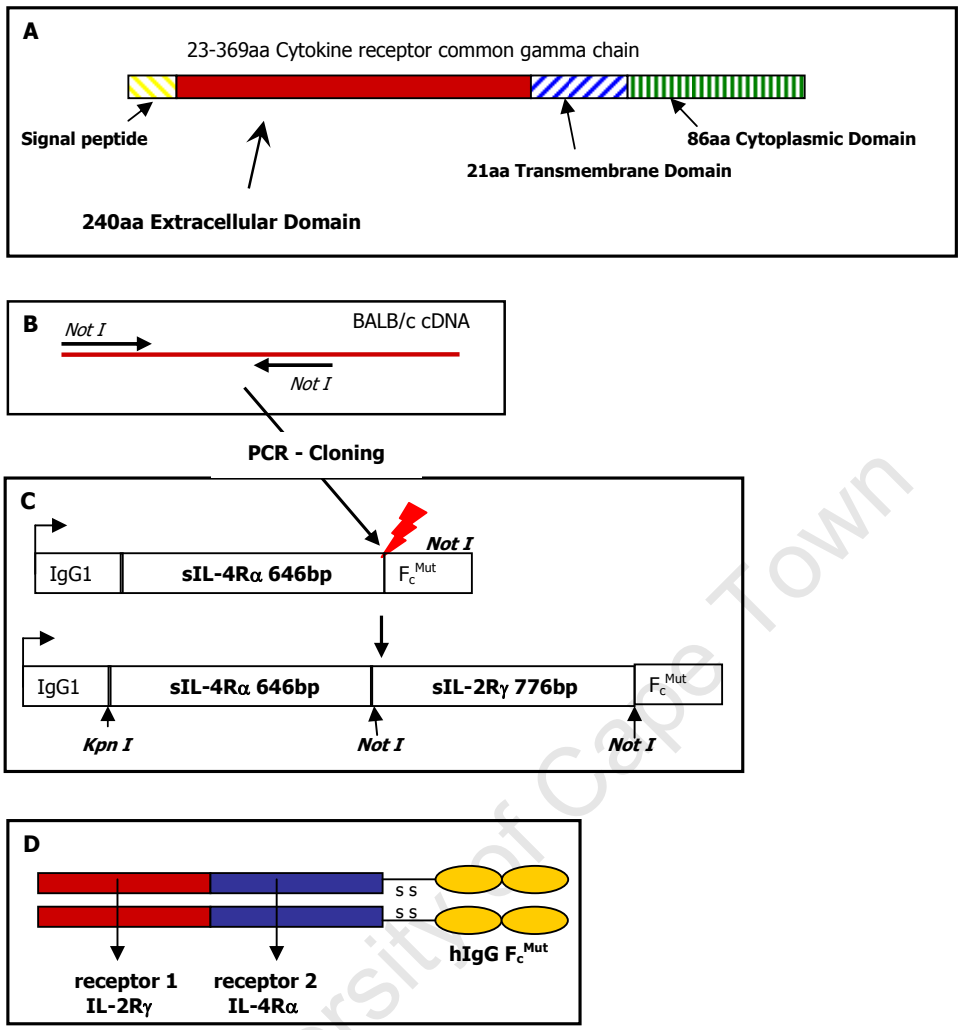

Figure 4.2.C Flow Diagram of pSecTag-F_c^{Mut}-sIL-2Rγ–sIL-4Rα Cloning Strategy

Panel A, *IL-2Rγ* map. Extracellular domain indicated. The coding region is 776bp in length and codes for 240 amino acids. **Panel B**, Primer design and PCR extracellular sIL-2Rγ transgene using BALB/c cDNA. **Panel C:** RE digestion of sIL-2Rγ cDNA and ligation into *Not I* digested pSecTag-F_c^{Mut} sIL-4Rα. pSecTag-F_c^{Mut} sIL-2Rγ-IL-4Rα eukaryotic expression cassette with ligation junctions indicated. **Panel D**, The sIL-2Rγ-IL-4Rα–F_c inline cytokine trap. Extracellular domains of IL-4Rα and IL-2Rγ arranged inline and fused to the mutated F_c fragment of human IgG1.

4.3.1.2.Molecular cloning and characterisation of F_c-tagged soluble.

4.3.1.2.1 The F_c-tagged soluble IL-4Rα eukaryotic expression vector.

In order to sub-clone, and ultimately express the soluble IL-4Rα the corresponding extracellular coding region was amplified using primer pairs that would introduce *Kpn I* and *Not I* restriction enzyme sites. These restriction sites would allow the subsequent ligation into the expression vector digested with the same set of enzymes.

The cDNA encoding the extracellular domain of IL-4Rα was amplified using the pBi-IL-4Rα (see chapter 3 for cloning details) plasmid as template. This vector contains the cDNA encoding the full-length transmembrane isoform of IL-4Rα. The cDNA was generated from RNA isolated from a BALB/c genotype. Primer pairs were designed to amplify the 646bp extracellular region on this fragment. The amplification produced the desired 646bp extracellular domain (Figure 4.3). The amplified cDNA fragment was isolated from a low melting agarose gel and digested with the *Kpn I* and *Not I*. The digested fragment was isolated in the same manner as the PCR product and subsequently ligated into the pSecTag-F_c^{Mut} vector digested with the same restriction enzyme set as those used on the amplified extracellular domain (refer to Figure 4.2.A for vector construction scheme). The ligation products were transformed into DH5α *E.coli* cells, and colonies screened by restriction enzyme (RE) digestion. *Nsi I* was used to identify the pSecTag-F_c^{Mut} colonies into which soluble/extracellular IL-4Rα (sIL-4Rα) had been ligated (Figure 4.4, Panel A). The enzyme has two recognition sites in pSecTag-F_c^{Mut}, which generates a single 974bp fragment upon *Nsi I* digestion. In the clones containing the sIL-4Rα cDNA three recognition sites are present, and digestion would produce an additional 1111bp fragment compared to that of the empty vector digestion. The digestion produced two putative positive clones (Fig.4.4.A), which were further screened for insert presence with the *Kpn I* and *Not I* enzymes, which would be present at the ligation junction of positive clones. This digestion produced the 646bp cDNA insert fragment (Panel B). Lastly; an additional enzyme screening (Fig.4.4.C), using enzymes that had single recognition sites in the insert sequence, confirmed the orientation of the ligated cDNA fragment in the vector. The sequences of inserts in positive constructs were subsequently verified by automated nucleotide sequencing (Fig.4.4.D). The construct was referred to as sIL-4RαF_c.

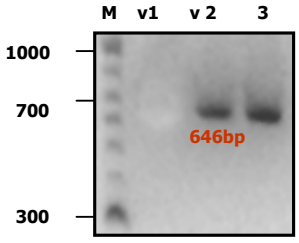

Figure 4.3 Amplification of extracellular IL-4Rα cDNA fragment.

PCR was performed to amplify the coding region of the extracellular IL-4Rα using oligonucleotides specific for the sequence and pBi-IL-4Rα as template. 1% (w/v) agarose gel in 1 × TAE containing ethidium bromide and visualized using short wavelength UV transillumination. **Lane M**, DNA molecular weight marker. **Lane 1**, The negative control, where the DNA template was omitted from the reaction mixture. **Lane 2** & **3**, Amplified 646bp sIL-4Rα cDNA fragments.

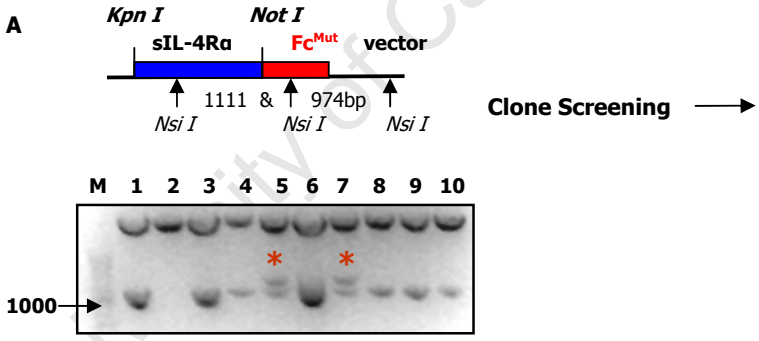

Figure 4.4 Restriction enzyme screening and sequence verification of the sIL-4RαF_c expression vector.

Panel A, Clone Screening. The cDNA insert was ligated into pSecTag-F_c^{Mut}. Following transformation and plasmid isolation the colonies were screened via RE digestion. The illustration shows the theoretical recognition sites and fragment sizes produced in colonies positive for the insert. 0.8% (w/v) agarose gel in 1 × TAE containing ethidium bromide and visualized using short wavelength UV transillumination. **Lane M**, DNA molecular weight marker. **Lanes 1-10**, 10 different isolated plasmid preparations (each from a single colony) digested with *Nsi I*. The clones positive for the correct fragment sizes are indicated.

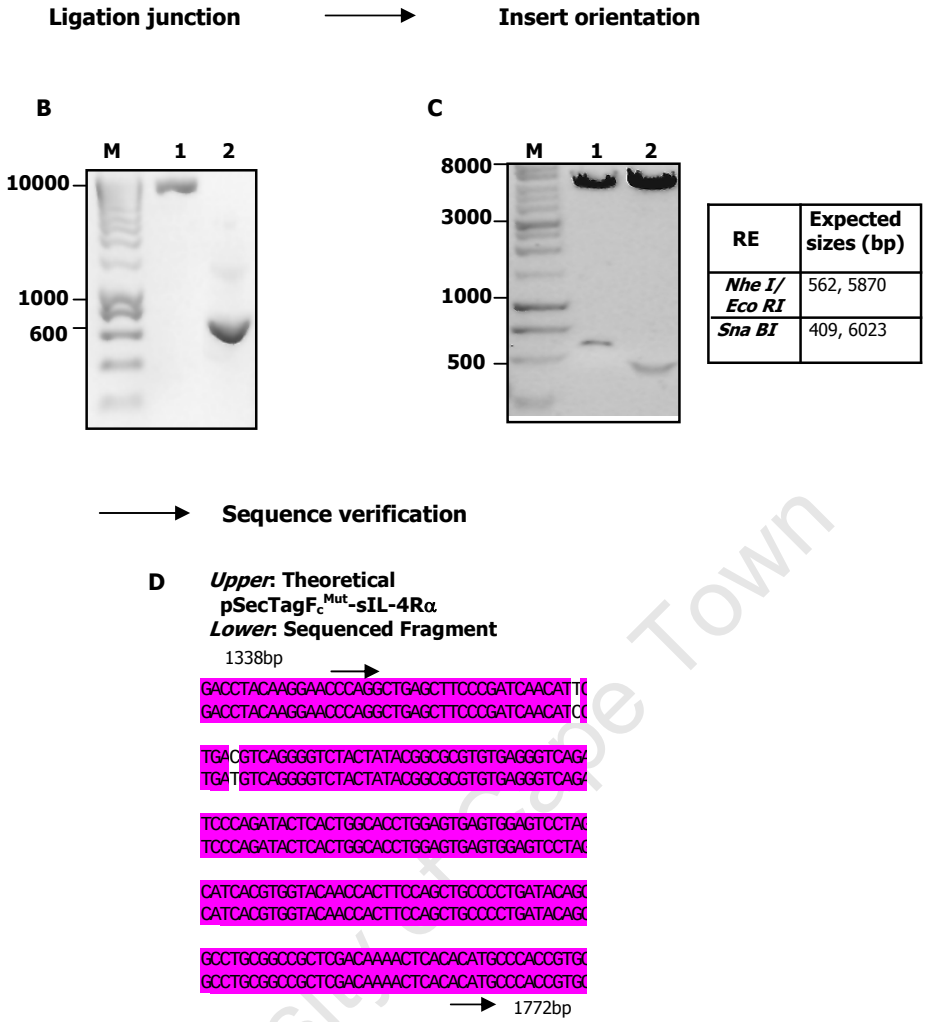

Figure 4.4 Restriction enzyme screening and sequence verification of the sIL-4RαF_c expression vector.

Panel B & **C**, 0.8% (w/v) agarose gel in 1 × TAE containing ethidium bromide and visualized using short wavelength UV transillumination. **Lane M**, DNA molecular weight marker. **Panel B**, Confirmation of the insert ligation junctions. The clones identified in Panel A were digested with *Kpn I / Not I*, confirming the insert size and presence of the ligation junctions. **Lane 1**, pSecTag-F_c^{Mut} empty vector digestion. **Lane 2**, pSecTag-F_c^{Mut}-sIL-4Rα digestion, showing the 646bp fragment generated. **Panel C**, Confirmation of the insert orientation. The clones positive for the insert were digested with the enzymes shown in the table. The expected sizes of the RE fragments generated in positive clones are indicated. **Lane 1**, Nhe *I / Eco RI* digestion showing the 562 and 5870bp fragments. **Lane 2**, *Sna BI* digestion showing the 409 and 6023bp fragments generated by the digestion. **Panel D**, Sequence verification via automated nucleotide sequencing. Illustration of post sequencing analysis, using *DNassist*. The theoretical sequence and sequenced DNA sequences showed a 98% similarity after alignment. Gaps indicate unmatched bases.

4.3.1.2.2 The F_c-tagged soluble IL-13Rα_2 eukaryotic expression vector.

Similar to the cloning strategy for pSecTag-F_c^{Mut}-sIL-4Rα, the vector construction of pSecTag-F_c^{Mut}-sIL-13Rα_2 started with identification of the extracellular IL-13Rα_2 coding region, followed by amplification using primer pairs that introduced the *Kpn I* and *Not I* restriction enzyme sites. These restriction sites permitted the ligation into the expression vector digested with the same set of enzymes.

To obtain the cDNA encoding the extracellular domain of IL-13Rα_2, total RNA was isolated from a BALB/c mouse after which cDNA was produced via reverse transcriptase PCR (Fig.4.5.A). In order to aid specific amplification of the extracellular domain, this cDNA pool was decreased. This was achieved by separating the amplification into two steps. In the first amplification step primers specific for the full-length IL-13Rα_2 coding region were designed, and used with the total pool of cDNA as template. The amplification produced the desired 1190bp full-length IL-13Rα_2 fragment, which was subsequently isolated from a low melting agarose gel (Fig.4.5.B). This isolated fragment served as PCR template in the second amplification step using primers designed specifically for the extracellular domain. This amplification produced a single product, the 970bp extracellular region of IL-13Rα_2 (Fig.4.5.C). Subsequent to gel isolation, the amplification products were digested with *Kpn I* and *Not I*. The digested fragments were isolated in the same manner as the PCR products and ligated into the pSecTag-F_c^{Mut} vector digested with *Kpn I* and *Not I* (refer to Figure 4.2.B, for vector construction scheme). The ligated constructs were transformed into DH5α *E.coli* cells, and colonies screened by RE digestion. To identify the pSecTag-F_c^{Mut} colonies into which soluble/extracellular IL-13Rα_2 (sIL-13Rα_2) had been ligated RE screening using *Fok I* was preformed. This enzyme has a single site in the empty vector and only if the IL-13Rα_2 is ligated in the correct orientation would a second site be present (Fig.4.6.A). The digestion identified two putative positive clones (Fig.4.6.B), which were further analyzed via insert digestion (Fig.4.6.C) with the enzymes used for vector cloning, namely *Kpn I* and *Not I*. The *Kpn I / Not I* digestion verified the ligation junctions and the subsequent RE digestion using enzymes with single recognition sites in the IL-13Rα_2 cDNA fragment confirmed the insert orientation (Fig.4.7.A). The sequence of insert in the positive constructs was subsequently verified by automated nucleotide sequencing (Fig.4.7.B). The construct was referred to as sIL-13Rα_2F_c.

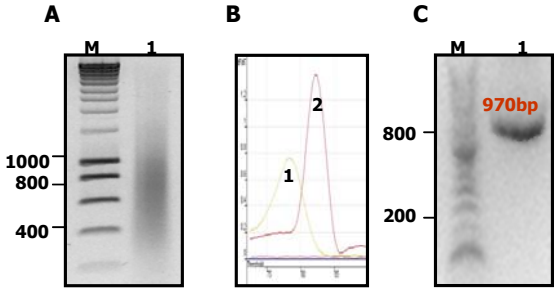

Figure 4.5 Amplification of the IL-13Rα_2 extracellular cDNA fragment.

In both **Panel A** & **C**, 1% (w/v) agarose gel in 1 × TAE containing ethidium bromide and visualized using short wavelength UV transillumination. **Lane M**, DNA molecular weight marker. **Panel A**, Products of the cDNA synthesis. RNA was isolated from the draining lymph node of BALB/c mouse and cDNA synthesised. **Panel B**, Melting Curve of first round PCR showing amplification of full length IL-13Rα_2. On graph, nr **1**; primer dimmers and nr **2**; amplification peak. **Panel C**, Second round PCR with extracellular IL-13Rα_2 primers.

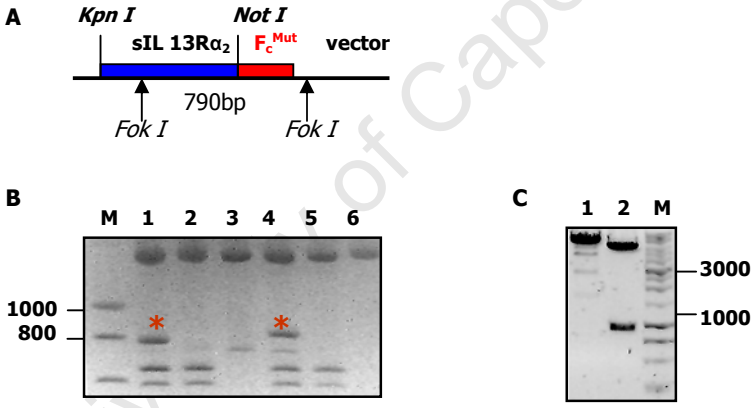

Figure 4.6 Restriction enzyme screening and sequence verification of the sIL-13Rα_2F$_c$ expression vector.

Panel A, Clone Screening. The cDNA insert was ligated into pSecTag-F$_c^{Mut}$. Following transformation and plasmid isolation the colonies were screened via RE digestion. The illustration shows the theoretical recognition sites and fragment sizes produced in plasmids positive for the insert. In both **Panel B** & **Panel C**, 0.8% (w/v) agarose gel in 1 × TAE containing ethidium bromide and visualized using short wavelength UV transillumination. **Lane M**, DNA molecular weight marker. **Panel B**, *Fok I* digestion. **Lanes 1-6**, 6 different isolated plasmid preparations digested with *Nsi I*. The clone's positive for the correct fragment sizes, lanes 1 and 4, are indicated. **Panel C**, Insert ligation junction confirmation. *Kpn I / Not I* digestion of positive clones (identified in Panel B). **Lane 1**, Digestion of empty vector only. **Lane 2**, pSecTagF$_c^{Mut}$-sIL-13Rα_2 digestion showing the 970bp insert fragment produced by the RE screening.

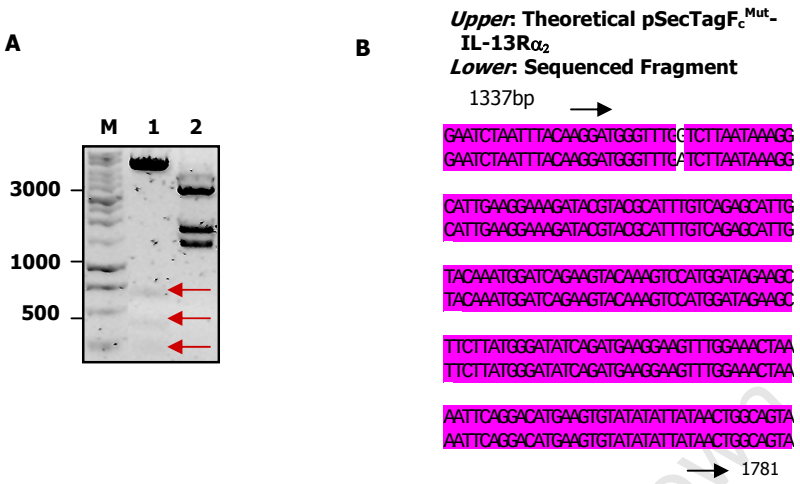

Figure 4.7 Insert orientation and sequence verification of the sIL-13Rα$_2$F$_c$ expression vector.

Panel A, Confirmation of insert orientation in vector. 0.8% (w/v) agarose gel in 1 × TAE containing ethidium bromide and visualized using short wavelength UV transillumination. **Lane M**, DNA molecular weight marker. **Lane 1**, *Sna BI* digestion showing the 266, 406 and 591bp fragments. **Lane 2**, *Bsa I* digestion showing the 1402 and 1758bp fragments generated via digestion. **Panel B**, Sequence verification via automated nucleotide sequencing. Illustration of the post sequencing analysis using *DNassist*. The theoretical sequence and sequenced DNA sequences showed a 99% similarity after alignment. Gaps indicate unmatched bases.

4.3.1.2.3 The inline F_c-tagged soluble IL-4Rα / soluble IL-2Rγ cytokine trap eukaryotic expression vector.

In order to generate a construct that would enable the expression of the extracellular domains of IL-2Rγ and IL-4Rα in the form of a fusion protein, the corresponding extracellular coding region of IL-2Rγ was amplified using primer pairs that introduced *Not I* restriction enzyme sites on both the 3' and 5' ends of the fragment. These restriction sites allowed for the subsequent ligation into the pSecTag-F_c^{Mut}-sIL-4Rα expression vector digested with the same enzyme (refer to Figure 4.2.C, for vector construction scheme). The cDNA encoding the extracellular domain of IL-2Rγ was generated from RNA isolated from a BALB/c mouse. Primer pairs were designed to amplify this region and the amplification produced the desired 776bp fragment coding for the extracellular domain (Figure 4.8). The amplified cDNA fragment was isolated from a low melting agarose gel and digested with *Not I*. The digested fragment was isolated in the same manner as the PCR product and subsequently ligated into the *Not I* digested pSecTag-F_c^{Mut}-sIL-4Rα vector. The ligation products were transformed into DH5α *E.coli* cells, and randomly picked colonies screened by RE digestion. Digestion with *Eco RV / Sca I* was used to identify the pSecTag-F_c^{Mut} colonies into which soluble/extracellular IL-2Rγ (sIL-2Rγ) had been ligated (Figure 4.9, Panel A & B). These enzymes both have unique sites in either the sIL-4Rα or sIL-2γ cDNA fragments, and none in pSecTag-F_c^{Mut}. Digestion of the clones into which the sIL-2Rγ cDNA had been ligated produced three putative positive clones (Fig.4.9.B). Further screening, with a *Pst I* digestion, confirmed the orientation of the ligated insert (Figure 4.10). The insert sequences in the positive constructs were subsequently verified by automated nucleotide sequencing. The construct was referred to as sIL-2Rγ-sIL-4RαF_c.

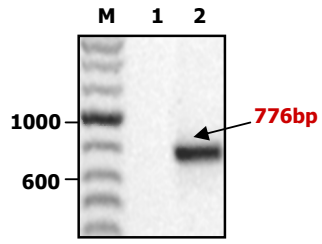

Figure 4.8 Amplification of the IL-2Rγ extracellular cDNA fragment.

PCR was performed for the amplification of the extracellular IL-2Rγ cDNA fragment using oligonucleotides specific for the sequence and BALB/c mRNA as template. 1% (w/v) agarose gel in 1 × TAE containing ethidium bromide and visualized using short wavelength UV transillumination. **Lane M**, DNA molecular weight marker. **Lane 1**, Negative control, where DNA was omitted from the reaction mixture. **Lane 2**, Amplified 776bp extracellular IL-2Rγ cDNA fragments.

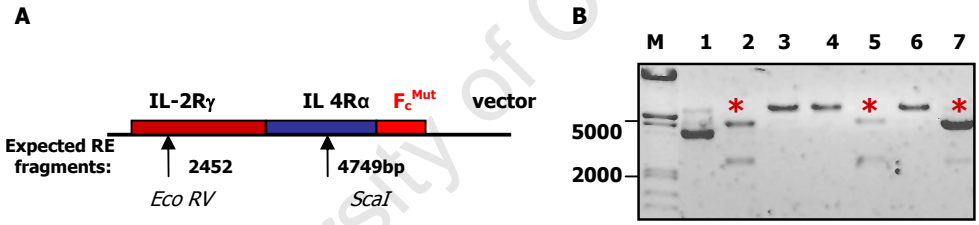

Figure 4.9 Restriction enzyme screening of sIL-2γ-sIL-4RαF_c clones.

Panel A, Clone Screening. The cDNA insert was ligated into pSecTag-F_c^{Mut}-sIL-4Rα. Following transformation and plasmid isolation the colonies were screened via RE digestion. The illustration shows the theoretical recognition sites and RE fragments produced in colonies positive for the insert. **Panel B**, 0.8% (w/v) agarose gel in 1 × TAE containing ethidium bromide and visualized using short wavelength UV transillumination. **Lane M**, DNA molecular weight marker. **Lanes 1-7**, 7 different isolated plasmid preparations digested with *Eco RV / Sca I*. The clone's positive for the correct fragment sizes, lanes 2, 5 and 7, are indicated.

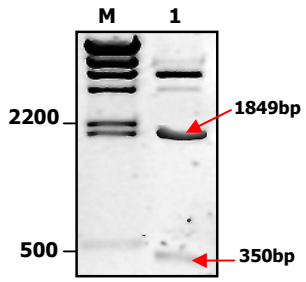

Figure 4.10 Insert orientation of sIL-2Rγ-sIL-4RαF_c expression vector.

Confirmation of the insert orientation. 0.8% (w/v) agarose gel in 1 × TAE containing ethidium bromide and visualized using short wavelength UV transillumination. **Lane M**, DNA molecular weight marker. **Lanes 1**, *Pst I* digestion of the expression vector showing the 1849bp and 350bp fragments produced.

4.3.3 Recombinant fusion protein expression and purification.

In order to perform functional studies and investigate IL-13 and IL-4 cytokine binding, the IL-13Rα_2, IL-4Rα soluble receptors and the sIL-2Rγ-sIL-4Rα cytokine trap were expressed as fusion proteins and purified. To produce sufficient quantities of the recombinant protein for the biochemical and functional analyses, proteins were over-expressed in Hek 293T cells, using the pSecTag-F_c^{Mut} eukaryotic expression system. Expression using this system, resulted in the IL-13Rα_2, IL-4Rα extracellular domains fused in-frame with the mutated human IgG1-F_c. In the case of the in-line sIL-2Rγ-sIL-4RαF_c cytokine trap, expression lead to the in-frame fusion of both the IL-2Rγ and IL-4Rα extracellular domains, with the IgG1-F_c tag. Fc-tagged proteins were purified from the cell supernatants via protein A Sepharose chromatography. The F_c tag directs the random formation of disulfide-linked dimmers between secreted peptides, in this way forming homodimeric proteins that have been shown to act as effective cytokine blockers (Caput *et al.*, 1996).

Both the purified sIL-4RαF_c and sIL-13RαF_c exhibited anomalous migration on SDS-PAGE gels (Figure 4.11, Panel A & B). The sIL-4RαF_c, has a predicted size of 58.5kDa (obtained from the peptide calculator at http://prowl.rockefellar.edu), but migrated at a region corresponding to approximately 65kDa (Fig.4.11.A, lane 2). The sIL-13RαF_c migrated at approximately 90kDa with an expected size of 63kDa (Fig.4.11.B, lane 2). This atypical migration by sIL-4Rα and sIL-13Rα_2 is attributed to N-linked glycosylation of the recombinant proteins (Donaldson *et al.,* 1998 and Schulte *et al.,* 1997). To assess the F_c tag directed protein dimerization, the proteins were electrophoresised under non-reducing conditions, in this way not disrupting and of the disulfide bonds. Both sIL-4RαF_c and sIL-13RαF_c formed homodimmers as illustrated by the protein migrated at a region approximately double in size to that of the proteins electrophoresised using reducing conditions (Lanes 1 in A and B). The sIL-2Rγ-sIL-4RαF_c cytokine trap migrated at the predicted 270kDa region on a SDS-PAGE gel (Fig.4.12). Under non-reducing conditions, it was also observed that the majority of the proteins were in the homodimeric cytokine trap formation. Subsequently, these results were confirmed via western blot analysis using an antibody against the mutated human IgG1-F_c portion of the purified fusion proteins. To asses the specificity of the antibody, protein was purified from the media only, from the supernatant of untransfected Hek 293T cells and from lysed untransfected Hek 293T (Figure 4.13, Panel A). There was no measurable detection, using this antibody on immobilized proteins purified from these groups. However, in cells transfected with the sIL-4RαF_c, sIL-13RαF_c or the sIL-2Rγ-sIL-4RαF_c expression vectors, F_c was detected

(Fig.4.13, B & C). Yet, as observed in Panel B, the level of expressed sIL-13RαF_c purified from the supernatant of the cells was much lower when compared to that obtained from the cell lysates. This decreased level, which was also confirmed with the BCA protein quantification assay, can possibly be attributed to a defect in the secretion of the expressed protein. The reason for this is yet to be investigated, but the possibility of incorrect protein folding leading to the decreased secretion could be analyzed further.

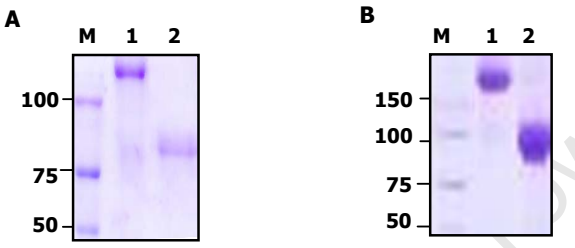

Figure 4.11 SDS-PAGE analyses of IL-4 and IL-13 soluble receptor blockers.

Panel A & **B**, 10% SDS-PAGE gels. Protein A Sepharose purified protein was visualized by Coomassie staining. **Panel A** & **B**: **lane M**, Protein molecular weight marker, with sizes indicated on the left. All other lanes contain Fc-tagged purified protein. **Panel A**, Purified sIL-4RαF_c **Lane 1**, Electrophoresis using non-reducing sample application buffer (SAB) and **lane 2**, using SAB supplemented with 5% (v/v) β-mercaptoethanol. **Panel B**, sIL-13R$\alpha_2 F_c$. **Lane 1**, Electrophoresis under non-reducing conditions and **lane 2**, Electrophoresis under reducing conditions.

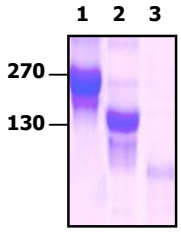

Figure 4.12 SDS-PAGE analysis of sIL-2Rγ-sIL-4RαF$_c$ cytokine trap.

10% SDS-PAGE gel of Protein A Sepharose purified sIL-2Rγ-sIL-4RαF$_c$ protein was visualized by Coomassie staining. Protein sizes indicated on the left. **Lane 1**, Electrophoresis using non-reducing conditions. **Lane 2**, Electrophoresis using reducing conditions. **Lane 3**, Control experiment; electrophoresis of protein purified from untransfected Hek 293T cells.

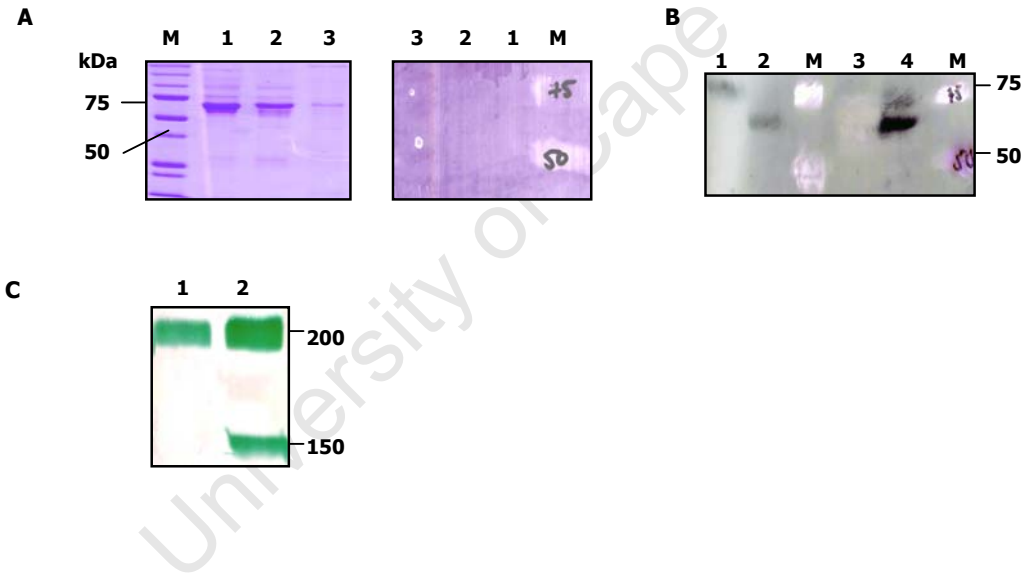

Figure 4.13 Western Blot detection of secreted proteins.

Protein A Sepharose purified proteins electrophoresised on 10% SDS-PAGE gels, visulaised via Coomassie. Protein was transferred to Nitrocellulose membrane, F$_c$ detected with Anti-Human IgG1 and visualized by chemiluminscence. **Panel A**, in both the SDS-Page gel and Nitrocellulose membrane; **Lane 1**, Media Only. **Lane 2**, Protein purified from untransfected Hek 293T cell supernatant. **Lane 3,** Protein purified from lysed untransfected Hek 293T cells. **Panel B**, **Lane 1**, Protein purified from lysed Hek 293T cells transfected with sIL-13Rα$_2$F$_c$. **Lane 2**, Protein purified from lysed Hek 293T transfected with sIL-4RαF$_c$. **Lane 3**, Protein purified from Hek 293T cell supernatant transfected with sIL-13Rα$_2$F$_c$. **Lane 4**, Protein purified from Hek 293T cell supernatant transfected with sIL-4RαF$_c$. **Panel C**, Protein purified from Hek 293T cell supernatant transfected with sIL-2Rγ-sIL-4RαF$_c$. **Lane 1**, Electrophoresis under non-reducing conditions and **Lane 2**, reducing conditions.

4.3.4 Biochemical protein characterisation.

4.3.4.1 Cytokine Binding assays.

To assess the binding potential and affinity of the expressed soluble receptors to their respective cytokines a modified version of the Sandwich Elisa technique was used (illustrated in Figure 4.14). Briefly, in parallel experiments, ELISA plates were either coated with the coating antibody for IL-13 or IL-4, or with different concentrations of sIL-13Rα_2F$_c$, sIL-4RαF$_c$ or sIL-2Rγ-sIL-4RαF$_c$. This was followed by a serial dilution of the respective cytokines, and lastly, the biotin-labelled detecting antibodies against these cytokines. The bound cytokine served as a measure of the cytokine binding to the soluble receptor blockers.

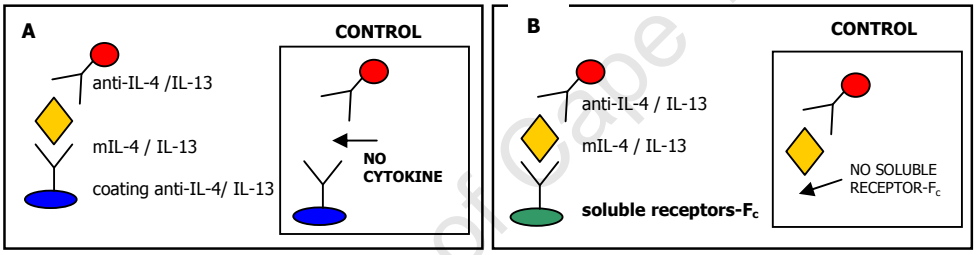

Figure 4.14 Diagram of F$_c$-tagged Soluble Receptor Elisa Protocol.

Panel A, Positive control ELISA, using coating antibody for the respective cytokines, cytokines and biotin-labelled antibody, for detection. Inset illustrates the control for this experiment where the cytokine is omitted in the procedure. **Panel B**, ELISA testing for the F$_c$-tagged soluble receptor cytokine binding. The coating antibody gets replaced by the respective F$_c$-tagged soluble receptors. This is followed by the respective cytokines and the biotin-labelled antibodies against these cytokines for detection. Inset illustrates the control for this experiment where the F$_c$-tagged soluble receptor is omitted in the procedure.

4.3.4.1.1 sIL-4Rα and sIL-13Rα$_2$.

Coating of the ELISA plates with sIL-4RαF$_c$ at a 10-fold concentration to that of the IL-4 coating antibody (0.025mg/ml) resulted in cytokine binding being equivalent to that shown by the cytokine antibodies (Figure 4.15, Panel A.1). For sIL-13Rα$_2$F$_c$, coating with a 10-fold concentration to that of the IL-13 coating antibody (0.02mg/ml) also resulted in cytokine binding but not to the degree shown by sIL-4RαF$_c$ (Fig.4.15.B.1). This data indicates that though the F$_c$-tagged soluble receptor blockers bind their respective cytokines effectively it is at a lower stoichiometric ratio than that shown by cytokine binding to the monoclonal coating antibodies. The cytokine binding results were not due to non-specific binding as demonstrated by the cytokine and coating antibody negative controls (Fig.4.15, A.2 & B.2).

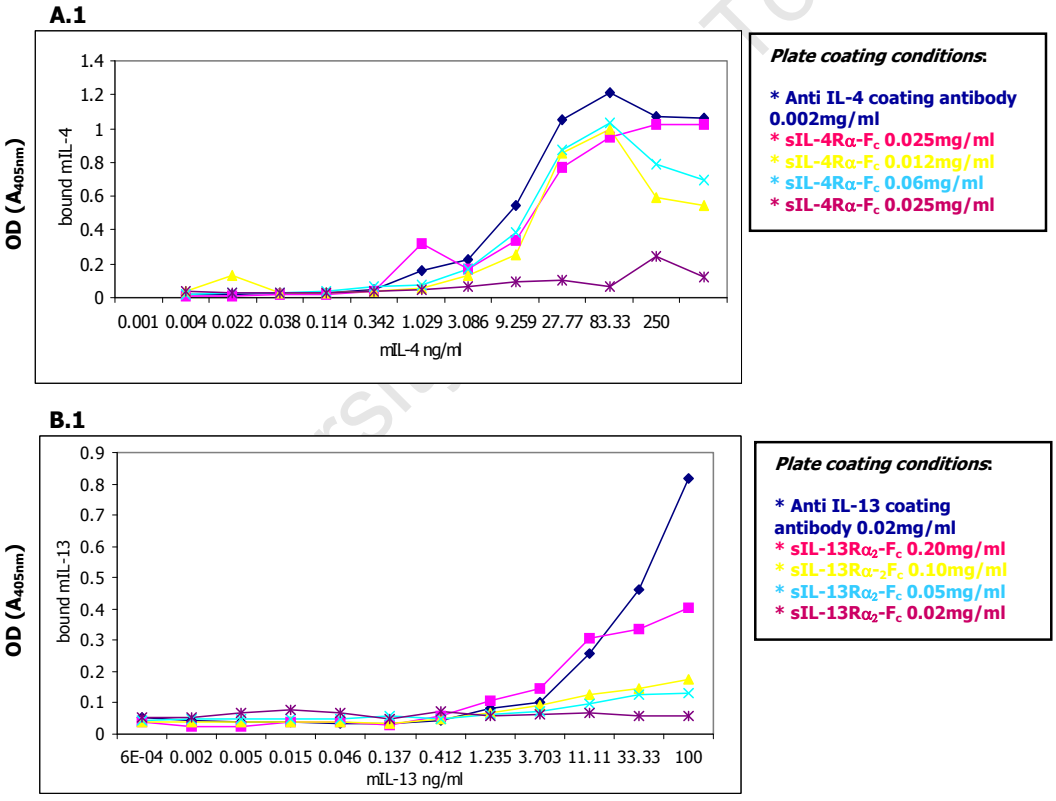

Figure 4.15 Cytokine Binding analyses of sIL-4RαF$_c$ and sIL-13Rα$_2$F$_c$.

Panel A.1 and **B.1**, Graphs of the cytokine - soluble receptor ELISA. sIL-4RαF$_c$ (A.1) and sIL-13Rα$_2$F$_c$ (B.1) were plated a 10-fold concentration as that of the coating antibody and then at 3-fold dilutions of this, as indicated in the legends. This was followed by the serial dilution of IL-4 (A.1) or IL-13 (B.1). Bound cytokine was measured by ELISA.

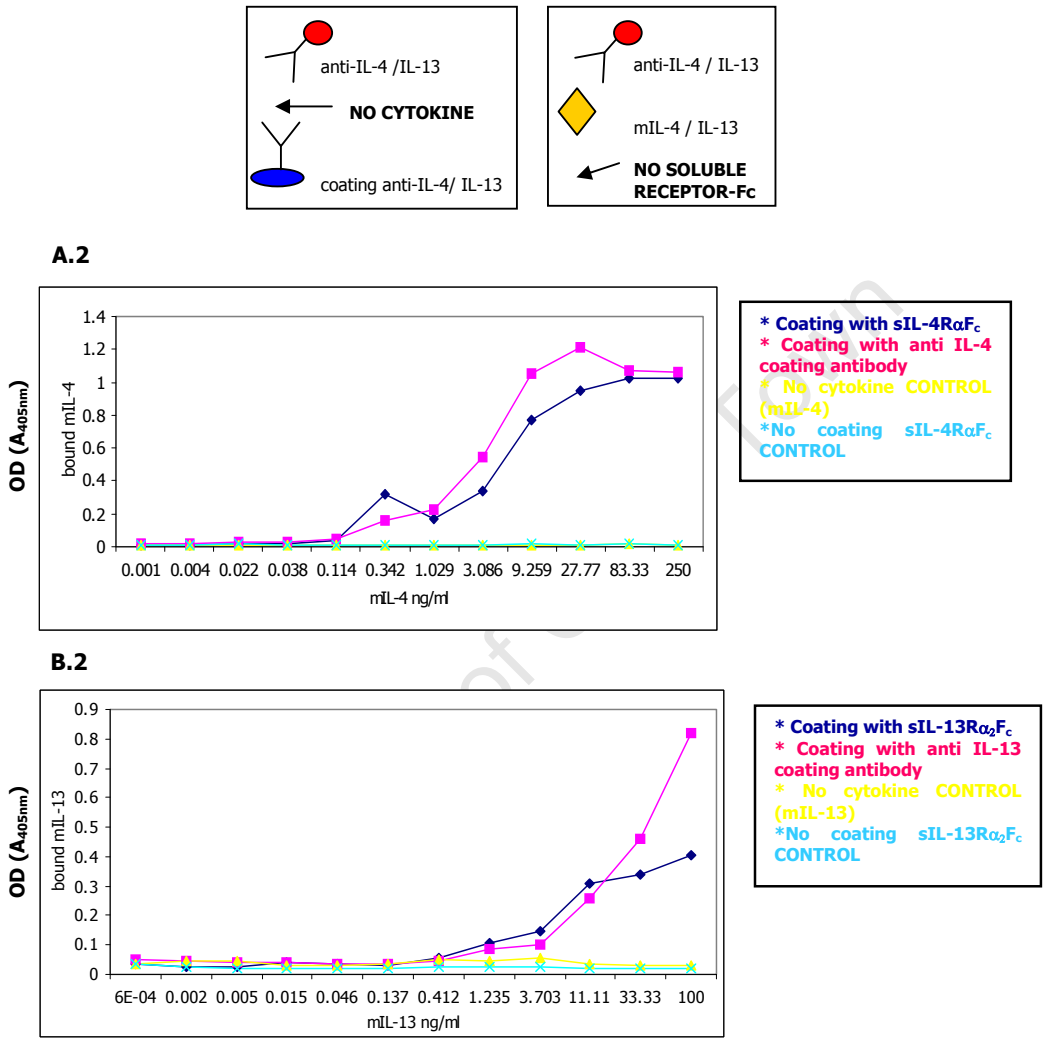

Figure 4.15 Cytokine Binding analyses of sIL-4RαF$_c$ and sIL-13Rα$_2$F$_c$ blockers.

Panel A.2 and **B.2**, Graphs of the cytokine - soluble receptor control ELISA (as illustrated in Figure 4.13). Bound cytokine was measured by ELISA. The results represent 1 of 3 independent experiments and show the average ± SEM of triplicate values.

4.3.4.1.2 sIL-2Rγ– sIL-4Rα cytokine trap.

Previously it was shown (Economides *et al.*, 2003) that the generated human form of the sIL-2Rγ-sIL-4RαF$_c$ cytokine trap displayed equivalent binding affinities to that shown by the monoclonal antibody for hIL-4.

To investigate if this was also the case for the binding affinity of the generated murine form of this trap the modified ELISA protocol (4.2.4.1) was preformed with the sIL-2Rγ-sIL-4RαF$_c$. Here when coating the plates with either the sIL-2Rγ-sIL-4RαF$_c$ cytokine trap or the anti IL-4 coating antibody (Figure 4.16) at the same concentrations (0.002mg/ml), equivalent binding was found by the trap and the IL-4 coating antibody with the cytokine. In parallel sIL-4RαF$_c$ was used to coat a plate at the same concentration as that of the cytokine trap and IL-4 coating antibody. From the results it was clear that the sIL-2Rγ-sIL-4RαF$_c$ cytokine trap showed a greater cytokine binding affinity as that of the sIL-4RαF$_c$ (Refer to Fig.4.15.A.1). This implies increased stoichmetry between the cytokine trap and the cytokine and indicates that the cytokine trap could potentially represent a more potent inhibitor of IL-4 cytokine binding.

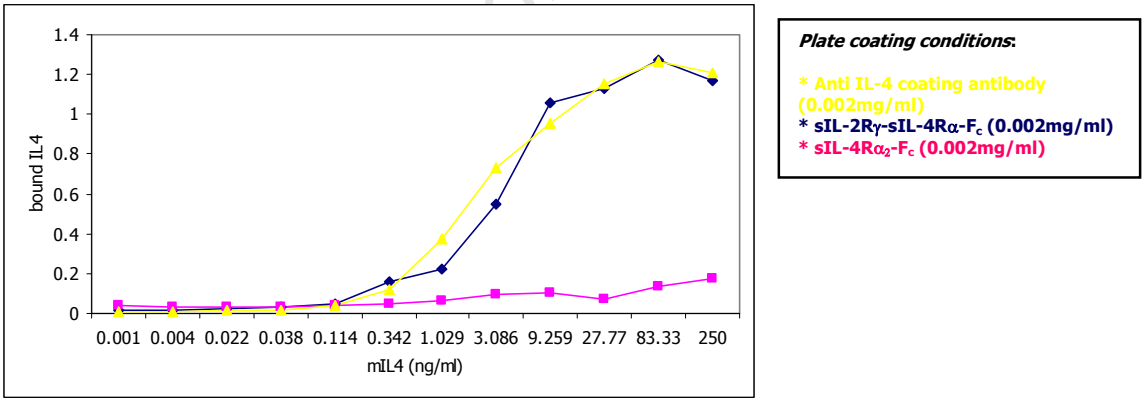

Figure 4.16 Cytokine Binding analysis of sIL-2Rγ-sIL-4RαF$_c$ cytokine trap.

Graph of the cytokine – cytokine trap ELISA. Plates coated with sIL-2Rγ-sIL-4RαF$_c$, sIL-4RαF$_c$ or the coating IL-4 antibody (11B11) at 0.002mg/ml. This was followed by the serial dilution of mIL-4. Different groups indicated in the legend. Bound cytokine was measured by ELISA. The results represent 1 of 3 independent experiments and show the average ± SEM of triplicate values

4.3.5 *In vitro* functional assays.

4.3.5.1 T cell Proliferation.

It is established that binding by IL-4 to type I IL-4R (IL-4Rα-γ chain heterodimer) induces *in vitro* proliferation of murine T lymphocytes (Kondo *et al.*, 1993 and Le Gros *et al.*, 1990). In order to demonstrate a biological effect of the generated sIL-4RαF_c, the effect of this dimeric form of mIL-4Rα on the proliferative response of $CD4^+$T cells to IL-4 was examined.

The $CD4^+$T cell enriched population was stimulated with recombinant mIL-4, at a saturating concentration, and with a combination of recombinant mIL-4 and purified sIL-4RαF_c. The soluble receptor blocker, sIL-4Rα-F_c, was added at the 10-fold concentration to the mIL-4, as this concentration was shown to be effective in the cytokine binding assays (refer to section 4.2.4.1.1). Stimulation of the cells with murine IL-2 served as a positive control and incubation with medium only as the negative control. As shown (Figure 4.17), $CD4^+$T cells proliferated significantly upon stimulation with either mIL-2 or mIL-4 ($p<0.05$) when assessed by BrdU absorbance values and compared to the media control. Where sIL-4RαF_c was added in combination to mIL-4 (bar D), the IL-4 induced proliferation was significantly decreased to a level equivalent to that of untreated cells (bar A). This proliferation assay clearly demonstrated sIL-4RαF_c to effectively block IL-4 induced $CD4^+$T cell proliferation.

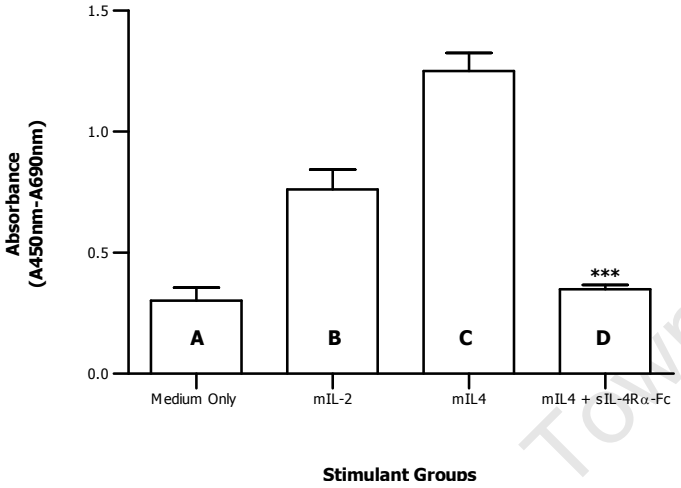

Figure 4.17 CD4$^+$T cell proliferation after stimulation with mIL-4, mIL-2, or mIL-4 with sIL-4RαF$_c$.

Cells were isolated from lymph node tissues of BALB/c mice and a CD4$^+$T cell enriched population was obtained by negative selection. Enrichment was confirmed by FACS analysis and all cell samples used were between 95-98% CD4$^+$T cell positive. CD4$^+$ T cells were plated with medium containing mIL-4 (**bar C**), mIL-2 (**B**) or mIL-4 in combination with sIL-4RαF$_c$ (**D**). Culture medium contained PMA (5ng/ml) and cells were stimulated for 48h with. Cell proliferation was measured by the BrdU incorporation during DNA synthesis in proliferating cells. Media was supplemented BrdU during the last 18h of culture incubation. BrdU incorporation was determined via the BrdU colorimetric immunoassay (described in methods section). The results represent 1 of 3 independent experiments and show the average ±_SEM of triplicate values. Statistical differences between groups calculated using unpaired Student's *t* test defining differences to cultures incubated with cytokine and PMA stimulated as significant (***, p ≤0.001).

4.3.5.2 T cell Differentiation.

To further confirm the biological effects of the sIL-4RαF_c on IL-4 driven $CD4^+$T cell responses the cytokine induced Th1 / Th2 differentiation was analyzed. It is well established that IL-4 induces the *in vitro* differentiation of naïve T helper (Th) cells to a Th2 phenotype (Zurawski *et al.*, 1993 and Manetti *et al.*, 1993) while IL-12 induces the differentiation to Th1 (Seder *et al.*, 1993).

$CD4^+$T cell enriched population was activated with plate bound anti-CD3/anti-CD28 and incubated for 72h with various combinations of the cytokines and Fc-tagged blockers (see Figure 4.18 for stimulant groups). The Th1 differentiation cells were cultured with IL-12 and anti-IL-4, with or without soluble receptor blocker. As a negative control cells were incubated in the absence of stimulants with medium only. Cells were restimulated for an additional 48h with anti-CD3 and differentiation determined by measuring the IFN-γ, IL-13 and IL-4 secretion.

As expected, stimulation with IL-12 / anti-IL-4 differentiated the T cells to Th1 (Figure 4.18, Panel A), as indicated by elevated IFN-γ secretion. Cells stimulated with the mIL-4 / anti-IFN-γ / sIL-4RαF_c combination showed a significant increase (calculated P value of 0.0053) to Th1 when compared to cells stimulated with mIL-4 / anti-IFN-γ only. The result suggests that the sIL-4RαF_c is blocking the IL-4 cytokine action. Panel B and C show the IL-4 and IL-13 secretion, respectively. The increase in cytokine secretion demonstrates that $CD4^+$T cells incubated with mIL-4 / anti-IFN-γ differentiated to Th2. Addition of sIL-4RαF_c to the cultures lead to impaired Th2 differentiation as observed with the reduced IL-4 and IL-13 levels. In the presence of IL-4 blocker the levels of IL-13 secretion also dropped significantly (C). $CD4^+$T cell stimulation with the mIL-13 / anti-IFN-γ combination had minimal effect on either IFN-γ or IL-4 production confirming previous data that IL-13 has no influence on *in vitro* T cell differentiation (Zurawski *et al.*, 1993; Sornasse *et al.*, 1996), due to the absence of a functional IL-13 receptor. This data confirmed the biological effect exerted by the generated sIL-4RαF_c on $CD4^+$T cells *in vitro*.

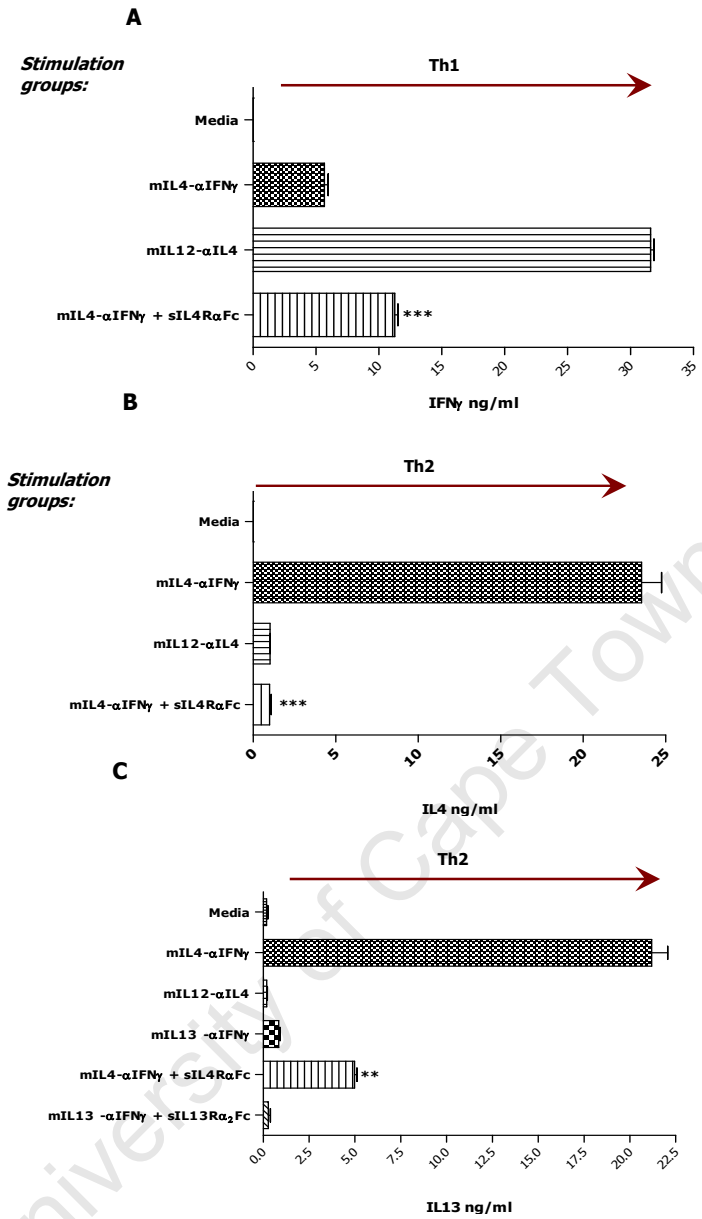

Figure 4.18 Effect by sIL-4RαF_c and sIL-13R$\alpha_2 F_c$ on *in vitro* Th1/Th2 differentiation of CD4$^+$ T cells from BALB/c mice.

Panel A, **B** & **C**, Isolated CD4$^+$ T cells (97% purity as determined with FACS analysis) from lymph node cells of naïve BALB/c mice. Cells were activated with plate bound anti-CD3/anti-CD28 in the presence of IL-2 and cultured with mIL-12/anti-IL-4 for Th1 differentiation. For Th2 differentiation cells were stimulated with mIL-4/anti-IFN-γ. As indicated sIL-4RαF_c and sIL-13R$\alpha_2 F_c$ were also added in different combinations. After 72h culture cells were restimulated with anti-CD3 for 48h. The levels of IFN-γ (**Panel A**), IL-4 (**B**) and IL-13 (**C**), secreted in the supernatant, were determined with ELISA. The results represent 1 of 3 independent experiments and show the average ±_SEM of triplicate values. Statistical differences compared to the mIL-12 / anti IFN-γ (**A**) cultures, the IFN-γ / LPS / mIL-4 cultures (**B**) and the IFN-γ / LPS / mIL-13 cultures (**C**) are indicated as ** p≤0.001 and *** p≤0.0001.

4.3.5.3 Influence of sIL-4RαF_c and sIL-13R$\alpha_2 F_c$ on macrophage responsiveness to mIL-4 and mIL-13.

It is established that macrophage differentiation to the classical activation status is driven by the IL-4Rα and is effected by both IL-4 and IL-13. This cytokine receptor interaction represents an excellent model for testing the generated F_c-tagged soluble receptor blocking function. Thus to establish the effect of sIL-13R$\alpha_2 F_c$ on cytokine-receptor binding bone marrow derived macrophages were used. These functional studies also served to further confirm the effect exerted by sIL-4RαF_c (as shown in section 4.2.5.2 and 4.2.5.3).

4.3.5.3.1 Bone marrow derived macrophage differentiation.

It has previously been shown that nitric oxide (NO) production is induced by IFN-γ / LPS, in classically activated macrophages (Ding *et al.*, 1988; Green *et al.*, 1990). Furthermore, IL-4Rα-dependent mechanisms counter this stimulation, leading to alternative activated macrophages with decreased production of NO but increased arginase I activity (Doyle *et al.*, 1994; Takeda *et al.*, 1996).

To illustrate the cytokine blocking effect of the soluble receptors the IFN-γ / LPS induced NO production and arginase I activity was analyzed using *in vitro* macrophage cultures. The BMDM cells were pre-incubated with medium only, mIL-4, mIL-13, mIL-4 / sIL-4RαF_c or mIL-13 / sIL-13R$\alpha_2 F_c$ for 24h. This was followed by a 24h IFN-γ / LPS stimulation. Subsequently, macrophages were analyzed for the levels of NO produced and for urea production which is a product of the arginase I activity. As shown (Figure 4.19, Panel A), the IFN-γ / LPS induced NO production was significantly decreased when the macrophages were cultured with mIL-4 or mIL-13 prior to IFN-γ / LPS stimulation. In contrast, preincubation with IL-4 or IL-13 increased the arginase I activity as demonstrated by increased urea production (B). With the addition of sIL-13R$\alpha_2 F_c$ or sIL-4RαF_c in combination with mIL-13 or mIL-4, respectively, the opposite effect was seen in both assays. Both the NO and urea production was decreased in these samples.

These results show that treatment with the generated F_c-tagged soluble receptors inhibits the effect by IL-4 and IL-13 on alternative macrophage activation, in this way leading to classically activated macrophages responsive to IFN-γ / LPS stimulation.

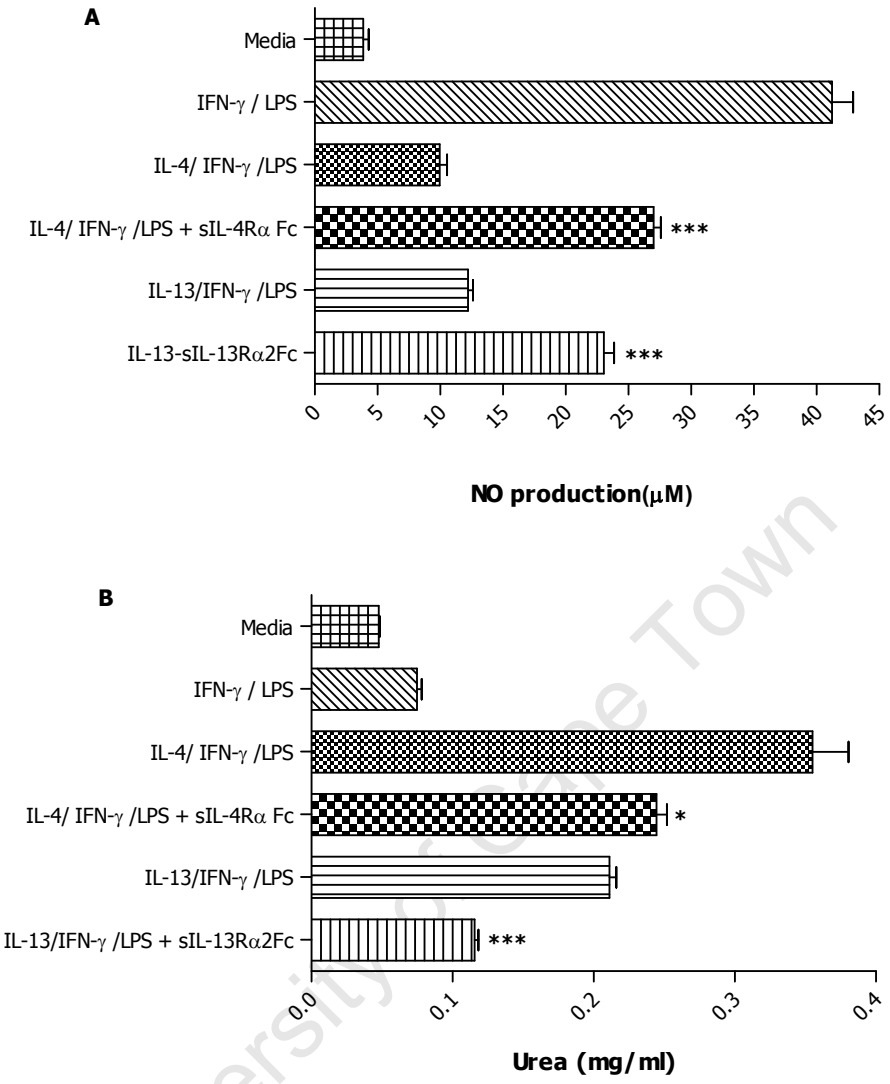

Figure 4.19 Suppression of IL-4 and IL-13 function in BMDM cultures.

Panel A, NO production determined with the Griess reaction. **Panel B**, Urea production after the addition of arginine substrate used to measure arginase I activity. Bone marrow derived macrophages from BALB/c mice were incubated with media only, mIL-4, mIL-4 / sIL-4RαF_c, mIL-13 and mIL-13 / sIL-13R$\alpha_2 F_c$ for 24h. Subsequently IFN-γ / LPS were added and cells stimulated for a further 48h. This was followed by the respective assays. Data is representative of one experiment, and show the average ± SEM of triplicate values. Statistical analysis was performed using unpaired Student's *t* test defining differences to cultures incubated with IL4 or IL13 / IFN-γ / LPS stimulated as significant (**, $p \leq 0.01$; ***, $p \leq 0.001$).

4.3.5.3.2 Macrophage mannose receptor expression.

To further define the effect of the generated F_c-tagged blockers on alternative activation of BMDM culture we also investigated the macrophage mannose receptor (MMR) expression was investigated, as this is considered a reliable marker for alternative activation. Both IL-4 and IL-13 (Ding *et al.*, 1988; Doyle *et al.*, 1994 and Stein *et al.*, 1992) have been shown to enhance the expression and activity of the macrophage mannose receptor (MMR). Thus to asses if the soluble receptor blockers would influence MMR expression in a fashion that mimics that of IL-4 and IL-13 unstimulated macrophages, MMR expression was determined via FACS analysis.

Bone marrow derived macrophages were incubated with medium only, mIL-4, mIL-13, mIL-4 / sIL-4RαF_c or mIL-13 / sIL-13R$\alpha_2 F_c$ for 72h. As expected, incubation of the macrophages with IL-4 or IL-13 led to increased expression of the MMR (Figure 4.20, Panel A). This increase in receptor activity was decreased to a level similar to that of the unstimulated control when cells were incubated with mIL-4 / sIL-4RαF_c or mIL-13 / sIL-13R$\alpha_2 F_c$ respectively. Quantification of this decrease by quadrant statistics of dot plots (panel B) illustrates this effect by the soluble receptor blockers to be greater than a 50% decrease in positive staining and thus MMR expression. These results suggest that the suppression of cytokine action was due to the presence of the F_c-tagged soluble receptor blockers.

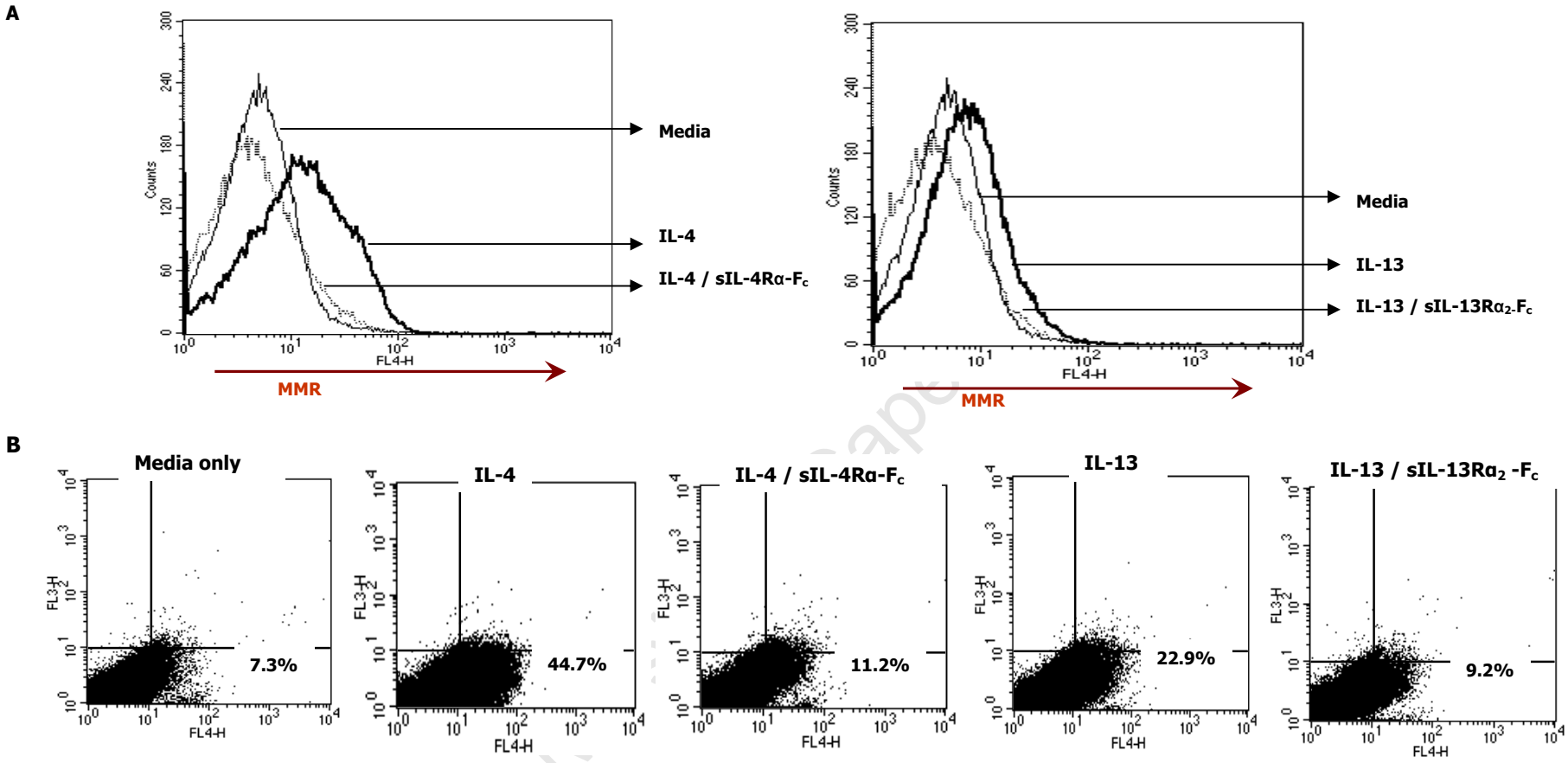

Figure 4.20 sIL-4RαF$_c$ and sIL-13Rα_2F$_c$ dependant suppression of MMR expression.

Panel A, Histograms indicating the shift in UV fluorescence due to MMR expression. **Panel B**, Dot plots indicating the percentage viable cells positive for MMR expression. BALB/c bone marrow derived macrophages were stimulated with mIL-4, mIL-13, mIL-4 / sIL-4RαF$_c$ or mIL-13 / sIL-13Rα_2F$_c$ for 72h. The cells were harvested, permeabilised and stained with biotin-labelled CD206 for the MMR and biotin-labelled Ly-2 as isotype control. Subsequently, the cells were stained with PE-labelled CD11b (macrophage marker) and with 7AAD (dead cell marker). Cells were then assessed for MMR expression in the various samples with FACS. Lines representing different stimulant groups are indicated (**A**). Both **A** and **B** are representative of populations gated for viable cells positive in CD11b surface expression.

4.4 Chapter Conclusions.

Subsequent to expression vector cloning and characterisation (section 4.3.1.2) the three fusion proteins were successfully expressed in Hek 293T cells and purified via protein A Sepharose chromatography (section 4.3.3). Protein purification was followed by the establishment of the cytokine binding affinities of the recombinant F_c-tagged fusion proteins. Results of the cytokine binding assays (section 4.3.4) demonstrated the following;

1. The generated F_c-tagged blockers namely, sIL-13Rα_2F_c, sIL-4RαF_c and sIL-2Rγ-sIL-4RαF_c successfully displayed binding, with differing affinities, to their respective cytokine ligands.
2. The sIL-2Rγ-sIL-4RαF_c cytokine trap showed a higher degree of binding affinity than that shown by the sIL-4RαF_c.

Having shown F_c-tagged soluble receptor - cytokine binding F_c-tagged soluble receptor biological function was tested *in vitro*. Here the $CD4^+$T cell proliferation assay (section 4.3.5.1) clearly demonstrated that the sIL-4RαF_c generated in this study is effective at preventing IL-4 dependant $CD4^+$T cell proliferation. Furthermore these data are comparable to previous studies using existing IL-4 cytokine blockers (Grunewald *et al.,* 1997 and Schulte *et al.,* 1997). From the $CD4^+$T cell differentiation assay (4.3.5.2) it was concluded that sIL-4RαF_c shows a definite blocking effect of the IL-4 cytokine - receptor binding. Even though stimulation with mIL-13 / anti-IFN-γ had a modest effect on either IFN-γ or IL-4 production in $CD4^+$T cells, when the cells were incubated with the sIL-13Rα_2F_c in combination with IL-13 there was a decrease in IL-13 and IL-4 secretion. This will have to be investigated further owing to the fact that to date T cells have been considered resistant to IL-13 stimulation (Zurawski *et al*., 1993; Sornasse *et al*., 1996). However, the data presented here challenges this dogma and points to the possibility of an undiscovered IL-13 signaling complex on $CD4^+$T cells.

To establish the biological functionality of the generated sIL-13Rα_2F_c, the effect of the F_c-tagged blockers on a defined IL-13 role was investigated utilising BMDM functional studies (section 4.3.5.3). These data demonstrated that both sIL-13Rα_2F_c and sIL-4RαF_c influenced the IL-4 and IL-13 cytokine driven alternative macrophage activation as assessed by the macrophage culture nitric oxide and urea production. This blockage of the IL-4 / IL-13 action lead to classically activated macrophages responsive to IFN-γ / LPS stimulation, which is indicative of sIL-13Rα_2F_c and sIL-4RαF_c suppression of cytokine-receptor interaction. This effect was further confirmed by the mannose receptor expression. These assays verified that sIL-4RαF_c and sIL-13Rα_2F_c both had an inhibitory

influence on the macrophage response to IL-4 and IL-13 stimulation. In conclusion, we have successfully generated 3 cytokine blockers of which 2 have demonstrated clear biological functionality.

Chapter 5: Discussion.

In the study presented here we describe the successful development of a range of novel tools for manipulating IL-4Rα function. As IL-4Rα and its associated cytokines are important components of the immune system the development of new tools to further our understanding of their role is of great importance to our understanding of the basic biology of the receptor and the development of potential future clinical applications. In this study we have developed three new approaches to further our understanding of IL-4Rα:

1. An IL-4Rα inducible model.
2. CD11c-Crec and CD11c-GFP constructs.
3. IL-4 and IL-13 soluble and a IL-4/IL-2 soluble receptor cytokine trap.

The generation of a mouse model, which allows the inducible and cell-specific deletion or reconstitution of IL-4Rα expression has the potential to define how controlling temporal expression of IL-4Rα contributes to immune responses. Such a model allows the development of a new dimension to our understanding of IL-4Rα signalling. Two transgenic (Tg) mouse lines were involved in generating the final double transgenic model. One line expresses the transactivator, tTA, from the Tet-Off expression cassette driven by the Vav promoter, ensuring hemopoeitic cell specificity of the expressed protein (Wiesner *et al.,* 2005). The second line, generated here, expresses the IL-4Rα cDNA under the dictates P^{CMV} minimal promoter supplemented with the Tet_O sequences, the operon thus serving as a binding site for the transactivator. Both lines were crossed to the IL-4R$\alpha^{-/-}$ BALB/c genetic background and then intercrossed to generate a double transgenic mouse on the IL-4R$\alpha^{-/-}$ backbone. In these double transgenic mice, the transactivator was synthesized in a cell specific manner leading to cell specific IL-4Rα reconstitution in the IL-4R$\alpha^{-/-}$ background.

Secondly we have generated constructs which will allow the production of a mouse model where Cre recombinase expression is driven by a dendritic cell (DC) specific promoter. This will enable the generation of dendritic cell-specific IL-4Rα deficient mice (CD11c-Cre-IL-4R$\alpha^{lox/-}$). This will be achieved by inter-crossing the newly generated CD11c-CreTg mice with floxed IL-4Rα and global IL-4R$\alpha^{-/-}$ mice. Cre recombinase transgene expression will be directed exclusively to DCs due to the incorporation of the cell specific promoter and Cre expression will lead to the inactivation of the lox P flanked

IL-4Rα gene. The study described here deals with the molecular cloning and characterisation of eukaryotic expression vectors containing the mouse dendritic cell specific promoter (CD11c) and the subsequent *in vitro* functional analysis of these constructs to show cell specific transcription and translation of the transgenes.

Finally, we aimed to build on the body of knowledge of the previously investigated cytokine blockers to generate F_c-tagged soluble receptor blockers for IL-4Rα, IL-13$R\alpha_2$ and the IL-2Rγ-IL-4Rα receptor complex. These Fc-tagged blockers have the ability to block cytokine function *in vitro* and *in vivo*. The design and generation of these fusion proteins represent an important refinement of previously described IL-4 and IL-13 cytokine blockers. We optimized the construct design and specifically used cDNA of a BALB/c genetic background, to skew the Th1 / Th2 response, and also incorporated the mutated human F_c-tag which decreases non-specific binding by these fusion proteins.

Together these models and molecular tools will provide excellent new strategies for investigating IL-4Rα functions both *in vivo* and *in vitro*.

5.1 Conclusions drawn from this study.

5.1.1 Chapter 2: Inducible deletion of IL-4Rα expression.

Immunological studies with IL-4R$\alpha^{-/-}$ mice have led to important advances in our understanding of immune system function. The continual development of more refined transgenic IL-4Rα models (such as cell specific mutants) has built on this understanding of IL-4Rα role considerably. In this study we have developed a new transgenic line which has the potential for inducible cell-specific reconstitution and deletion of IL-4Rα expression. This was achieved by combining the existing IL-4R$\alpha^{-/-}$ model with a newly generated line using the Tet system to induce expression in a hematopoietic cell-specific and temporal manner. This new model will allow the development of a new level of understanding of IL-4Rα function.

The role of IL-4Rα expression in controlling the immune system has been widely demonstrated. For example IL-4R$\alpha^{-/-}$ mice have provided invaluable information demonstrating IL-4 signalling to prevent the resolution of leishmaniasis in susceptible BALB/c mice, mice deficient in IL-4 (Kopf *et al.,* 1996), IL-13 and IL-4Rα (Matthews *et al.,* 2000; Mohrs *et al.,* 1999) being able to control the infection. IL-4R$\alpha^{-/-}$ mice have also demonstrated host protection against intestinal nematode parasites such as *Nippostrongylus brasiliensis* to be dependent on IL-4Rα and IL-13 for the worm

expulsion. Such mice have also shown that the protective host immune response to *Schistosoma mansoni* is also dependent on IL-4Rα expression (Wynn *et al.,* 1999 and Chiaramonte *et al.,* 1999, Chiaramonte *et al.,* 1999(b)). Further examples where IL-4Rα deficient mice have uncovered important roles in specific immunological scenarios include allergy, obesity and anaphylaxis.

However, if *L.major* and *N.brasiliensis* (commonly used in our studies) are to be highlighted as examples, the knowledge that these models though important is limited. An example being the dissection of cytokine function which has and will be facilitated greatly. To illustrate this, during *Nippostrongylus Brasiliensis* infection worm expulsion is dependent on IL-4Rα expression by non-bone marrow (goblet cells, intestinal epithelium, smooth muscle, vascular endothelium) derived cells and not by marrow-derived cells (T cells, B cells, mast cells dendritic cells or macrophages) (Katona *et al.,* 1988; Urban *et al.,* 2001). Although it has been shown that contributions by IL-4Rα expressing smooth muscle cells play a role (Horsnell *et al.;* 2007) the complete requirements for IL-4Rα expression on non-bone marrow derived cells remains to be defined. Thus, use of mice that express IL-4Rα in a spatial manner has and will contribute to defining the cell specific expression pattern required for disease resolution.

In addition to transgenic technology, a number of other tools are available for studying protein function both *in vitro* and *in vivo*. The immunomodulatory properties of antibodies represent a classic example of a technique that can specifically redirect host defenses against infectious agents. The strategy of using a combination of antibody and antigen to improve the host response is not new. The potential to modulate an immune response by immunization with antigen bound by antibody has been demonstrated in numerous studies (Alber *et al.,* 2000; Kunkl and Klaus, 1981; Wiersma *et al.,* 1989; Zheng *et al.,* 2001). These studies have illustrated the benefits of immunization, with immuno complexes consisting of either polyclonal or monoclonal reagents, in eliciting beneficial responses against human and animal pathogens. This can be attributed the recognized immunomodulatory potential of antibodies (Brady, 2005). Examples include the study of simian virus 5 (SV5) paramyxovirus, where monoclonal antibodies (MAbs) against the viral proteins were coupled to solid matrices of fixed *S. aureus* could be used to purify antigens from infected tissue culture cells. These could then be employed as immunogens that induced specific humoral and cytotoxic T-cell responses (Randall and Young, 1988).

Modulation of gene expression can also be achieved with the use of the small interfering RNA (siRNA) technique, which can activate or hinder transcription of a target gene. An example of this powerful tool has been shown for dendritic cell mediated regulatory mechanisms which control host self-tolerance. Here inhibited SOCS1 expression using siRNA demonstrated SOCS1 to be an antigen presentation attenuator, able to disrupt self-tolerance and lead to the induction of effective antitumor responses (Evel-Kabler et al., 2006).

However, the use of antibody complexes and iRNA technology has disadvantages including identifying precise spatial interactions and viral targeting of the reagents. Thus for the purposes of establishing a model that would allow temporal and spatial investigation trangenesis is still more appealing, although adenoviral iRNA technology is an invaluable tool and using it in conjunction with the inducible model could afford the investigator unprecedented scope.

We have therefore described here the successful generation of an inducible and cell specific model which will add a new dimension to our understanding of IL-4Ra function. Prior to applying this model to immunological studies a number of final characterisation steps remain which were beyond the scope of the current study. These include addressing the variability shown in expression between the transgenic male and females. The IL-4Rα transgene is X-linked and the difference shown in transgene expression could be due to the transgene being on both X chromosomes leading which could lead to X-chromosome inactivation (Dandolo *et al.,* 1993; Moulson *et al.,* 2007). It is thus essential to establish the final line lacking variability in translation before infectious studies using this model are commenced. Additionally, due to time constraints owing to a 4 month delay in the delivery of the initial chimeric mice and the lengthy breeding program the inducible repression of the transgene expression via the administration of doxycycline needs to be established.

5.1.2 Chapter 3: Dendritic Cell Specific Expression of Cre Recombinase.

Cell specific IL-4Rα defcient mice are a relatively recent development, which have already proved to be a superb tool for unraveling IL-4Rα functions. In *L. major* infections mice deficient in $CD4^+$T cell IL-4Rα developed disease phenotypes associated with mice genetically resistant (e.g. C57BL6 and BALB/c IL-$4R\alpha^{-/-)}$ to *L. major* infection, in this way confirming the importance of receptor expression on CD4+ T-cells in *L. major* disease progression (Radwanska *et al.,* 2007). Mice deficient in smooth muscle cell IL-4Rα expression have demonstrated an important role for IL-4Rα expression here in the expulsion of the parasitic worm *Nippostrongylus Brasiliensis* (Horsnell *et al.,* 2007). The macrophage/neutrophil-specific IL-4 receptor deficient mice were used to investigate the role of the receptor on myeloid cells during *Schistosoma mansoni* infection (Herbert *et al.,* 2004). These mice demonstrated host survival to be dependent on IL-4Rα signaling in macrophages.

The role of IL-4Rα expression on dendritic cells is limited but has been suggested to play a role in IL-4 dendritic cell maturation and the subsequent production of IL-4 in DC activated T cells (Feili-Hariri *et al.,* 2005). Additionally, IL-4 promotes the production of IL-4 by dendritic cells and the reason why IL-4 is rarely detected, in the secreted form, is due to the cytokines binding IL-4Rα on the dendritic cells, thus activating the dendritic cells in an autocrine fashion (Maroof *et al.,* 2005). Given the central role of these antigen presenting cells in immunity and tolerance, they are potentially ideal therapeutic targets for pharmacological modulation of immune responses (Banchereau *et al.,* 2000). The potential clinical implication of dendritic cell modulation via IL-4 (Maroof *et al.,* 2005, Sriram *et al.,* 2007), has also become more evident. An example is the suggestion that IL-4 could be candidate in novel therapeutic strategies for diseases in which an excessive exposure to type I IFNs is pathogenic (Theofilopoulos *et al.,* 2005). Furthermore, modulation of the effects of IL-4 on DCs may be therapeutic in the autoimmune diseases such as systemic lupus erythematosus (Sriram *et al.,* 2007).

Thus, the aim with this aspect of the study was the generation and *in vitro* functional analysis of constructs designed to express Cre recombinase (and Green Fluorescent Protein as a reporter line) under the control of the murine dendritic cell specific promoter, CD11c. Subsequent to intercrossing of this line with the existing IL-$4R\alpha^{lox/lox}$ line the dendritic cells specific deletion of IL-4Rα would be achieved and a new tool for the investigation of IL-4Rα mediated immune response would be available. Subsequent

to *in vitro* functional analysis the pCD11c-Cre and pCD11c-GFP constructs were sequence verified, the functionality of the constructs were confirmed in terms of transcriptional and translational analysis. We have thus successfully generated 2 functional transgenic constructs: the pCD11c-GFP that could potentially be utilised as a reporter for the CD11c activity in generated transgenic models and the pCD11c-Cre construct that after generation of the transgenic mouse and breeding into the IL-4R$^{lox/lox}$ line will lead to the DC specific disruption of IL-4Rα expression.

5.1.3 Chapter 4: Generation of molecular tools for the neutralization of signalling via IL-4Rα and IL-13Rα_2.

In the pursuit to find new clinical interventions in allergic and autoimmune diseases novel strategies to target cytokines are being developed, these include cytokine blockers such as monoclonal antibodies and soluble receptors. Additionally high-affinity blockers referred to as cytokine traps also show great potential, these recombinant proteins consist of fusion proteins between the constant region of IgG and the extracellular domain of two distinct cytokine receptor components involved in binding to the target cytokine. These potent cytokine blockers have shown cytokine blocking *in vivo* and *in vitro* and are a substantial advance in the generation of novel therapeutic candidates for cytokine driven diseases (Economides *et al.,* 2003). Additionally, cytokine blockers inhibiting the cytokine – receptor interaction have proven to be powerful tools in the pursuit to an enhanced understanding of cytokine function during certain disease states. The TNF-α blocker (Enbrel) is a prime example which has lead to clinical trails in patients suffering from rheumatoid arthritis (Goldenberg, 1999). Previously, an IL-13 blocker consisting of the extracellular domain of murine IL-13Rα_2 fused to the hinge-CH2-CH3 regions of hIg-γ1 had been generated (Donaldson *et al*., 1998). This soluble form of the IL-13 binding protein demonstrated high affinity binding and specificity for the IL-13 cytokine. Furthermore, it displayed an effective IL-13 antagonistic function (Urban *et al*., 1998; Grunig *et al*., 1998). The therapeutic efficacy this IL-13 inhibitor was demonstrated in the control of hepatic fibrosis. Fibrosis is a major pathological manifestation of a number of allergic, autoimmune, and infectious diseases and the IL-13 inhibitors demonstrated therapeutic benefit by means of preventing the damaging tissue fibrosis which is a result of the Th2-dominated inflammatory response (Chiaramonte *et al.,* 1999 (b)). Previous studies also describe the generation of IL-4 cytokine blockers. Examples of these blockers are; recombinant IL-4 soluble proteins, an IL-4 binding antibody (11B11),

recombinant mutated IL-4 proteins or IL-4/anti-IL-4mAb complexes (IL-4C) (Maliszewski *et al.*, 1990; Grunewald *et al.*,1997; Finkelman *et al.*, 1999).

The soluble isoform of IL-4Rα, sIL-4R, was shown to reduce airway inflammation *in vivo*, through inhibition of IgE production (Sato *et al.,* 1993), in this way illustrating it's possible use in treatment of IgE-mediated inflammatory diseases such as asthma. Subsequently a nebulised recombinant soluble human IL-4Rα has been investigated as a potential asthma therapy (Borish *et al.,* 2001).

A potential disadvantage of sIL-4R is that it does not block IL-13. In asthma the effects of allergic inflammation are mediated by both IL-4 and IL-13 thus blocking both cytokines is preferable. Alternative cytokine blocking / inhibition strategies include the use of IL-4R antagonists (Bayer, BAY 16-9996), and cytokine traps. These approaches are even more promising with the recent study demonstrating that IL-4Rα plays a vital role in the ligand binding properties of both receptors. Yet, the mechanism of formation and stabilization of ligand-bound IL-4R and IL-13R differ. Furthermore, these differences in binding affinity have functional implications for therapeutic agents that have been developed to antagonize these receptors. Its been demonstrated that soluble human IL-4Rα inhibits IL-4 induced responses and that this soluble receptor is able to act as a weak agonist through its ability to stabilize suboptimal doses of IL-13, in this way enhancing its activity(Andrews *et al.,* 2006). Additionally vaccines against IL-4 have been tested in mice, one in which IL-4 is chemically coupled to limpet haemocyanin (Le *et al.,* 2007)

Yet, the receptor binding and subsequent signalling mediated by IL-4 and IL-13 is not fully understood, and a complete understanding of these binding interactions between these cytokines and their related receptors will facilitate development of novel treatments for asthma that selectively target these cytokines without unexpected or harmful side effects.

The soluble IL-13Rα_2F_c fusion protein described in the current study differs from the recombinant mentioned previously, in two ways; firstly the RNA used to generate the coding region for the extracellular domain of IL-13Rα_2 was isolated from a BALB/c mouse strain as opposed to the C3H/HeJ RNA used in the above-mentioned study. For our purposes this represented a more relevant genetic background to study IL-4Rα, as the majority of the IL-4Rα transgenic mice available are on a BALB/c background. Secondly, the fusion of the extracellular domain is to a mutated form of the human IgG1. It is not clear how these differences will be represented in the phenotype, but should be borne in

mind when comparing binding affinity and antagonistic/agonistic roles. The IL-4 soluble receptor blocker described in this report was generated from BALB/c cDNA and fused to the human F_c tag, and as with the sIL-13Rα_2F_c blocker it isn't clear how these differences will be represented in the studies. Furthermore, the generation of the sIL-2Rγ-sIL-4Rα cytokine trap design was based on the molecular design of a previously generated IL-4 cytokine trap (Economides *et al.*, 2003). With differences being in the use of extracellular domains of BALB/c IL-4Rα and IL-2Rγ, as opposed to the human IL-4Rα and IL-2Rγ extracellular domains used in the above-mentioned study. Finally, we aimed to build on the vast body of knowledge of the previously investigated cytokine blockers to generate F_c-tagged soluble receptor blockers for IL-4Rα, IL-13Rα_2 and the IL-2Rγ-IL-4Rα receptor complex. These Fc-tagged blockers would have the ability to block cytokine function *in vitro* and subsequently *in vivo*. The design and generation of these fusion proteins were, although analogous to previous described IL-4 and IL-13 cytokine blockers, refinement of these. This optimization was in the construct design where we specifically used cDNA of a BALB/c genetic background (to skew the Th1 / Th2 response), and a mutated human F_c-tag which decreases non-specific binding by these fusion proteins.

Subsequent to recombinant protein over-expression the vectors were sequence verified. Protein purification was followed by the establishment of the cytokine binding affinities of the recombinant F_c-tagged fusion proteins. The results of these assays demonstrated the cytokine binding by all three generated F_c-tagged blockers namely; sIL-13Rα_2F_c, sIL-4RαF_c and sIL-2Rγ-sIL-4RαF_c, but there were distinct differences in the binding affinities shown by the blockers for their respective cytokine ligands. The sIL-13Rα_2F_c which binds to IL-13 showed binding affinities that were similar to those of the previously generated IL-13 blocker (Donaldson *et al.,* 1998). The generated sIL-4RαF_c displayed binding affinities that approached 3x less shown by an antibody against IL-4, a decreased affinity to that of the antibody was expected as it has been shown that the soluble isoform of IL-4Ra in BALB/c mice show reduced cytokine binding as that displayed by other mouse strains (Gessner *et al.,* 1994). Furthermore, there are no other reported murine F_c-tagged soluble receptors resulting in a lack of standard with which to compare the data. The sIL-2Rγ-sIL-4RαF_c cytokine trap showed a higher degree of binding affinity than that shown by the sIL-4RαF_c. This approached the binding affinity of the anti-IL-4 and was similar to that shown for the generated human sIL-2Rγ-sIL-4RαF_c, indicating the high degree of affinity that cytokine blockers afford (Economides *et al.,* 2003). The biological functions of these blockers were tested *in vitro*. The $CD4^+$T cell proliferation assay clearly

demonstrated that the sIL-4RαF_c generated in this study is effective at preventing IL-4 dependent $CD4^+$T cell proliferation. Furthermore these data are comparable to previous studies using existing IL-4 cytokine blockers (Grunewald *et al.,* 1997 and Schulte *et al.,* 1997). Furthermore the $CD4^+$T cell differentiation assay confirmed the sIL-4RαF_c blocking effect of the IL-4 cytokine-receptor interaction. Stimulation of the $CD4^+$T cells with mIL-13 / anti-IFN-γ had a modest effect on either IFN-γ or IL-4 production in, but when the cells were incubated with the sIL-13Rα_2F_c in combination with IL-13 there was a decrease in IL-13 and IL-4 secretion. This will have to be investigated further owing to the fact that to date T cells have been considered resistant to IL-13 stimulation (Zurawski *et al*., 1993; Sornasse *et al*., 1996). However, the data presented here challenges this dogma and points to the possibility of an undiscovered IL-13 signalling complex on $CD4^+$T cells. (Donaldson *et al.,* 1998; Aman *et al.,* 1996). To establish the biological functionality of the generated sIL-13Rα_2F_c, the effect of the F_c-tagged blockers on a defined IL-13 role was investigated utilising bone marrow derived macrophages (Doyle *et al*., 1994; Takeda *et al*., 1996). Here we demonstrated that both sIL-13Rα_2F_c and sIL-4RαF_c influenced the IL-4 and IL-13 cytokine driven alternative macrophage activation as assessed by the macrophage culture nitric oxide and urea production. This blockage of the IL-4 / IL-13 action lead to classically activated macrophages responsive to IFN-γ / LPS stimulation, which is indicative of sIL-13Rα_2F_c and sIL-4RαF_c suppression of cytokine-receptor interaction. This effect was further confirmed by the mannose receptor expression. These assays verified that sIL-4RαF_c and sIL-13Rα_2F_c both had an inhibitory influence on the macrophage response to IL-4 and IL-13 stimulation which was in accordance with previous studies (Ding *et al*., 1988; Doyle *et al*., 1994 and Stein *et al*., 1992).

5.2 Conclusion.

In this study we have successfully developed three new approaches to further our understanding of IL-4Rα.

Subsequent to the final establishment of the transgenic line and the studies confirming inducibility of the Tet system, the generated pVav-tTaTg/pBi-IL-4RαTg/IL-4R$\alpha^{-/-}$ transgenic model has the potential to allow great flexibility in the establishment of future transgenic models as the number of characterised effector lines, tTa expression mice, is continually increasing. Therefore the model affords the potential of inducible IL-4Rα expression on the cell-type of choice. Studies with this model can also potentially

overcome limitations inherent in conventional gene targeted mice. It could facilitate in the investigation of the precise role of IL-4Rα signalling in the generation and maintenance of organ specific immune responses, and of the role for cytokines in immune-mediated regulation of infectious disease. It also has the potential to assist in the design of novel therapeutic strategies to potentiate protection against debilitating infectious organisms.

In a similar fashion the CD11-Cre model will also broaden the scope of investigations into IL-4Rα function. Currently the chimeric mice are in development and the breeding program and subsequent characterisation will commence before the end of 2008.

Lastly we have also successfully generated 3 cytokine blockers. Two of these have shown clear biological functionality and if the binding assays were an indication, the ensuing studies on the biological functions of the cytokine trap could show an even greater IL-4 inhibiting effect. Having set-up the cloning strategies and expression and purification protocols, there is even scope to develop additional cytokine traps. One of interest could be the trap incorporating both soluble receptor components of IL-13$R\alpha_1$ and IL-4Rα which has the potential to be potent blockers of the cytokine responses displaying high affinity for both IL-4 and IL-13.

Appendix A

A.1 Plasmid Maps.

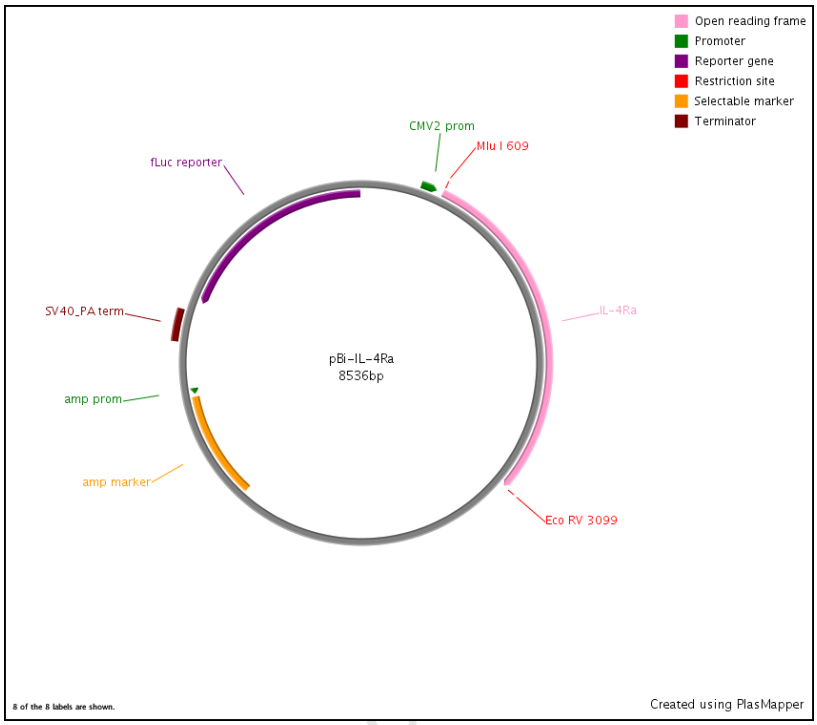

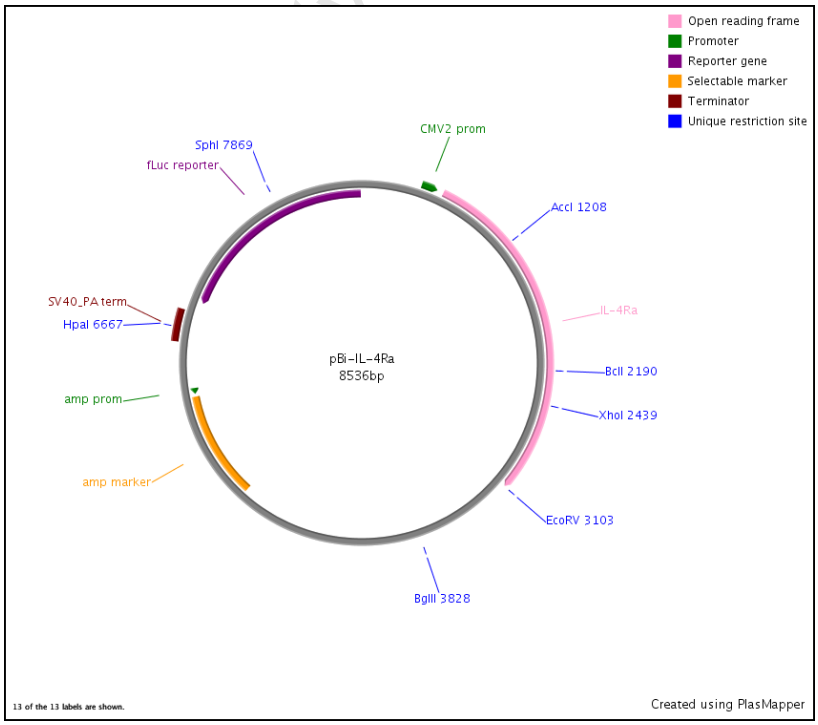

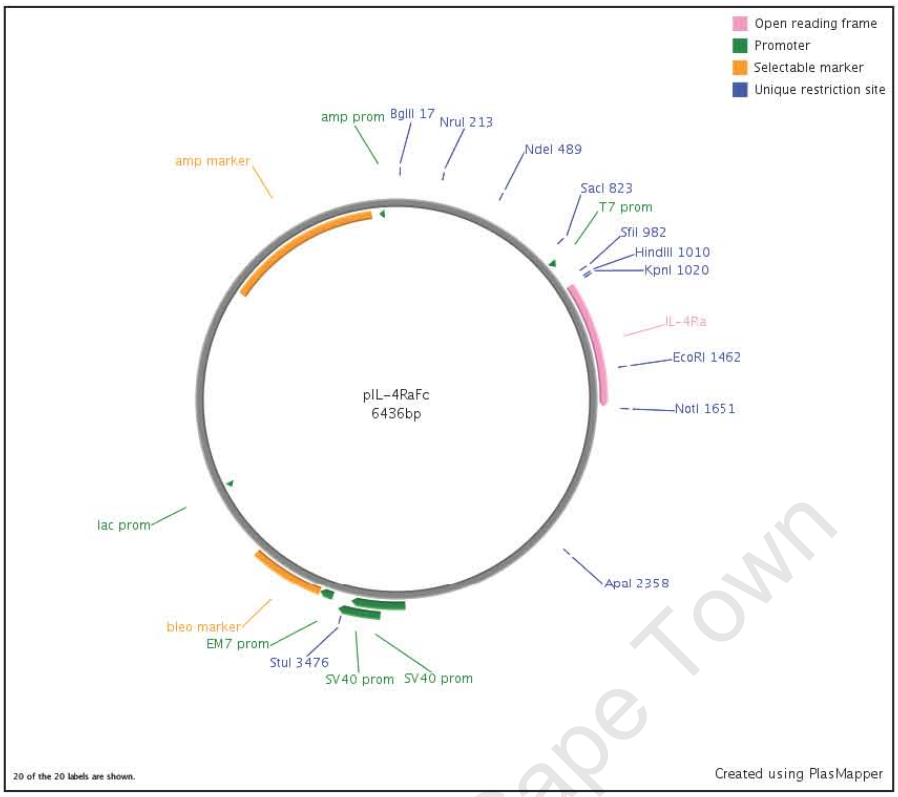

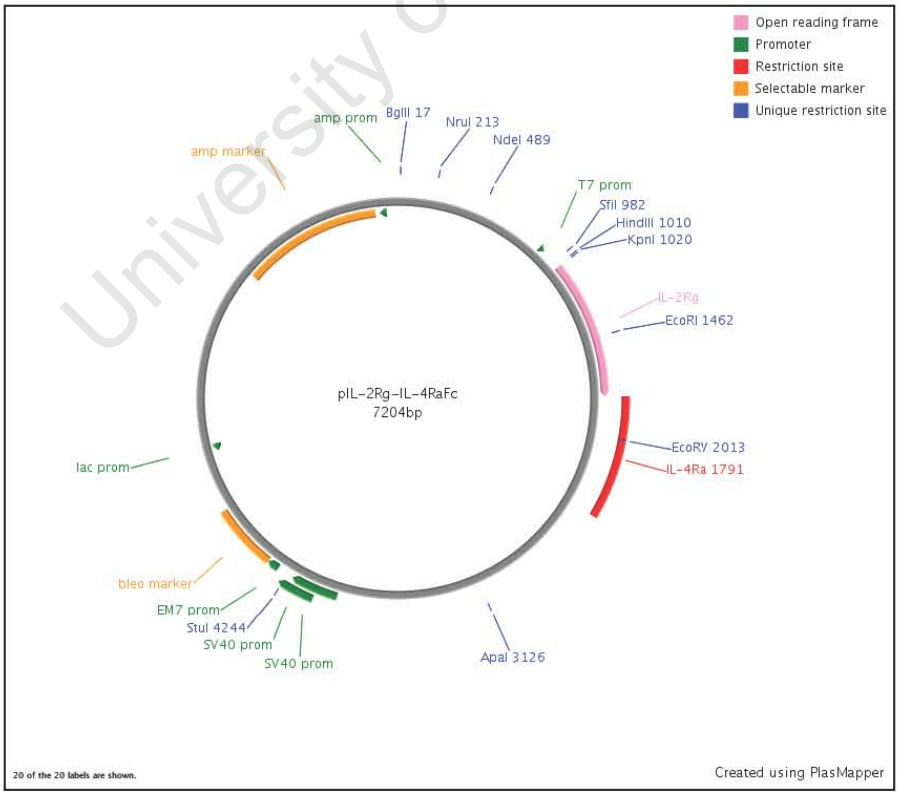

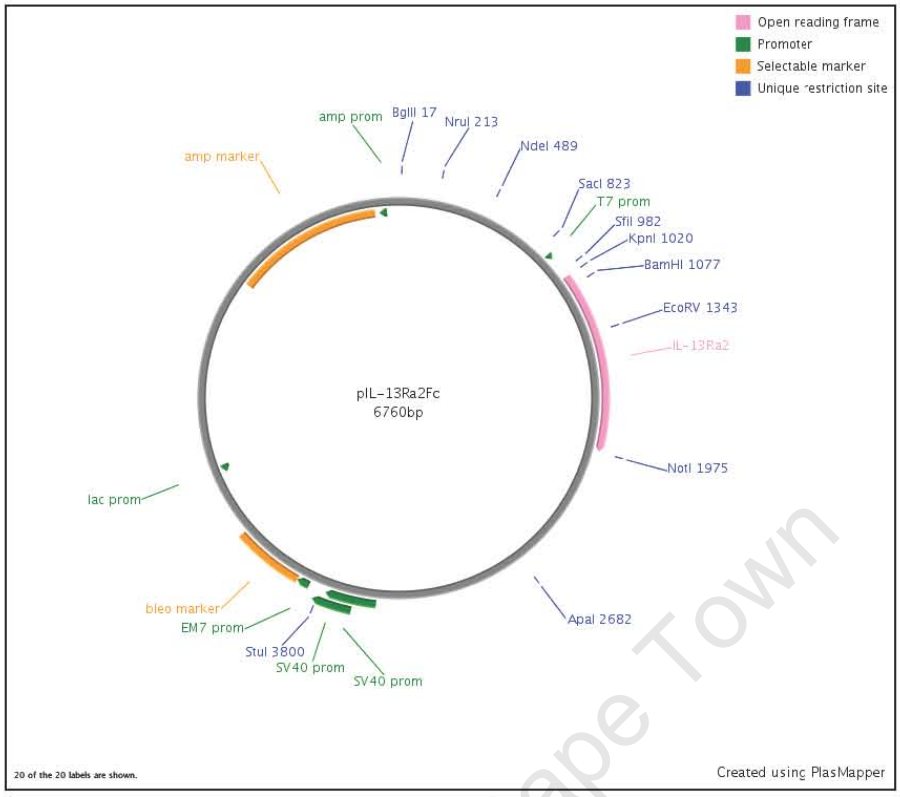

A.2 Reagents and Suppliers.

Reagent or Kit	Supplier
3,3',5,5'-tetramethylbenzidine (TMB)	Roche Diagnostics GmbH, Mannheim, Germany
5-bromo-4-chloro-3indolylphosphate (BCIP)	Roche Diagnostics GmbH, Mannheim, Germany
Acetone	Sigma-Aldrich, Munich, Germany
anti-CD11c-PE	BD Pharmigen, BD Biosciences, San Jose, CA, USA
anti-Cre-FITC (clone7-24)	Sigma-Aldrich, Munich, Germany
anti-human IgG-AP	Sigma-Aldrich, Munich, Germany
anti-MHC II-FITC	Sigma-Aldrich, Munich, Germany
anti- mouse IgG1	BD Pharmigen, BD Biosciences, San Jose, CA, USA
anti-I-Ab (clone KH74)	BD Pharmigen, BD Biosciences, San Jose, CA, USA
anti-rabbit $IgG_{2}\alpha$-FITC	Sigma-Aldrich, Munich, Germany
b-Mercaptoethanol	Sigma-Aldrich, Munich, Germany
Bovine Serum Albumin (fraction V)	Roche Diagnostics GmbH, Mannheim, Germany
Bovine Serum Albumin(BSA) (molecular grade at 20mg/ml)	Roche Diagnostics GmbH, Mannheim, Germany
calcium chloride	BDH Chemicals Ltd., Poole, England
Chloroform	BDH Chemicals Ltd., Poole, England
ImProm-II™ Reverse Transcription System	Promega, Madison, WI, USA
Iscoves's Modified Dulbecco's Modified Eagle's Medium (IMDMM) for Cell Culture	Gibco, Invitrogen Corporation, Carlsbad, CA, USA
isoamyl alcohol	Sigma-Aldrich, Munich, Germany
isopropanol	BDH Chemicals Ltd., Poole, England
Isopropanol (microarray)	Fisher Scientific
L-glutamine	Gibco, Invitrogen Corporation, Carlsbad, CA, USA

Reagent or Kit	Supplier
Lipopolysaccharide (LPS)	Sigma-Aldrich, Munich, Germany
low melting point agarose	Promega, Madison, WI, USA
magnesium chloride	BDH Chemicals Ltd., Poole, England
n-1-napthylethylenediamide	Sigma-Aldrich, Munich, Germany
nitroblue tetrazolium salt (NBT)	Roche Diagnostics GmbH, Mannheim, Germany
Oligonucleotide Primers	DNA Synthesis Laboratory, Dept. Molecular and Cellular Biology, University of Cape Town , South Africa
Penicillin G and Streptomycin Solution (100X)	Gibco, Invitrogen Corporation, Carlsbad, CA, USA
Peroxidase Substrate (Solution B)	Roche Diagnostics GmbH, Mannheim, Germany
phenol pH4.0	Sigma-Aldrich, Munich, Germany
phosphoric acid	BDH Chemicals Ltd., Poole, England
Polyacrylcarrier	Molecular Research Company, Cincinnati, USA
potassium chloride	BDH Chemicals Ltd., Poole, England
Proteinase K	Roche Diagnostics GmbH, Mannheim, Germany
Qiagen MiniElute RNA cleanup kit	Qiagen, Valencia, CA, USA
RNasin (1U/µl)	Promega, Madison, WI, USA
Reagent or Kit	**Supplier**
Teflon coated-bag	Max Planck Institute for Immunobiology, Max Planck, Freiberg, Germany
TMB Peroxidase Substrate (Solution A)	Roche Diagnostics GmbH, Mannheim, Germany
TriReagent	Molecular Research Company, Cincinnati, USA
TRIS-HCl	BDH Chemicals Ltd., Poole, England
Triton-X100	BDH Chemicals Ltd., Poole, England
Trypsin/EDTA Solution (10 X)	Gibco, Invitrogen Corporation, Carlsbad, CA, USA
tryptose-soy broth	Difco, Detroit, MI, USA
Tween-20	Merck Laboratory Supplies, South Africa
β-mercaptoethanol	Sigma-Aldrich, Munich, Germany

A.3 Software Resources.

Software	Supplier / URL
Axiovision version 3.1	Carl Zeiss, Göttingen, Germany
CellQuest	Becton-Dickinson, BD Biosciences, San Jose, CA, USA
DNAMAN version4.1.3.	Lynnon BioSoft, USA
Entrez Gene Database	http://www.ncbi.nlm.nih.gov/entrez/query.fcgi?db=gene
OMIM Database	http://www.ncbi.nlm.nih.gov/entrez/query.fcgi?db=OMIM
PubMed Database	http://www.ncbi.nlm.nih.gov/entrez/query.fcgi?db=PubMed

A.4 Specialized Equipment.

Equipment	Supplier
FACSCalibur	Becton-Dickinson, BD Biosciences, San Jose, CA, USA
Lightcycler	Roche Diagnostics GmbH, Mannheim, Germany
MJ thermocycler	Biozym, Hessisch Oldendorf, Frankfurt, Germany
NanoDrop ND-1000A UV-Vis Spectrophotometer	NanoDrop Technologies, Wilmington, DE, USA
SpeedVac	Savant Instruments Inc, Holbrook, NY, USA
VersaMax microplate reader	Molecular Devices Corporation, Sunnyvale, CA, U.S.A

A.5 Recipes.

A.5.1 General Lab Solutions

Mouse Tail Digestion Buffer

12.5ml 1M TRIS-HCL, pH8

50ml 500mM EDTA, pH8.0

12.5ml 1M NaCl

25ml 10% SDS

2.5ml 10mg/ml Proteinase K

Add 12.5ml of 1M TRIS-HCL (pH8), 50ml of 500mM EDTA (pH8.0), 12.5ml of 1M NaCl and 25ml of 10% SDS to 140ml of ddH_2O. Bring up the final volume to 250ml and filter sterilize with a 0.22µM filter (Millipore Corporation, Bedford, USA). Aliquot into sterile tubes and store at -20^oC. Thaw buffer and add 10mg/ml Proteinase K at a 1:100 dilution.

10mg/ml Proteinase K

1g Proteinase K

Weigh out 1g of Proteinase K and dissolve in 100ml of ddH_2O. Filter sterilize with a 0.22µM filter (Millipore Corporation, Bedford, USA) and aliquot into sterile tubes. Store at -20^oC and use at a 1:100 dilution in Mouse Tail Digestion Buffer.

0.5M EDTA, pH 8.0

93.06g EDTA

Weigh out 93.06g of EDTA and dissolve in 450ml ddH_2O. Adjust pH to 8.0 and bring final volume to 500ml. Autoclave and store at room temperature.

2M NaCl

11.688g NaCl

Weigh out 11.688g of NaCl and dissolve in 90ml of ddH_2O. Bring final volume to 100ml and autoclave. Store at room temperature.

10% SDS

10g SDS

Weigh out 10g of SDS and dissolve in 90ml of ddH_2O. Bring final volume to 100ml and autoclave. Store at room temperature.

1M TRIS-HCl, pH8.0

60.55g TRIS-HCl

Weigh out 60.55g of TRIS-HCl and dissolve in 450mlddH_2O. Adjust pH to 8.0 and bring final volume to 500ml. Autoclave and store at room temperature.

1 X Phosphate Buffered Saline (PBS)

8g NaCl

0.2g KCl

1.44g Na2HPO4

0.24g KH2PO4

Weigh out chemicals and dissolve in 900ml of ddH_2O and adjust pH to 7.4. Bring final volume to 1000ml and filter sterilize with a 0.22µM filter (Millipore Corporation, Bedford, USA). Store at 4^{o}C or room temperature.

1 X PBS (with $CaCl_2$ and $MgCl_2$)

8g NaCl

0.2g KCl

1.44g $Na_2HPO_4.2H_2O$

0.24g KH_2PO_4

100mg $CaCl_{2.}2H_2O$

100mg $MgCl_{2.}{}_{.}6H_2O$

Weigh out chemicals and dissolve in 900ml of ddH_2O and adjust pH to 7.4. Bring final volume to 1000ml and filter sterilize with a 0.22µM filter (Millipore Corporation, Bedford, USA). Store at 4^{o}C or room temperature.

3.7% formaldehyde (vol/vol in PBS)

48.68ml 38% formaldehyde

500ml 1 X PBS

Mix together 48.68ml of 38% formaldehyde and 400ml of 1 X PBS. Bring up volume to 500ml and filter sterilize with a 0.22µM filter (Millipore Corporation, Bedford, USA). Aliquot into sterile tubes and store at 4^{o}C.

10% glycerol

10ml 100% Glycerol
90ml 1 X PBS
Mix together 10ml of 100% of Glycerol and 90ml of 1 X PBS. Autoclave and store at temperature.

10% Triton-X100
10ml 100% Triton-X100
90ml 1 X PBS
Mix together 10ml of 100% Triton-X100 and 90ml of 1 X PBS. Autoclave and store at temperature.

1% BSA (Fraction V)
1g BSA (fraction V)
100ml 1 X PBS
Weigh out 1g of BSA (fraction V) and dissolve in 95ml of 1 X PBS. Bring up the final volume to 100ml and filter sterilize with a 0.22µM filter (Millipore Corporation, Bedford, USA). Aliquot into sterile tubes and store at -20^{o}C.

A.5.2 Bacterial Solutions

Luria broth (LB) (1ℓ)
10g tryptone peptone
5g yeast extract
5g NaCl
1ml 1M NaOH
Add water to volume. Mix together. Autoclave and store at room temperature.

LB-Agar

10g tryptone peptone
5g yeast extract
5g NaCl
1ml 1M NaOH
13g Bacto-Agar.

Add water to volume. Mix together. Autoclave and store at room temperature**.**

SOC medium

0.5% (w/v) yeast extract
2% (w/v) tryptone
10mM $NaCl_2$,
2.5mM KCl,
10mM $MgCl_{2,}$
20mM $MgSO_4$ and 20mM glucose

A.5.3 Cell Culture Solutions

Fetal Calf Serum (FCS)

500ml FCS

Thaw one 500ml bottle of FCS at 37°C and heat inactivate at 56°C for 30 minutes with intermittent agitation. Make 25ml aliquots and store at -20°C.

Horse Serum

500ml Horse Serum

Thaw one 500ml bottle of horse serum at 37°C and heat inactivate at 56°C for 30 minutes with intermittent agitation. Make 25ml aliquots and store at -20°C.

Dulbecco's Modified Eagle's Medium (DMEM)

13.38g DMEM powder
100ml Fetal calf serum
10ml 100X Penicillin G and Streptomycin Solution

Weigh out 13.38g of DMEM powder and 3.7g of sodium bicarbonate and dissolve in 800ml ddH_2O. Add 100ml heat decomplemented fetal calf serum and 10ml of 100X Penicillin G and Streptomycin Solution. Bring the final volume to 1000ml and filter sterilize with a 0.22µM filter (Millipore Corporation, Bedford, USA). Store at 4°C.

Iscoves's Modified DMEM (IMDM)

17.66g IMDM powder
100ml Fetal calf serum
10ml 100X Penicillin G and Streptomycin Solution

Weigh out 17.66g of IMDM powder and 3.024g of sodium bicarbonate and dissolve in 800ml ddH_2O. Adjust pH to between 7.2 – 7.4 with 1M NaOH. Add 100ml heat decomplemented fetal calf serum and 10ml of 100X Penicillin G and Streptomycin

Solution. Bring the final volume to 1000ml and filter sterilize with a 0.22µM filter Store at 4°C).

Plutznik Media

264ml DMEM (with 100U/ml penicillin G, 100µg /ml streptomycin)
50ml FCS (heat decomplemented)
25ml Horse serum (heat decomplemented)
5ml 200mM L-glutamine
5ml 100mM Na-pyruvate
1ml 1000X 2-β-Mercaptoethanol
150ml L929 cell-conditioned medium

Add all the reagents together and filter sterilize with a 0.22µM filter (Millipore Corporation, Bedford, USA). Always make fresh just before use.

200mM L-Glutamine

2.922g L-Glutamine

Weigh out 2.922g L-Glutamine and dissolve in 100ml of ddH_2O and filter sterilize with a 0.22µM filter (Millipore Corporation, Bedford, USA). Make 5ml aliquots and store at -20°C.

1000X 2-β-Mercaptoethanol

698µl 2-β-Mercaptoethanol

Add 698µl of 2-β-Mercaptoethanol to 100ml of ddH_2O. Filter sterilize with a 0.22µM filter (Millipore Corporation, Bedford, USA) and store at 4°C.

100mM Sodium Pyruvate

1.1g Sodium Pyruvate

Weigh out 1.1g sodium pyruvate and dissolve in 100ml ddH_2O. Filter sterilize with a 0.22µM filter (Millipore Corporation, Bedford, USA) and store at 4°C.

Red cell lysis Buffer

8.34g NH_4CL
0.037g EDTA
1.00g $NaHCO_3$

Weigh out chemicals and dissolve in 1000ml of ddH_2O. Filter sterilize with a 0.22µM filter (Millipore Corporation, Bedford, USA) and store at 4°C.

1 X Trypsin/EDTA Solution

10 X Trypsin/EDTA Solution (Gibco, Invitrogen Corporation, Carlsbad, CA, USA)
Add 10ml of 10 X Trypsin/EDTA Solution to 90ml of ddH_20, filter sterilize with a 0.22 µM filter (Millipore Corporation, Bedford, USA) and store at 4°C.

A.5.4 Immunology Solutions

ELISA Coating Buffer

0.2g NaN_3
Weigh out NaN_3 and dissolve in 900ml of 1 X PBS, bring the final volume to 1000ml and store at room temperature.

ELISA Blocking Buffer
20g Powder Milk
0.2g NaN_3
Weigh out chemicals and dissolve in 900ml of 1 X PBS, bring the final volume to 1000ml and store at 4°C.

ELISA Dilution Buffer

10g BSA
0.2g NaN_3
Weigh out chemicals and dissolve in 900ml of 1 X PBS, bring the final volume to 1000ml and store at 4°C.

ELISA Washing Buffer (20 X)
20g KCL
20g $KH_2HPO_4.2H_2O$
800g NaCl
50ml Tween-20
100ml 10% NaN_3
Weigh out chemicals and dissolve in 4500ml double distilled water (ddH_2O). Add 50ml of Tween-20 and 100ml of 10% NaN_3. Bring final volume to 5000ml and store at room temperature. Dilute 1:20 in ddH_2O for a 1 X working concentration buffer.

ELISA Substrate Buffer (for alkaline phosphatase conjugates)

0.2g NaN_3

97ml diethanolamine

0.8g $MgCl_2.6H_2O$

Weigh out chemicals and dissolve in 700ml of ddH_2O. Add 97ml of liquefied diethanolamine and adjust pH to 9.8. Bring the final volume to 1000ml and store at 4°C.

ELISA Substrate Buffer (for horseradish peroxidase conjugates)

TMB Peroxidase Substrate Solution A (Roche Diagnostics GmbH, Mannheim, Germany)

Peroxidase Substrate Solution B (Roche Diagnostics GmbH, Mannheim, Germany)

1M H_3PO_4

Just before use, mix equal volumes of TMB Peroxidase Substrate (Solution A) with Peroxidase Substrate Solution B. Add 50µl per well and let the reaction develop at room temperature for 5 minutes. Stop the reaction by adding 50µl of 1M H_3PO_4.

Griess Reagent Standard (1mM $NaNO_2$)

6.899mg $NaNO_2$

Weigh out 6.899mg of $NaNO_2$ and dissolve in 100ml of ddH_2O and store at 4°C.

Griess Reagent 1

1g sulfanilamide

100ml 2.5% phosphoric acid

Weigh out 1g sulfanilamide and dissolve in 100ml of 2.5 % phosphoric acid. Cover bottle in foil to protect from light and store at 4°C.

Griess Reagent 2

0.1g napthyl-ethylene-diamine

100ml 2.5 %phosphoric acid

Weigh out 0.1g napthyl-ethylene-diamine and dissolve in 100ml of 2.5 % phosphoric acid. Cover bottle in foil to protect from light and store at 4°C.

2.5% phosphoric acid

3ml 85% phosphoric acid

Add 3ml of 85% phosphoric acid slowly to 90ml of ddH_2O. Bring up volume to 100ml and store at room temperature.

NBT/BCIP Solution;
Add 200 µl of the stock solution to 10 ml 0.1 M Tris-HCl, pH 9.5
(20°C), 0.1 M NaCl, 0.05 M MgCl2 .

A.5.5 RNA Solutions

DEPC-treated H_2O
1000ml ddH_2O
1ml Diethylpyrocarbonate (DEPC)
Add 1ml of DEPC to 1000ml of ddH_2O and incubate overnight at 37°C with agitation. Autoclave to sterilize and heat deactivate the DEPC. Aliquot in RNAse-free tubes and store at room temperature.

70% Ethanol
70ml absolute ethanol
30ml DEPC-treated H_2O
Add 30ml of DEPC-treated H_2O to 70ml absolute ethanol and mix well. Aliquot in RNAse-free tubes and store at room temperature.

75% Ethanol
75ml absolute ethanol
25ml DEPC-treated H_2O
Add 25ml of DEPC-treated H_2O to 75ml absolute ethanol and mix well. Aliquot in RNAse-free tubes and store at room temperature.

Chloroform-Isoamyl Alcohol (49:1)
1ml isoamyl alcohol
49ml chloroform
Add 1ml of isoamyl alcohol to 49ml of chloroform in a in RNAse-free glass bottle. Cover bottle in foil and store at 4°C.

3M Sodium Acetate
408.3g sodium acetate.$3H_2O$
glacial acetic acid
1.0ml DEPC

Weigh and dissolve 408.3g of sodium acetate.$3H_2O$ in 700 ml of ddH_2O. Adjust the pH to 5.2 with glacial acetic acid and bring the final volume to 1000ml. Add 1ml of DEPC and incubate overnight at 37°C with agitation. Autoclave to sterilize and heat deactivate the DEPC. Aliquot in RNAse-free tubes and store at room temperature.

0.75M Sodium Citrate Ph7.0

110.29g of sodium citrate

Weigh 110.29g of sodium citrate and dissolve in 450ml of ddH_2O. Adjust the pH to 7.0 and bring the final volume to 500ml. Add 0.5ml of DEPC and incubate overnight at 37°C with agitation. Autoclave to sterilize and heat deactivate the DEPC. Aliquot in RNAse-free tubes and store at room temperature.

0.5% Sodium Lauryl Sarcosinate

5g sodium lauryl sarcosinate

Weigh out 5g of sodium lauryl sarcosinate and dissolve in 950ml of ddH_2O and bring the final volume to 1000ml. Add 1ml of DEPC and incubate overnight at 37°C with agitation. Autoclave to sterilize and heat deactivate the DEPC. Aliquot in RNAse-free tubes and store at room temperature.

RNA Denaturing Solution "Solution D"

250g guanidinium thiocyanate

17.6ml 0.75M sodium citrate pH7.0

26.4ml 0.5% (w/v) sodium lauryl sarcosinate

360µl 14.4M 2-β-mercaptoethanol

Weigh out and dissolve 250g of guanidinium thiocyanate in 293 ml of ddH_2O, 17.6 ml of 0.75M sodium citrate (pH 7.0) and 26.4 ml of 10% sodium lauryl sarcosinate. Dissolve using a heated magnetic stirrer set at 65°C. Cover the bottle in foil as this solution is sensitive to light. Solution D may be stored for months at 4°C but the guanidinium will precipitate out of solution, therefore pre-warm the solution before using it to dissolve the crystals. Add 360µl 14.4M 2-β-mercaptoethanol per 50 ml of Solution D just before use.

RNA Loading Buffer

14.0µl 12.3M Formaldehyde

50.0µl 100% Formamide

10.0µl 10 X MEA Buffer

1µl 10mg/ml Ethidium Bromide

Make up the buffer fresh each time. Add all reagents together and mix well. Add 7.4µl of loading buffer to 2.6µl of RNA. This recipe is enough for 10 samples

10 X MEA Electrophoresis Buffer

0.2 M MOPS, pH 7.0

6.67ml 3M sodium acetate, pH5.2

0.5M EDTA pH 8.0

Weigh out and dissolve 41.8 g of MOPS in 700 ml of sterile DEPC-treated H_2O. Adjust the pH to 7.0 with 1M NaOH. Add 6.67ml of DEPC-treated 3M sodium acetate and 20ml of DEPC-treated 0.5M EDTA (pH 8.0). Adjust the volume of the solution to 1000ml with DEPC-treated H_2O. Add 1ml DEPC and incubate overnight at 37^{o}C with shaking. Autoclave to heat deactivate the DEPC and to sterilize (autoclaving turns the solution yellow but does not affect the pH). Store at 4^{o}C wrapped in foil to protect from light.

A.6 Generation of pBi-IL-4Rα chimeras.

Find PDF file attached.

References

Aggarwal B. B. 2003. Signaling pathways of the TNF superfamily: a double-edged sword. *Nat Rev Immunol.* **3:**745-756.

Agger R., Crowley M.T. and Witmer-Pack M.D. 1990. The surface of dendritic cells in the mouse as studies with monclonmal antibodies. *Int. Rev. Immunol.* **6**:89-101.

Akashi K., Traver D., Miyamoto M. and Weissman I.L. 2000. A clonogenic common myeloid progenitor that gives rise to all myeloid lineages. *Nature*. **404:**193–197. [

Alber D. G., Killington R.A. and Stokes A. 2000. Solid matrix-antibodyantigen complexes incorporating equine herpesvirus 1 glycoproteins C and D elicit anti-viral immune responses in BALB/c (H-2K(d)) and C3H (H-2K(k)) mice. *Vaccine* **19:**895–901.

Alberts B., Johnson A.,Lewis J.,Raff M.,Roberts K. and Walters P. 2002. *Molecular Biology of the Cell; Fourth Edition.* New York and London: Garland Science. ISBN 0-8153-3218-1

Allen J.B., Wong H.L., Costa G.L., Bienkowski M.J. and Wahl S.M. 1993. Suppression of monocyte function and differential regulation of IL-1 and IL-1ra by IL-4 contribute to resolution of experimental arthritis. *J Immunol* **151:**4344–4351.

Aman M.J., Tayebi N., Oribi N.I. Puri R.K., Modi W.S. and Leonard W.J. 1996. cDNA cloning and characrteization of the human interleukin 13 receptor a chain. J. Biol Chem. 271:29265-29270.

Andrews A-L., Holloway J.W., Holgate S.T. and Davies D.E. 2006. IL-4 Receptor α is an important modulator of Il-4 and IL-13 receptor binding: Implications for the development of therapeutic targets. *J Immunology*. **176:**7456-7461.

Arai K., Lee F., Miyajima A., Miyatake S., Arai N. and Yokota T. 1990. Cytokines: Coordinators of Immune and Inflammatory Responses. *Annual Review of Biochemistry*. **59:**783-836

Ardavín C., Martínez del Hoyo G., Martín P., Anjuère F., Arias C.F., Marín A.R., Ruiz S., Parrillas V. and Hernández H. 2001. Origin and differentiation of dendritic cells. *Trends Immunol*.**22:**691-700.

Ardavín C. 2003. Origin, precursors and differentiation of mouse dendritic cells. *Nature*. **3:**1-9.

Arpinati M., Green C.L., Heimfeld S., Heuser J.E. and Anasetti C. 2000. Granulocyte-colony stimulating factor moblizes T helper 2-inducing dendritic cells. *Blood*. **95**:2484-2490.

Ausubel F., Brent., Kingston R.E., Moore D.D., Seidman., Smith J.A. and Struhl K. 1995. Short Protocols in Molecular Biology. Third Edition. Jhon Wiley & Sons Inc.

Bacchetta R., Gambineri E. and Roncarolo M. G. 2007. Role of regulatory T cells and FOXP3 in human diseases. *J. Allergy Clin. Immunol*. **120:**227–235.

Banchereau J. and Steinman R.M. 1998. Dendritic cells and the control of immunity. *Nature*. **392**:245-252.

Banchereau J., Briere F., Caux C., Davoust J., Lebecque S., Liu Y.J., Pulendran B. and Palucka K. 2000. Immunobiology of dendritic cells. *Annu. Rev. Immunol.* **18**, 767–811.

Baron U., Freundlieb S., Gossen M. and Bujard H. 1995. Co-regulation of two gene activities by tetracycline via a bidirectional promoter. *Nucleic Acids Res*. **17**:3605–3606.

Baron S., Peake R.C., James D.A., Susman M., Kennedy C.A., Singleton M.J.D. and Schuenke S. 1996. Medical Microbiology Fourth Edition. ISBN 0-9631172-1-1

Baron U., Gossen M. and Bujard H. 1997. Tetracycline-controlled transcription in eukaryotes: novel transactivators with graded transactivation potential.
Nucleic Acids Res. **25:**2723-2729.

Baron U. and Bujard H. 2000. Tet repressor-based system for regulated gene expression in eukaryotic cells: principles and advances. *Methods Enzymol.* **327:**401-421.

Belteki G., Haigh J., Kabacs N., Haigh K., Sison K., Costantini F., Whitsett J *et al*. 2005. Conditional and inducible transgene expression in mice through the combinatorial use of Cre-mediated recombination and tetracycline induction. *Nucleic Acids Res*. **33:**e51.

Bettelli E., Carrier Y., Gao W., Korn T., Strom T.B., Oukka M., Weiner H.L. and Kuchroo VK. 2006. Reciprocal developmental pathways for the generation of pathogenic effector TH17 and regulatory T cells. *Nature*.**441:**235-238.

Beutler B. 2004. Innate Immunity: an overview*. Mol Immunol*. **40:**845-859.

Björk I., Petersson B.A. and Sjöquist J. 1972. Some physicochemical properties of protein A from *Staphylococcus aureus*. *Eur.J.Biochem*. **29**: 579-584.

Bogdan C. 2000. The function of type I interferons in antimicrobial immunity. *Current Opinion in Immunology* **12:**419-424.

Borish L.C., Nelson H.S., Corren J., Bensch G., Busse W.W., Whitmore J.B. and Agosti J.M. 2001. Efficacy of soluble IL-4 receptor for the treatment of adults with asthma. *J Allergy Clin Immunol*. **107:**963-970.

Bradley A., Evans M., Kaufman M.H. and Robertson E. 1984. Formation of germ-line chimaeras from embryo-derived teratocarcinoma cell lines. *Nature.* **309:**255-256.

Brady L.J. 2005. Antibody-Mediated Immunomodulation: a Strategy To Improve Host Responses against Microbial Antigens. *Infection and Immunity*. **73:**671–678.

Broker T., Reidinger M. and Karjalainen K. 1997. Targeted Expression of major Histocompatibility Complex (MHC) Class II Molecules Demonstrates that Dendritic Cells Can Induce Negative but Positive Selection of Thymocytes In Vivo. *J Exp Med.* **185**:541-550.

Bronson S.K. and Smithies O. 1994. Altering mice by homologous recombination using embryonic stem cells. *J Biol Chem*. **269:**27155-27158.

Bullens D.M., Truyen E., Coteur L., Dilissen E., Hellings P.W., Dupont L.J. and Ceuppens J.L. 2006. IL-17 mRNA in sputum of asthmatic patients: linking T cell driven inflammation and granulocytic influx? *Respir Res.* **7:**135.

Camper S.A., Saunders T.L., Kendall S.K., Keri R.A., Seasholtz A.F., Gordon D.F., Birkmeier T.S., Keegan C.E., Karolyi I.J., Roller ML, et al. 1995. Implementing transgenic and embryonic stem cell technology to study gene expression, cell-cell interactions and gene function. *Biol Reprod*. **52:**246-257.

Caput D., Laurent P., Kaghad M., Lelias J.M., Lefort S., Vita N.and Ferrara P. 1996. Cloning and characterisatiohnof a specific interleukin (IL)-13 binding protein structurally related to the IL-5 receptor a chain. J.Biol Chem. 271:16921-16926.

Chang B.H., Liao W., Li L., Nakamuta M., Mack D. and Chan L. 1999. Liver-specific inactivation of the abetalipoproteinemia gene completely abrogates very low density lipoprotein/low density lipoprotein production in a viable conditional knockout mouse. *J Biol Chem*. **274:**6051-6055.

(a) Chiaramonte M.G., Schopf L.R., Neben T.Y., Cheever A.W., Donaldson D.D. and Wynn T.A. 1999. IL-13 is a key regulatory cytokine for Th2 cell-mediated pulmonary granuloma formation and IgE responses induced by Schistosoma mansoni eggs.
J Immunol. **162**:920-30.

(b) Chiaramonte M.G., Donaldson D.D., Cheever A.W. and Wynn T.A. 1999. An IL-13 inhibitor blocks the development of hepatic fibrosis during a T-helper type 2-dominated inflammatory response. *J Clin Invest*. **104**:777-85.

Chiaramonte M.G., Mentink-Kane M., Jacobson B.A., Cheever A.W., Whitters M.J., Goad M.E., Wong A., Collins M., Donaldson D.D., Grusby M.J. and Wynn T.A. 2003. Regulation and function of the interleukin 13 receptor alpha 2 during a T helper cell type 2-dominant immune reponse. *J Exp Med*. **197**:687-701.

Chomarat P. and Banchereau J. 1998. Interleukin-4 and interleukin-13: their similarities and discrepancies. *Int Rev Immunol*. **17**:1-52.

Clausen B.E., Burkhardt C., Reith W., Renkawitz R. and Förster I. 1999. Conditional gene targeting in macrophages and granulocytes using LysMcre mice. *Transgenic Res*. **8:**265-277.

Colotta F., Dower S.K., Sims J.E. and Mantovani A. 1994.The type II 'decoy' receptor: a novel regulatory pathway for interleukin 1*. Immunol Today*.**15:**562-566.

Corraliza I.M., Campo M.L., Soler G. and Modolell M. 1994. Determination of arginase activity in macrophages: a micromethod. *J Immunol Methods*. **174**:231-5.

Cote-Sierra J., Foucras G., Guo L., Chiodetti L., Young H.A., Hu-Li J., Zhu J. and William E. P. 2004. Interleukin 2 plays a central role in Th2 differentiation.101.
Cresswell P. 2005. Antigen processing and presentation. *Immunol Rev*. **207**:5-7.

Dabbagh K., Takeyama K., Lee H.M., Ueki I.F., Lausier J.A. and Nadel J.A. 1999. IL-4 induces mucin gene expression and goblet cell metaplasia in vitro and in vivo*. J Immunol. **162:**6233-6237.*

Dal Porto J.M., Gauld S.B., Merrell K.T., Mills D., Pugh-Bernard A. E and Cambier J. 2004. B cell antigen receptor signaling 101. *Mol Immunol*. **41:**599-613.

Dandolo L., Stewart C.L., Mattei M-G. and. Avner P.R. 1993. Inactivation of an X-linked transgene in murine extraembryonic and adult Tissues. *Development* **118:** 641-649

Darnell JE Jr. 1997. STATs and gene regulation. *Science*. 277:1630-1635

de Waal Malefyt R., Abrams J.S., Zurawski S.M., Lecron J.C., Mohan-Peterson S., Sanjanwala B., Bennett B., Silver J., de Vries J.E. and Yssel H. 1995. Differential regulation of IL-13 and IL-4 production by human CD8+ and CD4+ Th0, Th1 and Th2 T cell clones and EBV-transformed B cells. *Int Immunol*. **7:**1405-1416.

Deane J.A. and Furman D.A. 2004. Phosphoinositide 3-kinase: diverse roles in immune cell activation. *Annu Rev Immunol*. **22:**563-598.

Delespesse G., Sarfati M. and Peleman R. 1989. Influence of recombinant IL-4, IFN-alpha, and IFN-gamma on the production of human IgE-binding factor (soluble CD23).
J Immunol. **142**:134-138.

Ding, A.H., Nathan C.F. and Stuehr D.J. 1988. Release of reactive nitrogen intermediates and reactive oxygen intermediates from mouse peritoneal macrophages. Comparison of activating cytokines and evidence for independent production. *J Immunol* **141**:2407.

Doherty T.M., Kastelein R., Menon S., Andrade S. and Coffman R.L. 1993**.** Modulation of murine macrophage function by IL-13*. J Immunol*. 151:7151-7160.

Donaldson D.D., Whitters M.J., Fitz L.J., Neben T.Y., Finnerty H., Henderson S.L., O'Hara R.M. Jr., Beier D.R., Turner K.J., Wood C.R. and Collins M. 1998. The murine IL-13 receptor alpha 2: molecular cloning, characterization, and comparison with murine IL-13 receptor alpha 1. *J Immunol*. **161**:2317-2324.

Doucet C., Brouty-Boyé D., Pottin-Clemenceau C., Jasmin C, Canonica G.W. and Azzarone B. IL-4 and IL-13 specifically increase adhesion molecule and inflammatory cytokine expression in human lung fibroblasts. *Int Immunol.* **10:**1421-1433.

Doyle A.G., Herbein G., Montaner L.J., Minty A.J., Caput D., Ferrara P. and Gordon S. 1994. Interleukin-13 alters the activation state of murine macrophages in vitro: comparison with interleukin-4 and interferon-gamma. *Eur J Immunol*. **24:**1441-1445.

Dragon S., Rahman M.S., Yang J., Unruh H., Halayko A.J. and Gounni A.S. 2007. IL-17 enhances IL-1beta-mediated CXCL-8 release from human airway smooth muscle cells. *Am J Physiol Lung Cell Mol Physiol.* **292:**1023-1029.

Dymecki S.M. 1996. Flp recombinase promotes site-specific DNA recombination in embryonic stem cells and transgenic mice. *Proc Natl Acad Sci U S A*. **93:**6191-6196.

Economides A.N., Carpenter L.R., Rudge J.S., Wong V., Koehler-Stec E.M., Hartnett C., Pyles E.A., Xu X., Daly T.J., Young M.R., Fandl J.P., Lee F., Catver S., McNay J., Bailey K., Ramakanth S., Hutabarat R., Huang T.T., Radziejewski C., Yancopoulos G.D. and Stahl N. 2003. Cytokine traps: mulit-component, high-affinity blockers of cytokine action. *Nature Medicine.* **9**:47-52.

Essner R., Rhoades K., McBride W.H., Morton D.L. and Economou J.S. 1989.IL-4 down-regulates IL-1 and TNF gene expression in human monocytes.
J Immunol. **142:**3857-3861.

Evans M.J. and Kaufmann M.H.1981. Establishmnet in culture of pluripotential cells from mouse embryos. *Nature.* **292:**154-156.

Evel-Kabler K., Song X-T., Aldrich M., Huang X.F. and Chen S-Y. 2006. SOCS1 restricts dendritic cells' ability to break self tolerance and induce antitumor immunity by regulating IL-12 production and signaling. *The Journal of Clinical Investigation.* **116:**90-100.

Fallon P.G., Richardson E.J., Mckenzie G.J. and McKenzie A.N. 2000. Schistosome infection of transgenic mice defines distainct and contrasting pathogenioc roles for IL-4 and IL-13: IL-13 is a profibrotic agent. *J Immunol*. **164**:2585-2591.

Fanslow W.C., Clifford K., VandenBos T., Teel A., Armitage R.J. and Beckmann M.P.1990. A soluble form of the interleukin 4 receptor in biological fluids. *Cytokine***. 2:**398-401.

Fantuzzi G. and Faggioni R. 2000. Leptin in the regulation of immunity, inflammation, and hematopoiesis. *J Leukoc Biol***. 68:**437–446.

Feil R, Brocard J, Mascrez B, LeMeur M, Metzger D. and Chambon P. Ligand-activated site-specific recombination in mice. *Proc Natl Acad Sci U S A.* 93:10887-10890.

Feili-Hariri M., Falkner D.H. and Morel P.A. 2005. Polarization of naive T cells into Th1 or Th2 by distinct cytokine-driven murine dendritic cell populations: implications for immunotherapy. *J Leukoc. Biol* **78:**656–664.

Felgner P.L. and Ringold G.M. 1989.Cationic liposome-mediated transfection. *Nature*. **337**:387-8.

Feng N., Schnyder B., Vonderschmitt D.J., Ryffel B. and Lutz R.A. 1995. Characterization of interleukin-13 receptor in carcinoma cell lines and human blood cells and comparison with the interleukin-4 receptor. *J Recept Signal Transduct Res.***15:**931-949.

Fichtner-Feigl S., Strober W., Kawakami K., Puri R.K. and Kitani A. 2006. IL-13 signaling through the IL-13alpha2 receptor is involved in induction of TGF-beta1 production and fibrosis. *Nat Med*. **12:**99-106.

Finkelman F.D. and Morris S.C. 1999. Development of an assay to measure in vivo cytokine production in the mouse. *Int.Immunol*. **11**:1811-1818.

Finkelman F.D., Wynn T.A., Donaldson D.D. and Urban J.F. 1999. The role of IL-13 in helminth-induced inflammation and protective immunity against nematode infections. *Curr Opin Immunol*.**11**:420-6.

Fisher G.M., Iqball S. and Knight S.C. 1999. Gene expression during differentiation of human dendritic cells from cord blood CD34 stem cells. *Cytokine,* **11:**111–117.

Fitzsimons H.L., Bland R.J. and During M.J. 2002.Promoters and regulatory elements that improve adeno-associated virus transgene expression in the brain. *Methods*. **28**:227-36.

Fong L. and Engleman E.G. 2000. Dendritic cells in cancer immunotherapy. *Annu Rev Immunol.* **18:**245-273.

Fortschegger K., Wagner B., Voglauer R., Katinger H., Sibilia M. and Grillari J. 2007.Early embryonic lethality of mice lacking the essential protein SNEV.*Mol Cell Biol*. **27:**3123-3130.

Fukuda T. Fukushima Y. Numao T. Ando N. Arima M. Nakajima H. Sagara H. Adachi T. Motojima S. and Makino S. 1996. Role of interleukin-4 and vascular cell adhesion molecule-1 in selective eosinophil migration into the airways in allergic asthma. *Am J Respir Cell Mol Biol.* **14:**84-94.

Furlan R., Poliani P.L., Galbiati F *et al.* 1998. Central nervous system delivery of interleukin 4 by a nonreplicative herpes simplex type 1 viral vector ameliorates autoimmune demyelination. *Hum Gene Ther* **9:**2605–2617.

Furlan R., Poliani P.L., Marconi .PC *et al.* 2001. Central nervous system gene therapy with interleukin-4 inhibits progression of ongoing relapsingremitting autoimmune encephalomyelitis in Biozzi AB/H mice. *Gene Ther* **8:**13–9.

Galli S.J,. Maurer M. and Lantz C.S. 1999. Mast cells as sentinels of innate immunity. *Curr Opin Immunol.* **11:**53–59.

Gessner A., Schröppel K., Will A., Enssle K.H., Lauffer L. and Röllinghoff M. 1994. Recombinant soluble interleukin-4 (IL-4) receptor acts as an antagonist of IL-4 in murine cutaneous Leishmaniasis. *Infect Immun*. **62:**4112-4117.

Gleich G.J., Kita H. and Adolphson C.R. 1995. Eosinophils. In: *Samters Immunologic Diseases*, edn 5. 205–245.

Goldenberg M.M. 1999. Etanercept, a novel drug for the treatment of patients with severe, active rheumatoid arthritis. *Clin Ther*. **21**:75-87.

Gordon J.W., Scangos G.A., Plotkin D.J., Barbosa J.A. and Ruddle F.H. 1980. Genetic transformation of mouse embryos by microinjection of purified DNA. *Proc Natl Acad Sci U S A.* **77:**7380-7384.

Gordon S. 1986. Biology of the macrophage. *J. Cell Sci. Suppl.***4:**267–286.

Gossen M. and Bujard H. 1992. Tight control of gene expression in mammalian cells by tetracycline-responsive promoters. *Proc. Natl. Acad. Sci. USA* **89**:5547–5551.

Gossen M., Freundlieb S., Bender G., Muller G., Hillen W. and Bujard H. 1995. Transcriptional activation by tetracyclines in mammalian cells. *Science.* **268:**1766–1769.

Gossen M. and Bujard H. 2002. Studying gene function in eukaryotes by conditional gene inactivation. *Annu Rev. Genet*. **36:**153-173.

Green S.J., Crawford R.M., Hockmeyer J.T., Meltzer M.S. and Nacy C.A. 1990. *Leishmania major* amastigotes initiate the L-arginine-dependent killing mechanism in IFN-gamma-stimulated macrophages by induction of tumor necrosis factor-alpha. *J Immunol.* **145**:4290-4297.

Grunewald S.M., Kunzmanaa S., Scharr B., Ezernieks J., Sebald W. and Duschl A. 1997. A murine Interleukin-4 antagonistic mutant protein completely inhibits interleukin-4-induced cell proliferation, differentiation, and signal transduction. *JBC*. **272**:1480-1483.

Grünig G., Warnock M., Wakil A.E., Venkayya R., Brombacher F., Rennick D.M., Sheppard D., Mohrs M., Donaldson D.D., Locksley R.M. and Corry D.B. 1998. Requirement for IL-13 independently of IL-4 in experimental asthma. *Science*. **282**:2261-2263.

Gu H., Zou Y.R. and Rajewsky K. 1993. Independent control of immunoglobulin switch recombination at individual switch regions evidenced through Cre-loxP-mediated gene targeting. *Cell*. **73**:1155-1164.

Gu H., Marth J.D., Orban P.C., Mossmann H. and Rajewsky K. 1994. Deletion of a DNA polymerase beta gene segment in T cells using cell type-specific gene targeting. *Science.* **265:**103-106.

Guermonprez P., Fayolle C., Rojas M.J., Rescigno M., Ladant D. and Leclerc C. 2002. In vivo receptor-mediated delivery of a recombinant invasive bacterial toxoid to CD11c + CD8 alpha -CD11bhigh dendritic cells*. Eur J Immunol*. **32:**3071-3081.

Guermonprez P, Valladeau J, Zitvogel L, Théry C, Amigorena S. "Antigen presentation and T cell stimulation by dendritic cells". *Annu Rev Immunol* 20: 621-667.

Guidi C.J., Veal T.M., Jones S.N. and Imbalzano A.N. 2004. Transcriptional compensation for loss of an allele of the Ini1 tumor suppressor. *J Biol Chem*. **279:**4180-4185.

Guo J., Apiou F., Mellerin M.P., Lebeau B., Jacques Y. and Minvielle S. 1997. Chromosome mapping and expression of the human interleukin-13 receptor. *Genomics*. **15:**141-145.

Haas H., Falcone F.H, Holland M.J., Schramm G., Haisch G., Gibbs B.F., Bufe A. and Schlaak M. 1999. Early Interleukin-4: Its Role in the Switch towards a Th2 Response and IgE-Mediated Allergy. *Int Arch Allergy Immunol.* **119:**86-94

Hasan M.T., Schönig K., Berger S., Graewe W. and Bujard H. 2001. Long-term, noninvasive imaging of regulated gene expression in living mice. *Genesis.* **29:**116-122.

Hilton D.J., Zhang J.G., Metcalf D., Alexander W.S., Nicola N.A. and Willson T.A. 1996. Cloning and characterization of a binding subunit of the interleukin 13 receptor that is also a component of the interleukin 4 receptor. *Proc Natl Acad Sci U S A*. **93:**497-501.

Hofer T., Muehlinghaus G., Moser K., Yoshida T., Hebel K., Hause A., Hoyer B., Dorner T., Manz R.A., Hiepe F and Radbruch A. 2006. Adaptation of humoral memory. *Immunol Rev.* **211:**295-302.

Honma K., Udono H., Kohno T., Yamamoto K., Ogawa A., Takemori T., Kumatori A., Suzuki S., Matsuyama T. and Yui K. 2006. Interferon regulatory factor 4 negatively regulates the production of proinflammatory cytokines by macrophages in response to LPS. *PNAS.* **102:**18001-18008.

Horohov D.W., Crim J.A., Smith P.L. and Siegel J.P. 1988. IL-4 (B cell-stimulatory factor 1) regulates multiple aspects of influenza virus-specific cell-mediated immunity.*J Immunol.* **141:**4217-4223.

Horsnell W.G.C., Cutler A.J., Hoving C.J., Mearns H., Myburgh E., Arendse B., Finkelman F.D., Owens G.K., Erle D. and Brombacher F. 2007. Delayed goblet cell hyperplasia, acetylcholine receptor expression, and worm expulsion in SMC-specific IL-4Ra–deficient mice. *PLoS Pathog* **3**: 0046-0053.

Howard M., Farrar J., Hilfiker M., Johnson B., Takatsu K., Hamaoka T. and Paul W.E. 1982. Identification of a T cell-derived b cell growth factor distinct from interleukin 2. *J Exp Med*. **155:**914-23.

Hsieh C.S., Macatonia S.E., Tripp C.S., Wolf S.F., O'Garra A. and Murphy K.M. 1993. Development of TH1 CD4+ T cells through IL-12 produced by Listeria-induced macrophages. *Science.* **260:**547-549.

Hughes S., Boissonnas A., Amigorena S. and Fetler L. 2006. The dynamics of dendritic cell–T cell interactions in priming and tolerance. *Current Opinion in Immunology*. **18:**491-495

Igarashi H., Gregory S.C., Yokota T., Sakaguchi N. and Kincade P.W. 2002. Transcripition from the RAG1 locus marks the earliest lymphocyte progenitors in bone marrow. *Immunity.* **17:**117–130.

Ihle J.N. 1995. The Janus protein tyrosine kinases in hematopoietic cytokine signaling. *Adv. Immunol.* **7:**247-254.

Ing R., Su Z., Scott M.E. and Koski K.G. 2000. Suppressed T helper 2 immunity and prolonged survival of a nematode parasite in protein-malnourished mice. *Proc Natl Acad Sci U S A* .**97:**7078–7083.

Inoue H., Nojima H. and Okayama H. 1990. High efficiency transformation of *Escherichia coli* with plasmids. *Gene*. **96**:23-8.

Isola L.M. and Gordon J.W. 1991.Transgenic animals: a new era in developmental biology and medicine. *Biotechnology.* **16:**3-20.

Ivashkiv L.B. 1995. Cytokines and STATs: How can signals achieve specificity? *Immunity* **3:**1-4.

Izuhara K. and Harada N. 1996. Interleukin-4 activates two distinct pathways of phosphatidylinositol-3 kinase in the same cells. *Biochem Biophys Res Commun*. **13:**624-9.

Janeway C., Travers P., Walport M. and Shlomchik M. 2001. *Immunobiology; Fifth Edition*. New York and London: Garland Science. ISBN 0-8153-4101-6.

Jonuleit H., Schmitt E., Steinbrink K. and Enk A.H. 2001. Dendritic cells as a tool to induce anergic and regulatory T cells. *Trends Immunol*. **22:**394-400.

Kalderon D., Roberts B.L., Richardson W.D. and Smith A.E. 1984. A short amino acid sequence able to specify nuclear location. *Cell*. **39**: 499-509.

Kammer W., Lischke A., Moriggl R., Groner B., Ziemiecki A., Gurniak C.B., Berg L.J. and Friedrich K.1996. Homodimerization of interleukin-4 receptor alpha chain can induce intracellular signaling. *J Biol Chem*.. **271**:23634-23637.

Kansas GS. 1996. Selectins and their ligands: current concepts and controversies. *Blood* **88:**3259-3287.

Kapetanovic R and Cavaillon J.M. 2007. Early events in innate immunity in the recognition of microbial pathogens. *Expert Opin Biol Ther.* **7:**907-918.

Kaplan M.H., Sun Y.L., Hoey T. and Grusby M.J. 1996. Impaired IL-12 responses and enhanced development of Th2 cells in Stat4-deficient mice. *Nature*. **382**:174-177.

Katona I.M., Urban J.F., Jr. and Finkelman F.D. 1998. The role of L3T4+ and Lyt-2+ T cells in the Ige response and immunity to *Nippostrongylus Brasiliensis. J Immunol.* **140:**3206-3211.

Kellendonk C., Tronche F., Monaghan A.P., Angrand P.O., Stewart F. and Schütz G. Regulation of Cre recombinase activity by the synthetic steroid RU 486. *Nucleic Acids Res*. **24:**1404-1411.

Keyvani K., Baur I. and Paulus W. 1999.Tetracycline-controlled expression but not toxicity of an attenuated diphtheria toxin mutant. *Life Sci.* **64:**1719-1724.

Kistner A., Gossen M., Zimmermann F., Jerecic J., Ullmer C., Lübbert H. and Bujard H. 1996. Doxycycline-mediated quantitative and tissue-specific control of gene expression in transgenic mice. *Proc Natl Acad Sci U S A*. **93:**10933-10938.

Kopf M., Brombacher F., Köhler G., Kienzle G., Widmann K.H., Lefrang K., Humborg C., Ledermann B. and Solbach W. 1996. IL-4-deficient Balb/c mice resist infection with Leishmania major. *J Exp Med*. **184:**1127-1136.

Kondo M., Takeshita T., Ishii N., Nakamura M., Watanabe S., Arai K. and Sugamura K. 1993. Sharing of the interleukin-2 (IL-2) receptor gamma chain between receptors for IL-2 and IL-4. *Science*. **262**:1874-1877.

Kondo M., Weissman I.L. and Akashi K. 1997. Identification of clonogenic common lymphoid progenitors in mouse bone marrow. *Cell.* **91:**661–672.

Kondo M., Wagers A.J., Manz M.G., Prohaska S.S., Scherer D.C., Beilhack G.F., Shizuru J.A. and Weissman I.L. 2003. Biology of hematopoietic stem cells and progenitors: implications for clinical application*. Annu. Rev. Immunol.* **21:**759–806.

Koski K.G. and Scott M.E. 2001. Gastrointestinal nematodes, nutrition and immunity: breaking the negative spiral. *Annu Rev Nutr.* **21:**297–321.

Kouro T., Kumar V. and Kincade P.W. 2002. Relationships between early B-and NK-lineage lymphocyte precursors in bone marrow. *Blood.* **100:**3672–3680.

Kouskoff V., Fehling H.J., Lemeur M., Benoist C. and Mathis D. 1993. A vector driving the expression of foreign cDNAs in the MHC class II-positive cells of transgenic mice. *J. Immunol. Methods*. **166**:287-291.

Kozak M. 1984. *Nature*. **308**:241-246.

Kozak M. 1986. Point mutations define a sequence flanking the AUG initiator codon that modulates translation by eukaryotic ribosomes. *Cell*. **44**:283-92.

Kozak, M. 1987. An analysis of 5'-noncoding sequences from 699 vertebrate messenger RNAs. *Nucleic Acids Res*. **15**:8125–8148.

Krueger C., Danke C., Pfleiderer K., Schuh W., Jäck H.M., Lochner S., Gmeiner P., Hillen W. and Berens C. 2006. A gene regulation system with four distinct expression levels. *J Gene Med.* **8:**1037-1047.

Kubo M., Ransom J., Webb D., Hashimoto Y., Tada T. and Nakayama T. 1997. T-cell subset-specific expression of the IL-4 gene is regulated by a silencer element and STAT6.*EMBO J*. **16:**4007-4020.

Kunkl A. and Klaus G.G**.** 1981. The generation of memory cells. IV.Immunization with antigen-antibody complexes accelerates the developmentof B-memory cells, the formation of germinal centres and the maturationof antibody affinity in the secondary response. *Immunology* **43:**371–378.

Kwan K-M. 2002. Conditional alleles in mice: practical considerations for tissue-specific knockouts. *Genesis.* **32:**49-62.

Laemmli U.K. 1970. Clleavage of structural proteins during assembly of the head of bacteriophage T7. *Nature*. **227**:680-685.

Lai S.Y., Molden J., Liu K.D., Puck J.M., White M.D. and Goldsmith M.A. 1996. Interleukin-4-specific signal transduction events are driven by homotypic interactions of the interleukin-4 receptor alpha subunit. *EMBO J*. **15:**4506-4514.

Lakso M., Sauer B., Mosinger B. J.r, Lee E.J., Manning R.W., Yu S.H., Mulder K.L. and Westphal H. 1992. Targeted oncogene activation by site-specific recombination in transgenic mice. *Proc Natl Acad Sci U S A.* **89:**6232-6236.

Lanzavecchia A. and Sallusto F. 2004. Lead and follow: the dance of the dendritic cell and T cell. *Nature Immunology*. **5**:1201-1202.

Larche M. 2007. Regulatory T cells in allergy and asthma.*Chest* **132:**1007–1014.

Lavon I., Goldberg I., Amit S., Landsman L., Jung S., Tsuberi B.Z., Barshack I., Kopolovic J., Galun E., Bujard H. and Ben-Neriah Y. 2000.High susceptibility to bacterial infection, but no liver dysfunction, in mice compromised for hepatocyte NF-kappaB activation. *Nat Med.* **6:**573-577.

Le B. H. *et al.* 2007.Control of allergic reactions in mice by an active anti-murine IL-4 immunization. *Vaccine* **25:**7206–7216.

Le Gros G., Ben-Sasson S.Z., Seder R., Finkelman F.D. and Paul W.E. 1990. Generation of interleukin 4 (IL-4)-producing cells in vivo and in vitro: IL-2 and IL-4 are required for in vitro generation of IL-4-producing cells. *J Exp Med*. **172:**921-929.

Leary J.J., Brigati D.J. and Ward D.C. 1983. Rapid and sensitive colorimetric method for visualizing biotin-labelled DNA probes hybridized to DNA or RNA immobilized on nitrocellulose: Bio-blots*. Proc Natl Acad Sci U S A*. **80**:4045-9.

Lebman D.A. and Coffman R.L. 1988. Interleukin 4 causes isotype switching to IgE in T cell-stimulated clonal B cell cultures. J Exp Med. 168:853-62.

Ledermann B. 2000. Embryonic stem cells andgene targeting. *Experimental Physiology.* **85:**603-613.

Leeto M., Herbert D. R., Marillier R., Schwegmann A., Fick L.and Brombacher F. 2006. TH1-Dominant Granulomatous Pathology Does Not Inhibit Fibrosis or Cause Lethality during Murine Shistosomiasis.*Am J Pathol.* **169:**1701–1712.

Lefrançois L., Olson S. and Masopust D. 1999. A Critical Role for CD40–CD40 Ligand Interactions in Amplification of the Mucosal CD8 T Cell Response . *J Exp Med.* **190:**1275-1284.

Lewandoski M. 2001. Conditional control of gene expression in the mouse. *Nat Rev Genet*. **2:**743-755.

Lin J.X., Migone T.S., Tsang M., Friedmann M., Weatherbee J.A., Zhou L., Yamauchi A., Bloom E.T., Mietz J. and John S. 1995. The role of shared receptor motifs and common Stat proteins in the generation of cytokine pleiotropy and redundancy by IL-2, IL-4, IL-7, IL-13, and IL-15. *Immunity*. **2**:331-339.

Liu Y., Kanzler H., Soumelis V. and Gilliet M. 2001. Dendritic cell lineage, plasticity and cross-regulation. *Nature Immunology*. **2**:585-589.

Lobe C.G. and Nagy A. 1998. Conditional genome alteration in mice. *Bioessays.* **20:**200-208.

Lowenthal J.W., Castle B.E., Christiansen J., Schreurs J., Rennick D., Arai N., Hoy P., Takebe Y. and Howard M. 1988. Expression of high affinity receptors for murine interleukin 4 (BSF-1) on hemopoietic and nonhemopoietic cells. *J Immunol.* **140:**456-464.

Lumeng C.N., Bodzin J.L., Deyoung S.M. and Saltiel A.R. 2006. Increased inflammatory properties of adipose tissue macrophages recruited during diet induced obesity. *Diabetes*

Lumeng C.N., Bodzin J.L. and Saltiel A.R. 2007. Obesity induces a phenotypic switch in adipose tissuemacrophage polarization. *J Clin Invest.* **117:**175–84.

Luther S.A. and Cyster J.G. 2001. Chemokines as regulators of T cell differentiation. *Nat Immunol.* **2:**102-107.

Madden K.B., Urban J.F. Jr., Ziltener H.J., Schrader J.W., Finkelman F.D. and Katona I.M. 1991. Antibodies to IL-13and IL-4 suppress helminth-induced intestinal mastocytosis. *J Immunol.* **147**:1387-1391.

Maizels R.M and Yazdanbakhsh M. 2003. Immune regulation by helminth parasites: cellular and molecular mechanisms. *Nature Reviews Immunol*. **3:**733-744.

Majeau G.R., Meier W., Jimmo B., Kioussis D. and Hochman P.S. 1994. Mechanism of Lymphocyte Function-associated Molecule 3-Ig fusion proteins inhibition of T cell responses. *J Immunolgy*. **152**:2753-2767.

Malabarba M.G, Rui H., Deutsch H.H, Chung J., Kalthoff F.S., Farrar W.L. and Kirken R.A. 1996. Interleukin-13 is a potent activator of JAK3 and STAT6 in cells expressing interleukin-2 receptor-gamma and interleukin-4 receptor-alpha. *Biochem J.* **319:**865–872.

Malatesta P., Hack M.A., Hartfuss E., Kettenmann H., Klinkert W., Kirchhoff F. and Götz M. 2003. Neuronal or glial progeny: regional differences in radial glia fate. *Neuron.* **37:**751-764.

Maliszewski C.R., Sato T.A., Vanden Bos T., Waugh S., Dower S.K., Slack J., Beckmann P. and Grabstein K.H. 1990. Cytokine Receptors and B cell functions. *J Immunol.* **144**: 3028-3033.

Manetti R., Parronchi P., Giudizi M.G., Piccinni M.P., Maggi E., Trinchieri G. and Romagnani S. 1993. Natural killer cell stimulatory factor (interleukin 12 [IL-12]) induces T helper type 1 (Th1)-specific immune responses and inhibits the development of IL-4-producing Th cells. *J Exp Med*. **177**:1199-1204.

Mansour S.L., Thomas K.R. and Capecchi M.R. 1988. Disruption of the proto-oncogene int-2 in mouse embryo-derived stem cells: a general strategy for targeting mutations to non-selectable genes. *Nature*. **336:**348-352.

Mao J., Barrow J., McMahon J., Vaughan J. and McMahon A.P. 2005. An ES cell system for rapid, spatial and temporal analysis of gene function *in vitro* and *in vivo*. *Nucleic Acids Res*. **33:**e155.

Maroof A., Penny M., Kingston R., Murray C., Islam S., Bedford P.A. and Knight S.C. 2005. Interleukin-4 can induce interleukin-4 production in dendritic cells. *Immunology*, **117:** 271–279.

Martin G.R. 1981. Isolation of a pluripotent cell line from early mouse embryos cultured in medium conditioned by teratocarcinoma stem cells. *Proc Natl Acad Sci U S A.* **78:**7634-7638.

Martino G., Furlan R., Comi G. and Adorini L. 2001. The ependymal route to the CNS: an emerging gene-therapy approach for MS. *Trends Immunol*. **22:**483–490.

Matarese G. and La Cava A. 2004. The intricate interface between immune system and metabolism. *Trends Immunol*. **25:**193–200.

Matthews D.J, Emson C.L, McKenzie G.J, Jolin H.E., Blackwell J.M. and McKenzie A.N. 2000. IL-13 is a susceptibility factor for Leishmania major infection*. J Immunol*. **64:**1458-1462.

Mayer G. 2006. *Immunology***.** Chapter One: Innate (non-specific) Immunity. Microbiology and Immunology On-Line Textbook. USC School of Medicine.
McGuirk P. and Mills K.H. 2002. Pathogen-specific regulatory T cells provoke a shift in the Th1/Th2 paradigm in immunity to infectious diseases. *Trends Immunol*. **23:** 450-455.

McKenzie A.N., Culpepper J.A., de Waal Malefyt R., Brière F., Punnonen J., Aversa G., Sato A., Dang W., Cocks B.G., Menon S., et al. 1993. Interleukin 13, a T-cell-derived cytokine that regulates human monocyte and B-cell function. *Proc Natl Acad Sci U S A.***90:** 3735-3739.

Metcalfe D.D., Baram D. and Mekori Y.A. 1997. Mast cells. *Physiol Rev* **77:**1033–1079.

Metlay J.P., Witmer-Pack M.D., Agger R., Crowley M.T., Lawless D. and Steinman R.M. 1990. The distinct leukocyte integrins of mouse spleen dendritic cells as identified with new hamster monoclonal antibodies. *J.Exp.Med.* **171**:1753-1771.

Minvielle-Sebastia L. and Keller W. 1999**.** mRNA polyadenylation and its coupling to other RNA processing reactions and to transcription. *Current Opinion in Cell Biology*. **11**:352-357.

Miossec C., Genevee C., Hercend T. and Jitsukawa S. 1992. CD3.TCR1, a human CD3 epitope expressed on viable gamma/delta lymphocytes exclusively. *Cell Immunol*. **140:**173-183.

Miyazaki T., Kawahara A. Fujii H., Nakagawa Y., Minami Y., Liu Z.J., Oishi I., Silvennoinen O., Witthuhn B.A., and Ihle J.N. 1994. Functional activation of Jak1 and Jak3 by selective association with IL-2 receptor subunits.*Science.* 266:1045-1047.

Mohrs M., Ledermann B., Kohler G., Dorfmuller A., Gessner A. and Brombacher F. 1999. Differences Between IL-4- and IL-4 Receptor a-Deficient Mice in Chronic Leishmaniasis Reveal a Protective Role for IL-13 Receptor Signaling1. *The Journal of Immunology,* **162:** 7302–7308.

Monroe J.G., Haldar S., Prystowsky M.B. and Lammie P. 1988. Lymphokine regulation of inflammatory processes: interleukin-4 stimulates fibroblast proliferation. *Clin Immunol Immunopathol.* **49:**292-298.

Moreadith R.W. and Radford N.B. 1997. Gene targeting in embryonic stem cells: the new physiology and metabolism. *J Mol Med*. **75:** 208-216.

Morgan D.A., Ruscetti F.W. and Gallo R. 1976. Selective in vitro growth of T lymphocytes from normal human bone marrows. *Science.* **193:**1007–1008.

Morita Y., Yang J., Gupta R., Shimizu K., Shelden E.A., Endres J., Mulé J.J., McDonaghK.T. and Fox D.A. 2001. Dendritic cells genetically engineered to express IL-4 inhibit murine collagen-induced arthritis. *J. Clin. Invest.* **107**: 1275-1284

Moser M. and Murphy K.M. 2000. Dendritic cell regulation of TH1–TH2 development. *Nat. Immunol.* **1:** 199–205.

Moser R., Fehr J. and Bruijnzeel P.L. 1992. IL-4 controls the selective endothelium-driven transmigration of eosinophils from allergic individuals*. J Immunol*. **149:**1432-1438.

Mosley B., Beckmann M.P., March C.J., Idzerda R.L., Gimpel S.D., VandenBos T., Friend D., Alpert A., Anderson D. and Jackson J. 1989. The murine interleukin-4 receptor: molecular cloning and characterization of secreted and membrane bound forms. *Cell.* **59:**335-348.

Moulson C.L., Lin M-H., White J.M**.**, Newberry E.P., Davidson N.O. and Miner J.H. 2007**.** Keratinocyte-specific Expression of Fatty Acid Transport Protein 4 Rescues the Wrinkle-free Phenotype in *Slc27a4/Fatp4* Mutant Mice**.** *J. Biol. Chem.* **282:** 15912-15920.

Mueller R., Krahl T. and Sarvetnick N.1996. Pancreatic expression of interleukin-4 abrogates insulitis and autoimmune diabetes in nonobese diabetic (NOD) mice. *J Exp Med* **184:**1093–1099.

Muller U. 1999. Ten years of gen tarhgeting: targeted mouse mutants, from vector design to phenotype analysis. *Mechanisms of Development*. **82:**3-21.

Murata T., Noguchi P.D. and Puri R.K. 1996. IL-13 induces phosphorylation and activation of JAK2 Janus kinase in human colon carcinoma cell lines: similarities between IL-4 and IL-13 signaling. *J Immunol*. **156:**2972-2978.

Murata T., Husain S.R., Mohri H. and Puri R.K.1998. Two different IL-13 receptor chains are expressed in normal human skin fibroblasts, and IL-4 and IL-13 mediate signal transduction through a common pathway. *Int Immunol*. **10:**1103-1110.

Murphy K.M., Ouyang W. and Farrar J.D. 2000. Signaling and transcription in T helper development. *Annu Rev Immunol*. **18:**451-494.

Nagy A. 2000. Cre recombinase: the universal reagent for genome tailoring. *Genesis.* 26:99-109.

Nakae S., Asano M., Horai R., Sakaguchi N. and Iwakura Y. 2001. IL-1 Enhances T Cell-Dependent Antibody Production Through Induction of CD40 Ligand and OX40 on T Cells. *The Journal of Immunology*. **167:**90-97.

Nelms K., Keegan A.D., Zamorano J., Ryan J.J. and Paul W.E. 1999.The IL-4 receptor: signaling mechanisms and biologic functions. *Annu Rev Immunol*. **17:**701-738. 7

Neugebauer K.M. 2002. On the importance of being co-transcriptional. *Journal of Cell Science*. **115**:3865-3871.

Noelle R, Krammer PH, Ohara J, Uhr JW, Vitetta ES. 1984. Increased expression of Ia antigens on resting B cells: an additional role for B-cell growth factor. Proc Natl Acad Sci U S A. 81:6149-6153.

O'Garra A. 1998. Cytokines induce the development of functionally heterogeneous T helper cell subsets. *Immunity.* **8:**275-283.

O'Garra A., Vieira P.L., Vieira P. and Goldfeld A.E. 2004. IL-10-producing and naturally occurring CD4+ Tregs: limiting collateral damage. *J Clin Invest.* **114:**1372-1378.

O'hara J. and Paul W.E. 1988. Up-regulation of interleukin 4/B-cell stimulatory factor 1 receptor expression. *Proc Natl Acad Sci U S A.* **85:**8221-8225.

O'Shea J.J., Ma A. and Lipsky P. 2002. Cytokines and autoimmunity. *Nat Rev Immunol.* **2**:37-45.

Obiri N.I., Leland P., Murata T., Debinski W. and Puri R.K. 1997. The IL-13 receptor structure differs on various cell types and may share more than one component with IL-4 receptor*. J Immunol*. **158:**756-764.

Orban P.C., Chui D.and Marth J.D. 1992. Tissue- and site-specific DNA recombination in transgenic mice. *Proc Natl Acad Sci U S A.* 89:6861-6865.

Ouyang W., Löhning M., Gao Z., Assenmacher M., Ranganath S., Radbruch A. and Murphy K.M.2000. Stat6-independent GATA-3 autoactivation directs IL-4-independent Th2 development and commitment.*Immunity*.**12:**27-37.

Palmiter R.D., Brinster R.L., Hammer R.E., Trumbauer M.E., Rosenfeld M.G., Birnberg N.C. and Evans R.M. 1982. Dramatic growth of mice that develop from eggs microinjected with metallothionein-growth hormone fusion genes. *Nature.* **300:**611-615.

Palucka K.A. and Banchereau J. 1999. Dendritic cells: A link between innate and adaptive immunity. *J. Clin. Immunol*. **19**:12-25.

Paul W.E. and Seder R.A. 1994. Lymphocyte responses and cytokines. *Cell.* **76:** 241-251

Pène J, Rousset F, Brière F, Chrétien I, Bonnefoy JY, Spits H, Yokota T, Arai N, Arai K, Banchereau J, et al.1988. IgE production by normal human lymphocytes is induced by interleukin 4 and suppressed by interferons gamma and alpha and prostaglandin E2. Proc Natl Acad Sci U S A. 85:6880-4.

Peng Y., Martin D.A., Kenkel J., Zhang K., Ogden C.A. and Elkon K.B. 2007. Innate and adaptive immune response to apoptotic cells. *J Autoimmun*. **29:**303-309.

Pestka S., Krause C.D. and Walter M.R. 2004. Interferons, interferon-like cytokines, and their receptors. *Immunol Rev.* **202:**8-32.

Radwanska M., Cutler A.J., Hoving J.C., Magez S., Holscher C., Bohms A., Arendse B., Kirsch R., Hunig T., Alexander J., Kaye P. and Brombacher F. 2007. Deletion of IL-4Ra on CD4 T Cells Renders BALB/c Mice Resistant to Leishmania major Infection. *PLoS Pathog* **3:**0619-0629.

Raghavan M. and Bjorkman P.J. 1996. Fc receptors and their interactions with immunoglobulins. *Annu Rev Cell Dev Biol*. **12:**181-220.

Randall R. E. and Young D.F. 1988. Humoral and cytotoxic T cell immune responses to internal and external structural proteins of simian virus 5 induced by immunization with solid matrix-antibody-antigen complexes. *J. Gen. Virol*. **69:**2505–2516.

Randall R. E., Young D.F. and Southern J.A**.** 1988. Immunization with solid matrix-antibody-antigen complexes containing surface or internal virus structural proteins protects mice from infection with the paramyxovirus, simian virus 5. *J. Gen. Virol*. **69:**2517–2526.

Rapoport M.J., Jaramillo A., Zipris D *et al.* 1993.Interleukin 4 reverses T cell proliferative unresponsiveness and prevents the onset of diabetes in non obese diabetic mice. *J Exp Med* **178:**87–99.

Reiner S.L. and Locksley R.M. 1993. Cytokines in the differentiation of Th1/Th2 CD4+ subsets in leishmaniasis. *J Cell Biochem.* **53:**323-328.

Reis e Sousa C., Hieny S., Scharton-Kersten T. and Jankovic D. Et al 1997. "In vivo microbial stimulation induces rapid CD40 ligand-independent production of interleukin 12 by dendritic cells and their redistribution to T cell areas". *J. Exp. Med.* **186:**1819-1829.

Rickert R.C., Roes J. and Rajewsky K. 1997. B lymphocyte-specific, Cre-mediated mutagenesis in mice. *Nucleic Acids Res*. **25:**1317-1318.

Rudolph M.G., Stanfield R.L. and Wilson I.A. 2006. How TRCs bind MHCs, peptides, and coreceptors. *Annu Rev Immunol*. **24:** 419-466.

Russell S.M., Keegan A.D., Harada N., Nakamura Y., Noguchi M,. Leland P., Friedmann M.C., Miyajima A., Puri R.K., Paul W.E., et al. 1993. Interleukin-2 receptor gamma chain: a functional component of the interleukin-4 receptor*. Science.* **262:**1880-1883

Ryding A.D.S., Sharp M.G.F. and Mullins J.J. 2001. Conditional transgenic technologies. *Journal of Endocriniology*. **171:**1-14.

Sakaguchi S., Sakaguchi N., Asano M., Itoh M and Toda M. 1995. Immunologic self-tolerance maintained by activated T cells expressing IL-2 receptor alpha-chains (CD25). Breakdown of a single mechanism of self-tolerance causes various autoimmune diseases. *J Immunol.* **155:**1151-1164.

Sambrook J. and Russell D.W. 2001. *Molecular cloning: a laboratory manual*. Cold Spring Harbor Laboratory Press, Cold Spring Harbor, N.Y.

Sato T.A., Widmer M.B., Finkelman F.D., Madani H., Jacobs C.A., Grabstein K.H. and Maliszewski C.R. 1993. Recombinant soluble murine IL-4 receptor can inhibit or enhance IgE responses in vivo. *J Immunol*. **150:**2717-2723.

Sauer B. 1998. Inducible Gene Targeting in Mice Using the Cre/lox System. *Methods.* **14:** 381-392.

Savill J., I. Dransfi eld, C. Gregory. and Haslett C. 2002. A blast from the past: clearance of apoptotic cells regulates immune responses.*Nat. Rev. Immunol.* **2:**965–975.

Savina A and Amigorena S. 2007. Phagocytosis and antigen presentation in dendritic cells. *Immunol Rev*. **219:**143-156.

Schmidt E.V., Christoph G., Zeller R. And Leder P. 1989. The Cytomegalovirus Enhancer: a Pan-Active Control Element in Transgenic Mice. *Molecular and Cellular Biology*. **10**:4406-4411.

Schulte T., Kurrle R., Röllinghoff M. and Gessner A. 1997. Molecular characterization and functional analysis of murine interleukin 4 receptor allotypes. *J Exp Med*. **186**(9):1419-29.

Scott P., Natovitz P., Coffman R.L., Pearce E. and Sher A. 1988. Immunoregulation of cutaneous leishmaniasis. T cell lines that transfer protective immunity or exacerbation belong to different T helper subsets and respond to distinct parasite antigens. *J Exp Med.* **168:**1675-1684.

Seder R.A., Gazzinelli R., Sher A and Paul W.E. 1993. Interleukin 12 acts directly on CD4+ T cells to enhance priming for interferon gamma production and diminishes interleukin 4 inhibition of such priming. *Proc Natl Acad Sci USA*. **90**:10188-10192.

Siegal F.P., Kadowaki N., Shodell M., Fitzgerald-Bocarsly PA, et al (1999 June 11). "The nature of the principal type 1 interferon-producing cells in human blood". *Science.* **284:**1835-1837.

Silver L.M. 1995. Mouse genetics: Concepts and Applications. Oxford University Press, Oxford, UK.

Smerz-Bertling C. and Duschl A. 1995. Both interleukin 4 and interleukin 13 induce tyrosine phosphorylation of the 140-kDa subunit of the interleukin 4 receptor. *J Biol Chem.* **270:**966-970.

Smith A.D. (Ed). 1997. *Oxford dictionary of biochemistry and molecular biology.* Oxford University Press. ISBN 0-19-854768-4

Smithies O., Gregg R.G., Boggs S.S., Koralewski M.A. and Kucherlapati R.S. 1985. Insertion of DNA sequences into the human chromosomal beta-globin locus by homologous recombination. *Nature*. **317:**230-234.

Snapper C.M., Finkelman F.D., Stefany D., Conrad D.H. andPaul W.E. 1988. IL-4 induces co-expression of intrinsic membrane IgG1 and IgE by murine B cells stimulated with lipopolysaccharide*. J Immunol*. **141:**489-498.

Song X.T., Evel-Kabler K.,Rollins L., Aldrich M., Gao F., et al. 2006. An alternative and effective HIV vaccination approach based on inhibition of antigen presentation attenuators in dendritic cells. *PLoS Med* 3(1): e11

Soos T.J., Sims T.N., Barisoni L., Lin K., Littman D.R., Dustin M.L. and Nelson P.J. 2006. CX3CR1+ interstitial dendritic cells form a contiguous network throughout the entire kidney. *Kidney Int*. **70**:591–596.

Sornasse T., Larenas P.V., Davis K.A., de Vries J.E. and Yssel H. 1996. Differentiation and stability of T helper 1 and 2 cells derived from naive human neonatal CD4+ T cells, analyzed at the single-cell level. *J Exp Med*. **184**:473-483.

Spits H., Yssel H., Takebe Y., Arai N., Yokota T., Lee F., Arai K., Banchereau J. and de Vries J.E. 1987. Recombinant interleukin 4 promotes the growth of human T cells. *J Immunol*. **139:**1142-1147.

Sriram U., Biswas C., Behrens E.M., Dinnall J., Shivers D.K., Monestier M., Argon Y. and Gallucci S. 2007. IL-4 Suppresses Dendritic Cell Response to Type I Interferons. *The Journal of Immunology,* **179:** 6446–6455.

Stack R.M., Lenschow D.J., Gray G.S., Bluestone J.A. and Fitch F.W. 1994. IL-4 treatment of small splenic B cells induces costimulatory molecules B7-1 and B7-2. *J Immunol.* **152:**5723-3573.

Stäger S., Alexander J., Carter K.C., Brombacher F. and Kaye P.M. 2003. Both Interleukin-4 (IL-4) and IL-4 Receptor α Signaling Contribute to the Development of Hepatic Granulomas with Optimal Antileishmanial Activity. *Infect Immun*. **71:** 4804–4807.

Stäger S., Alexander J., Kirby A.C., Botto M., V Rooijen N., Smith D.F. Brombacher F. and. Kaye P. M**.** 2003. Natural antibodies and complement are endogenous adjuvants for vaccine-induced CD8_ T-cell responses. *Nat.Med*. **9:**1287–1292.

Standiford T.J., Strieter R.M., Chensue S.W., Westwick J., Kasahara K. and Kunkel S.L. 1990. IL-4 inhibits the expression of IL-8 from stimulated human monocytes. *J Immunol*. **145:**1435-1439.

Stein M., Keshav S., Harris N. and Gordon S. 1992. Interleukin 4 potently enhances murine macrophage mannose receptor activity: A marker of alternative immunologic macrophage activation. *J. Exp. Med.* **176**:287-292.

Stevens T.L., Bossie A., Sanders V.M., Fernandez-Botran R., Coffman R.L., Mosmann T.R. and Vitetta E.S. 1988. Regulation of antibodyisotype secretion by subsets of antigen-specific helper T cells. *Nature*. **334:**255-258.

Stockinger B. 2007.TH17 cells: an orphan with influence. *Immunol. Cell Biol*. **85**:83–84

Stoffel R., Ziegler S., Ghilardi N., Ledermann B., de Sauvage F.J. and Skoda R.C. 1999. Permissive role of thrombopoietin and granulocyte colony-stimulating factor receptors in hematopoietic cell fate decisions in vivo. *Proc Natl Acad Sci U S A.* **96:**698-702.

Strachan T. and Read A.P. 1999. Human Molecular Genetics. BIOS Scientific Publishers Ltd.

Svensson L., Nandakumar K.S., Johansson A., Jansson L. and Holmdahl R. 2002. IL-4-deficient mice develop less acute but more chronic relapsing collagen-induced arthritis. *Eur J Immunol* **32:**2944–2953.

Swain S.L., McKenzie D.T., Weinberg A.D. and Hancock W. 1988. Characterization of T helper 1 and 2 cell subsets in normal mice. Helper T cells responsible for IL-4 and IL-5 production are present as precursors that require priming before they develop into lymphokine-secreting cells. *J Immunol*. **141:**3445-3455.

Szabo S.J., Sullivan B.M, Stemmann C., Satoskar A.R., Sleckman B.P. and Glimcher L.H. 2000.Distinct Effects of T-bet in T_H1 Lineage Commitment and IFN-γ Production in CD4 and CD8 T Cells. *Science.* **295:**338-342.

Szabo S.J., Kim S.T., Costa G.L., Zhang X., Fathman C.G. and Glimcher L.H. 2000. A novel transcription factor, T-bet, directs Th1 lineage commitment *Cell.* **17:**655-669.

Takeda K., Tanaka T., Shi W., Matsumoto M., Minami M., Kashiwamura S., Nakanishi K., Yoshida N., Kishimoto T. and Akira S. 1996. Essentail role of Stat6 in IL-4 signaling. *Nature*. **380**:627-630.

Takeda K., Kaisho T., Yoshida N., Takeda J., Kishimoto T. and Akira S. 1998. Stat3 activation is responsible for IL-6-dependent T cell proliferation through preventing apoptosis: generation and characterization of T cell-specific Stat3-deficient mice.
J Immunol. **161:**4652-4660.

Taniguchi T. 1995. Cytokine signaling through nonreceptor protein tyrosine kinases. *Science*. **268:**251-255.

Theofilopoulos A. N., R. Baccala B., Beutler. and Kono D.H. 2005. Type I interferons (_/_) in immunity and autoimmunity. *Annu. Rev. Immunol.* **23:**307–336.

Thomas K.R and. Capecchi M.R. 1987.Site-directed mutagenesis by gene targeting in mouse embryo-derived stem cells. *Cell*. **51:**503-512.

Tet Expression Systems and Cell Lines (July 1996) CLONTECHniques **XI**(3):2–5.

Urban J.F Jr., Noben-Trauth N., Donaldson D.D., Madden K.B., Morris S.C., Collins M. and Finkelman F.D. 1998.IL-13, IL-4Ralpha, and Stat6 are required for the expulsion of the gastrointestinal nematode parasite Nippostrongylus brasiliensis*. Immunity*. **8:**255-264.

Urban J., Fang H., Liu Q., Ekkens M.J., Chen S.J., Nguyen D., Mitro V., Donaldson D.D., Byrd C., Peach R., Morris S.C., Finkelman F.D., Schopf L. and Gause W.C. 2000. IL-13-mediated worm expulsion is B7 independent and IFN-gamma sensitive. *J Immunol.* **164:**4250-4256.

Urban J.F. Jr., Noben-Trauth N., Schopf L., Madden K.B. and Finkelman F.D. 2001. Cutting edge: IL-4 receptor expression by non-bone marrow-derived cells is required to expel gastrointestinal nematode parasites. *J Immunol.* **167:**6078-6081.

Urlinger S., Baron U., Thellmann M., Hasan M.T., Bujard H. and Hillen W. 2000. Exploring the sequence space for tetracycline-dependent transcriptional activators: novel mutations yield expanded range and sensitivity. *Proc Natl Acad Sci U S A*. **97:**7963-7968.

Usui T., Preiss J.C., Kanno Y., Yao Z.Y., Bream J.H., O'Shea J.J. and Strober W. 2006. T-bet regulates Th1 responses through essential effects on GATA-3 function rather than on *IFNG* gene acetylation and transcription. *JEM.* **203:**755-766.

Utomo A.R., Nikitin A.Y. and Lee W.H. 1999.Temporal, spatial, and cell type-specific control of Cre-mediated DNA recombination in transgenic mice. Nat Biotechnol. 17:1091-1096.

Vats D., Mukundan L., Odegaard J.I., Zhang L., Smith K.L., Morel C.R., Wagner R.A., Greaves D.R., Murray P.J. and Chawla A. 2006. Oxidative metabolism and PGC-1beta attenuate macrophage-mediated inflammation. *Cell Metab.* **4**:13–24.

Vita N., Lefort S., Laurent P., Caput D. and Ferrara P. 1995. Characterization and comparison of the interleukin 13 receptor with the interleukin 4 receptor on several cell types. *J Biol Chem*. **270:**3512-3517.

Wang Y., Krushel L.A. and Edelman G.M. 1996. Targeted DNA recombination in vivo using a adenovirus carrying the cre recombinase gene. *Proc Natl Acad Sci USA*. **93:**3932-3936.

Weisberg, S.P., et al. 2005. CCR2 modulates inflammatoryand metabolic effects of high-fat feeding.*J. Clin. Invest.* **116**:115–124.

Wells K.D. Foster J.A. Moore K., Pursel V.G. and Wall R.J. 1999. Codon optimization, genetic insulation, and an rtTA reporter improve performance of the tetracycline switch. *Transgenic Res.* **8:**371-381.

Wiersma E. J., Coulie P.G. and Heyman B**.** 1989. Dual immunoregulatory effects of monoclonal IgG-antibodies: suppression and enhancement of the antibody response. Scand. *J. Immunol*. **29:**439–448.

Wiesner S. M., Jones J. M., Hasz D. E. and Largaespada D. A. 2005. Repressible transgenic model of *NRAS* oncogene–driven mast cell disease in the mouse. *Blood*, **106**:1054-1062.

Weiss G., Bogdan C. and Hentze M.W. 1997. Pathways for the regulation of macrophage iron metabolism by the anti-inflammatory cytokines IL-4 and IL-13. *J Immunol*. **158:**420-425.

Widmer M.B., Acres R.B., Sassenfeld H.M. and Grabstein K.H. 1987. Regulation of cytolytic cell populations from human peripheral blood by B cell stimulatory factor 1 (interleukin 4). *J Exp Med*. **166:**1447-55.

Wills-Karp M., Luyimbazi J., Xu X., Schofield B., Neben T.Y., Karp C.L. and Donaldson D.D. 1998. Interleukin-13: central mediator of allergic asthma. *Science*. **282**:2258-61.

Wilson M.S., Elnekave E. Mentink-Kane M.M., Hodges M.G., Pesce J.T., Ramalingam T.R., Thompson R.W., Kamanaka M.,. Flavell R.A., Keane-Myers A., Cheever A.W. and Wynn T.A. IL-13Ra2 and IL-10 coordinately suppress airway inflammation, airway hyperreactivity,and fibrosis in mice. *The Journal of Clinical Investigation* **117:** 2941-2951.

Wing K., Fehervari Z. and Sakaguchi S. 2006.Emerging possibilities in the development and function of regulatory T cells. *Int. Immunol.* **18:**991–1000.

Winzler C., Rovere P., Rescigno M., Granucci F., Penna G., Adorini L., Zimmermann V.S., Davoust J. and Ricciardi-Castagnoli P. 1997. Maturation Stages of Mouse Dendritic Cells in Growth Factor–dependent Long-Term Cultures. *J. Exp. Med*. **185**:317–328.
Wong P. and Pamer E.G. 2003. CD8 T cell responses to infectious pathogens. *Annu Rev Immunol.* **21:**29-70.

Wong T., Hildebrandt M., Thrasher S.M., Appleton J.A., Ahima R.S. and Wu G.D. 2007. Divergent Metabolic Adaptations to Intestinal Parasitic NematodeInfection in Mice Susceptible or Resistant to Obesity. *Gastroenterology*. **133:** 1979–1988

Wrighton N., Campbell L.A., Harada N., Miyajima A. and Lee F. 1992. The murine interleukin-4 receptor gene: genomic structure, expression and potential for alternative splicing. *Growth Factors*. **6:**103-118.

Yang D., Liu Z.H., Tewary P., Chen Q., de la Rosa G. and Oppenheim J.J. 2007. Defensin participation in innate and adaptive immunity. *Curr Pharm* **13:**3131-3139.

Ying S., Meng Q., Barata L.T., Robinson D.S., Durham S.R. and Kay A.B. 1997. Associations between IL-13 and IL-4 (mRNA and protein), vascular cell adhesion molecule-1 expression, and the infiltration of eosinophils, macrophages, and T cells in allergen-induced late-phase cutaneous reactions in atopic subjects. *J Immunol*. **158:**5050-5057.

Yoshimoto T. and Paul W.E. 1994. CD4pos, NK1.1pos T cells promptly produce interleukin 4 in response to in vivo challenge with anti-CD3*. J Exp Med.* **179:**1285-1295.

Yu H.M., Liu B., Chiu S.Y., Costantini F. and Hsu W. 2005. Development of a unique system for spatiotemporal and lineage-specific gene expression in mice. *Proc Natl Acad Sci USA.* **102:**8615-8620.

Zhang J., Hilton D.J., Willson T.A., McFarlane C., Roberts B.A., Moritz R.L., Simpson R.J. Alexander W.S., Metcalf D. and Nicola N.A. 1997**.** Identification, Purification, and Characterization of a Soluble Interleukin (IL)-13-binding Protein . *The American Society for Biochemistry and Molecular Biology, Inc.* **272:** 474-9480.

Zheng B. J., Ng M. H., He L.F., Yao X., Chan K.W., Yuen K.Y. and Wen Y.M. 2001. Therapeutic efficacy of hepatitis B surface antigen-antibodiesrecombinant DNA composite in HBsAg transgenic mice. *Vaccine* **19:**4219–4225.

Ziegler-Heitbrock H.W. 1989. The biology of the monocyte system.*Eur. J. Cell Biol.* **49:**1–12.

Zurawski S.M., Vega F. Jr., Huyghe B. and Zurawski G. 1993. Receptors for interleukin-13 and interleukin-4 are complex and share a novel component that functions in signal transduction. *EMBO J.* **12**:2663-2670.

Zurawski S.M., Chomarat P., Djossou O., Bidaud C., McKenzie A. N., Missec P., Banchereau J. and Zurawski G. 1995. The primary binding subunit of the human interleukin-4 receptor is also a component of the interleukin-13 receptor. *J.Biol Chem*. **270**:13869-13878.

Prof. Hermann Bujard webpage:
http://www.zmbh.uni-heidelberg.de/bujard/trouble/printingver.htm